SESSION VII

FILTRATION AND FILTRATION SYSTEMS

Wednesday, August 14, 1974
CHAIRMEN: Clifford A. Burchsted and
Humphrey Gilbert

AEROSOL FILTRATION BY FIBROUS FILTER MATS: PART III, GEOMETRIC RELATIONS
W.L. Anderson, W.S. Magee, L.A. Jonas

HIGH TEMPERATURE AEROSOL FILTRATION BY DIFFUSION
J.P. Kornberg, M.W. First

PERFORMANCE OF MULTIPLE HEPA FILTERS AGAINST PLUTONIUM AEROSOLS
M. Gonzales, J. Elder, H. Ettinger

IN-PLACE TESTING OF MULTIPLE STAGE HEPA FILTER PLENUMS
F.J. Linck, J.A. Geer

COMPARATIVE FILTER EFFICIENCY TESTING USING DIOCTYLPHTALATE AND SODIUM CHLORIDE AEROSOLS
O. Jovanović, M. Vidmar, M. Tubić, D. Patić, B. Radosavljević, R. Smiljanić

FLAME GENERATION OF SODIUM CHLORIDE AEROSOL FOR FILTER TESTING
J. Edwards, D.I. Kinnear

HIGH EFFICIENCY PARTICULATE AIR (HEPA)FILTER PERFORMANCE FOLLOWING SERVICE AND RADIATION EXPOSURE
L. R. Jones

THE HEPA-FILTER SMOKE PLUGGING PROBLEM
J.R. Gaskill, M.W. Magee

EVALUATION OF MULTISTAGE FILTRATION TO REDUCE SAND FILTER EXHAUST ACTIVITY
D.B. Zippler

THE OFF-GAS FILTER SYSTEM FOR THE SNR-300
L. Böhm, S. Jordan, W. Schikarski

DEEP-BED SAND FILTER AT SAVANNAH RIVER LABORATORY
R.A. Moyer, J.H. Crawford, R.E. Tatum

GOVERNMENT-INDUSTRY MEETING ON FILTERS, MEDIA AND MEDIA TESTING
W.L. Anderson

AEROSOL FILTRATION BY FIBROUS FILTER MATS: PART III GEOMETRIC RELATIONS

Wendell L. Anderson*, William S. Magee, Jr., Leonard A. Jonas
*Naval Weapons Laboratory, Dahlgren, VA 22448
Edgewood Arsenal, Aberdeen Proving Ground, MD 21010

Abstract

The aerosol filtration characteristics of ten randomly formed fibrous filter mats, of widely varying compositions and physical properties, were studied as a function of both the superficial linear flow velocity and the aerosol diameter size. The flow regime ranged from 7.2 to 141 cm/sec with ten discrete velocities. Four diameter sizes of dioctylphthalate (DOP) aerosol were used to challenge the filter mats over this velocity range, namely, 0.26, 0.28, 0.30, and 0.32 microns. Mathematical equations, derived from the original Dorman aerosol equations, provided insight on the interrelationships between aerosol size, flow velocity, and the diffusion, interception, and inertia mechanisms of aerosol filtration.

I. Introduction

In previous papers the aerosol filtration properties of a wide variety of fibrous filter mats were studied. The first paper, Part I in the series (Jonas, 1972), initiated the study and showed the applicability of the semi-empirical equations of Dorman (1960, 1966) with their concepts of diffusion, interception, and inertia as aerosol filtration mechanisms. Part II in the series (Magee, 1973) stressed the flow velocity relationships inherent in aerosol filtration theory; modified the original equations and derived a mathematical form which permitted the calculation of $\overline{V}_L$, the velocity at which maximum aerosol penetration occurred; and determined the Dorman parameters of diffusion, interception, and inertia for the various filter mats when challenged by 0.3 micron diameter DOP aerosols. This paper, Part III in the series, investigates the geometry dependent relations in filtration, as evidenced by challenges with 0.26, 0.28, 0.30, and 0.32 micron diameter DOP aerosols.

II. Purpose

The purpose of this work was to study aerosol penetration through fibrous filter mats as a function of aerosol size, and to augment the existing velocity dependent relations with geometric relations in the mathematical equations of the present theory.

III. Theory

Fuchs (1955) shows that the efficiency E for physical removal or filtration of fine aerosol particles by a fibrous filter mat is expressed by

$$E = 1 - \exp(-\alpha) \tag{1}$$

with α defined as the coefficient of absorption for the mat. Under the assumption that N independent mechanisms contribute additively to the total absorption, the coefficient for the mat becomes

$$\alpha = \sum_{i=1}^{N} \alpha_i \tag{2}$$

From the expression (1) and the fact that the % penetration of an aerosol through a mat is 100 times the ratio of the effluent to the influent concentration, it follows that

$$\% \text{ Pen} = 100(n/n_o) = 100(1 - E) = 100 \exp(-\alpha) \tag{3}$$

Substituting relation (2) in (3) and subsequently taking logarithms to the base ten yield the equation

$$\log \% \text{ Pen} = 2 - \left(\frac{1}{2.303}\right) \sum_{i=1}^{N} \alpha_i \tag{4}$$

Neglect of all mechanisms except inertial capture, diffusion, and interception reduces Equation (4) to the form

$$\log \% \text{ Pen} = 2 - \left(\frac{1}{2.303}\right) \left(\alpha_R + \alpha_D + \alpha_I\right) \tag{5}$$

where R, D, and I denote respectively inertia, diffusion, and interception.

These three dimensionless coefficients have been shown by Fuchs to be given by the following relations with the assumption of Poiseuille flow:

$$\alpha_R = \frac{\tau V_L \lambda}{2(3)^{1/2} h^2} \tag{6}$$

$$\alpha_D = \frac{2D^{2/3} \lambda V_L^{-2/3}}{3^{1/6}(d_f/2)\, h^{2/3} (1 + \frac{2h}{d_f})^{5/3}} \tag{7}$$

and

$$\alpha_I = \frac{3(d_p/2)^2 \lambda}{2(3)^{1/2} h^2 \left(\frac{d_f + 2h}{2}\right)} \tag{8}$$

where τ is the relaxation time imposed by viscous media forces on a particle during its travel in the interfiber volume of a filter mat, V_L (cm/sec) is the superficial linear face velocity, τ (in cm) is the mat thickness, h (in cm) is one half the average distance between nearest neighbor filtering fibers, D (in $cm^2\ sec^{-1}$) is the particle diffusion coefficient, d_f (in cm) is the diameter of a filtering fiber, and d_p (in cm) is the diameter of an aerosol particle.

Reducing the numerical coefficients in (6), (7) and (8) and substituting in (5), we find

$$\log \%\ \text{Pen} = 2 - \left(\frac{0.1254\tau\lambda}{h^2}\right) V_L - \left(\frac{1.4463\, D^{2/3} \lambda}{d_f\, h^{2/3} \left(1 + \frac{2h}{d_f}\right)^{5/3}}\right) V_L^{-2/3} - \left(\frac{0.1880\, d_p^2 \lambda}{h^2 (d_f + 2h)}\right) \tag{9}$$

In our Part II paper (Magee et al, 1973) we showed that the semi-empirical relation, originally developed by Dorman (Dorman, 1960a, b; 1966), could be generalized to describe aerosol penetration as

$$\log \text{DOP}\ \%\ \text{Pen} = 2 - k_R \lambda V_L^{\ x} - k_D \lambda V_L^{-y} - k_I \lambda \tag{10}$$

After justification for the assignments of x = 1 and y = 2/3 Equation (10) became

$$\log \% \text{ Pen} = 2 - k_R \lambda V_L - k_D \lambda V_L^{-2/3} - k_I \lambda \qquad (11)$$

where k_R, k_D, and k_I were the Dorman parameters for inertial, diffusion, and interceptional removal respectively. Since this equation predicts the existence of a velocity ($\bar{V}_L$) for which a maximum % penetration occurs, it can be shown, by setting the first derivative of Equation (11) to zero, that

$$k_D = 1.5\, k_R\, \bar{V}_L^{5/3} \qquad (12)$$

A term by term comparison of Equations (6), (7), (8), (9), and (11) showed the following relationships between the Fuchs' dimensionless coefficients and the Dorman parameters

$$\alpha_R = 2.303\, \lambda V_L\, k_R \qquad (13)$$

$$\alpha_D = 2.303\, \lambda V_L^{-2/3}\, k_D \qquad (14)$$

and

$$\alpha_I = 2.303\, \lambda\, k_I \qquad (15)$$

The equations used to evaluate the experimental data in our Part II paper, plotted as

$$\frac{\Delta \log \text{DOP \% pen}}{\Delta\, V_L^{-2/3}} \quad \text{vs.} \quad V_{L(m)}^{5/3}$$

were

$$\frac{\Delta \log \text{DOP \% pen}}{} = 1.5 \lambda k_R \left[V_{L(m)}^{5/3} - \bar{V}_L^{5/3} \right] \qquad (16)$$

where

$$V_{L(m)}^{5/3} = \left[\frac{V_{L(1)}^{-2/3} + V_{L(2)}^{-2/3}}{2} \right]^{-5/2} \qquad (17)$$

and

$$\bar{V}_L^{5/3} = \frac{-\text{intercept}}{\text{slope}} \qquad (18)$$

since all DOP aerosol challenging the various fibrous filter mats was at 0.30 micron diameter. Unique values were, therefore, obtained for the three Dorman parameters of each filter mat. In this study, however, four different diameters were used (0.26 to 0.32 microns) and, therefore, the effect of aerosol diameter, d_p, on the various Dorman filtration parameters had to be determined. Thus, the Fuchs relations, expressed by Equations (5) through (9) and (13) through (15), which involved d_p both directly and indirectly, e.g. through the diffusivity D, were added to the others to form a larger set of equations for evaluation of our experimental data.

IV. Materials

The DOP used in this study and manufactured by Union Carbide Co., New York, is commonly called dioctylphthalate (DOP) although its composition more closely corresponds to di-2-ethylhexylphthalate. It has a molecular weight of 390.5 g/mole, a boiling range of 229-233°C, a specific gravity of 0.986 g/cm^3 at 20°C, and a refrative index n_d^{20} of 1.4859.

The ten filter mats studied represented a wide range of fiber type and composition. Filter mat Type 5 was developed by Edgewood Arsenal in the 1940's and was composed of coarse matrix fibers (cotton floc, viscose rayon, and manila hemp) and Blue Bolivian crocidolite asbestos as the aerosol filtering fiber. The N11, N13, and N15 mats were developed by the Naval Research Laboraotory and each contained an 84.1 to 15.9 mixture of viscose and B.B. asbestos. The degree of acid beating of the asbestos fibers, though, was different for each. The remaining six filter mats were specially fabricated by the Naval Research Laboratory for aerosol filtration studies and were composed entirely of their fiber designations. Thickness λ values for the ten filter mats studied were as follows: 0.048, 0.112, 0.089, 0.122, 0.068, 0.095, 0.050. 0.071, 0.075, and 0.028 cm for the Type 5, N11, N13, N15, Esparto, Viscose 1.5D, Viscose 3.0D, A, AA, and AAA mats respectively. Other physical properties of these mats, such as bulk density, fiber density, volume fiber fraction, and volume void fraction (porosity), as well as methods of calculation, are described in our Part II paper (Magee, 1973). In addition, the Part II paper shows the pressure drop vs velocity relationships of the ten filter mats in terms of regression analysis polynomials, each conforming to the Darcy equation form (Collins, 1961) for the flow of an incompressible fluid through a porous medium.

Thickness values for many of the fibers present in the various filter mats are as follows:

Blue Bol. asbestos: 0.65μ diam Type 5, N11, and N15 filters;
0.50μ diam in N13 filter.

Esparto: fibers about 7μ diam.

Viscose 1.5D: fibers about 12μ diam; used in N series filter mats.

Viscose 3.0D: fibers about 17μ diam.

A glassfibers: range between 1.00 and 1.24μ diam with mean of 1.12μ.

AA glassfibers: range between 0.75 and 0.99μ diam with mean of 0.87μ.

AAA glassfibers: range between 0.50 and 0.74μ diam with mean of 0.62μ.

V. Equipment and Procedures

The equipment used to test the filtration characteristics of the filter mats was a DOP aerosol test apparatus. The DOP aerosol was generated at four discrete particle sizes; namely 0.26, 0.28, 0.30, and 0.32 micron diameter. The aerosol concentration for each size was established at 80 μg DOP per liter of air at 25°C. Aerosol diameter size was determined from forward angle light scattering and measured on the MIT-EIR2 particle size meter (the Owl). The superficial linear velocity flow range used in these tests was 7.1 to 141 cm/sec. Details of the component parts of the test apparatus, as well as its operating procedure, are fully described in the Part II paper, (Magee, 1973). All experimental tests on the fibrous filter mats were performed at the Naval Research Laboratory, Washington, DC.

VI. Results and Discussion

The aerosol filtration characteristics of the ten fibrous filter mats were studied using DOP aerosols, having the four discrete mean diameters of 0.26, 0.28, 0.30. and 0.32 microns, and measuring the present penetration of the aerosol through the mats over the superficial linear velocity range 7.2 - 141 cm/sec. These data are shown in Table I and plotted in Figures 1 to 3. The plots show that the DOP penetration vs. velocity values exhibit a maximum for all filter mats, and that $\overline{V}_L$, the velocity at which maximum penetration occurs, varies both in absolute value and discreteness depending upon the filter mat composition.

The experimental data in Table I were used to calculate values of Δ log DOP% penetration/Δ $V_L^{-2/3}$ for the ten filter mats at nine sequential flow velocity intervals for each of the four DOP aerosol diameter sizes, and are shown in Tables II to V. The dependence of these ratios on the 5/3 power of the root mean of the velocity interval $V_{L(m)}$, the means being calculated from Equation (17), was determined by regression analyses of Y on X as Y = aX + b using Equation (16).

Correlation coefficients for 29 of the 32 regression equations ranged between 0.903 and 0.999; for the remaining 3 equations the lowest was 0.844. Since the slope of the straight line curve was $1.5\lambda\ k_R$ and the Y-axis intercept was $-1.5\lambda\ k_R \bar{V}_L^{5/3}$, $\bar{V}_L$ could be calculated by taking the 3/5 power of the ratio of -intercept to slope, obtained from Equation (18). The regression equations, as well as both calculated and experimental $\bar{V}_L$ values, are shown in Table VI.

The calculated values of $\bar{V}_L$ for each filter mat and challenge DOP aerosol diameter compared closely with the experimental values obtained from all filter mats except the N13 and Viscose 3.0D filters. In the case of the N13 filter the experimental $\bar{V}_L$ was below the lowest velocity used and thus no discrete maximum was evidenced in the penetration vs. velocity plots. All experimental values, therefore, used in Equations (16) and (18) to derive a calculated $\bar{V}_L$ were of necessity taken only from the descending portion of the penetration vs. velocity plot. In the case of the Viscose 3.0D filter mat the experimental plot of penetration vs. velocity showed a prolonged plateau rather than a discrete $\bar{V}_L$ at which maximum DOP penetration occurred.

Using the calculated $\bar{V}_L$ values, the thickness (λ) values shown in the Materials section, and Equations(11), (12), and (16), the three Dorman parameters k_R, k_D, and k_I, representing inertial, diffusional, and interceptional mechanisms respectively, were calculated for the various DOP aerosol diameters challenging the various filter mats, and are shown in Table VII. As indicated the units for these parameters are cm^{-2} sec for k_R, $cm^{-1/3}$ $sec^{-2/3}$ for k_D, and cm^{-1} for k_I. The three dimensionless Fuchs' coefficients representing the same mechanisms, and denoted by α_R,α_D, and α_I, were calculated from Equations (13) to (15) using known thickness values and calculated Dorman parameters for each of the filter mats, and are shown in Table VIII. Although the Fuchs' coefficient for interception is velocity independent, the coefficients for inertia and diffusion are dependent on the 1 and -2/3 power of the velocity respectively. For these latter two coefficients, rather that calculating the values for each of the ten discrete velocities used, it was decided to show the range of the values over the experimental velocity interval 7.2 to 141 cm/sec. The calculated Fuchs' coefficients for the various fibrous filter mats at each of the four DOP aerosol diameters are shown in Table VIII.

The Fuchs' coefficients, although linearly dependent upon the Dorman parameters as indicated in Equations (13), (14), and (15), fail to illuminate the contribution of each of the mechanisms to the overall filtration for the various filter mats as well as the Dorman parameters because of the former's complex dependencies on velocity. This is especially evident in the ratio of the diffusional to inertial mechanisms for any filter mat, the α_D being decreased due to its dependence on $V_L^{-2/3}$ and α_R increased due to its dependence on V_L, thus smearing out their differences and decreasing the ability to discriminate between good and poor filter mats. Excellent examples of the smearing out effect can be seen by comparing the α_D/α_R and α_D/α_I ratios from Table VIII with the k_D/k_R and k_D/k_I ratios for an excellent filter such as N15 with corresponding ratios for a poor filter such as Esparto.

In view of this it was generally concluded that the Dorman parameters were much superior to the Fuchs' coefficients in assessing the aerosol filtration characteristics of fibrous filter mats. More specifically, the inertia parameter, k_R, although increasing slightly with increase in aerosol size, showed an insignificant contribution to the aerosol filtration of the various filter mats. The interception parameter, k_I, was essentially independent of aerosol size for each filter mat, although its contribution to the overall filtration was quite significant. The diffusion parameter, k_D, showed the greatest contribution to aerosol filtration for the highly efficient fibrous filter mats and revealed a nonmonotonic dependence on aerosol size.

TABLE I. DOP PENETRATION AS A FUNCTION OF VELOCITY AND AEROSOL SIZE

Lin Vel cm sec	Aer Diam μ	DOP% Penetration of 5	N11	N13	N15	Esp	Visc 1.5D	Visc 3.0D	A	AA	AAA
7.2	0.26	29	0.006	0.092	0.004	31	72	87	5.5	0.009	0.022
	0.28	32	0.004	0.033	0	29	74	85	3.2	0.006	0.015
	0.30	27	0.001	0.030	0	32	75	88	2.7	0.002	0.004
	0.32	19	0	0.015	0	24	74	86	1.5	0	0
10.7	0.26	31	0.009	0.089	0.006	33	74	87	6.0	0.019	0.038
	0.28	33	0.005	0.030	0.001	30	76	86	4.2	0.012	0.021
	0.30	28	0.003	0.027	0	33	80	90	3.6	0.004	0.006
	0.32	21	0	0.010	0	24	75	88	1.7	0	0
14.2	0.26	31	0.011	0.085	0.007	33	74	87	7.0	0.026	0.048
	0.28	33	0.005	0.025	0.002	30	78	86	4.8	0.016	0.027
	0.30	29	0.003	0.022	0	33	82	90	4.1	0.005	0.007
	0.32	21	0	0.006	0	25	77	88	1.8	0	0
17.6	0.26	33	0.012	0.084	0.007	34	78	87	7.5	0.035	0.054
	0.28	33	0.005	0.024	0.003	30	80	87	5.3	0.018	0.040
	0.30	29	0.002	0.020	0	33	83	90	4.3	0.005	0.007
	0.32	21	0	0.005	0	26	80	88	1.8	0	0
26.7	0.26	33	0.014	0.074	0.008	33	78	87	8.0	0.052	0.072
	0.28	33	0.004	0.016	0.004	30	80	87	5.8	0.025	0.044
	0.30	29	0.001	0.012	0	32	83	90	4.8	0.005	0.006
	0.32	21	0	0.001	0	23	81	88	1.7	0	0
35.3	0.26	33	0.010	0.062	0.009	33	78	87	8.5	0.062	0.078
	0.28	33	0.002	0.009	0.003	28	80	87	6.0	0.028	0.044
	0.30	29	0	0.007	0	30	83	90	4.8	0.004	0.005
	0.32	21	0	0	0	20	81	88	1.6	0	0
53.0	0.26	32	0.008	0.050	0.009	32	78	87	8.5	0.066	0.076
	0.28	32	0.001	0.005	0.002	26	80	87	6.0	0.027	0.038
	0.30	27	0	0.001	0	27	83	90	4.6	0.002	0.003
	0.32	19	0	0	0	14	81	88	1.4	0	0
71.0	0.26	30	0.006	0.029	0.007	28	78	87	8.5	0.058	0.074
	0.28	30	0	0.001	0.001	22	80	87	5.8	0.021	0.032
	0.30	25	0	0	0	23	83	90	4.0	0	0.002
	0.32	15	0	0	0	9	80	88	1.1	0	0
106.4	0.26	28	0.003	0.018	0.006	22	78	87	7.5	0.044	0.064
	0.28	27	0	0	0	16	80	87	5.0	0.012	0.025
	0.30	21	0	0	0	15	82	89	3.0	0	0
	0.32	11	0	0	0	4	78	80	0.6	0	0
141	0.26	24	0.001	0.008	0.003		78	83	6.5	0.028	0.040
	0.28	23	0	0	0		80	82	4.0	0.005	0.010
	0.30	17	0	0	0		80	86	1.6	0	0
	0.32	7	0	0	0			74	0.20	0	0

* DOP penetration of 0.000% shown as 0.

TABLE II. PENETRATION-VELOCITY SLOPES FOR FIBROUS FILTER MATS: 0.26μ DOP

Filter Mat	Δlog DOP% penetration/$\Delta V_L^{-2/3}$ * for the linear velocity interval (cm/sec) 7.2-10.7	10.7-14.2	14.2-17.6	17.6-26.7	26.7-35.3	35.3-53.0	53.0-71.0	71.0-106.4	106.4-141
5	-0.465	0	-1.194	0	0	0.606	2.233	2.173	8.784
N11	-2.829	-2.461	-1.662	-1.867	7.686	4.394	9.954	21.836	62.60
N13	0.231	0.564	0.226	1.535	4.041	4.236	18.847	15.024	46.208
N15	-2.829	-1.891	0	-1.618	-2.690	0	8.695	4.856	39.496
Esp	-0.436	0	-0.570	0.362	0	0.606	4.620	7.597	
Visc 1.5D	**								
Visc 3.0D	**								
A	-0.607	-1.891	-1.318	-0.782	-1.385	0	0	3.943	8.154
AA	-5.213	-3.847	-5.677	-4.796	-4.018	-1.231	4.471	8.703	25.754
AAA	-3.813	-2.865	-2.250	-3.485	-1.828	0.511	0.923	4.574	26.781

* Tabular values shown are truncated for convenience. Computer calculations, though, were made on the total number of computer-handled digits.

** Insufficient data points for calculation.

TABLE III. PENETRATION-VELOCITY SLOPES FOR FIBROUS FILTER MATS: 0.28μ DOP

Filter Mat	Δlog DOP% penetration/$\Delta V_L^{-2/3}$ * for the linear velocity interval (cm/sec)								
	7.2-10.7	10.7-14.2	14.2-17.6	17.6-26.7	26.7-35.3	35.3-53.0	53.0-71.0	71.0-106.4	106.4-141
5	-0.215	0	0	0	0	0.606	2.233	3.319	9.136
N11	-1.557	0	0	2.703	15.833	13.649			
N13	0.665	2.236	0.780	4.912	13.142	11.574	55.686		
N15		-8.502	-7.744	-3.485	6.571	7.984	23.983		
Esp	-0.237	0	0	0	1.576	1.459	5.780	10.032	
Visc 1.5D	**								
Visc 3.0D	-0.082	0	-0.221	0	0	0	0	0	3.373
A	-1.897	-1.638	-1.893	-1.092	-0.774	0	1.173	4.676	12.71
AA	-4.835	-3.528	-2.250	-3.979	-2.589	0.716	8.695	17.629	49.885
AAA	-2.347	-3.082	-7.507	-1.155	0	2.887	5.946	7.777	52.211

* Tabular values shown are truncated for convenience. Computer calculations, though, were made on the total number of computer-handled digits.

** Insufficient data points for calculation.

TABLE IV. PENETRATION-VELOCITY SLOPES FOR FIBROUS FILTER MATS· 0.30μ DOP

Filter Mat	$\Delta \log$ DOP% penetration/$\Delta V_L^{-2/3}$ * for the linear velocity interval (cm/sec)								
	7.2-10.7	10.7-14.2	14.2-17.6	17.6-26.7	26.7-35.3	35.3-53.0	53.0-71.0	71.0-106.4	106.4-141
5	-0.254	-0.430	0	0	0	1.407	2.663	5.493	12.041
N11	-7.665	0	7.744	8.396					
N13	0.735	2.512	1.820	6.188	12.312	38.317			
N15	**								
Esp	-0.215	0	0	0.373	1.474	2.075	5.548	13.466	
Visc 1.5D	-0.450	-0.303	-0.232	0	0	0	0	0.382	1.407
Visc 3.0D	-0.157	0	0	0	0	0	0	0.352	1.954
A	-2.007	-1.595	-0.910	-1.332	0	0.838	4.836	9.063	35.819
AA	-4.836	-2.737	0	0	5.097	13.649			
AAA	-2.829	-1.891	0	1.867	4.165	10.059	14.029		

* Tabular values shown are truncated for convenience. Computer calculations, though, were made on the total number of computer-handled digits.

** No data points for calculation since all show 0.000%.

TABLE V. PENETRATION-VELOCITY SLOPES FOR FIBROUS FILTER MATS: 0.32μ DOP

	$\Delta \log$ DOP% penetration/$\Delta V_L^{-2/3}$ * for the linear velocity interval (cm/sec)								
Filter Mat	7.2-10.7	10.7-14.2	14.2-17.6	17.6-26.7	26.7-35.3	35.3-53.0	53.0-71.0	71.0-106.4	106.4-141
5	-0.698	0	0	0	0	1.971	8.179	9.771	25.75
N11	**								
N13	2.829	6.265	3.482	19.496					
N15	**								
Esp		-0.501	-0.749	1.485	3.192	7.023	15.287	25.546	
Visc 1.5D	-0.094	-0.323	-0.730	-0.150	0	0	0.430	0.798	
Visc 3.0D	-0.016	0	0	0	0	0	0	3.003	4.442
A	-0.873	-0.701	0	0.693	1.385	2.629	8.344	19.095	62.600
AA	**								
AAA	**								

* Tabular values shown are truncated for convenience. Computer calculations, though, were made on the total number of computer-handled digits.

** No data points for calculation since all show 0.000% penetration.

TABLE VI. REGRESSION ANALYSIS EQUATIONS FOR FIBER MAT FILTRATION OF VARIOUS SIZE AEROSOLS

Filter Mat	DOP Aerosol Diameter μ	Regression Equation *	Max Penetration Vel $\overline{V}_L$, cm/sec	
			Calculated	Experimental
Type 5	0.26	Y = 0.003067X - 1.1743	35.5	35.0
	0.28	Y = 0.003153X - 0.8654	29.0	30.0
	0.30	Y = 0.004149X - 0.8149	23.8	25.0
	0.32	Y = 0.008805X - 1.8440	24.7	23.0
N11	0.26	Y = 0.020675X - 4.7294	26.0	27.0
	0.28	Y = 0.034285X - 1.0837	7.9	17.5
	0.30	Y = 0.124509X - 9.6263	13.6	13.0
N13	0.26	Y = 0.014719X - 0.9896	12.5	7.2
	0.28	Y = 0.056501X - 4.4519	13.7	7.2
	0.30	Y = 0.075814X - 4.6435	11.8	7.2
	0.32	Y = 0.124719X - 3.3647	7.2	7.2
N15	0.26	Y = 0.012925X - 5.0883	36.1	40.0
	0.28	Y = 0.036090X - 9.4371	28.2	29.0
Esparto	0.26	Y = 0.005139X - 0.9089	22.3	18.0
	0.28	Y = 0.006447X - 0.7462	17.3	19.0
	0.30	Y = 0.008333X - 1.2547	20.3	18.0
	0.32	Y = 0.016671X - 1.6218	15.6	17.5
Visc 1.5D	0.30	Y = 0.000571X - 0.3936	50.5	49.0
	0.32	Y = 0.000737X - 0.3771	42.2	39.0
Visc 3.0D	0.28	Y = 0.001206X - 0.2317	23.5	47.0
	0.30	Y = 0.000700X - 0.3777	43.6	55.0
	0.32	Y = 0.001574X - 0.0337	6.3	50.0
A	0.26	Y = 0.003267X - 1.6083	41.2	45.0
	0.28	Y = 0.004765X - 2.3205	41.0	42.0
	0.30	Y = 0.011810X - 3.9834	32.9	30.0
	0.32	Y = 0.020352X - 5.3547	28.3	28.0
AA	0.26	Y = 0.010318X - 6.2028	46.5	50.0
	0.28	Y = 0.017740X - 6.7296	35.3	40.0
	0.30	Y = 0.037061X - 5.7334	20.6	20.0
AAA	0.26	Y = 0.009272X - 4.9256	43.2	38.0
	0.28	Y = 0.017049X - 6.9766	36.9	35.0
	0.30	Y = 0.018786X - 2.1153	17.0	18.0

* $Y = \dfrac{\Delta \log \text{DOP\% penetration}}{\Delta V_L^{-2/3}}$ $\qquad X = V_{L(m)}^{5/3}$

TABLE VII. DORMAN PARAMETERS FOR FIBROUS FILTER MATS

Filter Mat	Dorman Parameter: Inertial k_R (cm^{-2} sec) 0.26 μ	0.28 μ	0.30 μ	0.32 μ	Diffusional k_D ($cm^{-1/3}$ $sec^{-2/3}$) 0.26 μ	0.28 μ	0.30 μ	0.32 μ	Interception k_I (cm^{-1}) 0.26 μ	0.28 μ	0.30 μ	0.32 μ
5	0.043	0.044	0.058	0.122	24.5	18.0	17.0	38.4	5.80	6.39	7.44	5.64
N11	0.123	0.204	0.741		42.2	9.68	85.9		26.3	33.8	15.5	
N13	0.110	0.423	0.568	0.934	11.1	50.0	52.2	37.8	30.7	24.5	22.9	26.9
N15	0.071	0.197			41.7	77.4			26.0	22.5		
Esp	0.050	0.063	0.082	0.163	13.4	11.0	18.5	23.9	3.88	4.70	2.64	2.22
Visc 1.5D			0.004	0.005			4.14	3.97			0.25	0.39
Visc 3.0D		0.016	0.009	0.021		4.63	7.55	0.67		-0.04*	-0.38*	0.27
A	0.031	0.045	0.119	0.191	22.7	32.7	56.1	75.4	11.9	12.3	8.23	8.96
AA	0.092	0.158	0.329		82.7	89.7	76.4		31.7	32.6	39.8	
AAA	0.221	0.406	0.447		176	249	75.5		85.1	77.8	131	

* Negative value probably occurred due to an artifact present in the three data points available for calculation. Values are equivalent to zero since negative values have no physical significance.

TABLE VIII. FUCHS' COEFFICIENTS FOR FIBROUS FILTER MATS

Filter Mat	DOP Aerosol Diameter μ	α_R * V_L range of 7.2 - 141 cm/sec	α_D * V_L range of 7.2 - 141 cm/sec	α_I *
Type 5	0.26	0.034 - 0.670	0.726 - 0.100	0.641
	0.28	0.035 - 0.686	0.533 - 0.073	0.706
	0.30	0.046 - 0.904	0.503 - 0.069	0.822
	0.32	0.097 - 1.902	1.137 - 0.156	0.623
N11	0.26	0.228 - 4.470	2.917 - 0.402	6.784
	0.28	0.379 - 7.419	0.669 - 0.092	8.718
	0.30	1.377 - 26.946	5.937 - 0.816	4.002
	0.32			
N13	0.26	0.162 - 3.173	0.610 - 0.084	6.292
	0.28	0.624 - 12.225	2.747 - 0.378	5.022
	0.30	0.838 - 16.418	2.868 - 0.395	4.696
	0.32	1.378 - 26.993	2.077 - 0.286	5.514
N15	0.26	0.143 - 2.806	3.140 - 0.432	7.305
	0.28	0.399 - 7.804	5.828 - 0.802	6.322
	0.30			
	0.32			
Esparto	0.26	0.056 - 1.104	0.562 - 0.077	0.608
	0.28	0.071 - 1.391	0.462 - 0.064	0.736
	0.30	0.092 - 1.811	0.777 - 0.108	0.414
	0.32	0.184 - 3.599	1.004 - 0.139	0.347
Visc 1.5D	0.26			
	0.28			
	0.30	0.006 - 0.123	0.243 - 0.033	0.055
	0.32	0.008 - 0.154	0.233 - 0.032	0.085
Visc 3.0D	0.26			
	0.28	0.013 - 0.260	0.143 - 0.020	0
	0.30	0.007 - 0.146	0.233 - 0.033	0
	0.32	0.017 - 0.341	0.021 - 0.003	0.031
A	0.26	0.037 - 0.715	0.995 - 0.137	1.929
	0.28	0.053 - 1.037	1.433 - 0.197	2.011
	0.30	0.140 - 2.742	2.459 - 0.338	1.345
	0.32	0.225 - 4.401	3.304 - 0.454	1.464
AA	0.26	0.114 - 2.240	3.828 - 0.527	5.475
	0.28	0.196 - 3.848	4.152 - 0.572	5.631
	0.30	0.406 - 7.962	3.538 - 0.487	6.875
	0.32			
AAA	0.26	0.103 - 2.009	3.042 - 0.419	5.488
	0.28	0.188 - 3.691	4.303 - 0.592	5.017
	0.30	0.207 - 4.064	1.304 - 0.179	8.449
	0.32			

*α_R calc. from Equation (13); α_D calc. from Equation (14); α_I calc. from Equation (15).

LITERATURE CITED

R. E. Collins, Flow of Fluids through Porous Materials, Reinhold, New York, New York, 1961, pp 10-11.

R. G. Dorman, Aerodynamic Capture of Particles, Permagon Press, Oxford, 1960 a.

R. G. Dorman, Air Water Pollution, 3, 112 (1960 b).

R. G. Dorman, Aerosol Science, Academic Press, New York, New York, 1966.

N. A. Fuchs, The Mechanics of Aerosols, Permagon Press, Macmillan, New York, 1964.

H. L. Green, and W. R. Lane, Particulate Clouds: Dusts, Smokes and Mists, E.&F.N. SPON LTD, London, 1957, pp 65-69.

L. A. Jonas, C. M. Lochboehler, W. S. Magee, Environ. Sci. Technol., 6, 821-6 (1972).

W. S. Magee, Jr., L. A. Jonas, W. L. Anderson, Environ. Sci. Technol., 7, 1131-5 (1973).

Figure 1. DOP PENETRATION AS A FUNCTION OF LINEAR FLOW VELOCITY FOR VARIOUS FILTER MATS

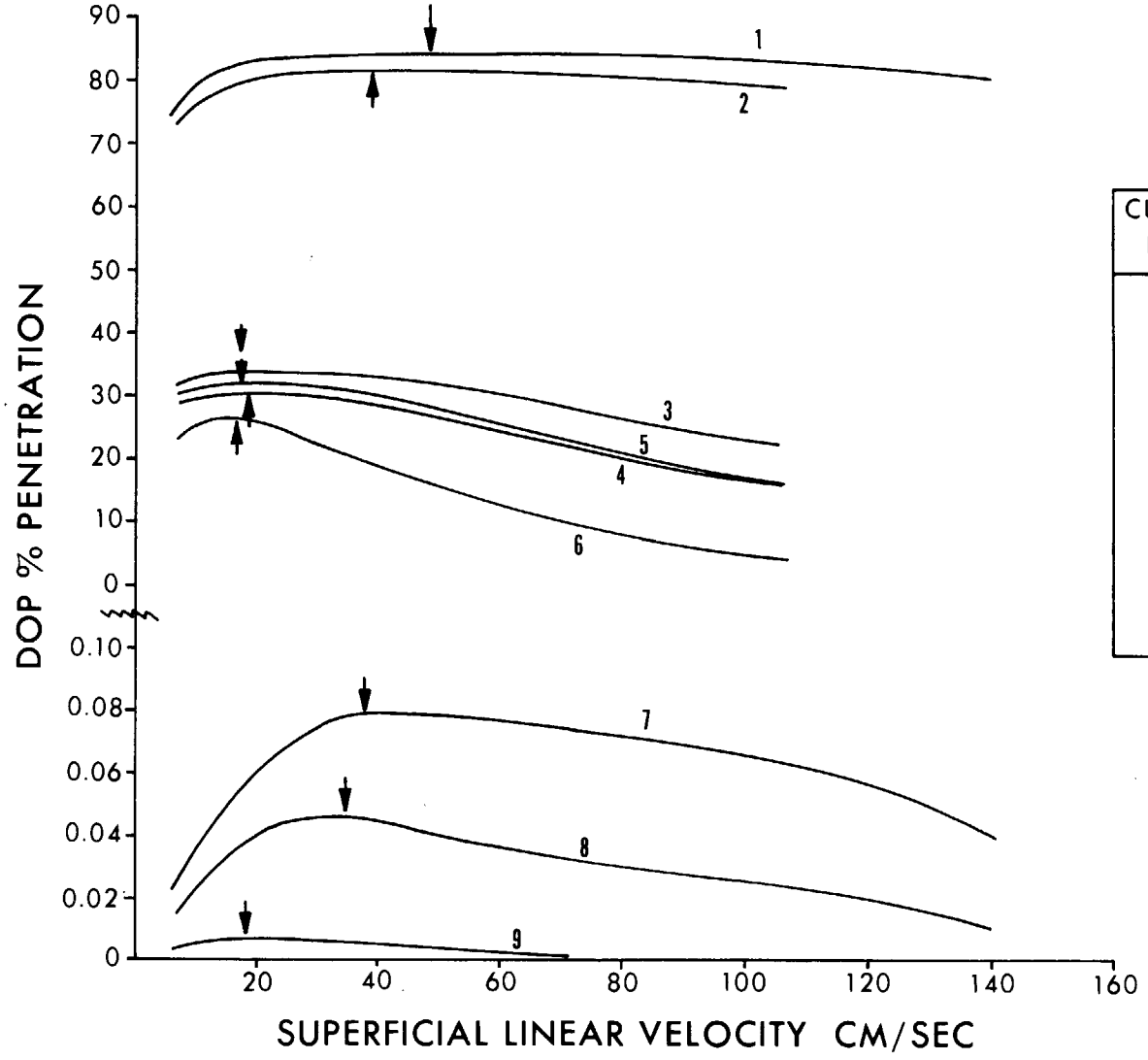

CURVE NO.	FIBER MAT.	AEROSOL DIAM
1	V 1.5	0.30
2	V 1.5	0.32
3	ESP	0.26
4	ESP	0.28
5	ESP	0.30
6	ESP	0.32
7	AAA	0.26
8	AAA	0.28
9	AAA	0.30

Figure 2. DOP PENETRATION AS A FUNCTION OF LINEAR FLOW VELOCITY FOR VARIOUS FILTER MATS

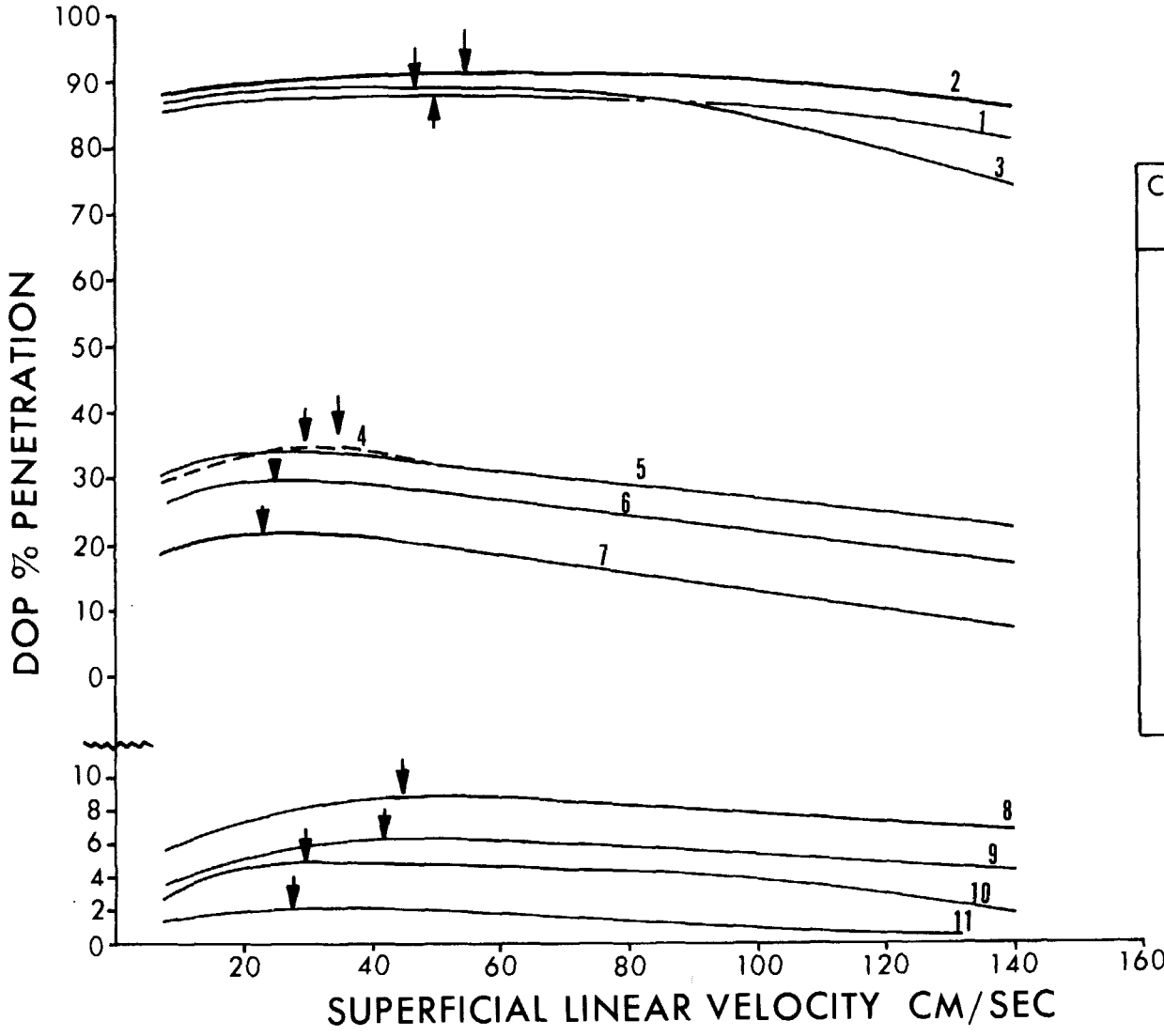

CURVE NO.	FIBER MAT.	AEROSOL DIAM.
1	V 3.0	0.28
2	V 3.0	0.30
3	V 3.0	0.32
4	TYPE 5	0.26
5	TYPE 5	0.28
6	TYPE 5	0.30
7	TYPE 5	0.32
8	A	0.26
9	A	0.28
10	A	0.30
11	A	0.32

Figure 3. DOP PENETRATION AS A FUNCTION OF LINEAR FLOW VELOCITY FOR VARIOUS FILTER MATS

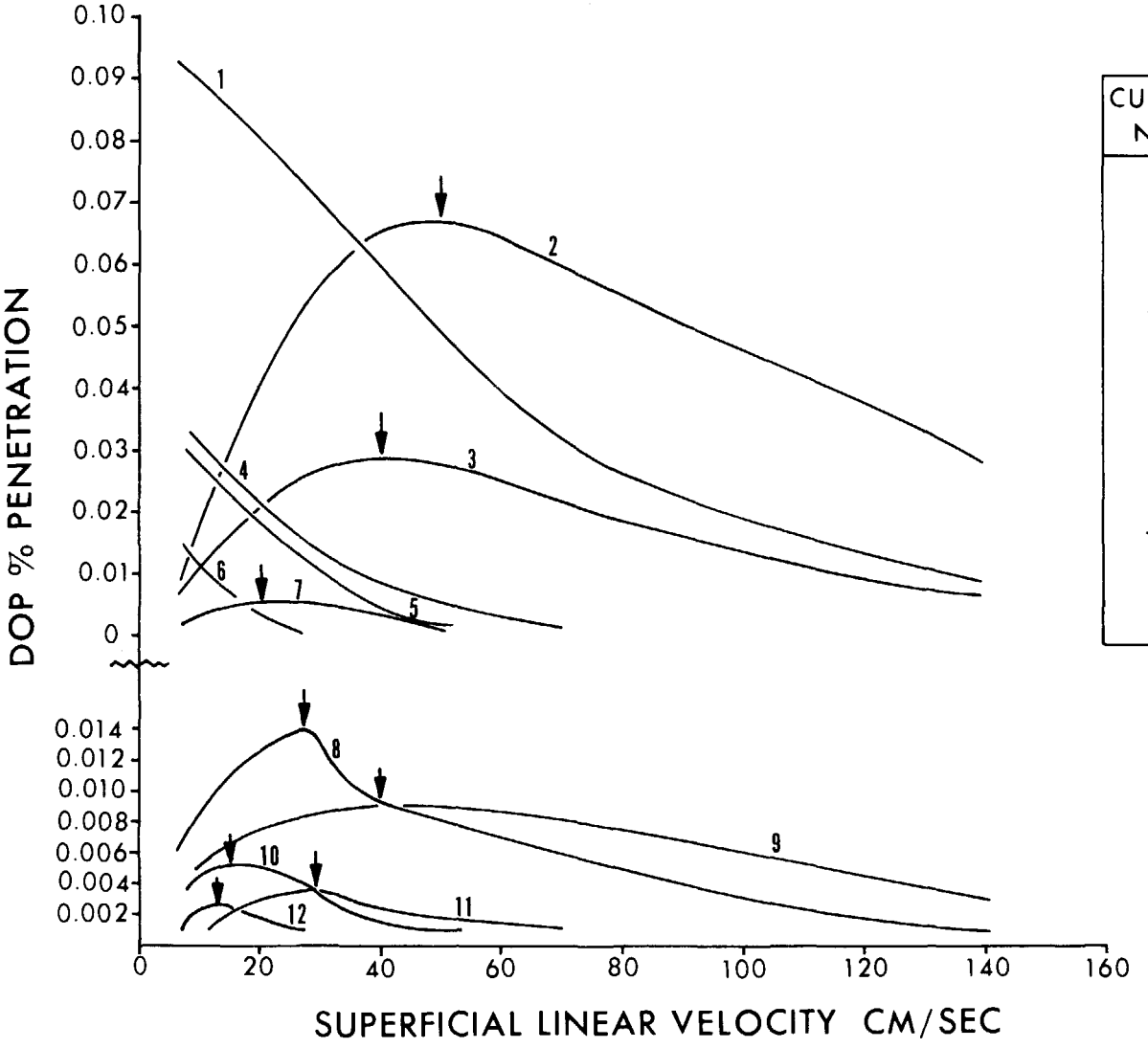

CURVE NO.	FIBER MAT.	AEROSOL DIAM
1	N13	0.26
2	AA	0.26
3	AA	0.28
4	N13	0.28
5	N13	0.30
6	N13	0.32
7	AA	0.30
8	N11	0.26
9	N15	0.26
10	N11	0.28
11	N15	0.28
12	N11	0.30

DISCUSSION

FIRST: I was wondering what the reliability of your particle measurement was in this series of experiments. The numbers are quite specifically defined in your tables. Are we to understand that these are absolute values, that there is no standard deviation around the mean, so to speak? Or are these absolutely uniform particle dispersions? In other words, is part of the unevenness of your coefficients related in some way to an uncertainty in the measurement of particle size?

JONAS: The experimental data on DOP were obtained from Mr. Anderson's work at the Naval Research Lab. For that, the liquid is vaporized and condenses in aerosol form due to temperature differential. The apparatus is equipped to measure the size of the aerosol particles with an OWL, which is based on the forward angle scattering of light. I don't have at hand the actual value of the geometric standard deviation. However, I believe that the distribution was quite sharply peaked.

DORMAN: I would like to congratulate Dr. Jonas and his co-workers for carrying the equations much farther than I did myself. I would like to ask him, following what Dr. First has said, whether there is any intention of going to smaller and larger sizes of particles? I know that the experimental effort would be very large, but it would be interesting to work from about 0.1 micron up to 1.0 micron. I have always felt that results would then help to elucidate the three mechanisms of capture, and to relate them all to fiber radius and packing density.

JONAS: We have no immediate plans for additional experimental work. What we are going through and reporting now is work that was done a few years ago, and, it represents very careful experimentation over these four particle sizes. However, there are additional experimental data for us to delve into, and we hope to continue the series and blend in more of the Fuchs equations in terms of the physical properties of filter mats. In our part four paper, we feel that we are just about at the point where we can calculate all of the parameters just from the physical properties of the filter mat. That paper is nearing completion and what we now have, at least in the initial draft form, is the Dorman parameters completely calculated without regard to experimental data.

HIGH TEMPERATURE AEROSOL FILTRATION BY DIFFUSION*

James P. Kornberg
Dartmouth Medical School
Hanover, New Hampshire

and

Melvin W. First
Harvard School of Public Health
665 Huntington Avenue
Boston, Massachusetts 02115

Abstract

Recent technological developments, such as the use of liquid metals to cool the forthcoming generation of breeder reactors, have created a need to examine whether diffusional filter theory adequately describes collection at high temperatures (500-1000°K) where both gas viscosity and the efficiency of deposition by diffusion increases. Three filters, each composed of monodisperse fibers with diameters of 4μm, 8μm, and 12μm were tested with spherical NaCl particles ranging in size from 0.022μm to 0.178μm at filter face velocities of 6.0, 11.6, and 20 cm/sec and at filter temperatures of 357°K, 561°K, and 711°K. Initial experiments were conducted to investigate the pressure drop characteristics of the test filters and to compare measured results with flow theory. For all values of filter solidity examined, measured pressure drop was lower than that predicted by all three theoretical flow models. Statistical examination of the data collected from the high temperature filtration experiments (97 paired values of single fiber efficiency, η_s, and Peclet number) led to the experimental relationship: $\eta_s \alpha Pe^{-0.467}$, which is in statistical disagreement with the theoretical relationship: $\eta_s \alpha Pe^{-0.667}$. A computer aided, multiple regression analysis, examining the dependence of single fiber efficiency upon temperature, fiber diameter, particle diameter and filter inlet velocity, identified fiber diameter as a variable responsible for part of the differences observed between theory and experiment. The conclusion was reached, therefore, that discrepancies between theory and experiment were caused, at least in part, by particle counting errors and difficulties encountered with the 12μm filter experiments. The observation that the experimental regression exponent of temperature is not in disagreement with that predicted by theory supports the conclusion that current diffusional filtration theory can be used to predict filter efficiencies at high temperatures.

---

*The research reported in this paper was supported by the U.S. Atomic Energy Commission (under Contract AT-(11-1) #3049) and by the General Electric Foundation.

I. Introduction

Important efforts have been made in the past few years, both in theory (1,2,3,6,7,20) and experiment (12,13,14,37), toward understanding diffusional collection of submicron aerosol particles at ambient temperatures. Recent technological developments, such as the use of liquid metals to cool the forthcoming generation of breeder reactors, have created the need to examine whether diffusional filter theory adequately describes collection at high temperatures (500-1000°k) where both gas viscosity and the efficiency of deposition by diffusion increases.

Past filtration studies[24,26-30] at high temperature have involved collection mechanisms in addition to diffusion and have used filters with non-uniform fiber sizes. The present high temperature filtration experiments, using a polydisperse NaCl aerosol and monodisperse fiber diameter filters, were conducted to investigate diffusional collection efficiency for values of Peclet number ranging from 18 to 5400 ($Pe = d_f U/D$, where d_f = fiber diameter; U = flow velocity; D = particle diffusion coefficient). Three filters, each composed of monodisperse fibers with diameters of 4μm, 8μm, and 12μm were tested with spherical NaCl particles ranging in size from 0.022μm to 0.178μm at filter face velocities of 6.0, 11.6, and 20 cm/sec and at filter temperatures of 357°K, 561°K, and 711°K. Experimental results were compared with the collection theory of Fuchs and Stechkina (1963)[32] [as originated by Friedlander (1957)[6] and Natanson (1957)[7]] and with the flow models of Spielman and Goren (1968)[1], Happel (1959)[3] and Kuwabara (1959)[2]. The high temperatures employed during these experiments required the development of appropriate methods of aerosol sampling and generation and provided an opportunity to test a new high temperature filtration material and filter holder design.

II. Theoretical Considerations

A. The Flow Field

The three theoretical flow fields which were examined [Spielman and Goren (1968)[1], Kuwabara (1959)[2], and Happel (1959)[3]] can be used to describe completely both the pressure drop characteristics of high porosity (> 0.9) filter media and, along with diffusional collection theory, the collection efficiency of a single fiber.

The Spielman and Goren flow field is structured upon the flow model of H.C. Brinkman[4], which accounts for the flow interference of neighboring fibers upon one another by including a damping term in the equation of motion of the flow. The advantages of this model over alternate flow models, as pointed out by Spielman and Goren (1, p. 280), are its application to:

i). non-monodisperse fibers.
ii). fibers with variable orientation with respect to fluid flow.
iii). mixtures of particles with different geometries.

In addition, predictions of filter pressure drop, based upon this flow model, are in better agreement than other flow models with pressure drops measured by experiment[1, 20].

The Brinkman model (and the Spielman and Goren elaboration of it) does not apply under the following circumstances:

i). At values of filter solidity, α (α = overall filter density/fiber density), >.1 to .2
The effects of large numbers of solid boundaries in immediate proximity of the fiber under investigation cannot be described by the simple damping coefficient found in Brinkman's equation of motion.

ii). At high filter velocity. Particle inertial effects become important and Darcy's Law (EQ. 3) no longer applies to the far field flow.

iii). In extremely porous media. Fibers act totally independently of one another. Under these circumstances, filter resistance increases with increasing fiber Reynolds number, Re, (where $Re = d_f U \rho/\hat{\eta}$, ρ = gas density; $\hat{\eta}$ = gas viscosity) and Lamb's[5] Reynolds number-dependent flow model should be used instead to describe the flow.

The flow models of Happel and Kuwabara are based upon a fluid cell concept. Kuwabara's cell model rests upon the assumption that fluid vorticity vanishes on the boundary between adjacent cells. Happel's model assumes that fluid shearing forces disappear on the same boundary. These cell models also take into account the spacing between fibers, but they do not provide a smooth transition in the flow fields between neighboring cells. They also break down under the same general circumstances outlined for the Brinkman model.

B. Filter Resistivity

Spielman and Goren solved Brinkman's equation of motion and the continuity equation ($\nabla \cdot U = 0$); and after demonstrating that pressure, P, obeys Laplace's equation ($\nabla^2 P = 0$), they derived a general expression for the total drag per unit length (F_D) on filter fibers oriented with their axes normal to flow in the filter. When no slip flow occurs at the fiber surface, the general expression reduces to:

$$F_D = 4\pi\hat{\eta}U \left[\frac{kd_f^2}{8} + \frac{k^{1/2}d_f K_1\left(\frac{k^{1/2}d_f}{2}\right)}{2K_0\left(\frac{k^{1/2}d_f}{2}\right)} \right] \qquad (1)$$

where: k = Darcy resistance coefficient or damping coefficient[4] (cm^{-2}) (See EQ. 3)
$K_0()$ = 0^{th} order modified Bessel function of the second kind
$K_1()$ = 1^{st} order modified Bessel function of the second kind

To determine the total pressure drop in the direction of flow when all fibers lie with their axes normal to the flow, F_D is multiplied by the total length of fiber per unit volume in the filter,

which equals $4\alpha/\pi d_f^2$.

Thus: $-dP/dL = 4F_D\alpha/\pi d_f^2$ where: dL = differential length of filter thickness (2)

From Darcy's Law: $-dP/dL = \hat{\eta}kU$ (3)

Substituting EQ. (3) into EQ. (2):

$$\frac{kd_f^2}{4} = F_D\alpha/\pi\hat{\eta}U = \Delta Pd_f^2/4L\hat{\eta}U \quad (4)$$

where: L = total filter thickness
ΔP = total pressure drop across the filter

Equating EQs. (4) and (1), it follows that:

$$\frac{kd_f^2}{4} = 4\alpha\left[\frac{kd_f^2}{8} + \frac{k^{1/2}d_fK_1(\frac{k^{1/2}d_f}{2})}{2K_0(\frac{k^{1/2}d_f}{2})}\right] \quad (5)$$

Now, let: $\frac{kd_f^2}{4} = \lambda^2$ (6)

Substituting EQ. (6) into EQ. (5), one finds that:

$$\lambda^2 = 4\alpha\left[\frac{\lambda^2}{2} + \frac{\lambda K_1(\lambda)}{K_0(\lambda)}\right] \quad (7)$$

λ^2 is called filter resistivity, and it can be evaluated experimentally by determining the measurable filter parameters in EQ. (4). By selecting values of λ, one can solve EQ. (7) for the corresponding value of α and can plot the theoretical λ^2 versus α. (See Figure 2).

For the Spielman and Goren model, F_D can be predicted using EQs. (4), (6), and (7).

$$F_D = 4\pi\hat{\eta}U\left[\frac{\lambda^2}{2} + \frac{\lambda K_1(\lambda)}{K_0(\lambda)}\right] \quad (8)$$

Expressions similar to EQ. (8) can be derived for Happel and Kuwabara. Namely:

Kuwabara: $F_D = 4\pi\hat{\eta}U(-.5\ln\alpha - .75 + \alpha - \frac{\alpha^2}{4})^{-1}$ (9)

Happel: $F_D = 4\pi\hat{\eta}U(-.5\ln\alpha - .5 + \frac{\alpha^2}{(1+\alpha^2)})^{-1}$ (10)

Since the definition of filter resistivity given in EQ. (6) applies, by using EQs. (9) and (10) with EQ. (4), graphs of resistivity versus solidity can be established for both models. (See Figure 2).

C. Diffusional Single Fiber Efficiency

For typical porosities (< 0.9) in a filter geometry in which all fiber axes are normal to the flow, Fuchs and Stechkina[32], and later Spielman and Goren[1], described the velocity profile around a fiber by the following stream function, Ψ, in polar coordinates (r, θ) with respect to the fiber axis as:

$$\Psi = \frac{Ud_f}{2\xi}\left(\frac{2r}{d_f} - 1\right)^2 \sin\theta \tag{11}$$

where ξ is a flow model parameter which has the following values:

Spielman and Goren: $$\xi = \frac{K_0(\lambda)}{\lambda K_1(\lambda)} \tag{12}$$

Happel: $$\xi = -0.5\ \ln\alpha - 0.5 + \frac{\alpha^2}{2(1+\alpha^2)} \tag{13}$$

Kuwabara: $$\xi = -0.5\ \ln\alpha - 0.75 + \alpha - \frac{\alpha^2}{4} \tag{14}$$

Initially derived by Langmuir[25], the equation for diffusional single fiber efficiency, η_s, was later modified by Friedlander[6] and by Natanson[7]. Fuchs and Stechkina[32] improved the work of Friedlander and Natanson by removing, from η_s, the influence of Reynolds number (which can correctly be applied only to predicting capture efficiency of an isolated cylinder) and replacing it with dependence upon ξ (strictly a function of filter solidity) which, in current theory, correctly describes the flow through filters [through EQ. (11)]. Fuchs and Stechkina gave the following theoretical expression for diffusional single fiber efficiency for Pe>10.

$$\eta_s = 2.9\xi^{-1/3}Pe^{-2/3} \tag{15}$$

The introduction of EQs. (12), (13), and (14) into EQ. (15) provides the three separate theoretical models with which experimental results were correlated.

The dependence of η_s, in EQ. (15), upon changes in temperature occurs through the Peclet number where:

$$Pe = Ud_f/D \tag{16}$$

Now:

$$D = C_c k_0 T/(3\pi\hat{\eta}d_p) \tag{17}$$

where: k_0 = Boltzmann constant
T = absolute temperature (°K)
C_c = Cunningham slip correction factor (dependent upon particle diameter and gas mean free path, λ', which in turn, is dependent upon T)

Using the exponential form of the Cunningham Correction factor[34] ($C_c = 1 - A\lambda'/d_p + B\lambda'/d_p(\exp(-C\ d_p/\lambda'))$, where A, B and C are constants) the introduction of EQs. (16), (17), and (18) into EQ. (15) shows the dependence of η_s on primary variables:

$$\eta_s = (\text{constant})\ T^{1.0}d_f^{-0.667}d_p^{-1.333}U^{-0.667} \tag{15a}$$

III. Experimentation

A. Filter Resistivity

Experimental filters consisted of three monodisperse, stainless steel (type 347) fiber* mats with diameters of 4μm, 8μm, and 12μm. They were mounted in the high temperature filter holder, shown in Figure 1. The filter was placed in the upstream half of the holder and clamped between stainless steel screens with the edges seated against an asbestos seal that prevented gas from entering the filter in a direction other than along the axis of the duct. The filter thickness was adjustable in 5mm increments over a range from 4mm to 104mm.

Experiments were conducted to characterize the resistivity of the filter media. At fixed values of filter inlet velocity and fiber diameter, pressure drop was measured at different values of overall filter solidity, and resistivity was calculated from EQ. (4). Resistivity measurements for the three filter fiber diameters examined are shown in Figure 2, with theoretical values of resistivity predicted from each of the three flow models mentioned in Section II. It may be seen that Spielman and Goren's theoretical line from EQ. (7) demonstrates closest agreement with experimental results. These measurements of resistivity at low solidities (0.003 - 0.012) support results obtained by others[8,9,10] at higher solidities (0.03 - 0.08) that show measured resistivity to be consistently less than predicted resistivity.

Fundamental to the use of the velocity independent flow models of Spielman and Goren, Happel, and Kuwabara is the assumption that the interaction of the flow fields about neighboring fibers prevents the fibers from acting totally independently of one another and that there should be, therefore, a range of fiber Reynolds number over which resistivity is constant. Filter resistivity was measured over a range of fiber Reynolds numbers between 0.02 and 0.30 for the 4μm, 8μm, and 12μm fiber filters at an overall solidity of 0.0057.

The data shown in Figure 3 indicate a range of fiber Reynolds number extending to about 0.2 over which filter resistivity remains essentially constant for all three filter types. This result indicates that it is appropriate to use the three flow models described in Section IIB to predict resistivity for values of Re <0.2. In addition, since resistivity is independent of Re for Re <0.2, the experimental curves given in Figure 2 are accurate for all values of Re <0.2, not just for those at which they were determined.

B. High Temperature Filtration by Diffusion

1. Experimental Apparatus

The equipment used for these experiments is shown schematically

*Brunsmet metal fibers ®: Technical Products Division, Brunswick Corporation, 69 W. Washington Street, Chicago, Illinois

FIGURE 1. HIGH TEMPERATURE FILTER HOLDER.

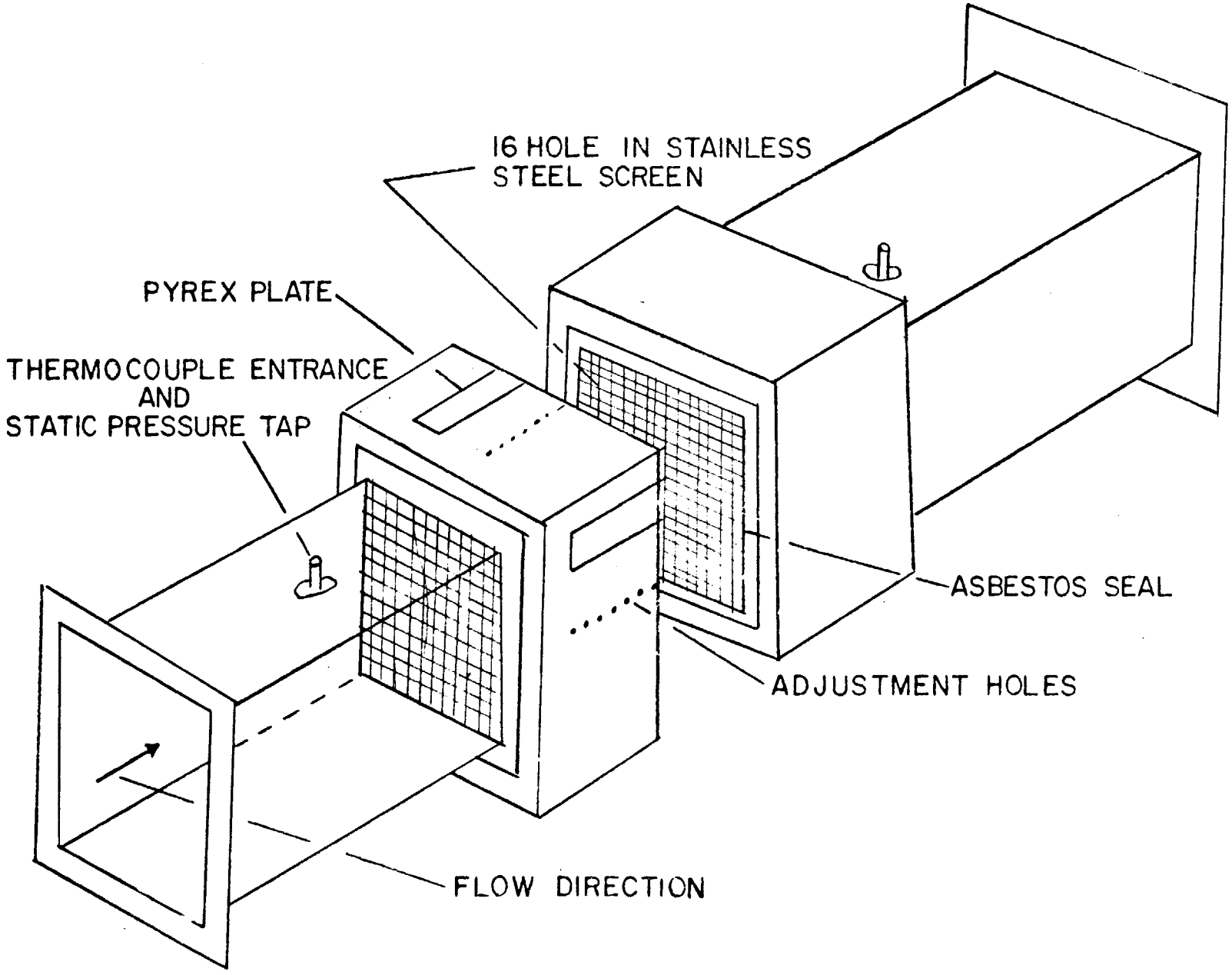

FIGURE 2. RESISTIVITY VERSUS SOLIDITY
THEORY AND EXPERIMENT

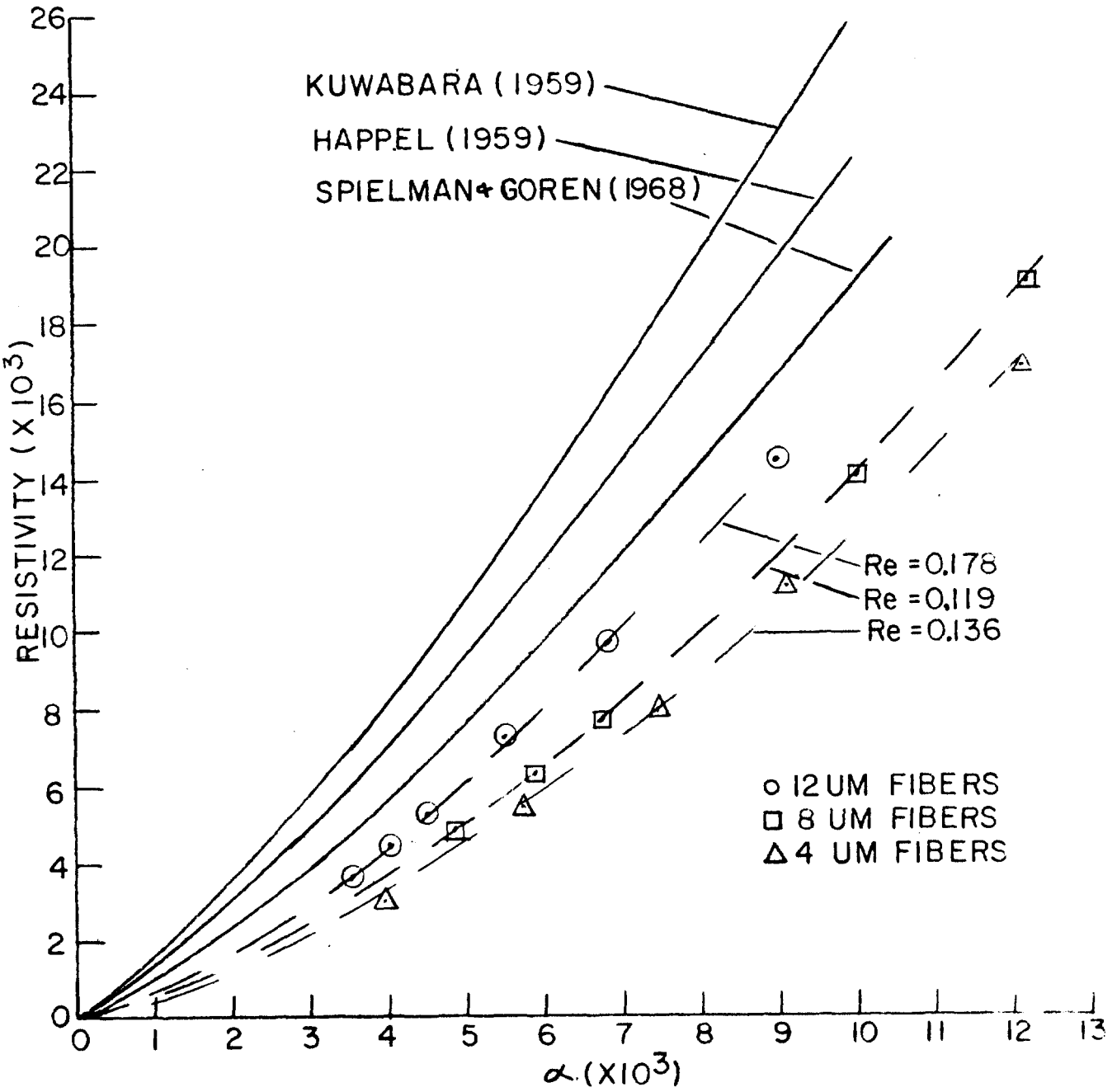

FIGURE 3. RESISTIVITY VERSUS Re (α=0.0057)

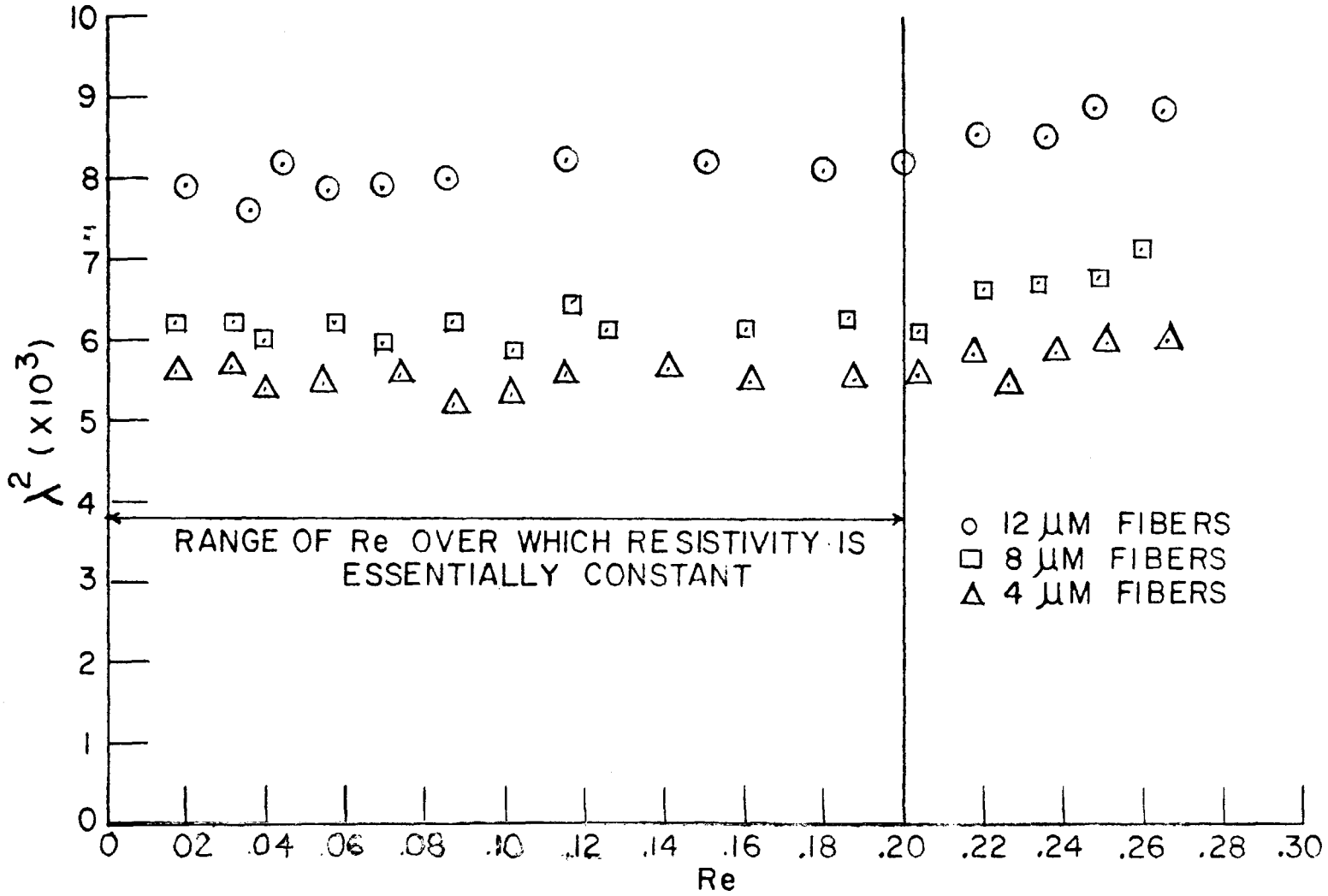

in Figure 4. A commercially available metalizing gun* was used to vaporize (in an oxygen-acetylene flame) finely ground sodium chloride crystals which formed a submicron aerosol upon cooling. The position of the gun with respect to the entrance to the duct helped to control the temperature of the aerosol entering the filter. Additional temperature control was obtained by employing one or two auxiliary oxygen-acetylene torches to heat the air from the sides of the entrance duct.

Particles in the test aerosol ranged in size from 0.022 to 0.178 microns in diameter. An impaction plate at the entrance to the test tunnel removed large salt particles released by the aerosol generator. About two meters downstream from the duct entrance, a probe guided a representative aerosol sample into a point-to-plane electrostatic precipitator.[35] Located slightly downstream, a second probe, connected to a peristaltic pump, sent a continuous aerosol sample to a differential flame photometer which was calibrated to indicate the mass concentration of NaCl in the duct.

Calculation of the vapor pressure of NaCl at 711°K (the highest temperature at which experiments were conducted) indicated that only 0.01% of the NaCl present in the test tunnel was in the vapor state.[38] Entrance ports located on both sides of the filter holder, permitted the measurement of pressure drop across the filter bed and determination of the temperature profile across the filter face. The flow through the test tunnel was maintained by a blower and measured with a calibrated brass orifice meter located downstream of the filter assembly. Gas temperature was measured at the orifice entrance so that proper temperature corrections could be made in calculating the flow rates through the orifice and the test tunnel.

2. Aerosol Sampling

The sodium chloride aerosol was sampled upstream and downstream of the filter with two point-to-plane electrostatic precipitators, at a flow rate of 0.8 liters/minute. At duct velocities between 6 and 20 cm/sec and aerosol concentrations of 1.0 mg/m^3, an appropriate sampling time for the precipitators was found to be about 5 seconds. The precipitators were switched during each experiment to overcome any bias which the devices might have had either with respect to overall collection efficiency or fractional size collection. Total particle counts at both sampling locations, therefore, included counts taken with both sampling precipitators. Particles were deposited on standard carbon-coated electron microscope grids and were examined in a Philips 200 electron microscope at a magnification of 40,000 X.

The presence of combustion water vapor in the sampled gases sometimes caused condensation to form on the electron microscope grids. To solve this problem the collection lines were wrapped in heating tape and the temperature in the vicinity of the sample was

*Model C, Wall Colmonoy spray welder unit. 19345 John R. Street, Detroit, Michigan 48203

FIGURE 4. EXPERIMENTAL ASSEMBLY.

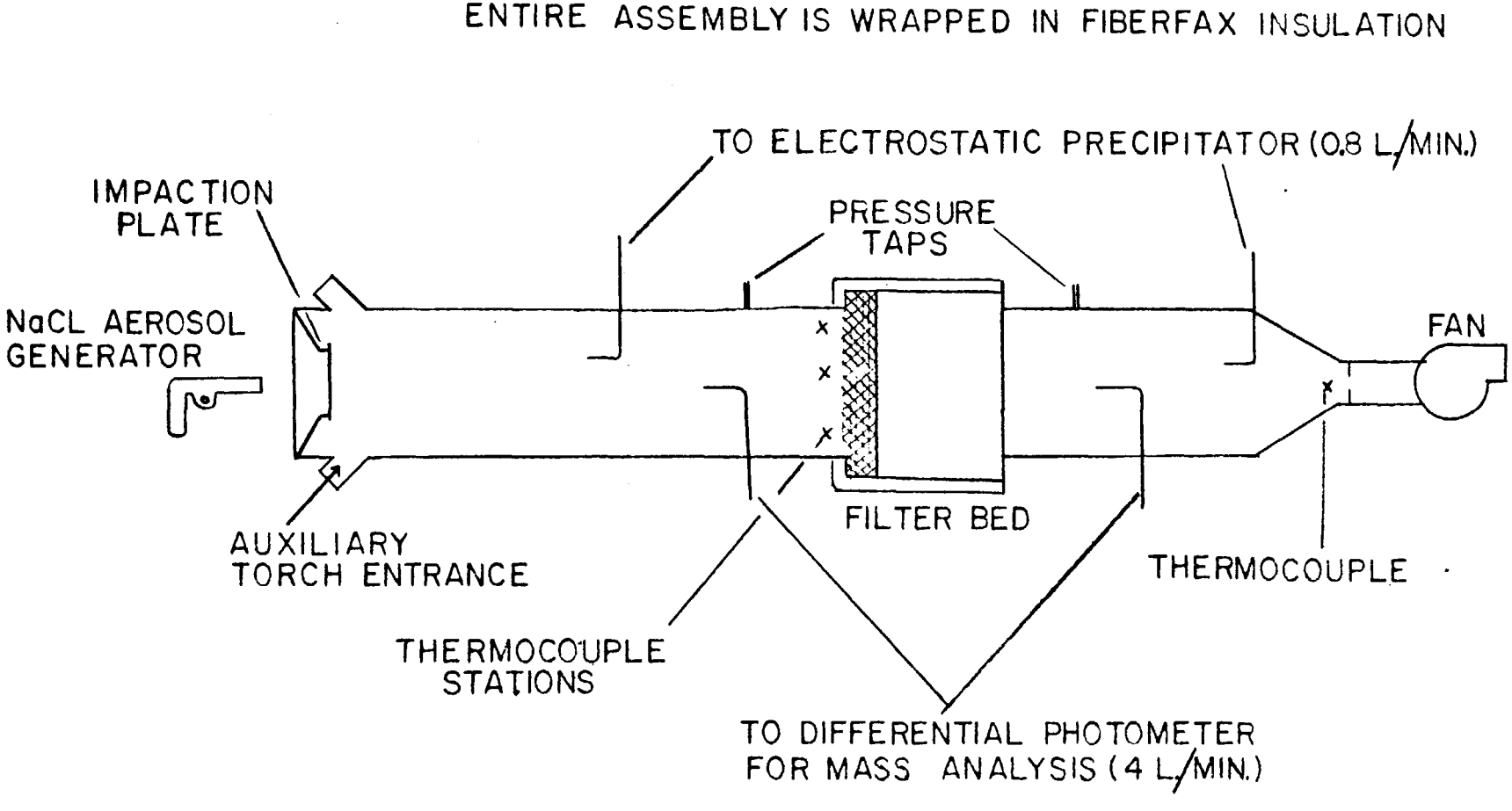

maintained at 250°F during sampling. To avoid water vapor adsorption during storage, the grids were stored in a sealed container flooded with dry nitrogen. The storage system was designed so that the samples could easily be transported from the experimental area to the electron microscope for examination without exposure to the atmosphere. For every experimental condition, at least four electrostatic precipitator samples were obtained and at least six electron micrographs were taken of each sample grid. Consequently, at least twelve upstream photographs and twelve downstream photographs were used in analyzing each experimental condition.

Magnification by the Philips 200 was usually about 40,000 X on the EM screen and about 15,000 X on the film negative which was enlarged approximately five times in the final printing process. Photographic prints were used for all upstream and downstream particle counting and sizing. From the pooled data derived from these prints, the upstream and downstream aerosols were characterized and the fractional size efficiency of each filter was determined.

A total of 418 8" x 10" electron micrographs were taken from which over 45,000 particles were counted and sized. All particle diameters usually fell within seven Porton size categories; the lowest was 0.022μm and the greatest 0.178μm. In all, 97 upstream and 97 downstream data counts were established from the EM photographs. In turn, these counts provided 97 measures of overall efficiency, which could be grouped into 17 major experimental cases in which fiber diameter, filter face velocity, and filter temperature were the major independent variables. These cases are summarized by the following experimental matrices:

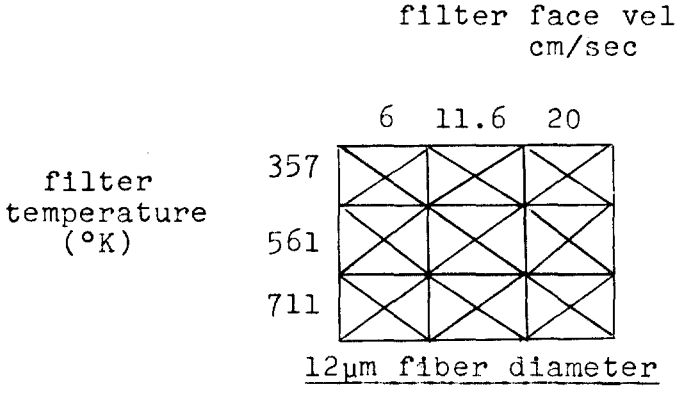

12μm fiber diameter

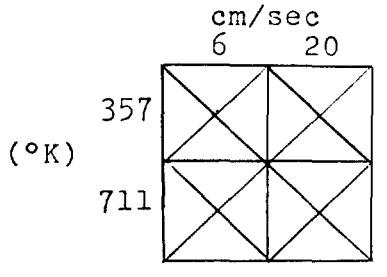

8μm fiber diameter

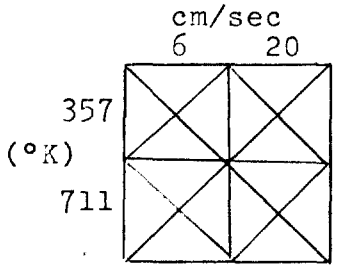

4μm fiber diameter

3. Analysis of Data

From the electron micrographs, total count efficiencies were compiled for each particle size in each of the experimental cases cited above. Loffler's[11] relationship for overall count efficiency (η_T) in terms of single fiber efficiency (η_S) was rearranged as the following equation to calculate η_S from experimentally measured values of η_T:

$$\eta_S = \frac{\pi d_f(1-\alpha)}{4\alpha L}\left[-\ln(1-\eta_T)\right] \qquad (18)$$

Experimental values of η_S and those predicted by the flow models of Spielman and Goren, Happel, and Kuwabara in combination with the collection equation of Fuchs and Stechkina are given in Figures 5-10. The theoretical models become straight lines on log-log axes as follows:

Spielman and Goren: $\log \eta_S = 0.330 - 0.667 \log Pe$ (15b)
Happel: $\log \eta_S = 0.356 - 0.667 \log Pe$ (15c)
Kuwabara: $\log \eta_S = 0.375 - 0.667 \log Pe$ (15d)

EQs. (15b-15d) were obtained by substituting a constant value of solidity, 0.0057 (maintained throughout all experiments) into EQs. (12)-(14) to obtain theoretical values of ξ and subsequently, substituting these values in EQ. (15). Figures 5-7 display the data at constant temperature and Figures 8-10 at constant fiber diameter. The entire data set is plotted with the three theoretical curves (15b)-(15d) in Figure 11.

Also shown in Figure 11 is the least squares fitted line through the experimental data. The equation of this line is:

$$\log \eta_S = -0.018 - 0.467 \log Pe \qquad (15e)$$
or: $$\eta_S = 0.96\, Pe^{-0.467} \qquad (15f)$$

The standard deviation of the residual in the regression equation, (15e), is 0.164; and the correlation coefficient is 0.847, indicating that Pe, alone, accounts for 71.2% of the variance in η_S. The 95% confidence limits for the exponent of Pe in equation (15f) are -0.407 to -0.527. On the basis of these limits, it is evident that the overall data set is not in agreement with the exponential trend predicted by theory in Equation (15) that $\eta_S \alpha Pe^{-0.667}$. Nevertheless, considering the difficulties involved with measuring diffusional collection efficiency at high temperatures, it does not appear that the observed disagreement is important enough to reject, without further analysis, the prediction of Equation (15).

As a first step to elucidate the basis for disagreement with theory, six experimental variables (T, d_f, d_p, U, Re, and Pe) were examined individually by the technique of stepwise multiple regression (by computer) to evaluate experimental variance in single fiber efficiency. The objective was to find the combination of variables which accounted for the highest percentage of the variance of η_S and which, at the same time, was associated with statistically significant regression coefficients. Computer results indicated that two

FIGURE 5. η_s VERSUS Pe (T = 356°K: d_f = 4μM, 8μM AND 12μM)

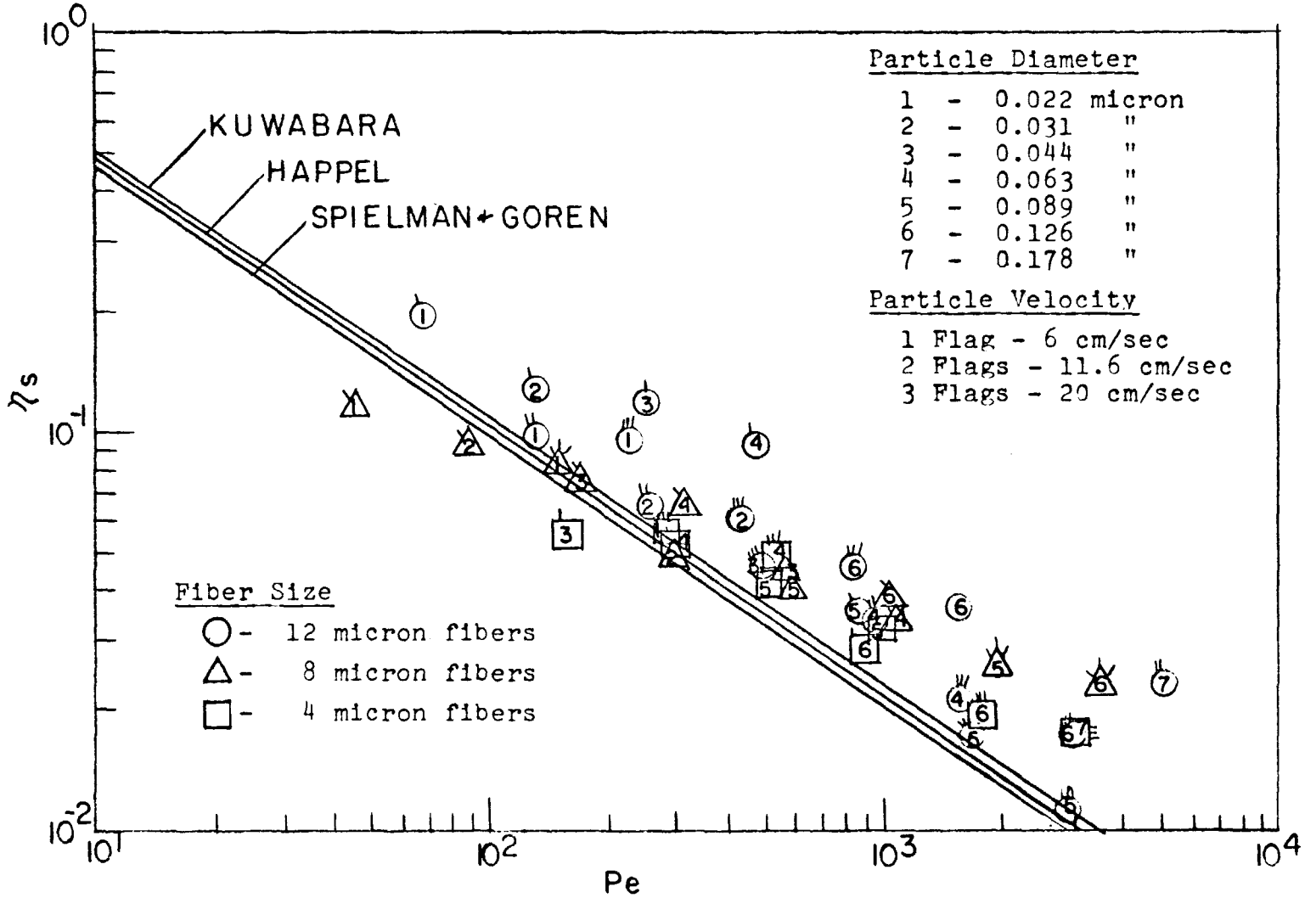

FIGURE 6. η_s VERSUS Pe ($T = 561°K$; $d_f = 12\,\mu M$)

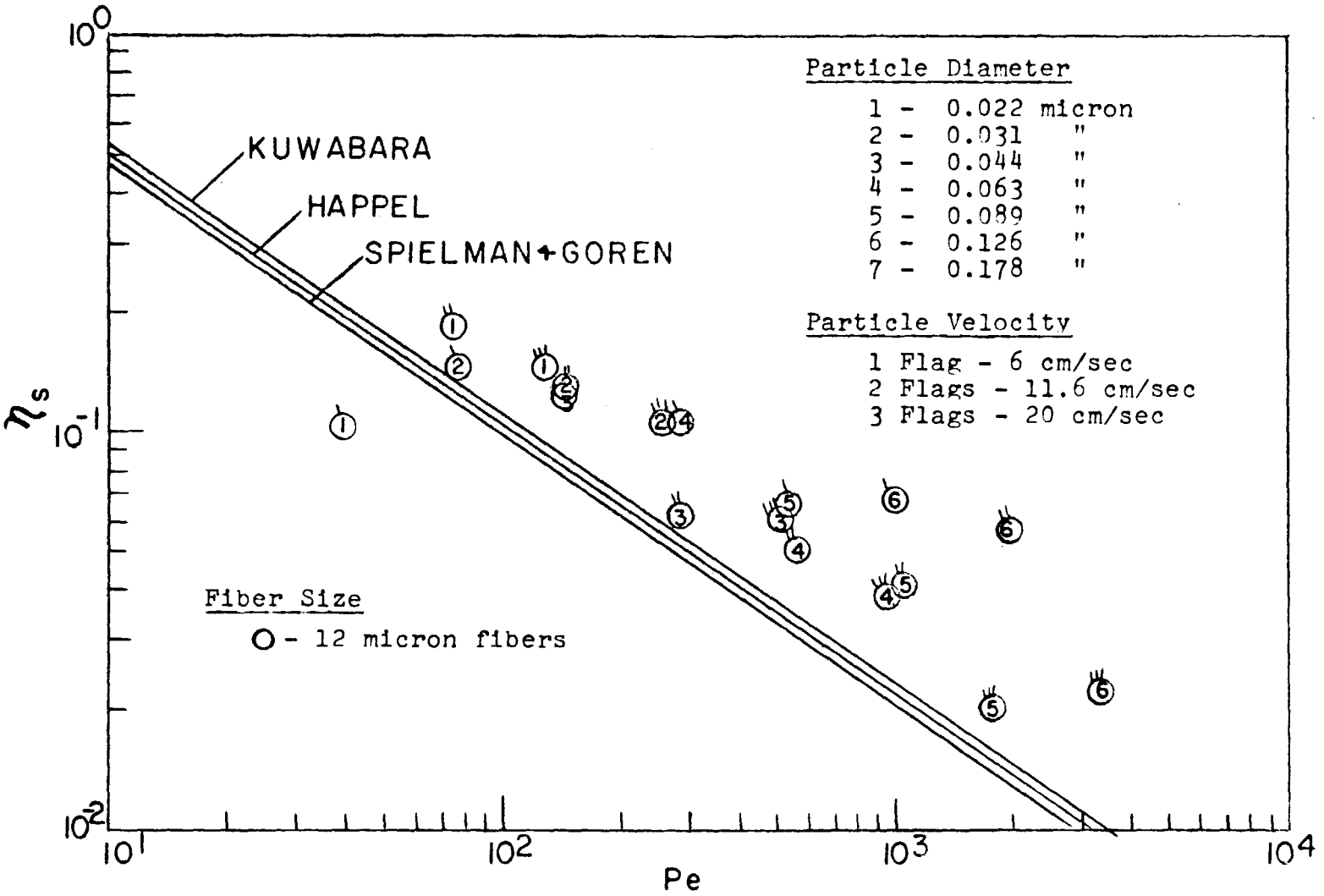

FIGURE 7. η_s VERSUS Pe (T = 711°F ; d_f = 12 μM , 8μM AND 4 μM)

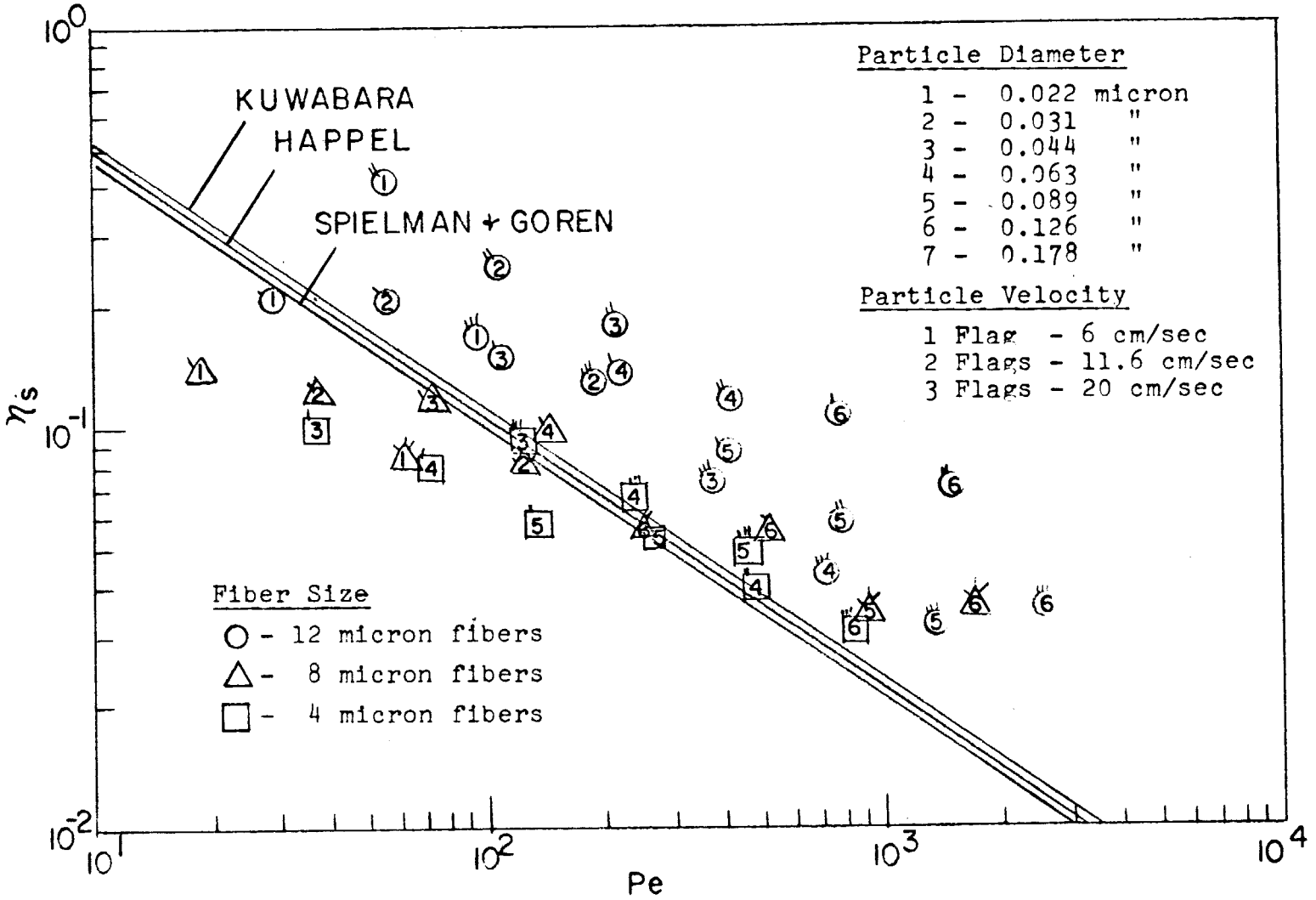

FIGURE 8. η_s VERSUS Pe ($d_f = 4\,\mu M$: T = 356°K AND 711°K)

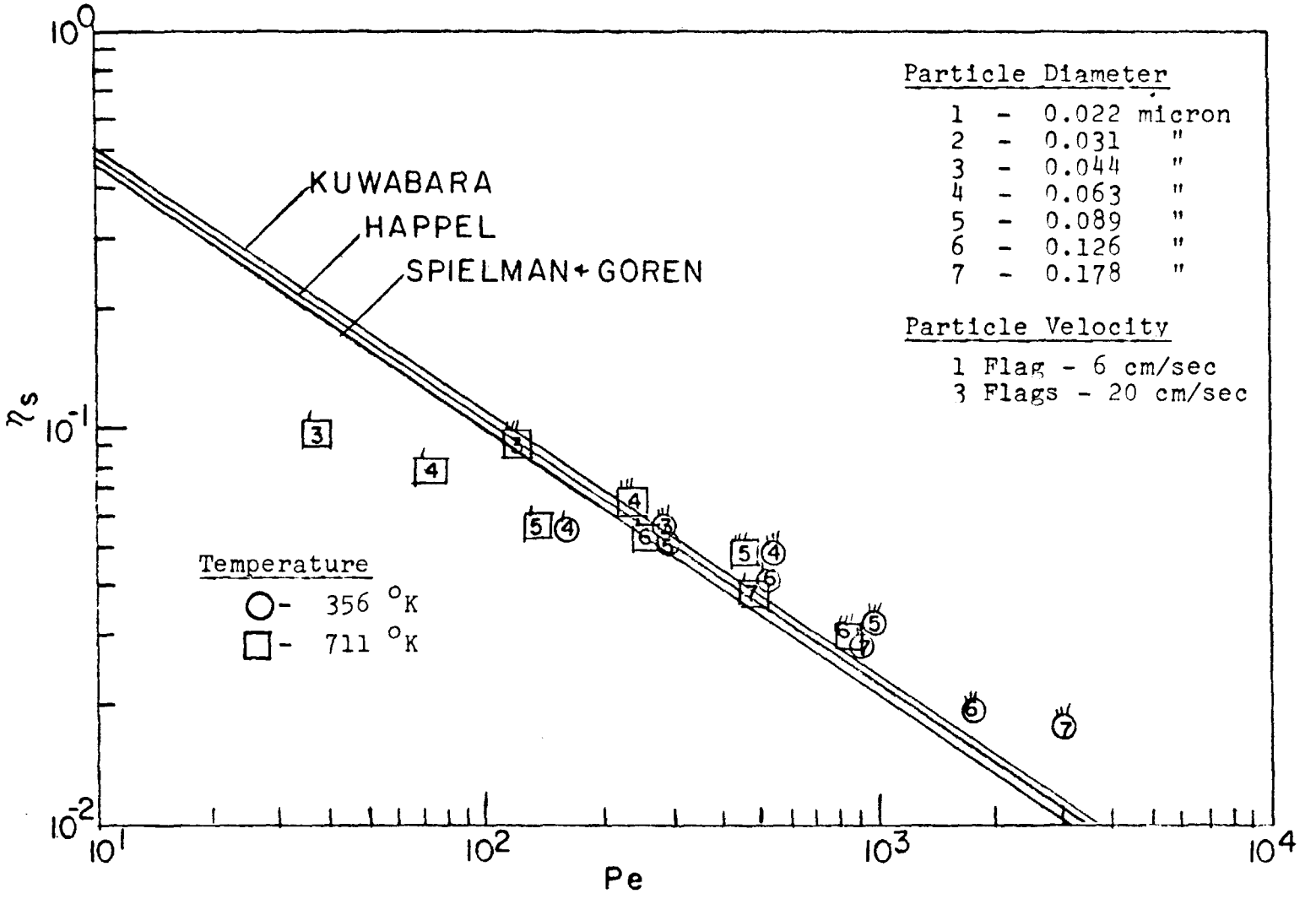

FIGURE 9. η_s VERSUS Pe (d_f = 8 μM: T = 356°K AND 711°K)

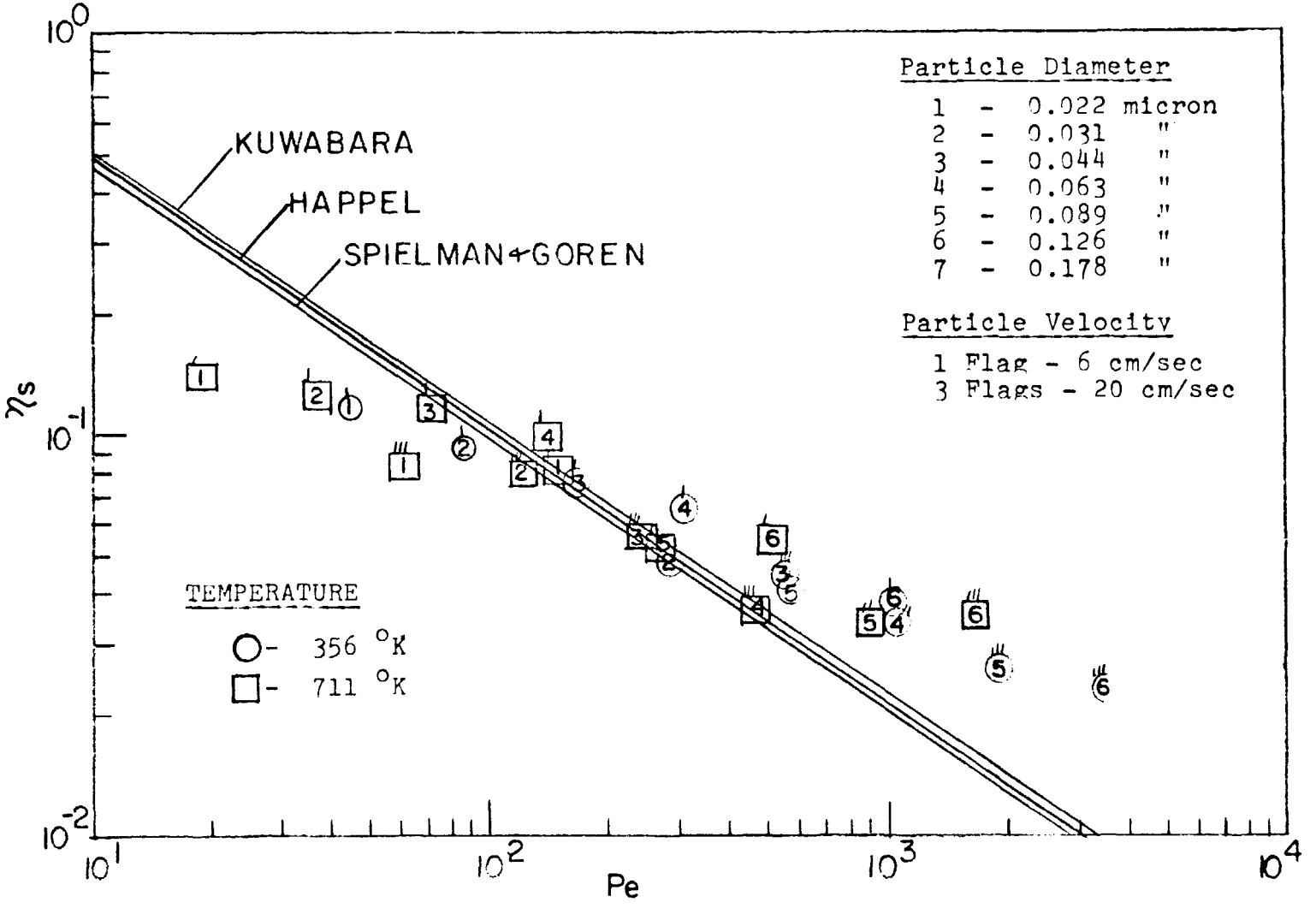

FIGURE 10. η_s VERSUS Pe (d_f = 12μM = T = 356°K, 561°K AND 711°K)

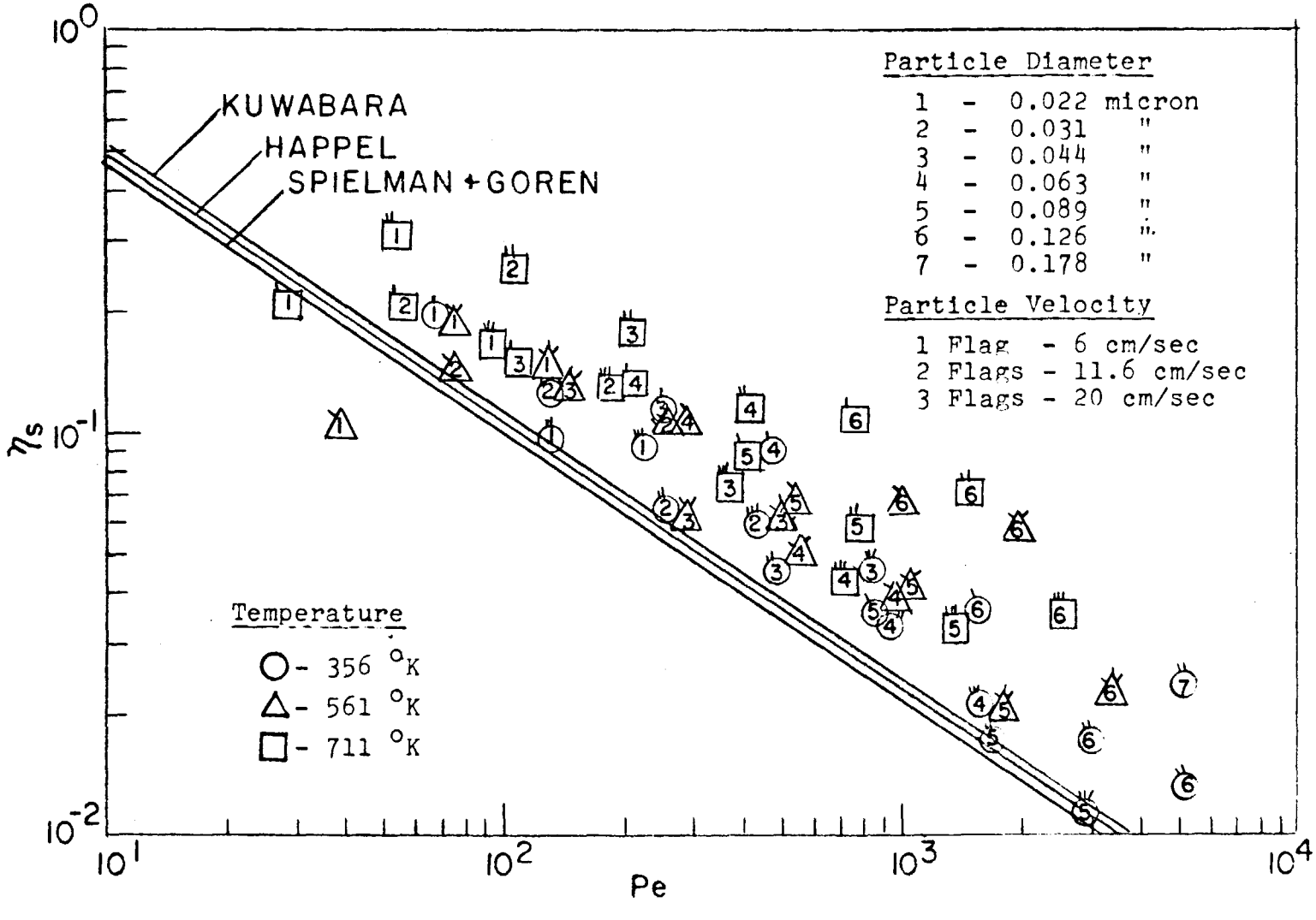

FIGURE II. ALL DATA (THEORY AND EXPERIMENT) η_s VERSUS Pe

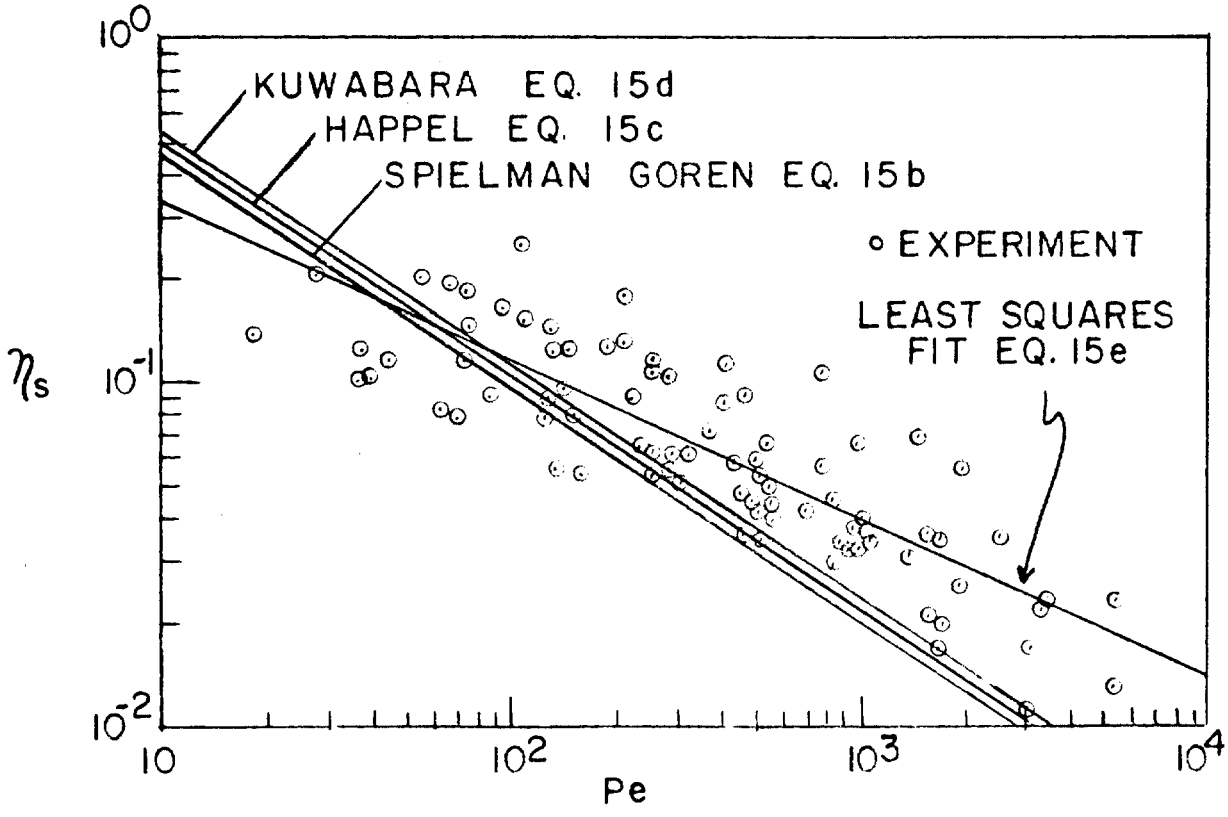

variables, Pe and d_f, met the above requirements (see Table I). Column 1 in Table I lists the variables in the order in which they were introduced into the regression analysis. Since each variable was expressed as a logarithm in the analysis, the regression coefficients ($\bar{B}$) listed in Column 2 are the exponents for the variables as they would appear in the regression equation. The values of the F statistic associated with $\bar{B}$, both of which are significant at less than the 5% level (94 degrees of freedom), are listed in Column 4. Finally, Column 5 lists the normalized regression coefficients, which reflect, in the same units, the relative strength of each variable in relation to the dependent variable.

Examination of theory (EQ. 15) shows that all independent variables influence η_s through the Peclet number. In support for collection theory, this regression analysis shows that Pe alone accounts for almost all of the variance in η_s as measured in our experiments. The appearance of fiber diameter as a separate term in the regression equation, however, indicates that this variable represents an important part of the differences between theory and experiment.

Consistent with the multiple regression equation (Table I), qualitative examination of all data plotted for different fiber diameters (Figures 8-10) indicates that the 12μm data (Figure 10) show greater disagreement with theoretical values of η_s than either the 4μm or the 8μm data.

Greater disagreement may have arisen because the 12μm filters were tested first and the experimental technique was not as well mastered as for later runs with the smaller fiber sizes. One source of error which influenced the 12μm experiments but was minimized during later work relates to the difficulty in keeping the filter mat at a uniform temperature throughout the experiment. The maintenance of thermal equilibrium in the duct system was improved during later high temperature tests by employing more thermal insulation around the filter holder and allowing longer warm-up times. The temperature differences across the filter face (measured by a thermocouple scan) averaged 5% of the filter inlet temperature during the 12μm experiments, but the deviations from the average were later reduced to 2-3%. Examining Figures 5-7, it can be seen that the 12μm data points show the most deviation from the theoretical lines. Undoubtedly, not all of the 12μm data points were influenced by this error, but increased off-axis convective flow in the duct system at the highest temperatures and enhanced diffusional deposition in hotter areas of the filter may explain the more anomalous 12μm points. In Figure 10, it may be seen that the data points obtained at temperatures closest to ambient deviate least from the theoretical line, and those at the highest temperatures deviate the most.

Having identified fiber diameter as contributing to the observed disagreement between theory and experiment, the next step in the analysis was to examine whether the individual exponent associated with each of the four basic parameters constituting Pe (i.e., T, U, d_f, and d_p) agreed with the exponent predicted by theory. Using all

Table I Multiple regression analysis.
(η_s with Pe and d_f)

(1) Independent Variable	(2) Regression Coefficient	(3) Standard Error	(4) F Value	(5) Normalized Regression Coefficient	(6) Cumulative % Variance in η_s Explained by Variables
Pe	-0.478	0.026	348.63	-0.867	71.8%
d_f	0.481	0.079	37.54	0.285	79.8%

Regression Equation: $\log \eta_s = 1.480 + 0.481 \log d_f - 0.479 \log Pe$

97 data points, in a separate regression analysis, an equation was determined for η_s that included the four experimental variables, T, U, d_p, and d_f. The results of this analysis are presented in Table II, from which it can be seen that the theoretically predicted exponents for two variables, U and T, lie within the 95% confidence limits for the exponenets in the experimental regression. The observation that the exponent of temperature from the multiple regression analysis is not in disagreement with that predicted by theory supports the conclusion that current diffusional filtration theory (EQ. 15) can be used for predicting filter efficiencies at high temperatures. Errors associated with particle counting and sizing (see Section IV, Part D) may be one reason why the regression exponent for d_p is in disagreement with that predicted by theory.

4. Comparison with Other Workers

Kirsch and Fuchs (1968)[12] conducted filtration experiments using polydisperse NaCl and dioctylsebacate particles having mean diameters ranging from 0.003 to 0.018μm. Fibers in all of their experimental filters had diameters ranging from 43 to 500μm, and solidities from 0.01 to 0.15. They reported the following relationship for their observed values of η_s:

$$\eta_s = 2.7\ Pe^{-0.667} \qquad (15g)$$

They state that EQ. (15g) is in agreement with EQ. (15), the collection model of Fuchs and Stechkina, and that their values of η_s were independent of α over the range of their data. EQ. (15g) can be rewritten:

$$\eta_s = 2.9(0.931)\ Pe^{-0.667} \qquad (15h)$$

In a term by term comparison of EQ. (15h) with EQ. (15), it can be seen that $\xi'^{-1/3} = 0.931$, and thus, $\xi' = 1.24$.

Stern, Zeller, and Schekman (1960)[13] examined the collection efficiency of an Institute of Paper Chemistry filter under reduced pressures, using monodisperse aerosols ranging in diameter from 0.026 to 1.71μm. The solidity of their filter was approximately 0.10. When their 9 data points are fitted to the form of EQ. (15), the equation with the highest correlation coefficient (0.83) is:

$$\eta_s = 2.9(2.13)\ Pe^{-0.667} \qquad (15i)$$

Paralleling the analysis with EQ. (15h), from EQ. (15i), it follows that their value of the flow parameter $\xi'' = 0.1034$.

Thomas and Lapple (1961)[14], used a super-cooled liquid aerosol in their investigations of the collection efficiency of glass fiber filters. Their aerosol, benzene azo β-napthol (mass median diameter = 0.29μm; geometric standard deviation = 1.4), was passed through various glass filters each with fiber diameters ranging from 1.0μm to 30μm and solidities from 0.0064 to 0.064. Flow velocities ranged from 0.6 cm/sec to 6000 cm/sec. Over such a wide range of experimental conditions, they were able to examine

Table II Multiple regression of primary independent variables.
(η_s with U, d_p, T, and d_f)

Variable	Regression Exponent	95% Confidence Limits	Theoretically Predicted Exponent (EQ. 15a)
U	-0.514	-0.514 ± 0.188	-0.667
d_p	-0.805	-0.805 ± 0.108	-1.333
T	0.815	0.815 ± 0.300	1.000
d_f	0.023	0.023 ± 0.027	-0.667

particle collection by diffusion, interception, and inertial impaction. Some of their experiments involved collection by diffusion alone. When the 21 data points from these experiments for diffusion alone are fitted to the form of EQ. (15), the equation with the highest correlation coefficient (0.491) is:

$$\eta_s = 2.9(0.944)\ Pe^{-0.667} \qquad (15j)$$

Paralleling the analysis with EQ. (15h), from EQ. (15j), it follows that $\xi''' = 1.189$.

When the data from our present experiments are fitted to the form of EQ. (15), the equation with the highest correlation coefficient (0.765) is:

$$\eta_s = 2.9(1.12)\ Pe^{-0.667} \qquad (15k)$$

Again, paralleling the analysis with EQ. (15h), from EQ. (15k), it follows that $\xi^{IV} = 0.7878$.

To compare the data of other workers with that from the current work, all data are plotted on axes which were chosen so that different values of ξ (hence, different experimental conditions) do not affect the comparison. To illustrate this approach, EQ. (15) can first be written as:

$$\log \eta_s = \log 2.9 - 0.667 \log (\xi^{1/2} Pe) \qquad (15\ell)$$

and then all data can be plotted as $\log \eta_s$ versus $\log (\xi^{1/2} Pe)$. It is important to note that each data set was first fitted to the form of EQ. (15ℓ) (which may not be the best fit) only because it facilitated the bringing together of all data sets for comparison and identifying the value of ξ at which the experiments were conducted. It is apparent upon examining all data sets together (Figure 12) that support for EQ. (15ℓ) is strong. It can be seen in Figure 12 that the present work provided most of the data points for values of $(\xi^{1/2} Pe) > 250$.

IV. Discussion

To provide explanation for the scatter in the data and the finding that calculated values of η_s were generally higher than those predicted by theory, the following investigations into sources of experimental error were made.

A. Electrical Charge on Test Aerosol Particles

The nature and the amount of electric charge present on the NaCl test aerosol particles were investigated with a simple mobility analyzer. Under different voltage conditions across the analyzer collection plates, comparisons were made between the observed behavior of the experimental aerosol (with an unknown charge distribution) and the predicted behavior of the same aerosol charged according to the Boltzmann Distribution Law[36]. By using the Boltzmann charge distribution as a standard, it is possible to make important inferences about the amount of charge on the experimental aerosol and the degree to which filter collection is influenced by

FIGURE 12

COMPARISON WITH OTHER WORKERS

(η_S Versus $\xi^{1/2}Pe$)

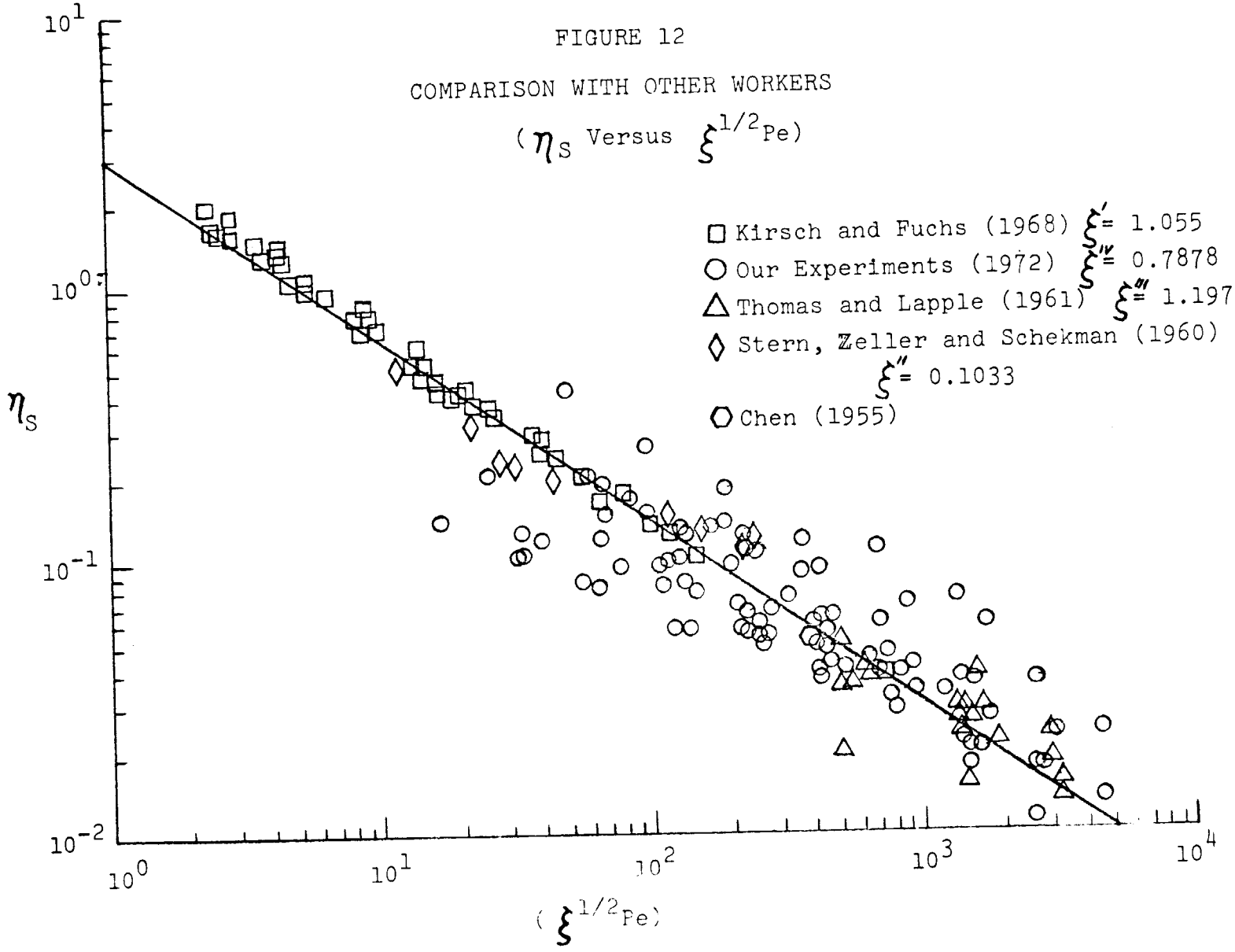

FIGURE 13. GEOMETRIC STANDARD DEVIATION OF THE DISTRIBUTION OF X VERSUS SCALE OF MEASUREMENT (LASER BEAM DIAMETER).

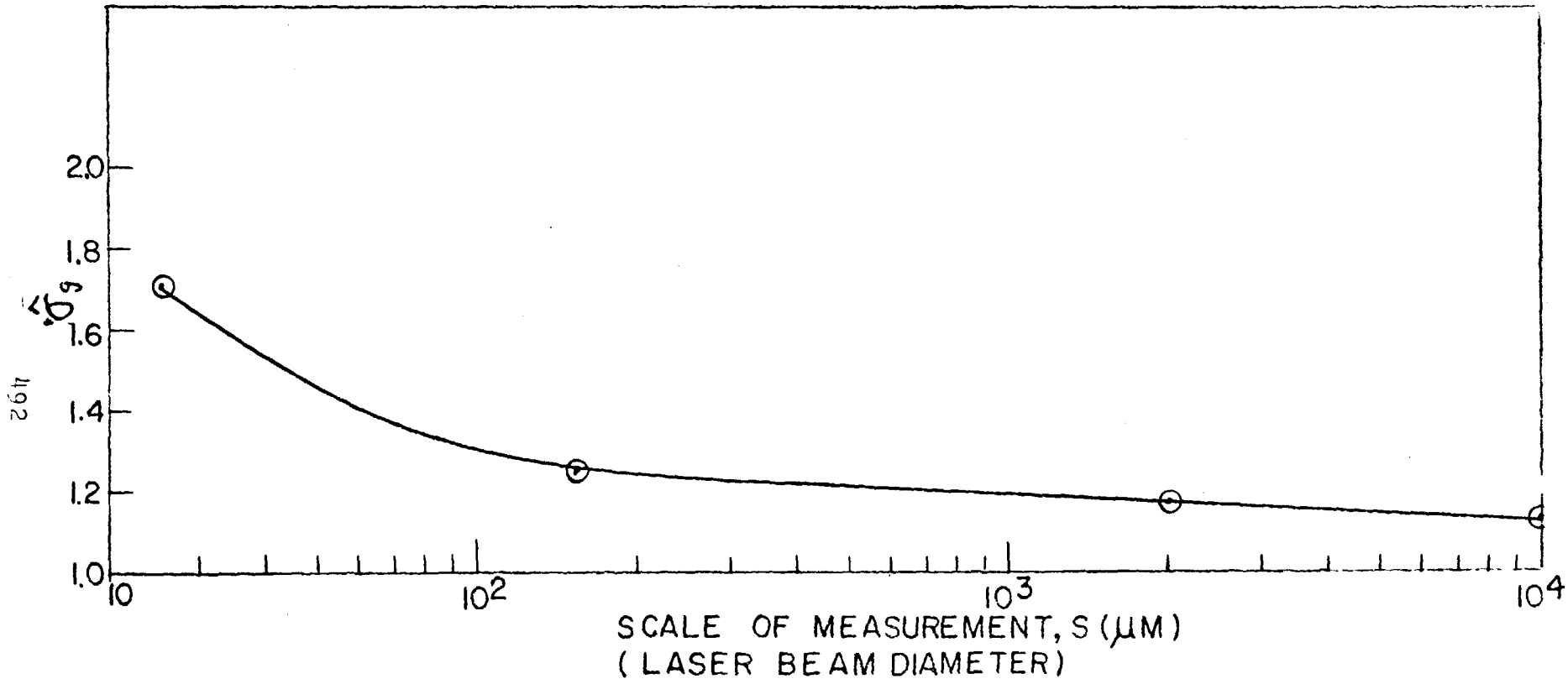

electrical effects. The following conclusions were drawn from this series of experiments:

1) The NaCl test aerosol, formed in the bipolar atmosphere present in the oxygen-acetylene flame, carried a bipolar charge.
2) The charge distribution present on the test aerosol was less than that present on an aerosol characterized in the following way as:
   i). having the same fraction of charged particles in each Porton size range as predicted by the Boltzmann Distribution Law,
   ii). but carrying only 20% of the Boltzmann charge on particles in each Porton size range.
3) The predicted values of electrical single fiber efficiency based upon the "20% Boltzmann" charge distribution are from 1/10 to 1/20 of the magnitude of the predicted values of diffusional single fiber efficiency.
4) The inclusion of electrical effects into the prediction scheme will not adequately explain the discrepancies observed between theory and experiment.

B. The Effects of Water Vapor on the Test Aerosol

During early experiments, the question was raised whether the presence of combustion water vapor in the aerosol generating system may have affected the shape of test aerosol particles, thereby introducing error into particle size measurements. Effort was made, throughout all experiments, to conduct sampling under the driest possible conditions (see section on aerosol sampling). According to a number of workers[15-19] when the preparation and collection of NaCl aerosol particles are carried out under dry conditions, spherical particles will result. These workers observed, further, that upon exposure to water vapor, the spherical particles changed to cubical in shape, presumably by the process of dissolution and recrystallization. Since the experimental particles were consistently spherical on all electromicrographs, it was concluded that no size change occurred from exposure to water vapor either during or after particle collection on the electron microscope grids.

C. The Non-Uniform Distribution of Solidity in the Fiber Media

The distribution of solidity in 12μm fiber filters was studied. These filters were assumed to be representative of filters composed of other monodisperse fibers, because all filters were manufactured in the same fashion. Filter solidity was evaluated so that theoretical predictions (which are based upon an assumption of uniform filter solidity) could be interpreted critically.

The distribution of solidity across the face of the filter mat was established by measuring the attenuation of light from a small laboratory laser with a photoresistor. The filter material was mounted in a frame and moved across the path of the laser by an electric, multispeed drive. The filter was stopped at 200 predetermined locations and resistance readings were taken. These were

converted to light intensities using the photoresistor calibration curve (ohms to foot-candles).

The intensity of the laser beam exiting from the filter (I) and the intensity of the unattenuated laser beam (I_o), were used to calculate 200 values of the quantity $X = -\ln I/I_o$, which from the Lambert-Beer Law[21], can be shown to be proportional to filter solidity. This routine was repeated for each of four different laser beam diameters (10,000μm, 2000μm, 152μm, and 25μm). The percentage frequency distribution of X values for each laser beam diameter was found to follow a log-normal distribution. Values of the geometric standard deviation ($\hat{\sigma}_g$) associated with each percentage frequency distribution of X are plotted with the laser beam diameters at which measurements were made in Figure 13.

Figure 13 suggests that the function relating $\hat{\sigma}_g$ and s is smooth over the range of s examined and that a relatively high degree of uniformity (i.e., low value of $\hat{\sigma}_g$) exists in the filter everywhere the scale of measurement is as small as the average interfiber spacing. Assuming a uniformly spaced parallel system of cylinders in the filter (12μm, α= 0.0057) the average value of interfiber spacing would be 145μm. For s = 145μm, $\hat{\sigma}_g$ = 1.27 (Figure 13) indicating a relatively uniform solidity distribution. For values of s less than 145μm, the observed degree of non-uniformity (as indicated by $\hat{\sigma}_g$) begins to increase. Very marked variations would be expected when the laser beam size begins to approach the diameter of the fiber.

The value of s that gives measured $\hat{\sigma}_g$ values equal to the theoretical σ_g of the filter solidity can be found with the aid of a multipathway pressure drop model developed by Dawson[20], which is based upon log-normal solidity distribution. This model can be used to predict the σ_g of filter solidity distribution when values of average solidity and W are known:

$$W = \frac{(\text{Resistivity})_{\text{based upon log-normal solidity distribution}}}{(\text{Resistivity})_{\text{based upon uniform solidity distribution}}}$$

The pressure drop measurements described earlier (Figure 2) compared experimental resistivity (measured in a filter assumed to have a log-normal solidity distribution) and theoretical resistivity (predicted from flow models based upon the assumption of uniform filter solidity). Values of W, therefore, can be obtained for different values of overall solidity from Figure 2. For 12μm filter fibers with overall solidity of 0.0057, W = 0.82, based upon measured resistance divided by resistance predicted by the Spielman and Goren flow model. For this value of W, Dawson's model predicts that σ_g = 1.51. For $\hat{\sigma}_g$ = 1.51, s is about 45μm in Figure 13 (depending upon the curve fit), a value equal to approximately four fiber diameters for this filter. When laser measurements are made with a beam diameter near fiber diameter, the value of $\hat{\sigma}_g = \sigma_g$. When used in Dawson's model this accounts for observed differences between resistivity measured in real filters and resistivity predicted by flow models based upon the assumption of uniform filter solidity.

At a scale of measurement of 45μm (ϑ_g = 1.51), filter solidity varies by a factor of about three for ± one geometric standard deviation from the mean. This variation was responsible for a small error in η_s when, during data reduction, values of overall count efficiency were converted to single fiber efficiency with EQ. (18). The evaluation of this equation requires substitution of the average (mean) filter mat solidity which is measured by dividing the density of the filter by the density of the fiber material. As solidity is log-normally distributed in the filter, solidity is more correctly described by the median of the solidity distribution than by the mean, (see Silverman, Billings, and First, p. 237)[23]. The relationship (in a log-normal distribution) between the mean solidity and the median solidity is given by:

$$\log (\alpha_{mean}) = \log (\alpha_{median}) + 1.15 \log^2 \sigma_g \qquad (19)$$

For σ_g = 1.51 and α_{mean} = 0.0057, α_{median} = 0.0052. Using the value of α_{median} in EQ. (19) will result in a small overall increase in η_s, a change which will not help to explain experimental values of η_s which are already greater than those predicted by theory.

Examining flow theory, on the other hand, it can be shown that large changes in solidity (in the range in which our experiments were conducted) will hardly affect theoretical collection by diffusion. Changes in solidity of 200-300% account, in theory, (according to Spielman and Goren; Fuchs and Stechkina) for changes of only 6-8% in single fiber efficiency.

D. Error Associated with Particle Counting

The standard deviation association with each of the experimental values of single fiber efficiency was calculated, based upon the assumption that our counting procedures follow Poisson statistics.[33] Count penetration through the filter is defined:

$$P' = (1 - \eta_s) = c_d/c_u \qquad (20)$$

where: c_d = total downstream count
c_u = total upstream count

From EQ. (18), let $\frac{\pi d_f(\alpha-1)}{4\alpha L} = C_1$ (21)

then, substituting EQ. (20) and (21) into EQ. (18), we find:

$$\eta_s = C_1 \ln(c_d/c_u) \qquad (22)$$

Volk's[24] expression for the variance of a general function is:

$$\sigma^2_{\eta_s} = \left(\frac{\partial \eta_s}{\partial c_u}\right)^2 \sigma^2_{c_u} + \left(\frac{\partial \eta_s}{\partial c_d}\right)^2 \sigma^2_{c_d} \qquad (23)$$

where: σ^2_s = variance associated with η_s
$\sigma^2_{c_u}$ = variance associated with c_u
$\sigma^2_{c_d}$ = variance associated with c_d

From Poisson statistics, one finds:

$$\sigma_{c_u} = (c_u)^{1/2}; \quad \sigma_{c_d} = (c_d)^{1/2} \qquad (24)\&(25)$$

A simple relation for $\sigma^2_{\eta_s}$ then follows:

$$\sigma^2_{\eta_s} = C_1^2/c_u + C_1^2/c_d \qquad (26)$$

For each of the experimental cases, the mean filter solidity was maintained at 0.0057 and L was always 2.9 cm. Thus:

$$C_1 = -47.24\ d_f \qquad (27)$$

Using EQs. (26) and (27) and experimental particle counts, Table III was constructed in which is tabluated (according to mean particle diameter) the percentage frequency of values of the coefficient of variation of measured single fiber efficiency, (σ_{η_s}/η_s). The information in this table indicates a greater counting error in the larger particle size ranges. This fact emerges because of the fewer number of large particles counted both upstream and downstream of the filter. Although low particle counts were found downstream in the smaller size ranges, the relatively high upstream counts tended to reduce the overall error. Examining the Pe number range associated with the data points in each size range, one can see that high coefficient of variation points are scattered over most of the Pe range (although not uniformly) for the entire experiment.

The magnitude of the counting errors listed in Table III helps to explain the scatter seen in the data. When the 95% confidence limits are placed on 77 of the 97 experimental points shown in Figure 11, the range of possible data results (for these points) extends to values of single fiber efficiency which are both 50% higher and 50% lower than those indicated in Figure 11.

V. Summary of Findings

A. Statistical examination of experimental values of η_s and Pe (ranging between 18 and 5400) from the present high temperature filtration research leads to the experimental relationship that $\eta_s \alpha Pe^{-0.467}$. This relationship is in statistical disagreement with that predicted by theory: $\eta_s \alpha Pe^{-0.667}$ (EQ. 15).

B. Comprehensive error analysis, including a stepwise multiple regression of experimentally measured variables indicated that statistical counting errors and experimental errors with the 12μm fiber filters account for most of the deviations between theory and experiment. This conclusion is supported by examination of Figures 8 and 9, which show better agreement (within the reliability limits of the data) between theory and experiment for the 4μm and the 8μm results.

C. Multiple regression analysis indicates that the experimental relationships: $\eta_s \alpha\ T^{0.815\pm0.300}$ and $\eta_s \alpha U^{-0.514\pm0.188}$ are not in

TABLE III

PARTICLE COUNTING STATISTICS

% Frequency of Values of $\frac{\sigma\eta_s}{\eta_s}$

Size Range µm at mean	# Data Points	$\frac{\sigma_{\eta_s}}{\eta_s} < 0.1$	$0.1 \leq \frac{\sigma_{\eta_s}}{\eta_s} < 0.2$	$0.2 \leq \frac{\sigma_{\eta_s}}{\eta_s} < 0.3$	$\frac{\sigma_{\eta_s}}{\eta_s} \geq 0.3$	Pe Range of Data	By Count - % of Particles in Upstream Aerosol
0.022	13	54%	39%	7%	0%	18.9- 224.4	12.7%
0.031	13	92%	0%	8%	0%	37.1- 435.3	41.4%
0.044	16	50%	44%	6%	0%	36.3- 834.0	19.4%
0.063	17	35%	53%	12%	0%	70.5-1570.1	17.4%
0.089	17	0%	65%	18%	17%	135.0-2891.8	5.9%
0.126	17	0%	35%	18%	47%	254.2-5171.3	2.1%
0.178	4	0%	0%	0%	100%	468.0-5181.0	1.1%
TOTAL	97						

disagreement with those predicted by theory: $\eta_s \alpha T^{1.000}$ and $\eta_s \alpha U^{-0.667}$ (EQ. 15a). The observation that the experimental regression exponent of temperature is not in disagreement with that predicted by theory supports the conclusion that current diffusional filtration theory can be used to predict filter efficiencies at high temperatures.

D. Within the range of significance of the present experimental results, it can be concluded that none of the three flow models studied (in combination with the collection theory of Fuchs and Stechkina) accounts for the present experimental observation more reliably than either of the other two.

E. The flow model of Spielman and Goren predicts values of filter pressure drop which are closest to those measured in the laboratory.

References

1. Spielman, L. and Goren, S., "Model for Predicting Pressure Drop and Filtration Efficiency in Fibrous Meida," Environ. Sci. Tech., 2, 279-287, (1968).

2. Kuwabara, S., "The Forces Experienced by Randomly Distributed Parallel Circular Cylinders and Spheres in a Viscous Flow at Small Reynolds Numbers," J. Phys. Soc. Japan, 14, 527-532, (1959).

3. Happel, J., "Viscous Flow Relative to Arrays of Cylinders," A.I.Ch.E.J., 5, 174-177, (1959).

4. Brinkman, H.C., "A Calculation of the Viscous Force Exerted by a Flowing Fluid on a Dense Swarm of Particles," Appl. Sci. Res. A1, 27-34, (1947a).

5. Lamb, H., Hydrodynamics, 6th Edition, Cambridge University Press, Cambridge, England, (1932).

6. Friedlander, S.K., "Mass and Heat Transfer to Single Spheres and Cylinders at Low Reynolds Numbers,: A.I.Ch.E.J., 3, 43, (1957).

7. Natanson, G.L., "Diffusion Precipitation of Aerosols on a Streamlined Cylinder with a Small Capture Coefficient," Dolk. Akad. Nank. SSSR., 112, 100-103, (1957a).

8. First, M.W., et al., Air Cleaning Studies, Progress Report for Feb. 1, 1950 to Jan. 31, 1951, School of Public Health, Harvard University, Boston, Massachusetts, June 30, 1951, issued April 21, 1952, NYO-1581.

9. Wright, T.E., Stasny, R.J., and Lapple, C.E., "High Velocity Air Filters," WADC TR 55-457, AD-142075, PB-131570, Oct., 1957.

10. Baumstark, J., et al., Upper Atmosphere Monitoring Program, Seventh Progress Report to Atomic Energy Commission Division of Biology and Medicine, General Mills No. 1907, July 1, 1959, AECU-4280.

11. Loffler, F., "Collection of Particles by Fiber Filters," in Air Pollution Control, part I edited by Werner Strauss, Wiley-Interscience, New York, (1971).

12. Kirsch, A.A., and Fuchs, N.A., "Studies on Fibrous Aerosol Filters II. Pressure Drops in Systems of Parallel Cylinders," Ann. Occup. Hyg., 10, 23-30, (1967).

13. Stern, S.C., Zeller, H.W., and Schekman, A.I., "The Aerosol Efficiency and Pressure Drop of a Fibrous Filter at Reduced Pressures," J. Colloid Sci., 15, 546-562, (1960).

14. Thomas, D.G. and Lapple, C.E., "Deposition of Aerosol Particles in Fibrous Filters," A.I.Ch.E.J., 1, 203-210, (1961).

15. Matijevic, E., Espenscheid, W.F., and Kerker, M., "Aerosols Consisting of Spherical Particles of Sodium Chloride," J. Colloid Sci., 18, 91, (1963).

16. Lodge, J.P. and Tufts, B.J., "An Electron Microscope Study of Sodium Chloride Particles Used in Aerosol Generation," J. Colloid Sci., 10, 256, (1955).

17. Schiff, D., Schiff, H.I., and Gendron, P.R., "The Use of a Diffusion Cloud Chamber to Characterize Condensation Nuclei," Can. J. Chem., 31, 1108, (1953).

18. Craig, A. and McIntosh, R., "The Preparation of Sodium Chloride of Large Specific Surface," Can. J. Chem., 30, 448, (1952).

19. Mclauchlan, T.A., Sennett, R.S., and Scott, G.D., "Continuous Observations with the Electron Microscope on the Formation of Evaporated Films of Silver, Gold, and Tin," Can. J. Res., A28, 530, (1950).

20. Dawson, S.V., Theory of Collection of Airborne Particles by Fibrous Filters, Doctoral thesis, Harvard University, School of Public Health, (July, 1969).

21. Hodkinson, J.R., "The Optical Measurement of Aerosols," Aerosol Science, edited by C.N. Davies, Academic Press, New York, (1966)

22. Silverman, L., Billings, C.E., and First, M.W., Particle Size Analysis in Industrial Hygiene, Academic Press, New York, (1971).

23. Volk, William, Applied Statistics for Engineers, McGraw-Hill Book Company, Inc., New York, (1958).

24. First, M.W., "Performance of Absolute Filters at Temperatures from Ambient to 1000°F," 12th A.E.C. Air Cleaning Conference, Oak Ridge, Tenn., (1972).

25. Langmuir, I., "Report on Smokes and Filters," OSRD Report, 865, (1942).

26. First, M.W., et al., "High Temperature Dust Filtration," Ind. Engr. Chem., 48, #4, (1956).

27. Billings, C.E., Silverman, L., and Small, W.D., "Pilot-Plant Studies of a Continuous Slag-Wool Filter for Open Hearth Fume," J.A.P.C.A., 5, 159, (1955).

28. Billings, C.E., Silverman, L., Levenbaum, L.H., Kurker, C., and Hickley, E.C., "Further Investigations of Slag-Wool Filters," J.A.P.C.A., 8, 53, (1958).

29. Billings, C.E., Silverman, L., and Kurker, C., "Simultaneous Removal of Acid Gases, Mists, and Fumes with Mineral Wool Filters," J.A.P.C.A., 8, 185, (1958).

30. Billings, C.E., Silverman, L., and Kurker, C., Industrial Wastes, (reprint).

31. Billings, C.E., Silverman, L., Dennis, R., and Levenbaum, L.H., "Shock Wave Cleaning of Air Filters," J.A.P.C.A., 10, 318, (1960).

32. Fuchs, N.A., and Stechkina, I.B., "A Note on Theory of Fibrous Filters," Ann. Occup. Hyg., 6, 27-30, (1963).

33. Herdan, G., Small Particle Statistics, Academic Press, New York, (1960), page 47.

34. Zebel, G., "Coagulation of Aerosols," Aerosol Science, edited by C.N. Davies, Academic Press, New York, (1966).

35. Billings, C.E., and Silverman, L., "Aerosol Sampling for Electron Microscopy," J.A.P.C.A., 12, 586, (1962).

36. Keefe, D., Nolan, P.J., and Rich, T., Proc. Royal Irish Acad., A4, 25, (1959).

37. Chmielewski, R.D., and Goren, S.L., "Aerosol Filtration with Slip Flow," Envir. Sci. Tech., 6, 1101, (1972).

38. Kaufman, D.W., Sodium Chloride, ACS Monograph #145, Reinhold Publishing Corporation, New York, (1960).

PERFORMANCE OF MULTIPLE HEPA FILTERS AGAINST PLUTONIUM AEROSOLS*

M. Gonzales, J. Elder and H. Ettinger
Health Division
Los Alamos Scientific Laboratory
University of California
Los Alamos, New Mexico 87544

Abstract

Performance of multiple stages of High Efficiency Particulate Air (HEPA) filters against aerosols similar to those produced by plutonium processing facilities has been verified as part of an experimental program. A system of three (3) HEPA filters in series was tested against $^{238}PuO_2$ aerosol concentrations as high as 3.3×10^{10} d/s-m^3. An air nebulization aerosol generation system, using ball milled plutonium oxide suspended in water, provided test aerosols with size characteristics similar to those defined by a field sampling program at several different AEC plutonium processing facilities. Aerosols have been produced ranging from 0.22 μm activity median aerodynamic diameter (amad) to 1.6 μm amad. The smaller size distributions yield 10 to 30% of the total activity in the <0.22 μm size range allowing efficiency measurement as a function of size for the first two HEPA filters in series. The low level of activity on the sampler downstream of the third HEPA filter (~0.01 c/s) precludes aerosol size characterization downstream of this filter. For the first two HEPA filters, overall efficiency, and efficiency as a function of size, exceeds 99.98% including the <0.12 μm and the 0.12 to 0.22 μm size intervals. Efficiency of the third HEPA filter is somewhat lower with an overall average efficiency of 99.8% and an apparent minimum efficiency of 99.5%. This apparently lower efficiency is an artifact due to the low level of activity on the sampler downstream of HEPA #3 and the variations due to counting statistics. Recent runs with higher concentrations, thereby improving statistical variations, show efficiencies well within minimum requirements.

I. Introduction

Most AEC facilities use multiple stages of HEPA filters to provide the necessary level of control associated with the release of radioactive particulates. While emission standards have not been established for radioactive particulates, AECM 0524 [1] has been interpreted to require that emission concentrations be controlled so that effluent concentrations at the boundary between controlled and uncontrolled areas does not exceed specified limits without any credit for atmospheric diffusion and dilution between the point of discharge and the boundary. This extremely conservative interpretation limits the release of plutonium to 6×10^{-14} μCi/ml, as measured at the point of discharge. Some operations involving plutonium will generate exhaust air streams with concentrations as high as 10^{-5} μCi/ml just upstream of the building air cleaning system [2] and to reduce this contaminant concentration to that specified by AECM 0524, the building air cleaning system must provide a decontamination factor of approximately 10^9.

*Work supported by the U. S. Atomic Energy Commission

To satisfy this requirement, multiple stages of HEPA filtration have generally been used, and these are quality control tested to assure a media efficiency ≥ 99.97% against 0.3 μm monodisperse dioctyl phthalate (DOP) [3].

Because of the potential problems associated with handling and installing these filters [4], most designs assume that the installed filters will perform at a somewhat lower level (99.9 to 99.95%) [5, 6, 7] with this performance level confirmed by in-place testing the entire system with 0.8 μm polydisperse DOP aerosols[8,9].

While these concepts are generally accepted for a single stage HEPA filter, unresolved problems are introduced by the need for multiple filter stages to provide the decontamination factors of 10^9 required to satisfy the previously noted conservative interpretation of AECM 0524. While filtration theory predicts that 0.3 μm aerodynamic diameter aerosols are the most difficult to remove[10], and the 99.97% quality control efficiencies will be exceeded by the first HEPA filter, and at least satisfied by back-up filters, substantiating experimental data does not exist for the specific problem at hand. In addition, existing multiple HEPA filter system designs generally do not permit routine testing to assure that efficiencies for each bank continuously satisfy or exceed 99.9%, nor do the existing test methods provide sufficient sensitivity to confirm decontamination factors (over several HEPA filters in series) of 10^9.

To guarantee the adequacy of existing HEPA filter systems or designs which do not permit routine in-place testing of each successive stage, it is necessary to provide assurance that the filter media will perform against plutonium aerosols at the levels suggested by theory, and monitored by DOP quality control tests on individual filters. To provide this information, an experimental program was initiated to (1) define size characteristics of the source terms from the major AEC operations using plutonium; (2) simulate these aerosols under laboratory test conditions; and (3) define the performance of multiple stages of HEPA filters against these laboratory aerosols. The possibility of obtaining similar information via a field test program was considered, but this approach was discarded since existing HEPA filter systems handling large quantities of plutonium do not permit testing of individual stages, and it would not be possible to distinguish between plutonium aerosol penetration due to the inadequacy of the media in successive stages (due to changes in the aerosol size characteristics), in contrast to leaks around the filters, due to improper installation.

II. Field Sampling--Source Term Characterization

Field sampling to determine Pu particle size characteristics and alpha activity concentration was performed immediately up-stream of the exhaust HEPA filters at five locations: two each at Mound Laboratory and Rocky Flats Plant, and one at LASL. These locations were selected to monitor Pu aerosols produced by typical research and production operations utilizing both ^{238}Pu and ^{239}Pu. Samples were obtained during the most active periods of the working day, when activity concentrations could be termed "worst normal" and most source

operations would be normally contributing plutonium aerosols to the process ventilation system. Many variables were expected to affect size characteristics and activity concentration, resulting in a range of these parameters for each facility. The relationship between some of these variables and the individual sampling sites are summarized in Table I. The predominant chemical form at each plant was reported to be PuO_2, although a detailed chemical analysis of each sample was not performed.

Aerodynamic diameter was considered the significant aerosol parameter of concern in preference to physical (microscopic) diameter since inertial impaction is the chief mode of particle collection by HEPA filters operating at rated capacity [10]. Activity median aerodynamic diameter (amad) is a convenient unit because it is not affected by changes in isotopic ratio, particle shape, or particle density. Particle size characteristics were determined by radiometric analysis of each of the nine stages of Andersen impactors (eight impaction stages plus backup membrane filter). Errors due to possible rebound of particles were minimized by covering the impaction surface with filter media.

Table II summarizes the results of this field sampling program in terms of the mean values of amad and geometric standard deviation (σ_g). Detailed analysis of the individual sampling results[11] shows that the two fabrication facilities have aerosols with amad's ranging from 2 to 5 μm; the two research and development facilities indicate amad's ranging from 1 to 4 μm; and the recovery facility consistently shows a sub-micron aerosol with a typical amad of 0.3 to 0.5 μm. This recovery facility (location 11) also produces aerosols as small as 0.1 μm amad, has the highest activity concentration, and constitutes the most difficult air cleaning problem.

III. Performance of Multiple HEPA Filters

A. Experimental Procedures

A two-module laboratory test system was designed and constructed to permit testing three HEPA filters in series, using ^{238}Pu test aerosols with size characteristics similar to those defined by the field sampling program. HEPA filter efficiency would be determined in terms of gross plutonium activity passing each filter as well as a function of aerosol size. Figure 1 shows the first module, a 9 ft. glove box housing the aerosol generators, (1); sampler #1, (2); and HEPA filter #1, (3). Each test HEPA filter has a design flow rate of 0.012 m^3/s (25 cfm) and its construction and filtration velocity is identical to the typical 0.472 m^3/s (1000 cfm) units used in most air cleaning systems. The only difference is that the 0.472 m^3/s (1000 cfm) units are generally open faced, while the test filter is designed for in-line installation with 2-inch pipe nipples at each end. Figure 2 shows the second module and its major components which consists of sampler #2 (4) immediately upstream of HEPA filter #2 (5); sampler #3 (6) immediately upstream of HEPA filter #3 (7); sampler #4 (8) downstream of HEPA filter #3; and a vacuum pump (9).

Samplers #1, #2 and #3 are dual samplers simultaneously collecting a gross membrane filter sample for aerosol concentration, and an Andersen impactor sample for measuring aerosol aerodynamic size characteristics. The gross filter measurements determine overall HEPA filter efficiencies, while impactor data are used to calculate HEPA filter efficiency as a function of plutonium aerosol aerodynamic size. Sampler #4 consists of nine 2-inch open face glass fiber filters (Figure 3) and is designed to filter all the exhaust air. This was required because of the very low levels of activity existing at this point which preclude impactor measurements to define aerosol size characteristics downstream of the third HEPA filter.

To obtain sufficient activity downstream of the third HEPA filter in series it was calculated that an activity concentration of $\sim 10^{10}$ to 10^{11} d/s-m^3 had to be produced by the aerosol generating system. This high activity level upstream of the first HEPA filter resulted in activity levels collected on the first impactor which are virtually impossible to handle with the counting facilities available. To circumvent this problem, a sample dilution system was designed to draw a relatively small sample 2.33×10^{-5} m^3/s (0.05 cfm) at the sampling probe, to be diluted with 4.48×10^{-4} m^3/s (2.95 cfm) filtered air. Even so, samples obtained from this first sampler required preparation of extensive serial dilutions prior to counting. Andersen impactors located downstream of the first and second HEPA filters did not need dilution systems because the activity concentration at those positions are sufficiently low. A gross filter sampler was used at each location, concurrently with the Andersen samplers, to monitor total aerosol concentration. Sampling times varied for each sampling position with one minute being sufficient for position number one (upstream of first HEPA filter) and up to two hours for position number three (downstream of second HEPA filter). With these gross differences in sampling times, it was necessary to take several samples at position number one during each run to monitor the degree of variation in aerosol generator output as a function of time.

Several plutonium aerosol generating methods were investigated before choosing the modified ReTec nebulizer[12]. Modification entailed enlarging holes in the cap and jet to twice their original size to provide a threefold increase in aerosol output, from $\sim$300 µl/min to $\sim$900 µl/min at 3.45×10^5 pascals (50 psig) operating pressure. The generator solution reservoirs were constructed of brass to a capacity of 70 ml to allow generation times up to one hour per loading, O-ringed for elimination of leaks and Teflon coated to minimize wall losses. Six of these nebulizers attached to a central duct (Figure 4), with a generator solution concentration of up to 8.0 mg/ml $^{238}PuO_2$ suspended in water, yielded the plutonium aerosol concentrations required to test three HEPA filters in series.

To keep the suspension well stirred and achieve a constant aerosol output, the reservoirs were partially immersed in an ultrasonic bath throughout the aerosol generation run. Because the aerosol was produced from a water suspension, care was exercised to assure that all water was dried from the particles before arriving at the samplers and the first HEPA filter. This required supplying heated air at the system air inlet, raising the temperature of the system air about 10°C.

To approximate plutonium aerosols with 0.1 to 5 μm amad's measured under field conditions, $^{238}PuO_2$ powders were dry ball milled for various time intervals and suspended in water to a concentration of 2.5 -8.0 mg/ml. Ultrasonic agitation of the suspension broke up agglomerates, and addition of anionic surfactant kept the suspensions well dispersed. Selective ball milling provided some control of size characteristics over the range of interest with some limitations at either end. By adjusting the ball milling time, it was possible to produce aerosol with amad's ranging from 0.7 to 1.6 μm, with σ_g's ranging from 2.1 to 2.9. Even with extensive dry ball milling, it was not possible to produce an aerosol with an amad smaller than 0.7 μm. However, these aerosols contained a significant fraction of particles smaller than 0.4 μm, which is the smallest size fraction which can be characterized by the Andersen impactor operated at its normal sampling rate of 0.48×10^{-3} m^3/s (1 cfm).

To provide aerosols similar to those measured at the chemical processing facility (location 11; amad ranging from 0.1 to 1.0 μm) a centrifugal ball mill was used to mill various batches of $^{238}PuO_2$ for varying time intervals. Smaller sizes could be attained because of higher rate of energy input. Milling was carried out using a carrier liquid to reduce agglomeration. Initially, ethanol was used, but high pressures generated within the mill enclosure necessitated a change to water as the carrier liquid. Additional problems were encountered as a result of alpha activity breaking down the water to H_2, O_2, and H_2O_2, again creating high pressures and explosive mixtures within the mill jar. A continuously vented mill enclosure was developed to eliminate these problems. The new milling procedures yielded aerosol amad's ranging from 0.22 μm to 0.66 μm for milling times ranging from 44 to 167 hours. Though not reaching the desired 0.1 μm amad, these size distributions yield 10 to 30% of the material in the size range of interest, i.e., <0.22 μm.

The previously described sampling system ahead of each HEPA stage was modified to allow impactor sampling at 1.42×10^{-3} m^3/s (3.0 cfm). As previously utilized in the field sampling program at location 11, operation of these impactors at higher flow rates shifts the effective range of particle size classification downward to include the lower limit of the range of interest (0.1 μm). Calculated and experimentally measured effective cutoff diameters[13] for 1.42×10^{-3} m^3/s (3.0 cfm) flow rates are in adequate agreement to permit characterization of the test aerosol using this technique.

B. Test Results

For the plutonium aerosols produced through dry ball milling (amad range of 0.7 to 1.6 μm), overall HEPA filter efficiencies determined by gross filter samples for each filtration stage are detailed in Table III and summarized in Table IV. HEPA filter stages are numbered 1-3 with stage 0 representing the aerosol concentration and size characteristics upstream of HEPA filter #1. Aerosol size characteristics in terms of amad and σ_g generally decrease at succeeding stages. Activity concentrations upstream of HEPA #1 ranged between 10^9 to 2.3×10^{10} $d/s\text{-}m^3$. As expected, filter efficiency is highest

for the first stage, but the measured HEPA filter efficiencies remain well within the present minimum AEC performance guidelines for each stage[14]; i.e., 99.95% for first stages and 99.8% for succeeding stages. In fact, the second HEPA filter efficiency always exceeds 99.99%.

Minimum efficiency noted for the third stage is slightly below the 99.8% guideline. This is due to statistical problems encountered with count rates below .01 c/s downstream of the third HEPA filter, and counting problems due to gaseous contaminants from radon-thoron daughters. Contamination probably accounts for the two tests indicating an efficiency less than 99.8%. Greater confidence in third HEPA stage efficiencies was obtained using longer run times with greater aerosol concentration (10 mg/ml), and longer counting times, allowing a minimum of one week for decay of gaseous contaminants. These modifications to the original test procedure have resulted in consistently higher efficiencies for the third HEPA filter (for the last seven test runs), and indicate that a third HEPA filter in series will satisfy existing AEC guidelines[14].

Table V shows HEPA filter efficiencies as a function of aerosol aerodynamic size. The first column denotes the impactor stages for an 8-stage impactor plus a backup filter (MF #2). The next column gives the impactor particle collection interval for each stage in μm. Mean efficiencies of HEPA filters #1 and #2 are well above the minimum criteria, and actually exceed the DOP quality control requirement of 99.97% for all size intervals characterized by the impactor. Although impactor data downstream of HEPA #3 are not available, the efficiencies reported for HEPA #3 are essentially against particles <1.1 μm aerodynamic diameter, with particles <.43 μm aerodynamic diameter accounting for approximately 40% of the total activity.

Based on the field data obtained at location 11, the need for characterizing HEPA filter performance for aerosols as small as 0.1 μm was indicated. As previously detailed, wet centrifugal milling provided plutonium aerosols with amad's as small as 0.22 μm, with a significant fraction of the aerosol smaller than 0.22 μm. Overall HEPA filter efficiencies against these aerosols are detailed in Table VI, and summarized in Table VII. The first and second stages were all well within minimum criteria guidelines[14], with the minimum measured efficiency for each of the first two filters in series of >99.98%. HEPA filter #3 in the series shows an average efficiency of 99.84, with a minimum efficiency of 99.50%, significantly lower than HEPA #1 or #2. However, these lower efficiencies are probably an artifact, and can be attributed to poor count statistics at sampler #4 downstream of HEPA #3. More recent tests (last 8 tests in Table VI) having higher initial aerosol concentrations, thereby increasing the challenge aerosol to HEPA filter #3, show efficiencies exceeding the minimum criteria guidelines.

Table VI also shows that aerosol size distributions do not change significantly with subsequent filter stages, in contrast to the observation previously noted with larger plutonium test aerosols. The σ_g

is decreased somewhat, indicating an aerosol with a narrower size range downstream of successive HEPA filters. However, these minor aerosol size variations suggest that the aerosol challenging the third HEPA filter is comparable to that for the second HEPA, and filter performance for these filters should be the same.

Efficiency of the first and second HEPA filters in series as a function of size was also well within minimum requirements. A typical computer print-out is reproduced as Table VIII. This shows the HEPA filter efficiency as function of particle size; the combined protection factor (HEPA's #1 and #2) as a function of particle size for the first two HEPA's; filter efficiency based on gross MF-1 filter samplers upstream and downstream of each HEPA; and the overall protection factors for two or three HEPA's in series. For all tests completed, protection factors for two HEPA's in series ranged from 1.6×10^{8} to 1.7×10^{11} against aerosols 0.22 to 0.66 µm amad, while for three HEPA's the protection factor ranged from 2.1×10^{12} to 4.7×10^{13}. Table VIII shows these protection factors to be 1.97×10^{10} and 2.35×10^{13}. Overall efficiencies based on total Andersen impactor activity agreed quite closely with the overall efficiencies as given by the gross MF-1 filter samplers. Aerosol concentrations for these runs have ranged from 3.3×10^{9} d/s-m^3 up to approximately 1.9×10^{10} d/s-m^3. The closer the initial aerosol concentration is to 1.9×10^{10} d/s-m^3, the fewer are the low level counting problems associated with the sampler downstream of HEPA #3.

Summary

Recent effort in the area of test methods and efficiency studies on multi-bank HEPA filter systems has been prompted primarily by a need to specify design requirements of air cleaning systems for several new plutonium processing plants. Primary interest lay in attaining decontamination factors above 10^{9}, and establishing test methods to permit routine efficiency testing of each stage. In the absence of experimental data to substantiate individual stage efficiency against an actual plutonium aerosol, a laboratory study was initiated using $^{238}PuO_2$ as the test aerosol. A field study preceding the laboratory phase determined the source term at three AEC plants for typical plutonium processing operations in terms of aerosol size characteristics and activity concentrations. It was against similar aerosols that efficiency of a three stage HEPA test system was evaluated.

Aerosol size characteristics in terms of amad and σ_g of the generated aerosol and the aerosol passing the first two stages were determined by Andersen 8-stage cascade impactor samples. Efficiency of each stage was provided by gross samples on membrane filters. Quality of the HEPA filter installation was removed as a variable by utilizing fully enclosed, quality control tested filters. Aerosols of $^{238}PuO_2$ ranging from 0.22 µm to 1.6 µm amad were generated upstream of the three stage system in activity concentration as high as 2.3×10^{10} d/s-m^3. Measured HEPA filter efficiencies remained high for all three stages and was, as expected, highest for the first stage. Mean efficiencies by stage, including values obtained against 0.22 µm amad, were as follows:

first stage, 99.99+%; second stage, 99.99+%; and third stage, 99.84%. Several early tests indicated stage 3 efficiencies below the 99.8% guideline (99.49% minimum) but these observations have been considered artifacts after improved test methods resulted in efficiencies consistently above 99.8%. The tests show that second and third stages do not suffer gross efficiency loss for plutonium aerosol as small as 0.22 μm amad.

This study was done under idealized conditions to assure that only aerosol penetration, and not leakage around the filter media was monitored. Therefore, proper installation of good, quality control tested HEPA filters is of prime importance to achieve the protection factors determined by this study.

Acknowledgement

The cooperation, guidance and assistance of the following people in completing the field sampling program and initiating the laboratory program are gratefully acknowledged: D. G. Carfagno and W. H. Westendorf, Monsanto Research, Mound Laboratory; W. D. Kittinger and E. A. Putzier, Dow Chemical, Rocky Flats Plant; and C. E. Klatt and F. Miley, Los Alamos Scientific Laboratory.

References

1. AEC Appendix 0524, Standards for Radiation Protection, (Nov. 1968).

2. Ettinger, H., J. Elder, M. Gonzales: Performance of Multiple HEPA Filters Against Plutonium Aerosols, Progress Report for period Jan. 1 through June 30, 1973. Report LA-5349-PR, (July 1973).

3. U. S. Army Chemical Corps and U. S. Navy Bur. Ships: Filter Units, Protective Clothing, Gas Mask Components and Related Products: Performance-Test Methods. Report MH-STD-282, (May 1956).

4. Gilbert, H. and J. H. Palmer: High Efficiency Particulate Air Filter Units, Report TID-7023, (Aug. 1961).

5. Panchuk, F. and W. Rachuk: Filter Testing Program Atomic Energy of Canada Limited. Proceedings of the 9th AEC Air Cleaning Conference, CONF. 660904, pp. 979-1020, (Sept. 1966).

6. Proceedings of the 8th AEC Air Cleaning Conference: In-Place Filter Testing, Round Table Session, Report TID-7677, pp. 433, (1963).

7. Collins, J. T., Jr.: Criteria for High Efficiency Filter Installations at the National Reactor Testing Station, Report IDO-12045, pp. 30-31, (Dec. 15, 1965).

8. Burchsted, C. A. and A. B. Fuller: Design Instruction and Testing of High Efficiency Air Filtration Systems for Nuclear Application, ORNL-NSIC-65, (Jan. 1970).

9. ANSI Standard N101.1, Efficiency Testing of Air Cleaning Systems Containing Devices for Removal of Particles, (1972).

10. Chen, C. Y.: Filtration of Aerosols by Fibrous Media, Chemical Review, 55, 595, (1955).

11. Ettinger, H., J. Elder, M. Gonzales: Performance of Multiple HEPA Filters Against Plutonium Aerosols, Progress Report for period July 1 through Dec. 31, 1972. Report LA-5170-PR, (Jan. 1973).

12. Manufacturer's Bulletin, ReTec Development Laboratory, Portland, Oregon.

13. Hu, J. N. H.: An Improved Impactor for Aerosol Studies - Modified Andersen Impactor, Envir. Sci. and Tech., 5, #3, 251, (1971).

14. HEPA Filtration Guidelines (draft), AEC Division of Operational Safety, and Division of Engineering and Construction, (Dec. 9, 1971).

TABLE I

SUMMARY OF OPERATING CONDITIONS AT EACH SAMPLING LOCATION

Location	Operations	Isotope	Prefilter[c] Efficiency	Relative Quantities Handled
00	R & D	Both	Unknown	Small
04	R & D	238	High[a]	Moderate
08	Fabrication	238	High[a]	Moderate
11	Recovery	239	Unknown[b]	Large
14	Fabrication	239	Unknown	Large

[a] Routine monitoring and replacement.

[b] Probably unreliable due to presence of high concentrations of corrosive acid vapors.

[c] Prefilter is small HEPA located at glove box.

TABLE II

MEAN Pu AEROSOL SIZE CHARACTERISTICS* AND ACTIVITY CONCENTRATION

Location	Type	Isotope	amad (μm)	σ_g	Activity Concentration d/s-m^3
00	R & D	Both	1.9	2.1	2.0×10^2
04	R & D	238	2.9	3.0	2.0×10^3
08	Fabrication	238	4.1	1.7	1.0×10^3
11	Recovery	239	0.5	3.9	1.5×10^5
14	Fabrication	239	2.6	2.9	2.7×10^4

*Assuming particle diameters are lognormally distributed.

TABLE III

OVERALL HEPA FILTER EFFICIENCY

Run	HEPA Filter Stage	Plutonium Aerosol amad (μm)	σ_g	Activity Concentrations d/s-m^3	HEPA Filter Efficiency
P2-1	0	0.7	2.26	2.80×10^9	
	1	0.6	1.50	9.60×10^3	99.99+
	2	0.7	1.8	2.38×10^{-1}	99.99+
	3	--	--	1.20×10^{-3}	99.49*
P2-3	0	1.3	2.94	2.12×10^9	
	1	0.59	1.6	5.17×10^3	99.99+
	2	0.57	1.84	8.63×10^{-2}	99.99+
	3	--	--	CONTAMINATED	
P2-4	0	1.3	2.7	1.86×10^9	
	1	0.45	2.04	5.55×10^3	99.99+
	2	0.48	2.54	4.04×10^{-2}	99.99+
	3	--	--	CONTAMINATED	

*Probable contamination from radon-thoron daughters.

TABLE III (continued)

OVERALL HEPA FILTER EFFICIENCY

Run	HEPA Filter Stage	Plutonium Aerosol amad (μm)	σ_g	Activity Concentrations d/s-m^3	HEPA Filter Efficiency
P2-5	0	0.65	2.2	5.04×10^{9}	
	1	0.64	1.6	9.22×10^{4}	99.99+
	2	0.55	1.4	1.68	99.99+
	3	--	--	CONTAMINATED	
P2-6	0	0.75	2.7	4.36×10^{9}	
	1	0.59	1.6	6.25×10^{4}	99.99+
	2	0.51	1.5	1.39	99.99+
	3	--	--	7.67×10^{-4}	99.94
P2-7	0	1.61	2.70	1.68×10^{9}	
	1	0.64	1.70	7.52×10^{3}	99.99+
	2	0.43	1.31	7.69×10^{-2}	99.99+
	3	--	--	1.67×10^{-4}	99.78
P2-8	0	0.79	2.51	1.24×10^{9}	
	1	0.67	1.74	2.35×10^{4}	99.99+
	2	0.56	1.47	2.50×10^{-1}	99.99+
	3	--	--	1.21×10^{-3}	99.52*
P2-9	0	0.84	2.07	5.17×10^{9}	
	1	0.45	1.93	8.10×10^{4}	99.99+
	2	0.42	1.66	2.07	99.99+
	3	--	--	5.77×10^{-4}	99.97

*Probable contamination from radon-thoron daughters.

TABLE III (continued)

OVERALL HEPA FILTER EFFICIENCY

Run	HEPA Filter Stage	Plutonium Aerosol amad (μm)	Plutonium Aerosol σ_g	Activity Concentrations d/s-m^3	HEPA Filter Efficiency
P2-10	0	0.80	2.09	7.34×10^{9}	
	1	0.52	1.67	1.04×10^{5}	99.99+
	2	0.36	1.79	2.15	99.99+
	3	--	--	4.02×10^{-4}	99.98
P3-1	0	0.71	2.12	1.59×10^{10}	
	1	0.66	1.58	3.34×10^{5}	99.99+
	2	0.42	1.79	8.79	99.99+
	3	--	--	9.64×10^{-4}	99.99
P3-2	0	0.77	2.18	2.14×10^{10}	
	1	0.61	1.65	3.78×10^{5}	99.99+
	2	0.60	1.40	1.12×10^{1}	99.99+
	3	--	--	7.80×10^{-4}	99.99+
P3-3	0	1.45	2.79	7.30×10^{9}	
	1	0.82	2.00	1.99×10^{5}	99.99+
	2	0.50	1.60	2.57	99.99+
	3	--	--	9.36×10^{-4}	99.96
P3-4	0	0.78	2.55	7.31×10^{9}	
	1	0.57	1.75	8.39×10^{4}	99.99+
	2	0.50	1.65	1.37	99.99+
	3	--	--	3.71×10^{-4}	99.97

TABLE III (continued)

OVERALL HEPA FILTER EFFICIENCY

Run	HEPA Filter Stage	Plutonium Aerosol amad (μm)	σ_g	Activity Concentrations d/s-m^3	HEPA Filter Efficiency
P3-5	0	0.80	2.54	2.28×10^{10}	
	1	0.58	1.69	2.12×10^{4}	99.99+
	2	0.49	1.49	3.31×10^{-1}	99.99+
	3	--	--	3.22×10^{-4}	99.90

TABLE IV

OVERALL HEPA FILTER EFFICIENCY

HEPA Filter Stage	Range of Size amad (μm)	σ_g	Efficiency Range (%) Min.	Mean	Max.
1 *	0.70 - 1.6	2.07 - 2.9	99.99+	99.99+	99.99+
2 *	0.45 - 0.82	1.5 - 2.04	99.99+	99.99+	99.99+
3 **	0.36 - 0.70	1.31 - 2.54	99.49	99.86	99.99+

*Total of 14 test runs.

**Total of 11 test runs.

TABLE V

HEPA FILTER EFFICIENCY AS A FUNCTION OF AEROSOL SIZE

Sampling Impactor Stage Number	Aerodynamic Diameter Range μm	Mean Efficiency (%) HEPA #1	HEPA #2
0	>11	99.999	99.999
1	7.0 - 11	99.999	99.996
2	4.7 - 7.0	99.999	99.999
3	3.3 - 4.7	99.999	99.998
4	2.1 - 3.3	99.999	99.999
5	1.1 - 2.1	99.999	99.999
6	0.65 - 1.1	99.997	99.998
7	0.43 - 0.65	99.997	99.998
MF#2	<0.43	99.998	99.997
OVERALL	-	99.998	99.998

TABLE VI

HEPA FILTER EFFICIENCY

Run	HEPA Filter Stage	Plutonium Aerosol amad (μm)	σ_g	Activity Concentrations d/s-m^3	HEPA Filter Efficiency(%)
P4-1	0	0.31	2.87	8.06×10^{8}	
	1*	0.31	2.01	3.79×10^{3}	99.99+
	2*	0.40	1.69	6.19×10^{0}	99.98+
	3	--	--	3.67×10^{-4}	99.94
P4-2	0	0.37	2.46	1.42×10^{9}	
	1**	--	--	4.90×10^{3}	99.99+
	2	0.34	1.65	0.10×10^{0}	99.99+
	3	--	--	4.33×10^{-4}	99.50

* Broken backup filter.
**Broken backup filter - no activity.

TABLE VI (continued)

HEPA FILTER EFFICIENCY

Run	HEPA Filter Stage	Plutonium Aerosol amad (μm)	Plutonium Aerosol σ_g	Activity Concentrations d/s-m^3	HEPA Filter Efficiency(%)
P4-3	0	0.38	2.51	3.26×10^{9}	
	1	0.37	1.76	2.90×10^{3}	99.99+
	2	0.36	1.68	6.86×10^{-2}	99.99+
	3	--	--	2.98×10^{-4}	99.55
P4-4	0	0.34	3.00	4.06×10^{9}	
	1	0.36	1.99	2.78×10^{4}	99.99+
	2	0.34	1.89	1.47×10^{-1}	99.99+
	3	--	--	9.23×10^{-5}	99.92
P4-5	0	0.66	3.28	5.22×10^{9}	
	1	0.38	2.10	6.52×10^{3}	99.99+
	2	0.39	2.09	9.95×10^{-2}	99.99+
	3	--	--	3.30×10^{-4}	99.63
P4-6	0	0.48	3.76	9.14×10^{9}	
	1	0.44	1.69	2.21×10^{3}	99.99+
	2	0.42	1.66	5.01×10^{-1}	99.99+
	3	--	--	1.81×10^{-4}	99.60
P4-7	0	0.48	2.98	4.74×10^{9}	
	1	0.47	1.96	2.60×10^{4}	99.99+
	2	0.42	1.68	2.08×10^{-1}	99.99+
	3	--	--	1.95×10^{-4}	99.89

TABLE VI (continued)

HEPA FILTER EFFICIENCY

Run	HEPA Filter Stage	Plutonium Aerosol amad (μm)	Plutonium Aerosol σ_g	Activity Concentrations d/s-m^3	HEPA Filter Efficiency(%)
P4-8	0	0.47	3.26	6.29×10^{9}	
	1	0.48	1.70	2.11×10^{4}	99.99+
	2	0.41	1.69	1.81×10^{-1}	99.99+
	3	--	--	6.23×10^{-5}	99.96
P4-9	0	.36	3.17	3.56×10^{9}	
	1	.40	1.85	4.12×10^{3}	99.99+
	2	.37	2.00	4.04×10^{-2}	99.99+
	3	--	--	1.29×10^{-4}	99.64
P4-10	0	.44	3.06	1.07×10^{10}	
	1	.53	2.28	1.66×10^{6}	99.99+
	2	.42	1.72	5.83×10^{1}	99.99+
	3	--	--	4.23×10^{-3}	99.99+
P4-11	0	.43	3.36	1.94×10^{10}	
	1	.47	2.36	1.94×10^{6}	99.99
	2	.39	1.86	6.49×10^{1}	99.99+
	3	--	--	3.87×10^{-3}	99.99+
P4-12	0	.33	3.56	1.38×10^{10}	
	1	--	--	1.09×10^{5}	99.99+
	2	.15	1.93	1.07×10^{1}	99.99
	3	--	--	9.67×10^{-4}	99.99

TABLE VI (continued)

HEPA FILTER EFFICIENCY

Run	HEPA Filter Stage	Plutonium Aerosol amad (μm)	Plutonium Aerosol σ_g	Activity Concentrations d/s-m^3	HEPA Filter Efficiency(%)
P4-13	0	.27	3.86	1.04×10^{10}	
	1	--	--	9.29×10^{4}	99.99+
	2	.20	2.5	9.15×10^{0}	99.99
	3	--	--	6.11×10^{-4}	99.99+
P4-14	0	.22	2.59	1.68×10^{10}	
	1	--	--	2.54×10^{5}	99.99+
	2	.28	2.34	1.41×10^{1}	99.99+
	3	--	--	1.10×10^{-3}	99.99+
P4-15	0	.26	3.20	1.12×10^{10}	
	1	.29	2.18	9.12×10^{4}	99.99+
	2	--	--	1.29×10^{1}	99.98
	3	--	--	1.14×10^{-3}	99.99
P4-18	0	.37	3.16	9.29×10^{9}	
	1	.30	2.52	4.23×10^{4}	99.99+
	2	.22	2.50	2.90×10^{0}	99.99+
	3	--	--	1.69×10^{-4}	99.99+
P4-19	0	.32	3.65	5.40×10^{9}	
	1	.30	2.10	1.08×10^{5}	99.99
	2	.28	2.44	1.31×10^{1}	99.98
	3	--	--	3.25×10^{-4}	99.99

TABLE VII

SUMMARY OF HEPA FILTER EFFICIENCY

HEPA Filter Stage	Pu Aerosol amad Range (μm)	HEPA Filter* Efficiency (%) Minimum	Avg.	Maximum
1	0.22 - 0.66	99.99+	99.99+	99.99+
2	0.29 - 0.53	99.98+	99.99+	99.99+
3	0.15 - 0.42	99.50	99.86	99.99+

*Total of 17 experimental runs.

TABLE VIII

MULTIPLE HEPA FILTER EFFICIENCY RUN NUMBER P4-7

RATIO CONCENTRATION ANDERSEN TO CONCENTRATION MF1

SAMPLE LOCATION	ONE	TWO	THREE
RATIO	1.2662	1.2038	1.0907

ECD*	INDIVIDUAL FILTER EFFICIENCIES BY CASCADE IMPACTOR STAGES FILTER 1	FILTER 2	PROTECTION FACTOR FILTER ONE AND TWO FILTER 1 & 2
>5.40	99.999954	100.000000	.20397E.13
5.40	99.999950	100.000000	.18518E.13
3.39	99.999951	100.000000	.19279E.13
2.30	99.999886	99.999903	.45993E.12
1.54	99.999674	99.999915	.17018E.12
.96	99.999070	99.998994	.10935E.11
.44	99.999264	99.999188	.16697E.11
.22	99.999645	99.998973	.28075E.11
.12	99.999748	99.998957	.39029E.11
SUM	99.999478	99.999170	100.000000

TOTAL FILTER EFFICIENCY AS GIVEN BY MF 1 FILTERS AND FINAL STAGE FILTERS

FILTER 1	FILTER 2	FILTER 3
99.999451	99.999056	99.890966

PROTECTION FACTORS AS GIVEN BY FILTER COLLECTIONS

FILTER 1+2= .19681E+11 FILTER 1+2+3= .23456E+14

*Effective cutoff diameter.

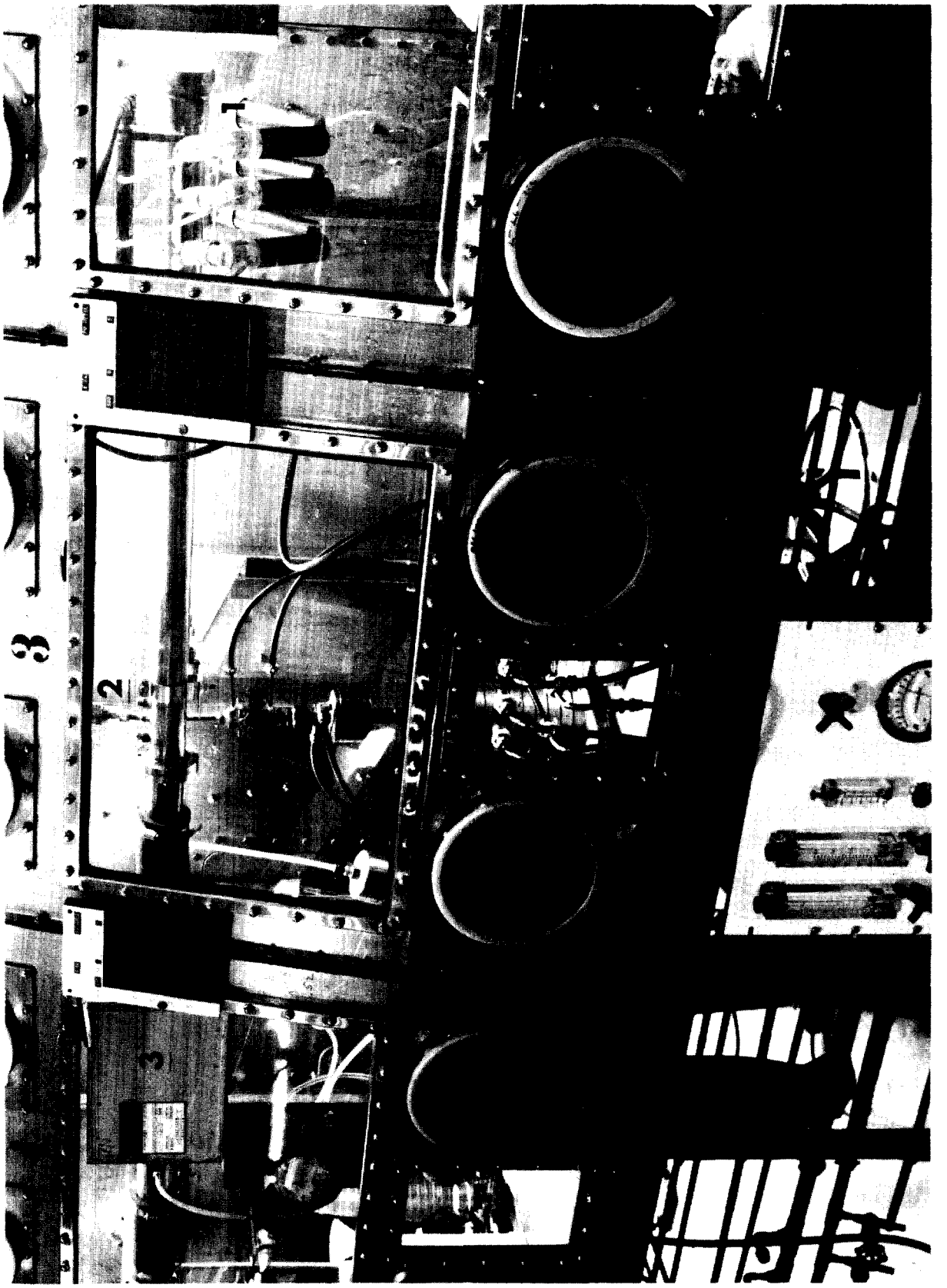

Figure 1. Glovebox module.

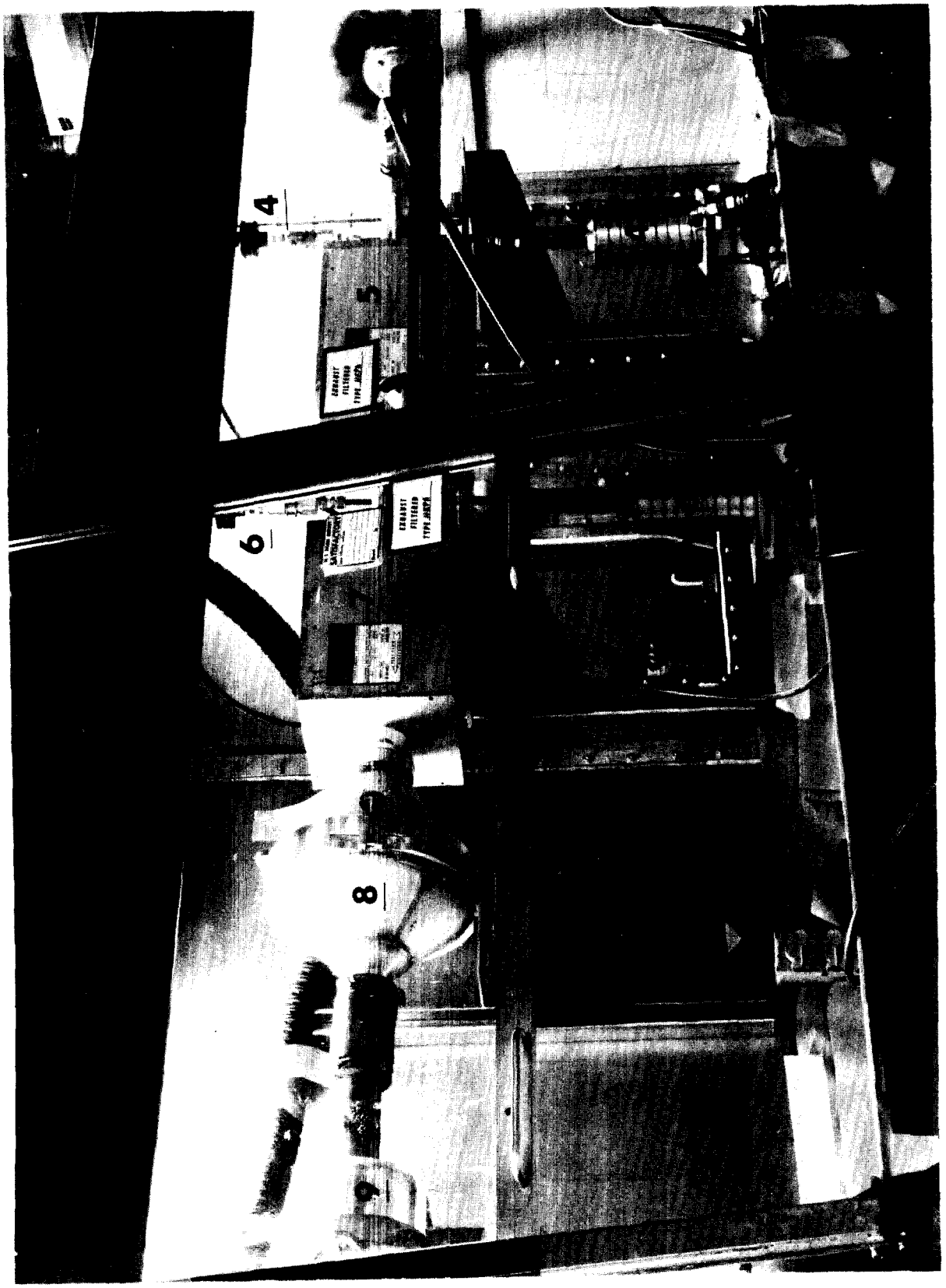

Figure 2. Hood module.

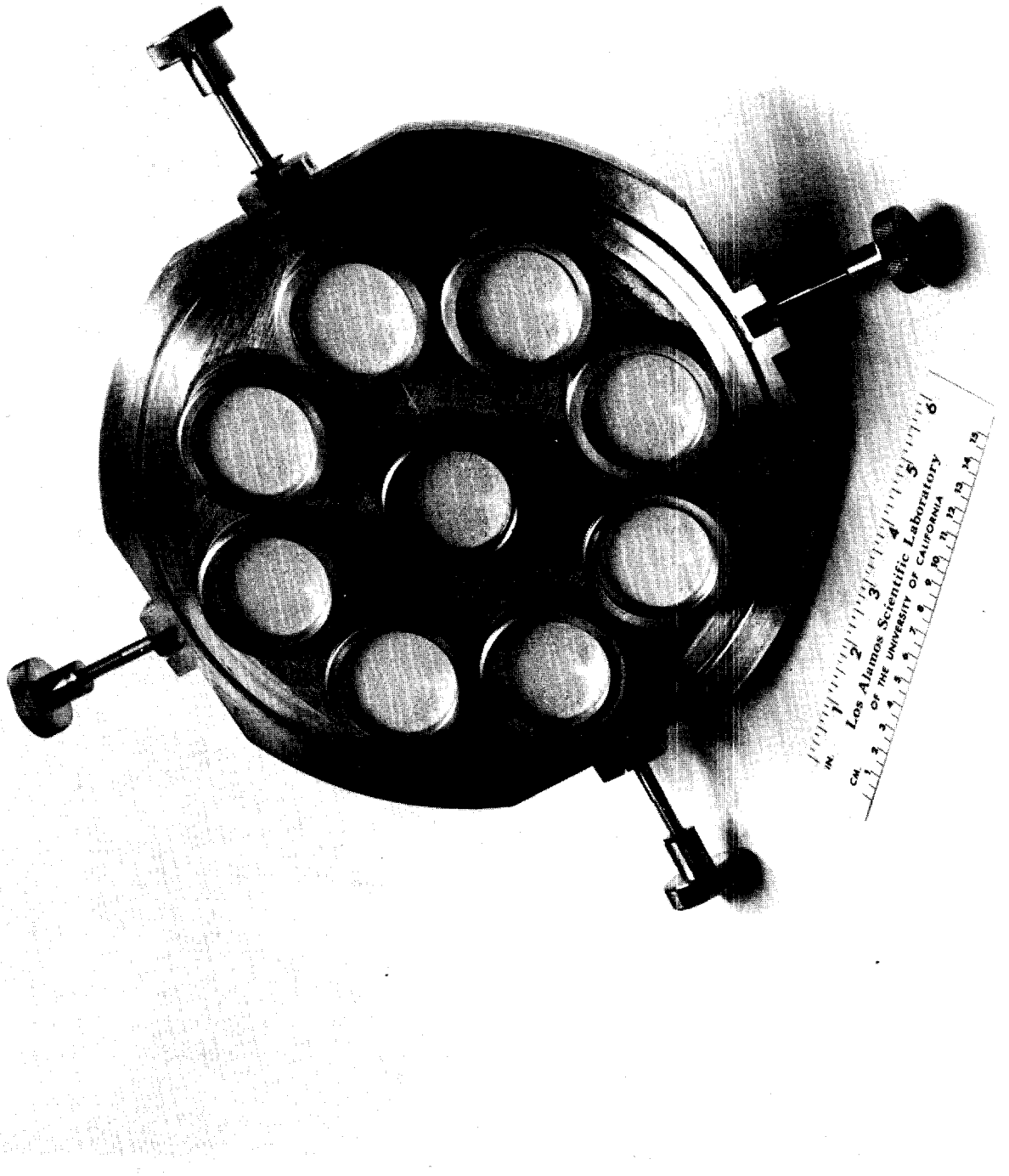

Figure 3. Sampler #4.

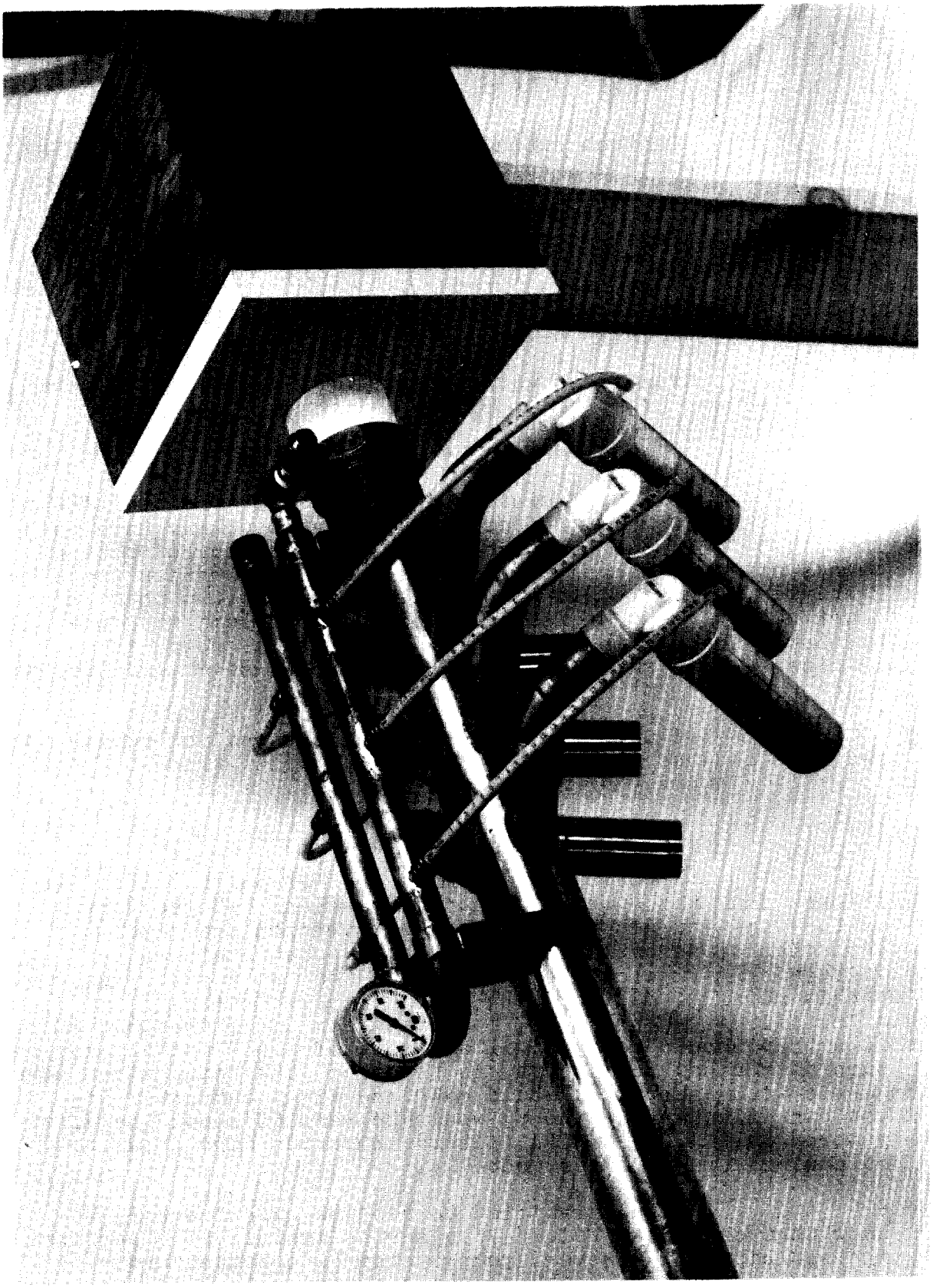

Figure 4. Aerosol Generation System.

DISCUSSION

FIRST: Can you explain the mechanisms that are taking place whereby the particles grow when you go from one HEPA filter to another?

GONZALES: Particle growth?

FIRST: That is what shows in almost every case. Your minimum size is larger on your second filter than your first in almost every slide shown.

GONZALES: What I showed in these particular slides were averages or minimums of several different runs.

FIRST: What comes to the second filter?

GONZALES: The 0.22 micron aerosol was for one or a few of the 17 runs. Now, for HEPA filter two, that aerosol may have been approximately 0.2 microns or slightly smaller but, out of both of these blocks of runs, there were only one or two instances where we saw slightly larger sizes out of HEPA filter number two than in HEPA filter number one. We found we had some problems with our sampling, but I don't think the data show we had a growth in particle sizes. As I said, these are minimums of several different runs.

FIRST: I understand that, but I suggest you review the displayed data because the change in particle size struck me rather strongly while viewing your slides.

GONZALES: The paper shows all of the data.

FIRST: I would like to make another point. I think you mentioned that the uncertainty of measurement becomes very large by the time you get to measuring penetration and size characteristics of aerosols after they have penetrated two or three filters. In view of the material in the two papers presented earlier this morning, dealing with theoretical equations for calculating filter penetrations, it would seem to me that one of the things that should be done, in any sort of experimental examination such as you have conducted, is to see if the results you have gotten agree with theory. I would make one final comment: I think you can calculate by theory what the results should be after passing through 2, 3, or 4 HEPA filters in series more accurately than you can measure it experimentally.

BLANCO: I was gratified to see the experimental data which show that each HEPA filter in a series installation performs with high efficiency. However, your system is operated under strict control conditions. Other speakers have described problems in the construction and operation of field installations.

BLANCO (cont.): What efficiency ratings should the design engineer assume for banks of HEPA filters that are operated in series?

GONZALES: The system will only be as good as the installation. We attempted to show that the filter media will attain these efficiencies. That is one of the critical points. The installation is extremely important. I don't know what engineers can do about that. I think Bob Mitchell showed a study yesterday on ways of in-place testing of HEPA filters and I believe this is very important. I think in-place testing is the only way we are going to be able to keep a good handle on something like that.

GILBERT: Thank you, Mr. Gonzales. Yesterday afternoon you saw a method for in-place testing on multiple-stage filters, both for an existing facility and a proposed facility at Los Alamos. Dow Chemical have their own procedure, developed by John Geer and Fred Linck, and they are prepared to describe it now. I will let you compare the methods.

IN-PLACE TESTING OF MULTIPLE STAGE HEPA FILTER PLENUMS

F. J. Linck and J. A. Geer
Dow Chemical, U.S.A.
Rocky Flats Division
Golden, Colorado

Abstract

Multiple stage High Efficiency Particulate Air (HEPA) filter plenums are required for plutonium processing facilities. This report reviews a method used for dioctylphthalate (DOP) aerosol testing in multiple stage plenums at Rocky Flats. A brief review is presented on aspects of the plenum design which relate to filter testing.

I. Introduction

Plutonium processing facilities at Rocky Flats have large exhaust ventilation systems containing two to four stages of HEPA filtration. Testing of these plenums is difficult because the streamline airflow conditions between stages prevents mixing of the test aerosol as well as obtaining representative samples of the aerosol. ANSI Standard ANSI N101.1-1972 on in-place testing therefore cannot be fully applied. Since the in-place test procedure is really a leak test, a different method of accomplishing the same thing was investigated.

II. Discussion

Rocky Flats has replaced or modified most of its filter plenums within the last few years. Each stage of filtration within the new or modified plenum is tested and certified to be at least 99.95% efficient with a pneumatically generated DOP aerosol. The criteria for plutonium building ventilation systems requires that all general building air will get two stages of filtration before release and all glovebox process air will get at least four stages of filtration.

The new filter plenums are designed with certain features which facilitate the testing. A few of these features will be reviewed briefly.

All plenums are of the walk-in variety (Fig. 1) which permit direct access to the filters and framework. This allows careful installation and inspection. The recommended minimum center-to-center spacing between stages in all plenums is seven feet, which assures adequate access space for both filter installation and leak testing.

Process air plenums are of all metal, welded construction with marine bulkhead type doors (Fig. 2). Penetrations of the skin of the plenum are minimized, but where necessary are sealed and pressure tested. The filter mounting framework (Fig. 3) is fabricated of rectangular steel structural tubing (usually four inches square). Special attention is given to flatness and surface finish to assure good gasket seal. All filter framework designs now provide eight-bolt holddown, a detail found essential to proper filter gasket sealing.

Each stage of filtration has a designated air lock to assure no possibility of leakage by bypassing air through a common air lock arrangement.

Since some plenums operate at substantial negatives, access is assured by a pressure equalizing valve which has been provided between the plenum and its associated air lock. Ball valves are used for this service and can be manipulated from within either the plenum or the associated air lock.

All plenums have viewports (Fig. 4) and good illumination to permit observation during testing. The viewports are used for routine Operator surveillance of the condition of the filter banks. A local panel (Fig. 5) containing temperature and pressure monitoring points provides additional surveillance of the filter conditions. All of these items help assure filter integrity after initial testing.

To facilitate testing, filter plenum size has been limited to a maximum of 44 filters, with no designs permitting an array of more than four filters in height. Older plenums (Fig. 6) often had hundreds of filters and looked about like this. One can easily project the problems of testing a plenum of this size.

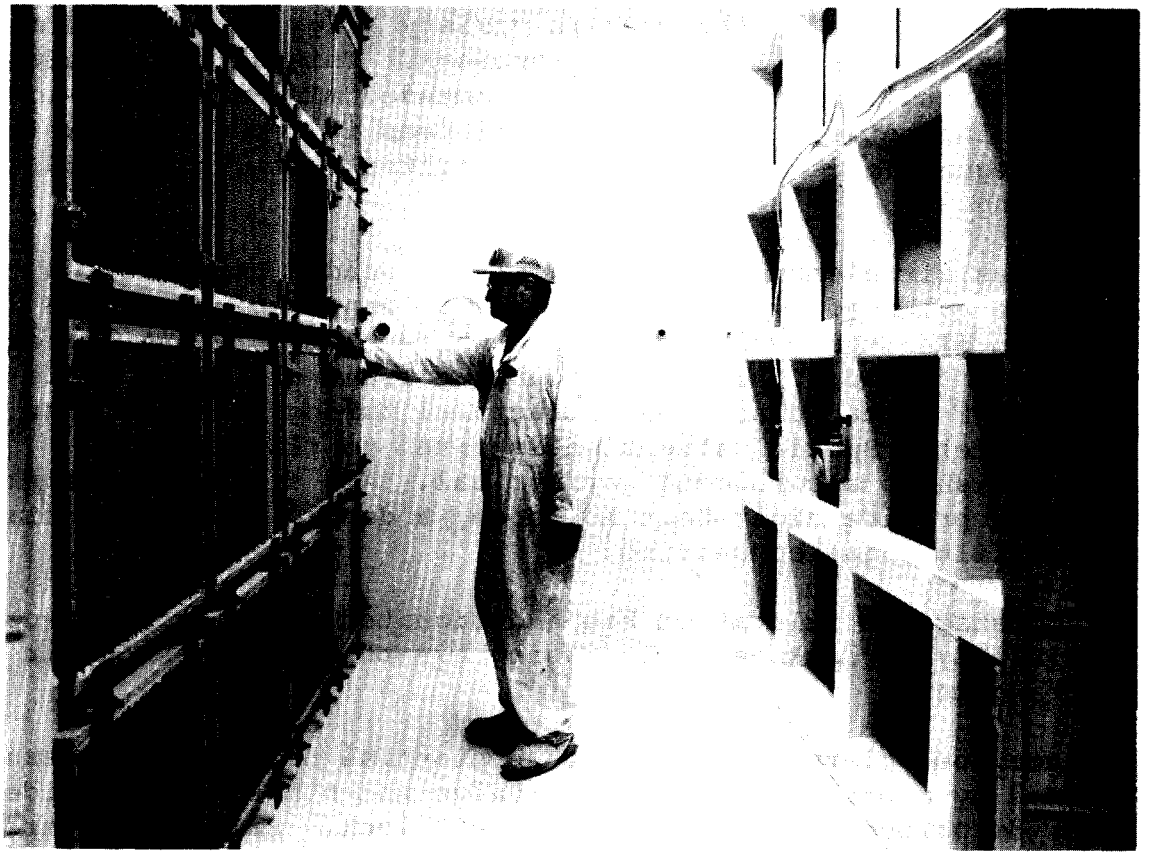

Fig. 1 View of plenum interior

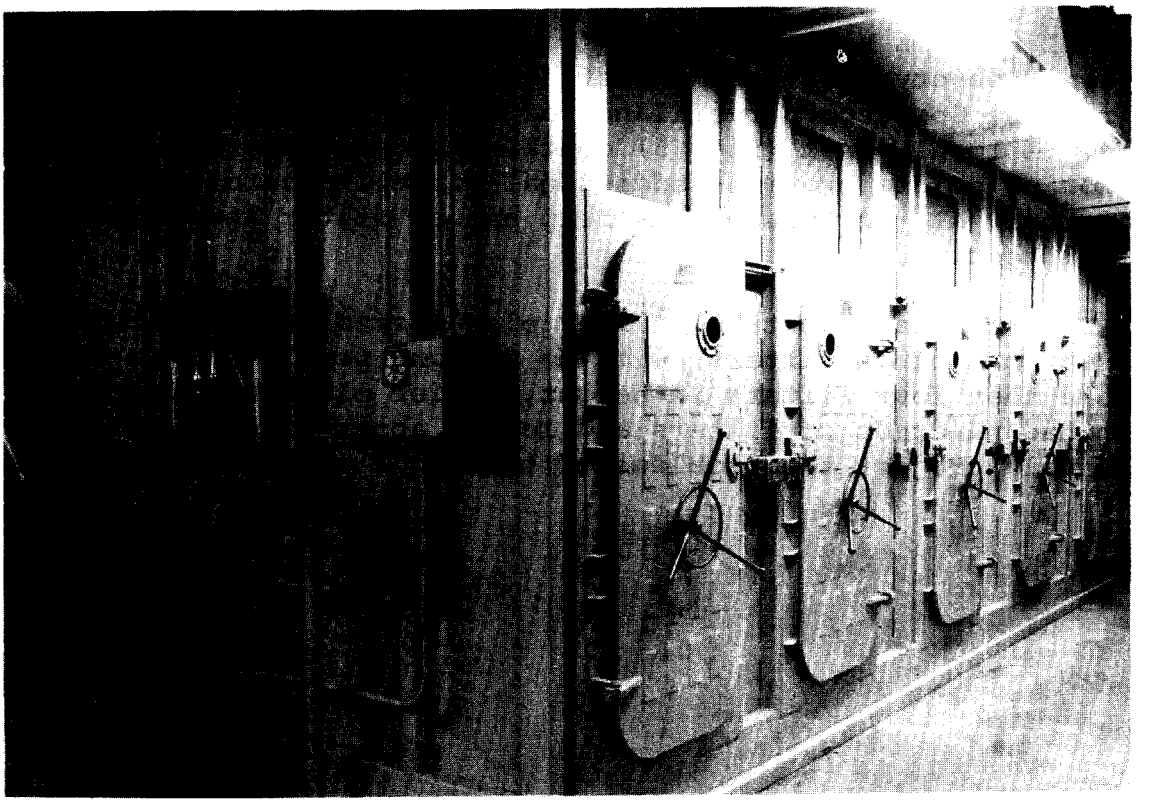

Fig. 2 View of plenum exterior

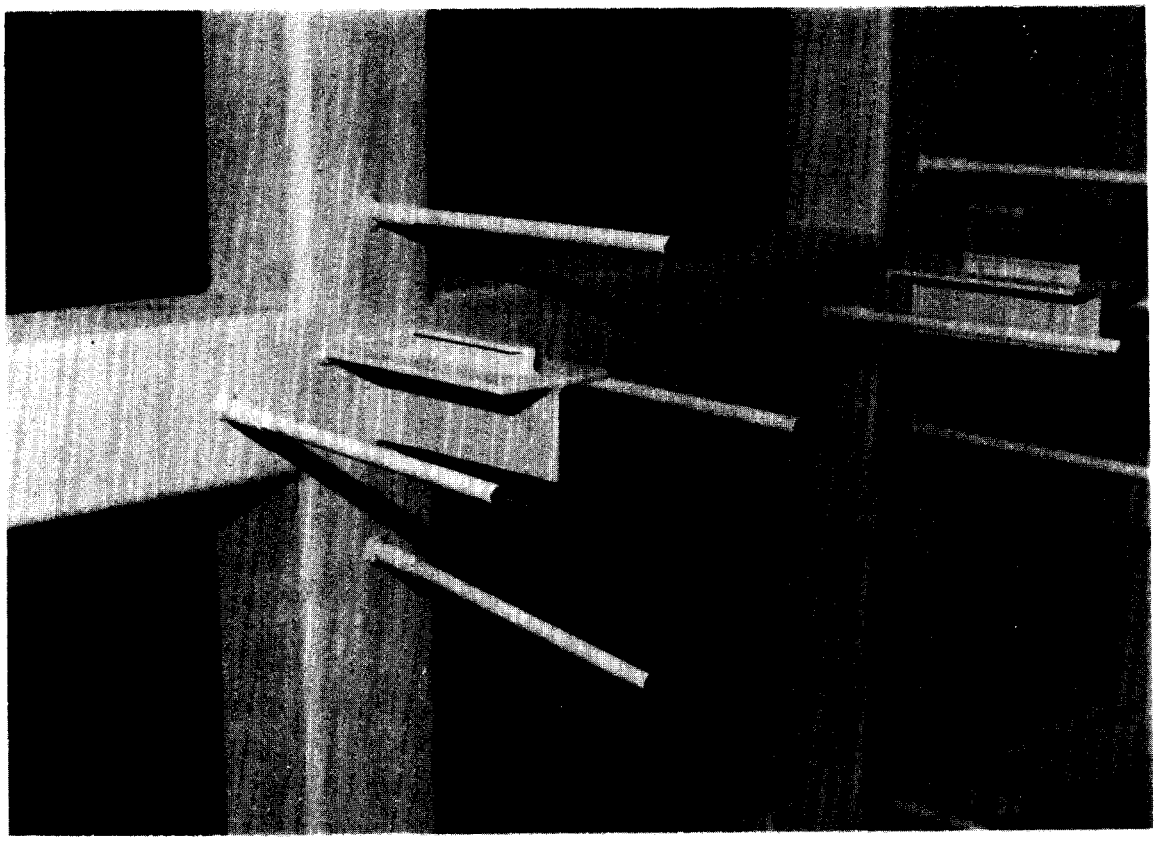

Fig. 3 Filter mounting framework

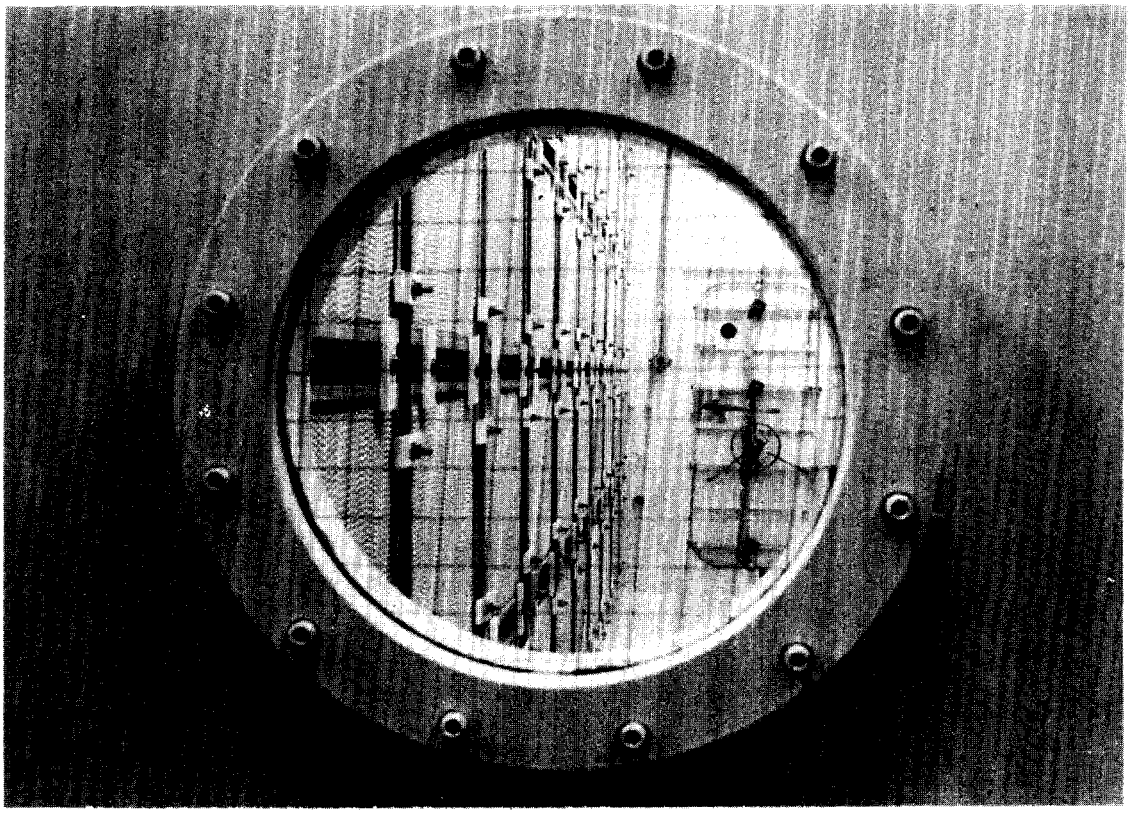

Fig. 4 Plenum viewport

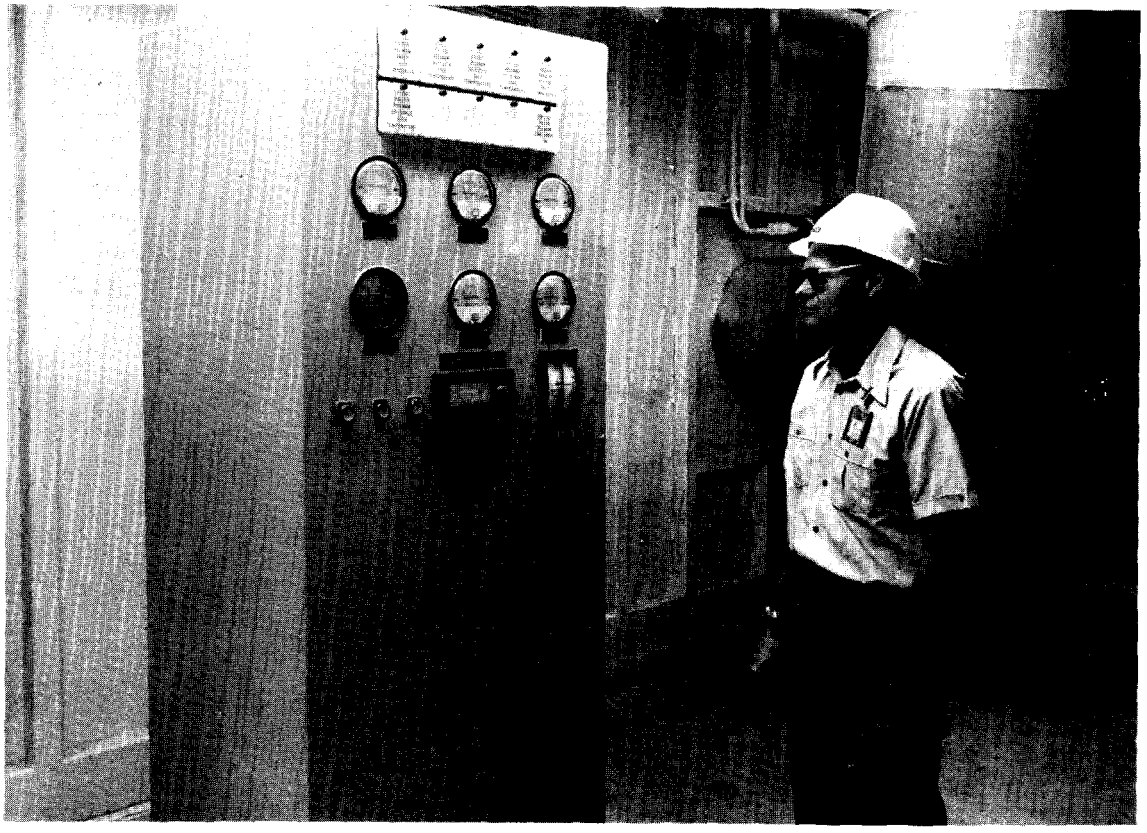

Fig. 5 Local panel

Fig. 6 Large filter plenum

With this brief description of the conditions under which the HEPA filters are installed and used, the following discussion will describe the testing developed for the plenums.

The first problems encountered in filter testing involve testing new plenums before they are put into service. Thorough testing involves not only the filters but also the plenum unit itself, the fans, and interconnecting ducting. The testing is somewhat simplified if the final stage of filtration is installed first. An overall efficiency test and/or a leak test can then be run on this stage.

Testing is done with a forward light scattering photometer and pneumatically generated dioctylphthalate aerosol. With the final stage installed and tested, aerosol can be injected into the surrounding room to check the plenum, its air locks, and the fans. This testing supplements the pressure and leak tests which should be performed before construction is completed. The fans and at least a portion of the exhaust system must be operable to establish a desired test airflow.

When these tests are completed, preceding filter stages are installed and tested one at a time, from the last stage forward to the first stage. In this manner, the upstream aerosol is well distributed and the only problem is determining the downstream concentration. This is accomplished by surveying the downstream face of the bank in question with a remote probe attached to the photometer. The remote probe contains a meter in the handle for ease of use.

This method of surveying for leaks or "leak probing" is a very sensitive method. When the probe samples the air from a leak, it is sampling some amount of straight 100% aerosol (assuming the upstream concentration is at a 100% level). The photometer meter reading is dependent upon the amount of leakage air up to a rate equal to the sample flow rate.

Since the photometer meter deflection is dependent upon the leakage airflow and the upstream concentration, it was thought that the leak probe readings might be used to estimate the amount of leakage air. The probe would have to capture most of this leakage air, or at least a reasonably constant percentage. A series of tests were devised to determine whether or not it might be practical to use this as a means of determining overall efficiency.

The forward light scattering photometers in use draw about 0.028 cubic meters per minute (m^3/min.) or one cubic foot per minute (cfm) of air through the probe (Fig. 7). A point source leak of only 0.0028 m^3/min. would therefore produce a photometer reading of 10% if the leakage aerosol was all captured by the probe. This is 100 times the quantity needed to produce a full scale meter deflection on the normally used 0 to 0.1% scale.

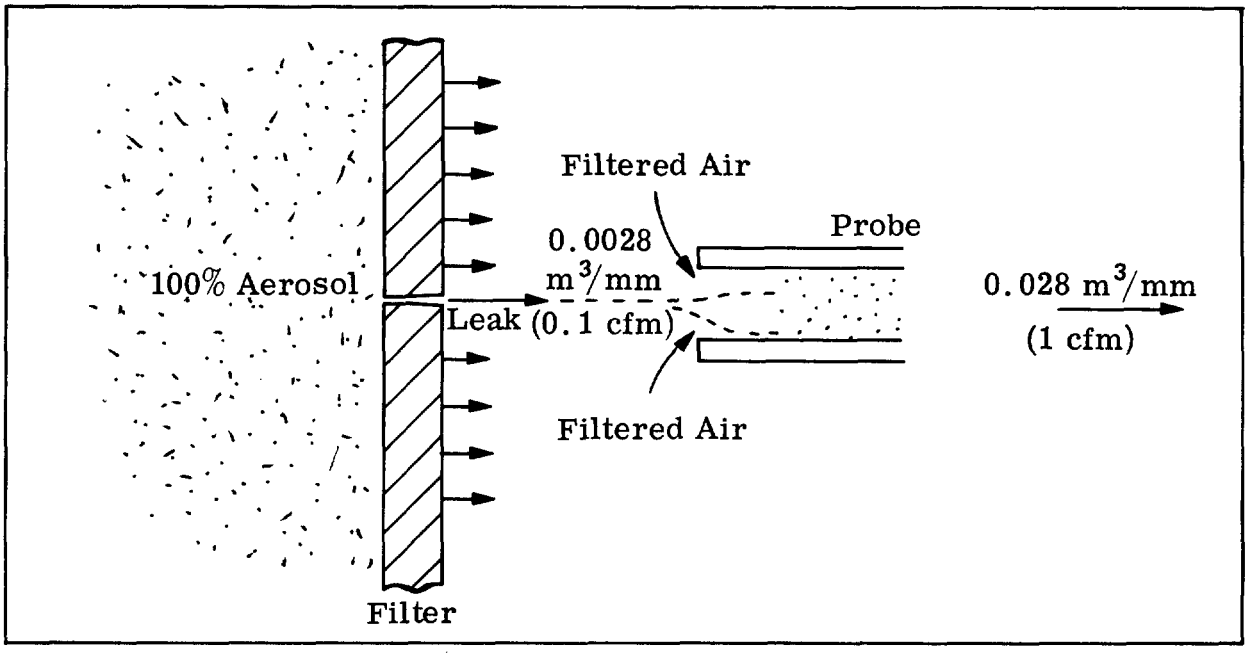

Fig. 7 Illustration of leak probing airflow

This discussion assumes that no DOP aerosol penetrates the filter media. It should be mentioned that the filters used in the following tests were checked at the Quality Assurance Test Station and found to have an average penetration for 0.3 micrometer particles of only 0.006%. This is extremely good and, as a result, the penetration of the approximately 0.7 micrometer pneumatically generated aerosol was found to be essentially zero except where filter media damage or a leak occurred. In fact, any time the Quality Assurance Station penetration exceeded 0.01% it was possible to find one or more leakage points in the filter by probe testing.

Because of the extremely high efficiency of modern day media, the leak probe method is very effective. It is easy to differentiate between good media which shows no penetration and a leak which does.

A single stage of 24 HEPA filters was installed in a new plenum which could be accurately tested for overall efficiency. A plate with orifices of different sizes was installed in place of one of the filters to permit correlating leakage airflow with efficiency.

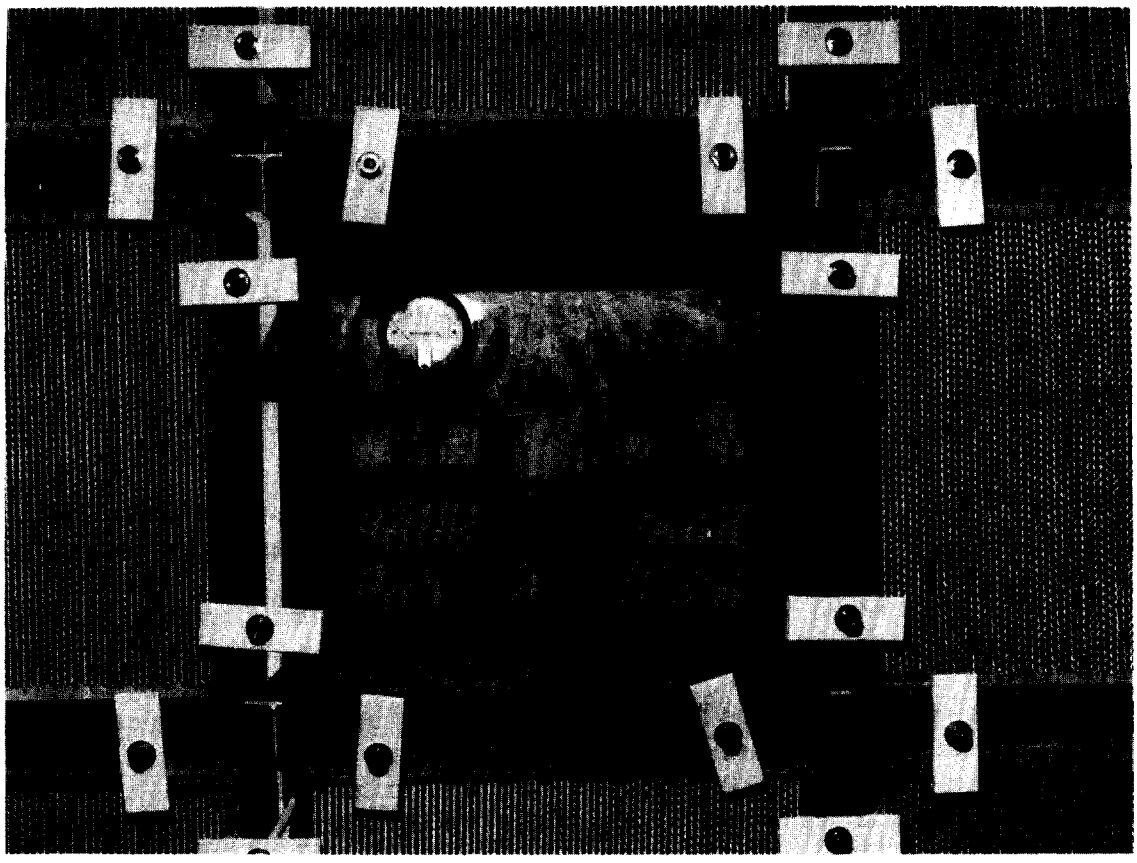

Fig. 8 Orifice plate

Airflow through the orifices was measured with a hot wire anemometer. In the larger opening sizes the airflow was found to agree well with that predicted by a simplified orifice equation:

$$Q = 0.0163A\sqrt{\Delta P}$$

Where Q = Airflow in m^3/min.
A = Orifice area in square centimeters (cm^2)
P = Pressure drop in millimeters of water (mm H_2O)

The installed orifice plate is shown in Fig. 8. The various orifices are covered with masking tape in this illustration.

The filter bank was first checked for overall efficiency and then leak probed to make certain no significant individual leaks were present. The orifices were then checked one at a time and the overall efficiency measured. Table I shows a comparison between the measured efficiency and the efficiency calculated from the airflows for the larger orifices.

Table I. Measured vs. calculated efficiency

Orifice Diameter (Centimeters)	Measured Flow (m^3/min.)	Measured Efficiency (Percent)	Calculated Flow (m^3/min.)	Calculated Efficiency (Percent)
5.1	0.99	99.59	0.98	99.55
2.5	0.25	99.84	0.25	99.89
1.3	0.056	99.96	0.061	99.97

No instrumentation was available for accurately measuring the airflow through orifices smaller than 1.3 cm.

These tests confirmed that the filter penetration was low enough to permit calculating the installed efficiency by means of the leakage airflow. Results also indicated that the overall efficiency test, even when it can be performed, may not be suitable for Rocky Flats. It does not differentiate between a large number of very small leaks (which are permissible) and a few large leaks (which may be unacceptable because of their size). A surprisingly large amount of leakage air is permissible in this large a bank of filters (approximately 0.06 m^3/min. or 2.0 cfm) with the bank still showing what is normally an acceptable efficiency.

Several pinholes were then made in one filter to determine small leak characteristics, using 0.3 mm diameter wire. Larger holes, approximately one mm diameter, were also made using a sharp pencil. A leak probing of these holes indicated that the aerosol dispersed very little horizontally because of the vertical alignment of the separators but dispersed vertically approximately 2.5 cm each way from the hole because of turbulence in and behind the filter. These small leaks, whether on the front or back filter surfaces, were easily detected as long as the filter surface was scanned horizontally with each pass within 5 cm of the previous one. This information was used to develop the probing pattern shown in Fig. 9 where each filter is scanned for leaks by leak probing first around the gasket surface, then along the back face of the filter. Scanning approximately 5 cm from the back of the filter gives good sensitivity without any leaks being missed.

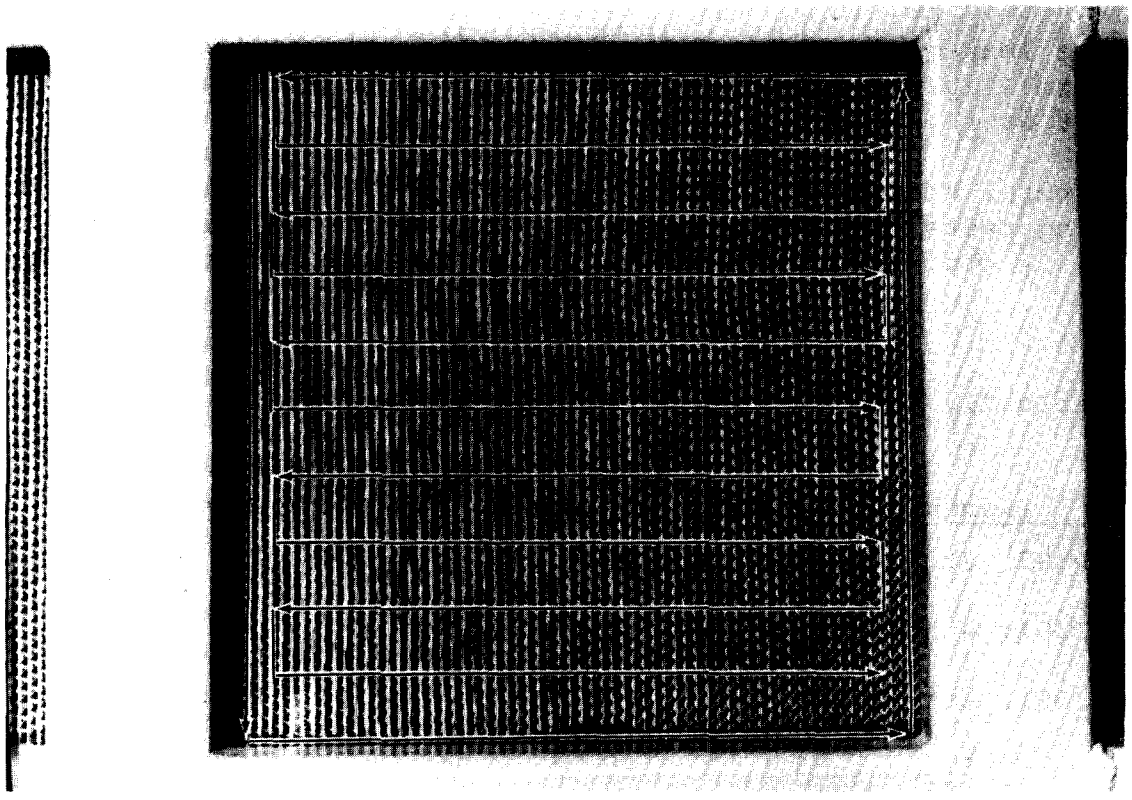

Fig. 9 Filter scanning pattern

Once a leak is found, it is carefully scanned to determine its exact location, if possible, and its shape (i.e., Is it a puncture or a slit?). Filters with slit leaks are rejected since the probe cannot capture most of the leakage airflow. The probe is carefully located at the point of maximum aerosol concentration and a reading taken. This reading is used to calculate the leakage airflow. All the leakage flows are then summed up to obtain an overall leak rate.

The technique as finally developed consisted of (1) introducing DOP aerosol in the upstream ductwork to assure proper dispersion, (2) measuring the upstream concentration by sampling ahead of the filters being tested, (3) adjusting the photometer to a 100% reading when possible, (4) leak probing the downstream surface as outlined previously, (5) rejecting or repairing off-limit leaks, (6) recording values of acceptable leaks, and (7) calculating the overall efficiency.

The leak calculation is made as follows:

$$\frac{\text{Leak probe meter reading}}{\text{Upstream concentration}} \times \text{Probe flow} = \text{Leak flow}$$

$$\text{Penetration} = \frac{\sum \text{Leak flow}}{\text{Total flow}}$$

The leakage locations, magnitude, and calculations are recorded on a form (Fig. 10) which is kept on file until the filters are retested or replaced.

Several stages of filtration, including the one used in the preceding tests, have been both overall efficiency tested and leak tested. A comparison of three of these plenums is shown in Table II.

Table II. Comparison of overall and leak test efficiencies

Plenum	Overall Eff. (Percent)	Leak Test Eff. (Percent)
FP302, 4th stage	> 99.99	99.996
FP301, 4th stage	99.997	99.998
FP601, 1st stage	99.997	99.999

A more difficult problem is the retesting of multiple stage plenums while in use. Normally, radiometric monitoring is used to continually check plenum operation. However, if filters are changed or the radiometric monitoring indicates a potential problem, it is necessary to perform a DOP test without interrupting the system. In this case, the distribution of aerosol on the upstream side of the filters is the major problem.

The method developed for this testing, when a reasonable upstream aerosol dispersion cannot be obtained, is as follows:

1. The upstream area in the vicinity of the filter to be checked is blanketed with visible quantities of aerosol.

2. The downstream surface of the filter and frame are leak probed.

3. The general magnitude of all leaks is determined; i.e., is it in the range of 0 to 0.1, 0 to 1.0, or 0 to 10% on the photometer scale?

4. Any significant leaks are corrected and any other leaks are rechecked to make certain they are not significant.

HEPA FILTER TEST REPORT

Bldg. _____ Plenum _____

Test Date _____ Stage ____ Date filters changed _____

☐ Overall Efficiency Method ☐ Leak Test Method

I. Leak locations and size.

	1	2	3	4	5	6	7	8	9	10
A										
B										
C										
D										
E										

View looking upstream

II. Calculations.

Total airflow _____ cfm, determined by: _____

Filter bank ΔP: ____ inches H_2O. Upstream conc. _____%

III. Results.

Leak flow _____ cfm÷total airflow _____cfm=_____Pen.

Efficiency: _____% Certified by: _____

Remarks:

Fig. 10 HEPA filter test report

This approach does not provide an overall efficiency value for the stage of filters but experience has shown it to be consistent in producing an acceptable filtering capability. Trained hourly personnel performing this test have a tendency to "oversmoke" the area being tested. This results in finding and repairing smaller leaks than would otherwise be necessary. A well designed and constructed plenum will have so few leaks, this unnecessary repair presents no serious problem from the cost standpoint.

III. Conclusions

The approach outlined in this presentation provides Rocky Flats with better assurance than does the overall efficiency method that a bank of filters will perform satisfactorily. The high sensitivity of the method, coupled with its ability to determine quantity and approximate size of leaks, makes it a valuable step in the filtering operations.

DISCUSSION

SHEARER: I am interested in the inference you made that large holes were present in the filtering media. I would like to ask if it is a common occurrence that large holes could occur in a filter as opposed to the structural member itself?

LINCK: It isn't common. I have found only two such cases in checking plenums. We found these holes by the leak test. Once you locate the leak you can easily see it visually. Our people had inspected the filters before we closed the plenums, but had overlooked these leaks. We found only a couple of these cases where we found significant holes.

MARBLE: In the power plant industry, they won't allow patching of HEPA filters. The military specification says no leak can be patched, and yet I saw in your slides,filters which obviously had been patched. Do you wish to comment?

LINCK: Normally we don't patch leaks. One photograph was of a 560 filter plenum. It is on a room ventilation system and we may or may not patch the leaks until we get a chance to change out the filters. In the smaller plenums we don't patch leaks, we change filters.

MURROW: The framing you showed for the filter holders was of excellent construction. However, contrary to what is recommended in ORNL-NSIC 65, I noticed that you used one bolt common to two filters. This is also contrary to the AEC requirement in power plants. Do you find this method of using one bolt for more than one filter is capable of providing a good seal on all filters, especially after you change out one filter?

LINCK: We have checked this out. As long as we maintain tension along the remaining bolts around the filter, we don't have trouble with the seal on the surrounding filters. Generally, we change the whole bank at once and this usually isn't a problem. The filters will generally have to be changed because they are plugged. The common holddowns across the filters actually work out very well. If you have one holddown per filter, you have a torque or bolt bending problem to correct. With the common holddown, the torque balances across the filters.

YORK: With regard to feeding smoke into the filter, do you supply it one filter at a time or do you apply smoke to the entire bank and then do your probing operation filter by filter?

LINCK: When we can, we apply smoke to the entire bank, such as on the first stage. On downstream filters, we can't. When we can't apply it to the entire bank, we have to do it modularly. The aerosol has a tendency to disperse between the filters and stay there for quite a while, since there is not too much air flow. Then, we essentially do it one filter at a time.

YORK: When probing, do you keep the smoke on the entire bank?

LINCK: When we can disperse it across the entire bank, yes.

YORK: Do you worry about the total amount of smoke you have injected into the filters?

LINCK: No. The tests don't take that long and we have never found any increase in pressure drop because of the tests. We usually complete a test in about half an hour.

COMPARATIVE FILTER EFFICIENCY TESTING USING DIOCTYLPHTALATE AND SODIUM CHLORIDE AEROSOLS*

O.Jovanović, M.Vidmar, M.Tubić, D.Patić
R.Radosavljević and R.Smiljanić
Boris Kidrič Institute of Nuclear Sciences,
Beograd - Vinča, Yugoslavia

Abstract

Efficiencies of high efficiency particulate air (HEPA) filters were tested using dioctylphatalate (DOP) and sodium chloride (NaCl) aerosol methods. Commercial generator and detecting unit were used for the DOP test. In the NaCl test a commercial sodium flame photometer and home made generator were used. The aerosols produced and used in both DOP and NaCl tests had similar particle size distribution and MMD. Particle size distribution of both DOP and NaCl aerosols was determined by means of a six-stage Andersen cascade impactor. The MMD were determined from the cumulative per cent mass probability curves. In the paper the description of the sodium chloride generator and its characteristics (production rate, particle size distribution and MMD) are also given.

Introduction

Several experiments have been reported up today dealing with the comparison of high efficiency particulate air filter penetration measurements using DOP and NaCl aerosols [1-3]. As it is known, most of the authors came to a conclusion that NaCl aerosol is practically as applicable as DOP aerosol and has, at the same time, several advantages. However in all these experiments the particle size distribution of both aerosols was different. Mostly a monodisperse 0.3 /um DOP and polydisperse sodium chloride aerosol with different

*Work supported by the U.S.Environmental Protection Agency through the special foreign currency program

MMD were used. One author [3] used polydisperse DOP and NaCl aerosols, but made no conclusion due to difficulties he faced when detecting the NaCl aerosol.

In our work were used polydisperse DOP and NaCl aerosols having similar MMD and particle size distribution.

Ecuipments and methods

Filter testing facility

The filter testing facility built at the Boris Kidrič Institute is shown in Figure 1.

The air flow rate through the facility was measured by means of a orifice air flowmeter the calibration of which was performed by Heat and Mass Transfer group of the Institute Boris Kidrič. The ventilator used was capable of producing 100 mm w.g. pressure drop and a flow rate through the filter up to 90 m^3/h. The dimensions of the facility are given in the Figure 2.

DOP aerosol test equipment

A commercial ATI - DOP generator (model TDA - 41) and detector (model TDA - 2D) were used in the experiments. Only one nozzle was used for aerosol production and the desired particle size distribution was obtained by using proper air flow rate (1750 l/h) through the generator.

NaCl test equipment

A commercial Moore´s portable NaCl detection unit was used. The unit was calibrated by the Chemical Defence Establishment, Porton Down, England. The NaCl concentration range, which can be measured by this instrument, is 0.16 - 13000 $\mu g/m^3$.

NaCl aerosol generator shown in Figure 3 was designed and built at the Boris Kidrič Institute. The aerosol is produced from NaCl water solution. Characteristics of the generator (aerosol production and particle size distribution) were determined for different working con-

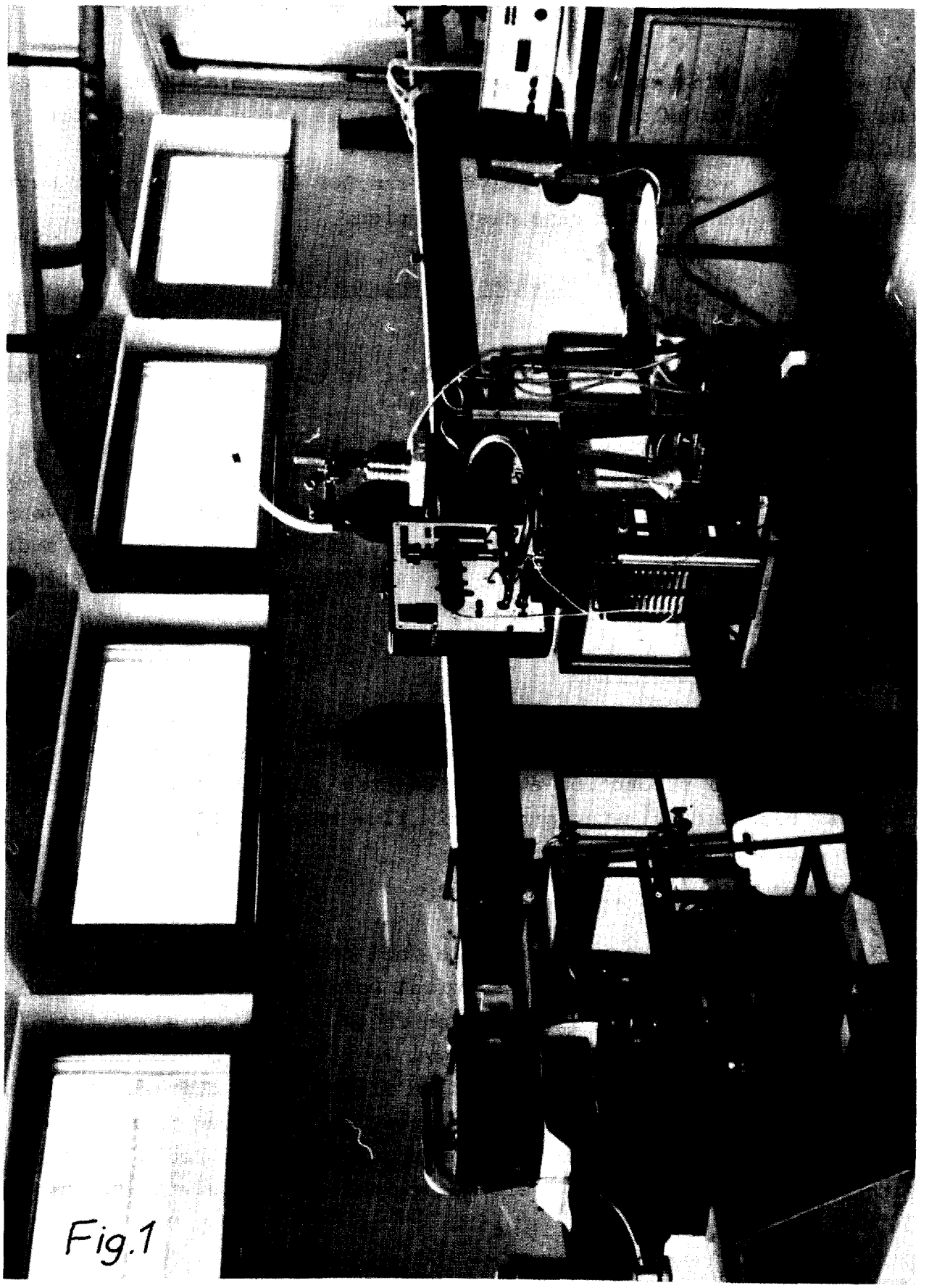

Fig.1

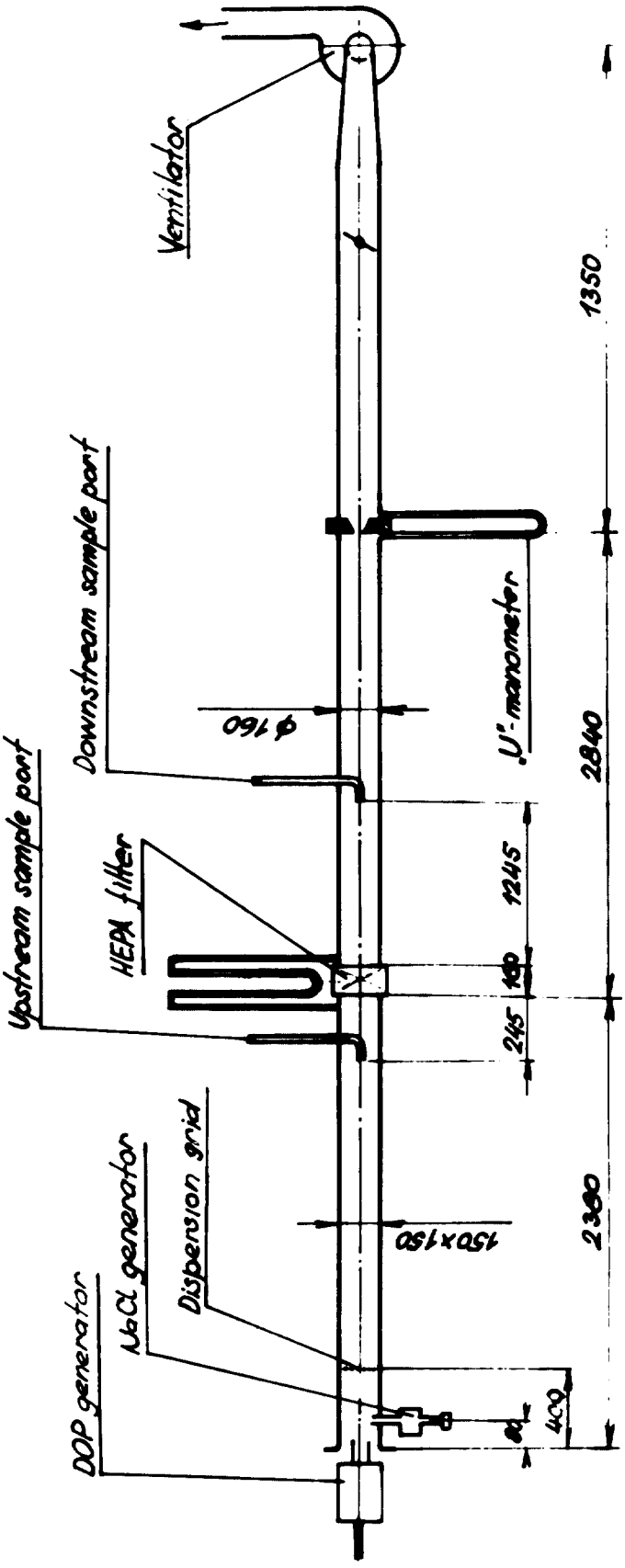
Ventilator
Downstream sample port
Upstream sample port
HEPA filter
DOP generator
NaCl generator
Dispersion grid
U-manometer
ϕ160
150x150
1350
2840
1245
100
245
2380
400

Fig. 2

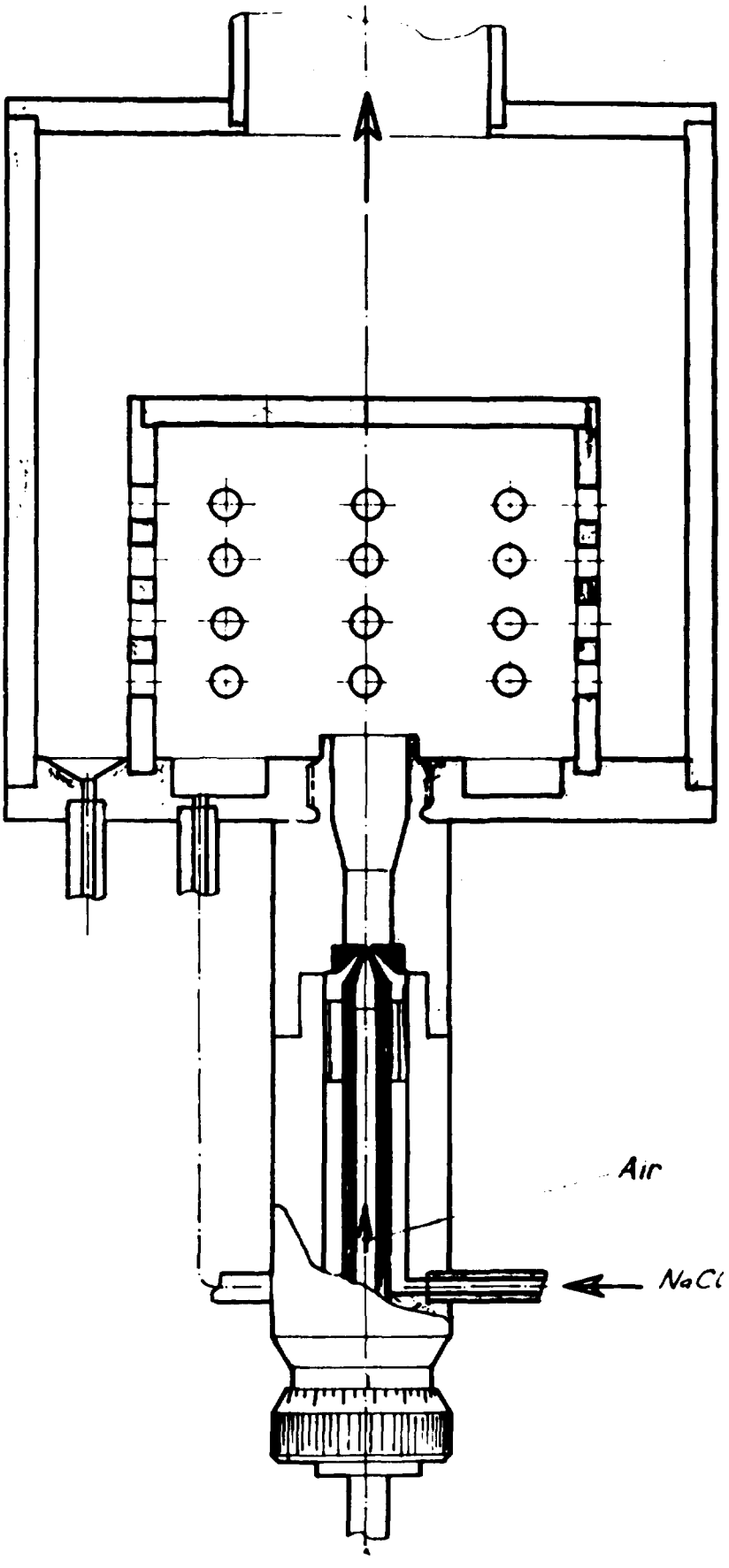

NaCl AEROSOL GENERATOR

Fig. 3

ditions (nozzle diameter, air flow rate through the nozzle, solution concentration, temperature and feed rate). Some of them are given in Figures 4 - 6.

Determination of particle size distribution

Particle size distribution of DOP and NaCl aerosols was determined by means of a six-stage Andersen cascade impactor. Mass median diameter was determined from the cumulative per cent mass versus particle diameter curves.

Since the data of the effective cut-of size (ECS) for individual stages of the Andersen cascade impactor given in the literature are for materials having density $\rho = 1$, the ECS for NaCl particles were calculated using the well known relation:

$$\rho d^2 = \text{const}$$

where:

d = ECS for particular impactor stages.

Test results

Two types of high efficiency particulate air filters* were tested. The manufacturer's standard test at 50 cfm flow rate for the filters of each type showed the following results:

		Resistance (mm W.G.)	Penetration (%)
Filters with Separators	No 1	0.68	0.022
	2	0.70	0.014
Filters w/c Separators	3	0.84	0.120
	4	0.84	0.090
	5	0.90	0.030
	6	0.90	0.150

Test conditions were the following:Air flow rate through the filter 71 m^3/h,air flow rate through the DOP generator 1750 l/h (0.65 atü),air flow rate through the NaCl generator 260 l/h (4.6 atü), NaCl aerosol production round 0.355 g/h,duration of the penetration measurement 2 minutes.

*Flanders Filters Inc. 6x8x6 inch stock number 7 C 70-L and 7070-L

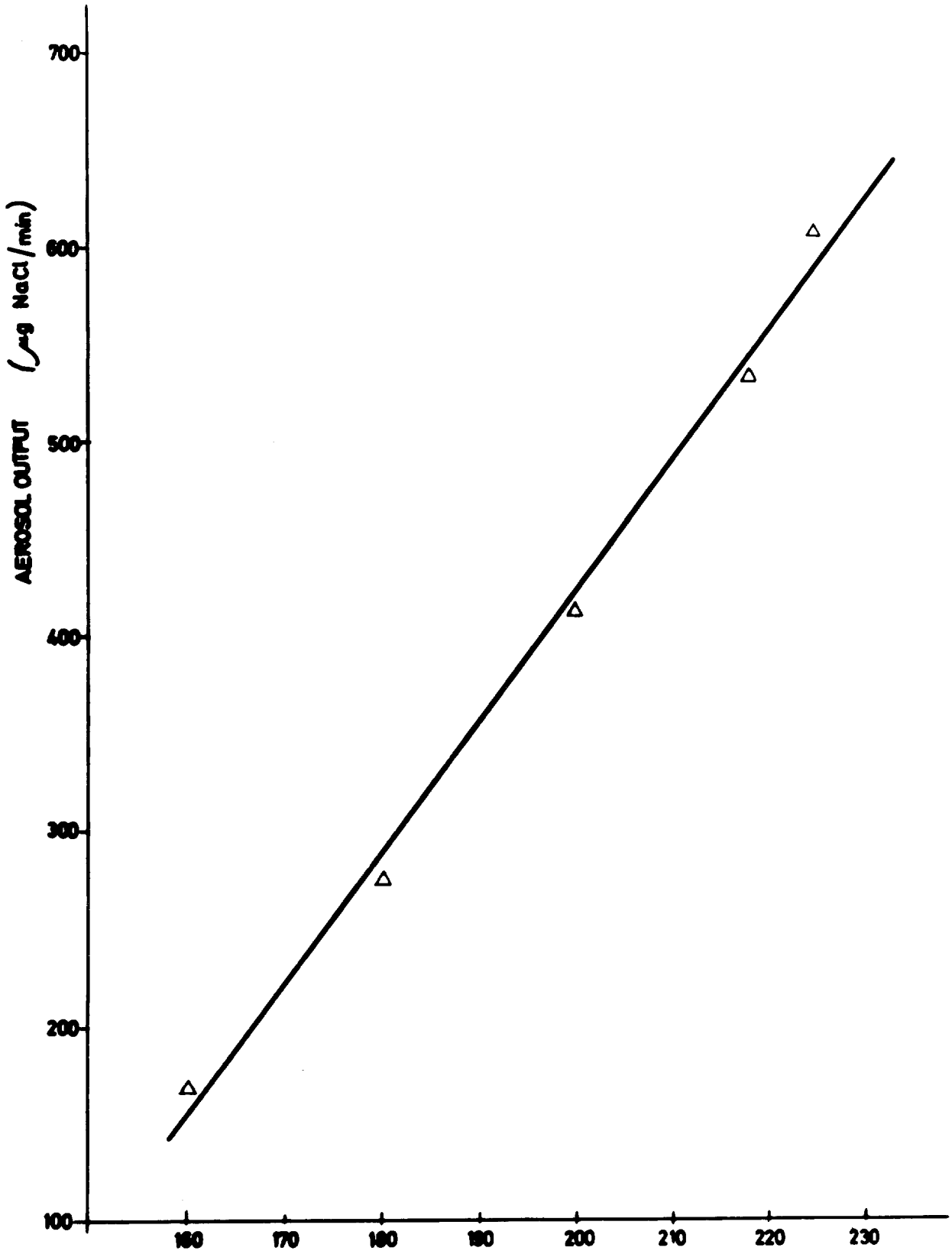
AEROSOL OUTPUT (µg NaCl/min)
700
600
500
400
300
200
100
160
170
180
190
200
210
220
230
AIR FLOW RATE THROUGH THE NOZZLE l/h

Fig. 4

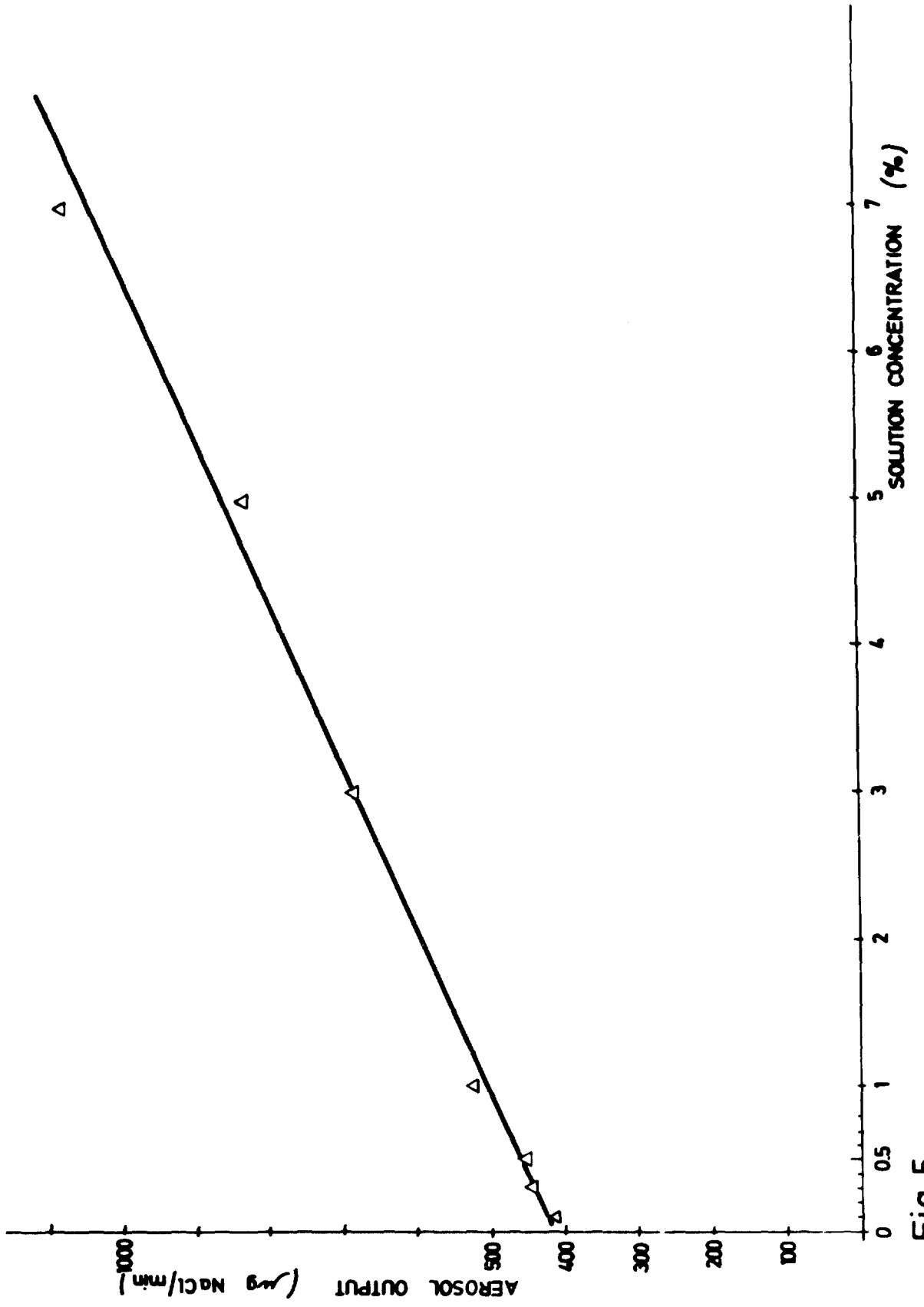
AEROSOL OUTPUT (mg NaCl/min)
1000
500
400
300
200
100
0
0.5
1
2
3
4
5
6
7
SOLUTION CONCENTRATION (%)

Fig. 5

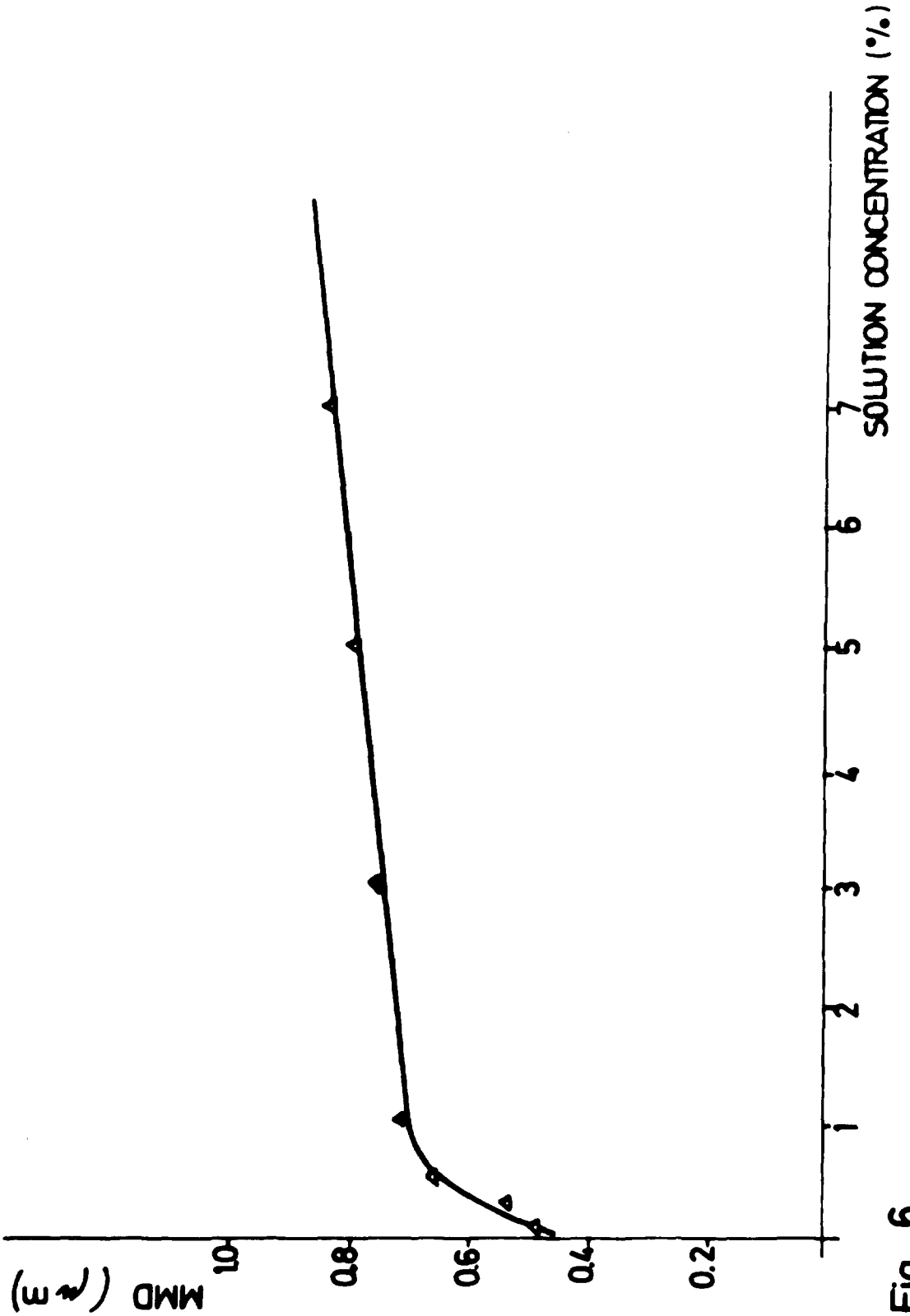

Fig. 6

Figure 7 shows the cumulative per cent mass versus particle diameter curves of DOP and NaCl aerosols used in the experiments.

The aerosol homogeneity i.e. sodium chloride or DOP particles and air mixing was checked up and down stream by moving the sampling probe across the duct. This check showed a good upstream aerosol homogeneization since there was no difference in instrument reading in the region between 12 mm from one and 28 mm from the opposite duct wall. The same was down stream exept for filters No 3,4,5 and 6 where the check performed discovered pinholes. Being these pinholes close to the filter edge the sampling probe was positioned in the centre of the duct when measuring filter penetration.

The measured penetrations for the tested filters are given in the Table 1.

Table 1

Filter No	Penetration %	
	DOP	NaCl
1	0.0080	0.0084
2	0.0040	-----
3	0.0350	0.0250
4	0.0070	0.0060
5	0.0090	0.0080
6	0.0190	0.0160

Sodium chloride aerosol data for filter No 2 are not avalable due to claging of the filter.

One can conclude from the Table 1 that no matter what kind of aerosol is used (solid or liquid) the penetration is practically the same as long as the particle size distribution and MMD are similar. Slightly higher penetration obtained with DOP is probably due to the small difference in MMD. The great discrepance between the values given in the Table 1 from those given by the manufacturer are in our opinion due to the much smaller diameter of the monodisperse DOP aerosol used by the manufacturer.

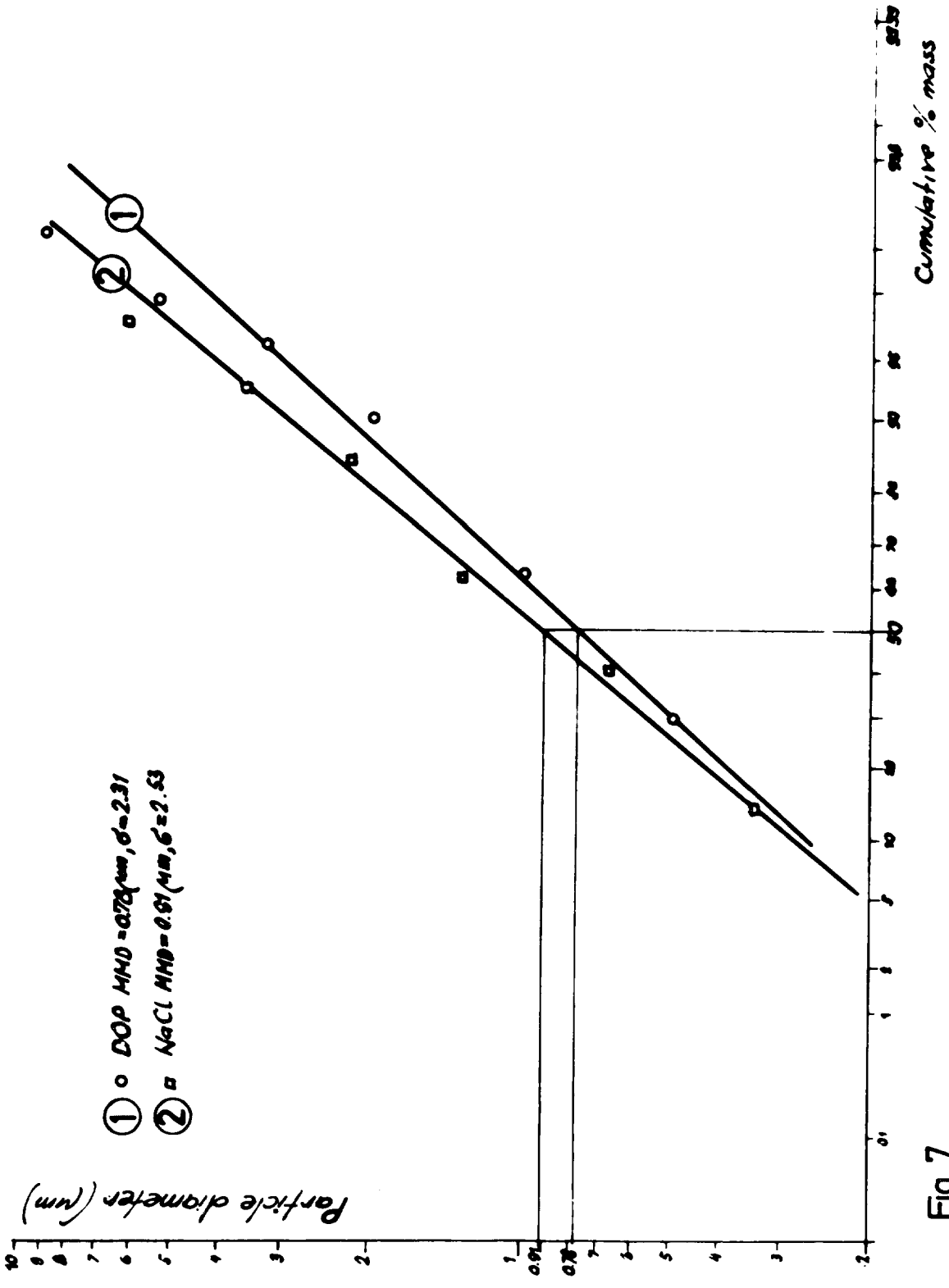
Particle diameter (μm)
Cumulative % mass
① ○ DOP MMD = 0.78 μm, σ = 2.31
② □ NaCl MMD = 0.91 μm, σ = 2.53

Fig. 7

References:

1. Murrow J.L. and Nelson G.O., "HEPA Filter Testing: Comparison of DOP and NaCl Aerosols", Proceedings 12th AEC Air Cleaning Conference, 808 (1972).

2. Mitchell R.N., Bevis D.A., and Hyatt E.C., "Comparison of Respirator Filter Penetration by Dioctyl Phathalate and Sodium Cloride", Am.Ind.Hyg.Assoc.J. 32, 357 (June, 1971).

3. Grady B.J.Jr. and Henry K.H., "In-Place Efficiency Tests of a Large Scale Ventilation Exaust filter", Proceedings 12th AEC Air Cleaning Conference, 646 (1972).

4. Andersen A.A., "A Sampler for Respiratory Health Hazard Assessment", Am.Ind.Hyg. Assoc. J., 27 (March-April, 1966).

FLAME GENERATION OF SODIUM CHLORIDE AEROSOL FOR FILTER TESTING

J. Edwards and D. I. Kinnear*
United Kingdom Ministry of Defence
Chemical Defence Establishment,
Porton Down, Salisbury SP4 OJQ

Abstract

A generator for sodium chloride aerosol is described, which, when used in conjunction with a sensitive portable sodium flame detector unit, will permit the in-place testing of large filter installations having air throughputs up to about 80,000 m^3/h, at penetrations down to at least 0.005 per cent.

I. Introduction

The particulate penetration of high efficiency air filters may be tested by using a sodium chloride aerosol in conjunction with a sensitive sodium flame photometer (penetrometer). The British Standard test for high efficiency filters (BS 3928), which gives penetrations ranging from a half of to equality with those recorded by the American DOP test, employs an aerosol generated by atomization and evaporation of an aqueous salt solution. An output of 250 mg/min of aerosol is obtained from a battery of compressed air atomizers and with the standard photometer capable of measuring to rather better than 0.01 $\mu g/m^3$ tests on filter units of capacity up to 80,000 m^3/h are theoretically possible, at penetrations down to about 0.005%. This performance probably represents about the limit for spray-generated aerosols; however, the high consumption of compressed air by the atomizers, with resulting lack of portability of the compressor, and the size of the duct required to allow the aerosol the two seconds residence time necessary to ensure dry particles, generally preclude the use of the BS 3928 apparatus for in-place installation testing.

When considering the requirement for a relatively cheap, portable method for the in-place testing (primarily leak-testing) of large filter installations of throughputs up to 80,000 m^3/h it was clear that the existing CDE portable photometer(1), which can measure salt concentrations as low as 0.1 $\mu g/m^3$ and is now available commercially(2), would suffice as a detector provided that a fine salt aerosol could be generated at the rate of about 2.5 g/min. Of the possible methods of generation the most promising seemed to be the flame atomization method used by Dyment(3,4), in which salt is evaporated by the application of a high temperature flame and on cooling condenses to form a cloud of sub-micron particles. Dyment employed an oxygen-acetylene powder fed blowtorch ("spray welder") to generate aerosol at the rate of several grammes per minute. An apparatus very similar to his was made and tested.

* Read by Richard G. Dorman

II. Performance of Powder-Fed Blowtorches

Three problems were encountered in operating the equipment.

1. The salt had to be supplied to the blowtorch as a finely-ground powder, via a metering mechanism. To ensure a constant powder feed rate a relatively complex pre-treatment of the salt was required, comprising ball-milling with colloidal graphite, drying, sifting and storing at elevated temperature.

2. Even with the most careful pre-treatment of the salt occasional blockages occurred both in the powder feed apparatus and in the fine internal passages of the blowtorch.

3. Only a somewhat variable fraction, about 30%, of the salt entering the torch was evaporated and condensed to form an aerosol. The remainder emerged from the flame as particles ranging in size up to about 100 μm equivalent diameter. Clearly, the dwell time of the powder in the flame was too short to allow evaporation of the larger particles.

These problems persisted with other designs of spray-welder and powder feed apparatus; the best conversion to submicron aerosol, about 60%, was achieved only by using very bulky, complex and expensive apparatus consuming large volumes of fuel gas. Because of these shortcomings an alternative, simple way of introducing salt to the flame was sought, which would allow a much longer dwell time to ensure complete vaporization. A solution was found in feeding a specially formulated solid rod or stick, consisting mostly of salt, into the flame of a modified blowtorch.

III. Development of a Rod-Fed Blowtorch

The first experiments, in which rods of pure salt were fed into blowtorch flames, were unsuccessful. Molten salt dripped freely from the rods and very little aerosol was produced. Various materials were added to the salt in an attempt to form a sponge-like matrix which would retain the molten salt and prevent loss by dripping. This aim was achieved by using a mixture of salt with a proportion of a refractory material and a small amount of binding agent. When such a rod is fed into a flame the refractory material supports the molten salt until evaporation is complete, practically all of the salt thus being converted into aerosol. The first tests of this system indicated that complete evaporation of the salt could be achieved by an oxygen-propane flame which was adopted in preference to the hotter oxygen-acetylene flame, for reasons of safety and convenience.

A conventional blowtorch was adapted for aerosol generation by fitting a specially designed flame nozzle and a feed mechanism for the salt stick. The basic apparatus is shown in Figures 1 and 2. The standard commercial torch (British Oxygen Co type

"Saffire 3" with propane mixer) is fitted with an annular flame nozzle which is finned to assist cooling. The salt stick, of 12.5 mm diameter, passes through the nozzle from the rear; additional support for the stick is provided by a short tubular guide. The fuel gas issues from a ring of 14 holes, each of diameter 0.89 mm, forming a tube of flame surrounding the stick. The stick is gripped between a serrated driving roller and a smooth idler roller, mounted on two calliper arms. The arms are sprung and pivoted to facilitate stick insertion and to accommodate slight variations in stick diameter and straightness. The driving roller is powered by a constant-speed battery-operated motor/gearbox unit (Escap type 26) which is available with a wide range of gear ratios, enabling various stick feed rates to be achieved. In operation, when the rear of the salt stick nears the stick guide a further stick may be inserted behind it, and will be held in place temporarily by pressure from the plunger unit until the new stick is gripped by the rollers. The interruption in the aerosol supply due to changing sticks is thus minimized. The modified torch is mounted in a tubular steel frame with the necessary gas flow meters and the dry cell battery pack for the stick drive unit. The complete apparatus is shown, operating, in Figure 3.

IV. Salt Stick Preparation

An acceptable stick must possess the following properties:

1. Almost complete conversion of salt to aerosol by the flame.

2. Adequate mechanical strength.

3. Ease of formation to accurate dimensions.

The formula which has given the best results to date is:

Sodium chloride	85% by weight
Magnesium oxide (heavy)	13% by weight
Hydroxy ethyl cellulose	2% by weight

('Natrosol 250 HHR' manufactured by Hercules Inc., USA)

The ingredients are ground together for 2 minutes in a domestic food grinder (Kenwood). Approximately 25% by weight of water is added to the ground powder and the mixture is worked quickly, forming a thick dough. A piece of the dough weighing 62-63 g is rolled on a flat surface, using a smooth flat piece of wood, to produce a stick 350 mm long. The freshly rolled sticks are placed on a suitably grooved slab of 'Tufnol' and dried under infra-red lamps, turning the sticks occasionally in their grooves, until the sticks weigh less than 52 g each. This gives a residual water content not greater than 4%. With practice strong, straight sticks of

effectively uniform cross-section can be produced by this method. In experiments with an extrusion process, apparently well formed sticks were made, but, during aerosol generation tests the extruded sticks were found to be prone to the premature detachment, in the flame, of portions of stick from which the salt had not completely evaporated, with consequential variation in the rate of aerosol output. Until this defect is overcome, rolled sticks are preferred. The sticks require no special treatment or precautions in storage.

V. Performance of the Rod-Fed Blowtorch

1. Efficiency of Aerosol Generation

The apparatus was set up with a stick feed rate of 41 mm/min, giving an aerosol generation rate of 5 g/min, assuming complete conversion of the salt. For maximum flame temperature, propane and oxygen should be used in the ratio 1:4.3 by volume[5]. Using these gas proportions the minimum flows required for consistent complete vaporization of the salt were found by experiment to be 4 l/min of propane and 17 l/min of oxygen. With this flame the salt content of the stick residue (ie the refractory component) after burning was less than 0.1%, which suggested that the efficiency of aerosol generation is probably high.

The aerosol was drawn into a small wind tunnel having an air throughput of 2700 m^3/hr and the concentration at the tunnel working section was measured, using the CDE portable sodium flame photometer. It was necessary to reduce the aerosol concentration by a further factor of 70, using an air dilution rig consisting of several large jars in cascade. The average concentration measured was about 90% of the theoretical, assuming complete conversion of the salt. This is regarded as satisfactory; the 10% loss is attributed to deposition on the tunnel walls and within the dilution apparatus.

2. Aerosol Particle Size

Sampling of the aerosol in the tunnel, for particle size determination, was initially by cascade impactor, operating isokinetically and backed by a high efficiency paper filter. More than 99% by mass of the aerosol proved to be smaller than 1 μm equivalent diameter, over 80% being caught on the paper filter. Subsequent sampling by point to plane electrostatic precipitator for examination by electron microscopy indicated a particle size range of from about 0.55 μm down to 0.03 μm with mass median diameter of 0.32 μm. Some aggregation was present but the largest aggregates were generally below 0.7 μm. A typical micrograph is shown in Figure 4.

At low feed rates the aerosol is rather finer than the generally considered optimum size for high efficiency filter testing, ie 0.3 μm, and the possibility of modifying the apparatus to produce a coarser cloud has been investigated, briefly. Tubular sheaths of steel and of silica, of various lengths and

diameters were placed around the flame in the attempt to prolong the condensation process. Somewhat coarser aerosols were produced but further work is needed to establish whether it is possible to generate 'made to measure' aerosols consistently.

3. Aerosol Generation at Reduced Rate

For some applications an aerosol generation rate of 5 g/min may be too high. Lower outputs are obtained by reducing the salt stick feed rate, diameter and salt content. Output rates down to 0.01 g/min are achieved easily; an electron micrograph of a sample from a cloud generated at 0.2 g/min is shown in Figure 5.

VI. Conveyance of Aerosol by Ducting

When carrying out an in-place test it may not be possible to site the aerosol generator immediately adjacent to the inlet of the air cleaning system; it will then be necessary to use an air blower and duct to convey the aerosol to the inlet. Tests were made in which aerosol generated at 5 g/min was passed through a small high speed centrifugal blower of capacity 170 m^3/hr (Secomak type 74/37) followed by a 3 m length of 64 mm diameter brass tubing with two right angle bends. Losses by deposition in the blower and ducting were less than 5%.

VII. Filter Tests

Although the aerosol generator has not been employed to test a large high efficiency installation results are available for several 1700 m^3/h (1000 cfm) high-efficiency filters and for a medium-sized electrostatic precipitator. Penetrations through the filters were measured with the torch operating at the rate of 0.2 g/min and compared with penetrations measured employing the standard sodium chloride aerosol of British Standard 3928. Results are shown in Table 1 below:

Table 1 Filter penetration by spray-generated and flame-generated aerosols

Filter No	% Penetration	
	Aerosol from thermal generator	BS 3928 aerosol
1	0.002	0.004
2	0.00036	0.0008
3	0.026	0.03
4	0.05	0.05
5	0.011	0.017

The electrostatic precipitator was tested at two flow rates with the following results:

a. 27,000 m^3/h, salt feed rate 0.2 g/min, 5.5% penetration.

b. 13,500 m^3/h, salt feed rate 0.2 g/min, 1.3% penetration.

No comparison could be made with the BS 3928 aerosol.

VIII. Discussion

This paper has described the development and characteristics of a generator of particles of common salt fine enough to give measureable penetrations through high efficiency filters. Constancy of mass ouput is good and is controllable over the range 0.01 g/min to 5 g/min. Work so far points to smaller particle size distributions at the lower feed rates; further work is necessary to establish the magnitude and importance of such changes. The possibility of keeping the size distribution constant is under investigation.

It should be stressed that the testing of large installations involves more than adequate generators and sensitive detectors. There may be difficulties in distributing the test aerosol across the face of the installation and in ensuring a representative sample from the downstream ducting. Such difficulties will vary from installation to installation and will require an intelligent and flexible approach to each problem.

The portable detector employed in these tests has been a cadmium sulphide cell which has a rather slow recovery rate after exposure to high light levels. Although this is not of prime importance in on site tests, consideration is being given to the use of a PIN diode which recovers almost instantaneously after exposure.

IX. Future Developments

A second aerosol generator has been made which has a set of interchangeable flame nozzles to accept salt sticks of diameters 6 mm, 12 mm and 24 mm. It is hoped that this apparatus will prove capable of generating aerosol at rates of 0.01 to 10 g/min or more. The possibility of close control of particle size will be investigated further.

The generator is the subject of a British patent application.

References

1. Dorman R.G., "Industrial filter test services provided by CDE., Porton Down." J. Instn Heat. Vent. Engrs 38: 178-180 (1970).

2. "Portable flame photometer." Manufactured by: Moore's (Wallisdown) Ltd., Wallisdown Road, Bournemouth, BH11 8QN, England.

3. Dyment J., 11th AEC Air Cleaning Conference Conf. 700816 1: 128-137 (1970).

4. Boyne L., Dyment J. and Thomason I.D., "Generation of a sodium chloride aerosol for in-place testing of air filters." Filtr. (& Sep.) 8: 709-712 (1971).

5. Hewitt A.D., "Technology of oxy-fuel gas processes. Part 2. Comparative combustion properties of fuel gases." Weld. Metal Fabric. 40: 382-389 (1972).

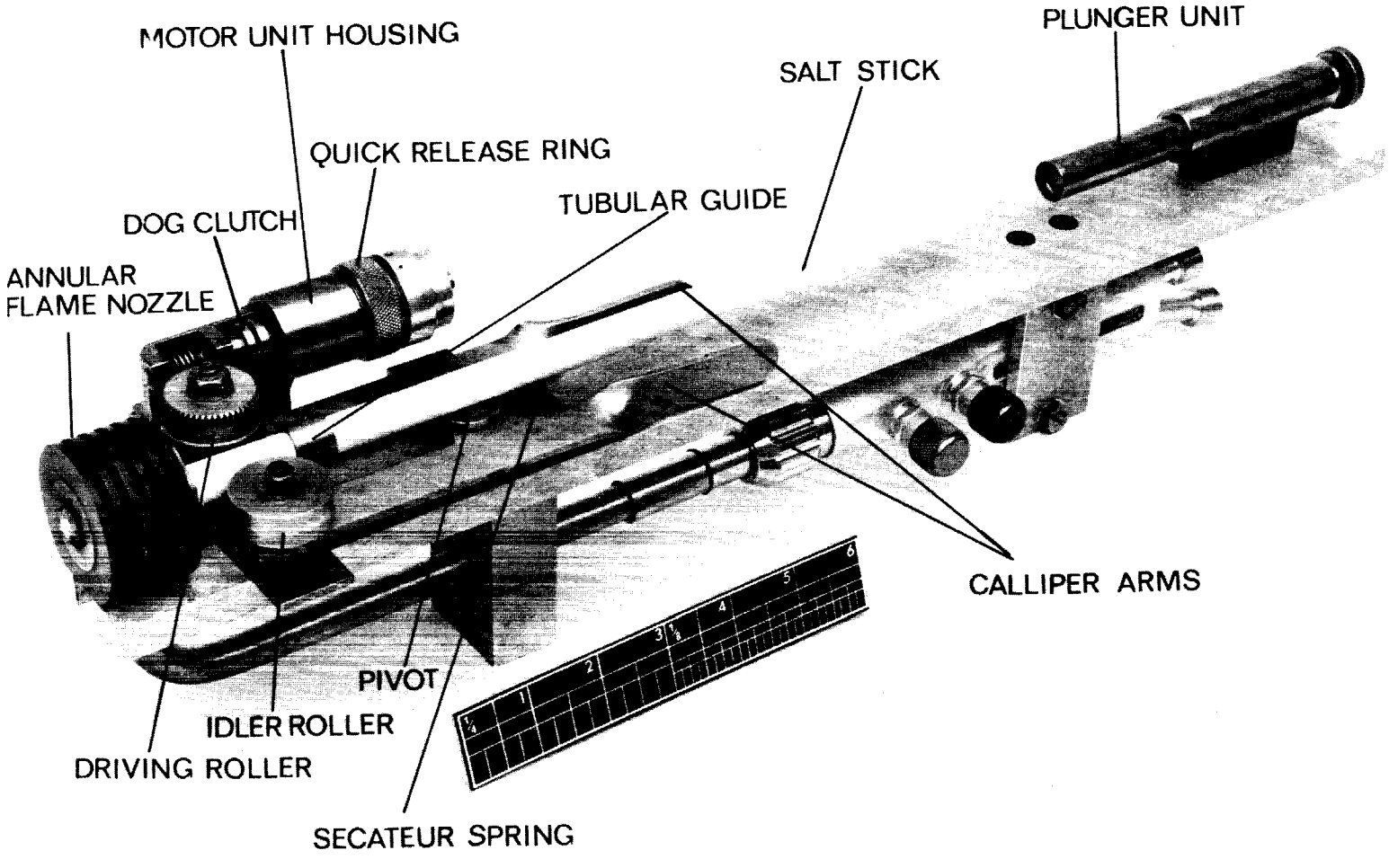

Figure 1. Rod-fed sodium chloride aerosol blowtorch.

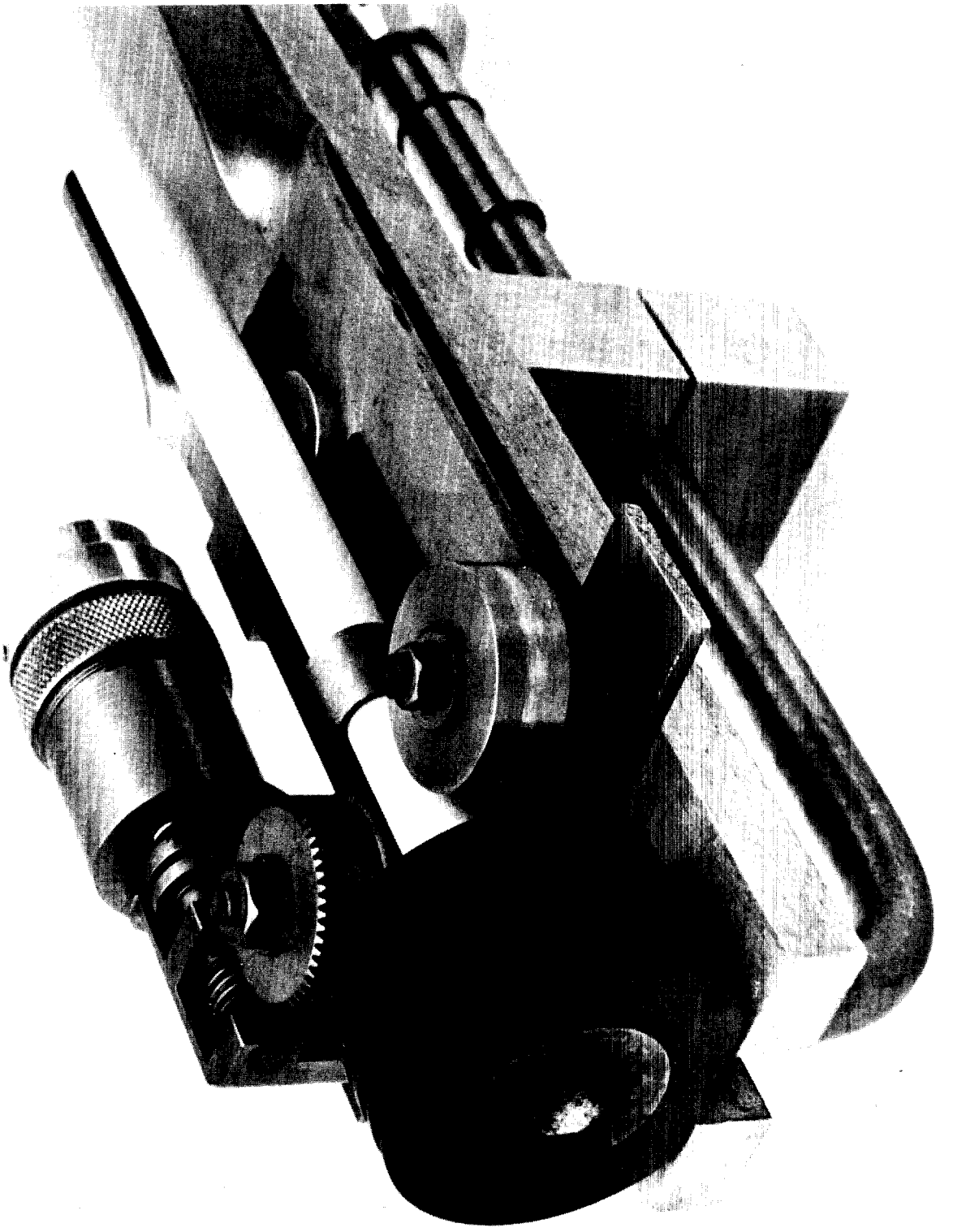

Figure 2. Flame nozzle and salt rod drive mechanism.

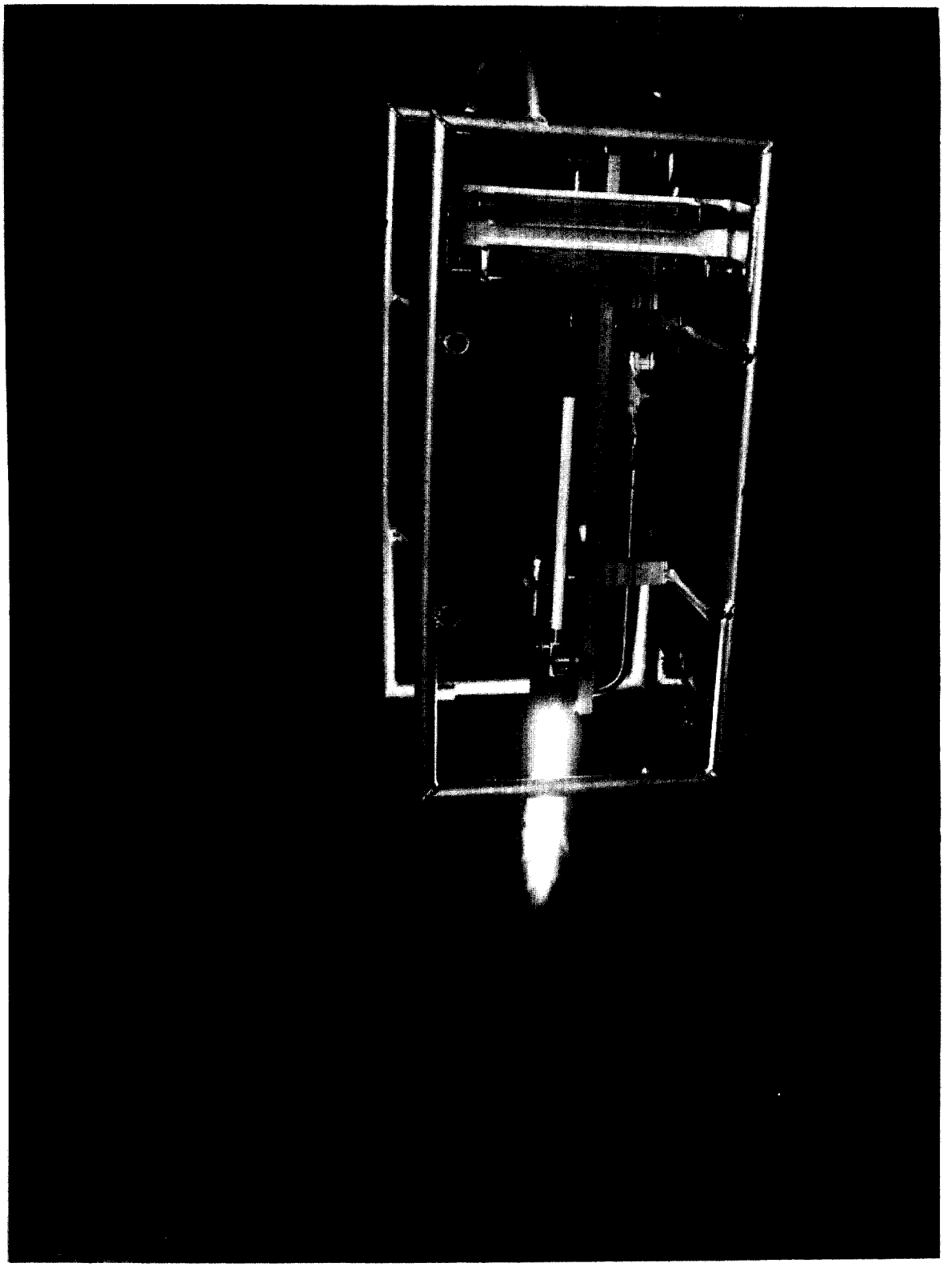

Figure 3. Generation of aerosol at 5 g/min.

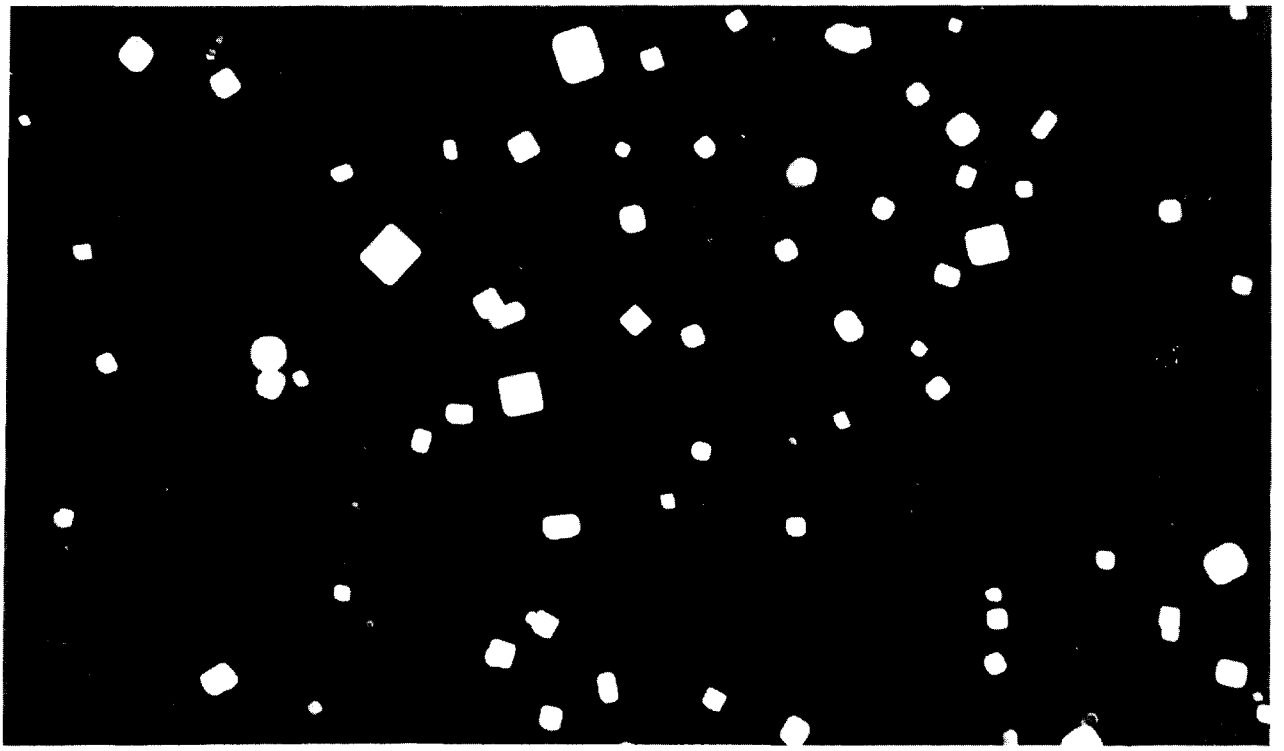

Figure 4. Aerosol generated at 5 g/min.

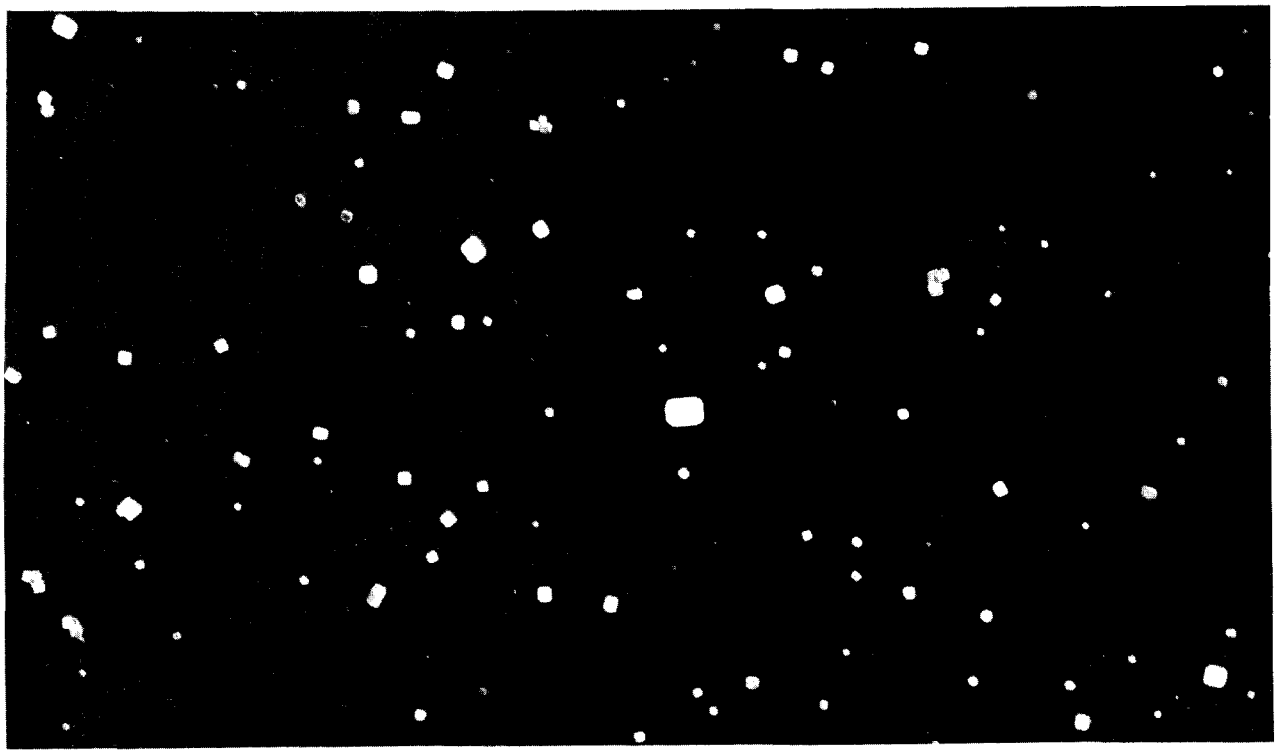

Figure 5. Aerosol generated at 0.2 g/min.

DISCUSSION

JONAS: I might have missed it in the paper. When you measured penetration, what was the time factor? How long after you start your aerosol into the filter do you get a penetration result?

DORMAN: I'm sorry, Dr. Jonas. You didn't miss it, because I didn't say it. It was a mistake on my part. The generator starts to give a fairly constant output within 20 seconds of being opened up, and the output remains constant within 20% variation. Now, the time of the test obviously depends on how far down the duct system you are going to put your detection system. If you want to test just behind the filter bank, the test can be over in 30 seconds or so, but if you wish to test 100 feet down the duct, which one must do sometimes, you have to allow time for the aerosol to travel that distance. The system itself is instantaneous once the salt gets into the detector. While one might take a reading in about 45 seconds, I think it would be unwise; I would leave the generator and detector working until there was a steady reading for at least a minute to make sure there was a proper mixing of aerosols down the duct.

HALLIGAN: What is the smallest and the biggest system you can test with that generator?

DORMAN: We can test 1000 CFM filters at salt feed rates of 0.1 or 0.2 grams of salt per minute but, as I said, the particle size is then somewhat different from the 1 to 5 gram a minute feed rate the system was designed for. We intend to test up to 50 thousand cubic feet per minute filter systems with penetration of, say, 0.005 percent. If you only want to test at 0.1 percent penetration, you may increase flow rates by something like a factor of 10, but if you wish only to test to one percent you can increase even more. But you're going to find what has been stressed this week; that you must get the aerosol to your detector, insuring thorough mixing in the duct. The actual flow rate is no trouble as the instrumentation is sensitive enough. Further, you must ensure that the test aerosol gets to the correct place on the filter installation so that the test is valid. Someone said on Monday that the test crew should be men of integrity. While agreeing with that sentiment, I would add they should also be men of sound common sense.

FIRST: If you are designing a system for in-place leak testing, why are you concerned about changes in particle size? The leak doesn't know the difference between particle sizes passing through it.

DORMAN: No, that's quite right. I said we still use low feed rates but we don't think we shall get exactly the same percent penetration as at high salt feed rates. Besides getting a qualitative result, we would also like to get something better than an order of magnitude. I believe that, with a very low feed

DORMAN (cont.): rate of salt and sampling a long way down the duct, there may be diffusion of some of the smaller particles to the duct walls. For this reason, we like to keep the mean particle size larger than that found at very low feed rates. However, I agree that holes in filters are not size selective.

HIGH-EFFICIENCY PARTICULATE AIR (HEPA) FILTER PERFORMANCE FOLLOWING SERVICE AND RADIATION EXPOSURE*

L. R. Jones
E. I. du Pont de Nemours & Company
Savannah River Laboratory
Aiken, South Carolina 29801

Abstract

Small HEPA filters were exposed to a ^{60}Co source with a radiation strength of 3×10^7 rads per hour and then exposed to steam-air mixtures at several times filter design flow, followed by extended exposure to steam and air at reduced flow. Additional filters were exposed to air flow in a reactor confinement system and then similarly tested with steam-air mixture flows. The test data and calculated effects of filter pluggage with moisture on confinement system performance following potential reactor accidents are described.

Gamma radiation exposure impaired the performance of new filters only slightly and temporarily improved performance of service aged filters. Normal confinement system service significantly impaired filter performance although not sufficiently to prevent adequate performance of the SRP confinement system following an unlikely reactor accident. Calculations based on measured filter pluggage indicate that during an accident air flow could be reduced ∿50% with service-degraded HEPA filters present, or ∿10% with new filters damaged by the radiation exposure.

I. Introduction

In the highly unlikely event of a major reactor accident, radioiodine and radioactive particulates would accumulate on filter and adsorber units in the airborne activity confinement system. The radiation intensity produced by this accumulated radioactivity could be sufficient to alter the performance of confinement system components following the accident. Filter and adsorber units also collect atmospheric pollutants during normal service. Effects of radiation and normal service exposure on filter and adsorber units are being measured at the Savannah River Laboratory (SRL) as part of a continuing program in support of reactor confinement facilities at the Savannah River Plant (SRP).[1-4] Presently, filters are replaced every 13 months.

Effects of gamma radiation on material properties of confinement system components, reported at the Twelfth AEC Air Cleaning Conference,[5] included degradation of water repellency and wet strength of glass fiber HEPA filter media and disintegration of *Teflon*** fibers in moisture separators following irradiation. Degradation of SRP HEPA filter media following normal service in the confinement system was also reported.

This paper reports the results of simulated accident performance testing of filter media found to be the most radiation resistant in filter units following irradiation and/or service exposure.

---

* Work performed under USAEC Contract No. AT(07-2)-1.

** Tradename, E. I. du Pont de Nemours and Co., Wilmington, Delaware, for polytetrafluoroethylene resin.

II. Test Development

SRP Confinement System

The airborne confinement system for each SRP reactor building provides continuous once-through ventilation air flow of about 100,000 cfm. This high flow maintains process areas at subatmospheric pressures. All potentially contaminated air is filtered by a highly efficient filter adsorber system before discharge to the atmosphere through a 200-foot stack. A simple schematic of this system is shown in Figure 1. HEPA filter and moisture separator units become plugged with atmospheric pollutants (dust, soot, fly ash, etc.) during months of service. This necessitates periodic replacement with clean components so that adequate ventilation air flow can be maintained by exhaust fans.

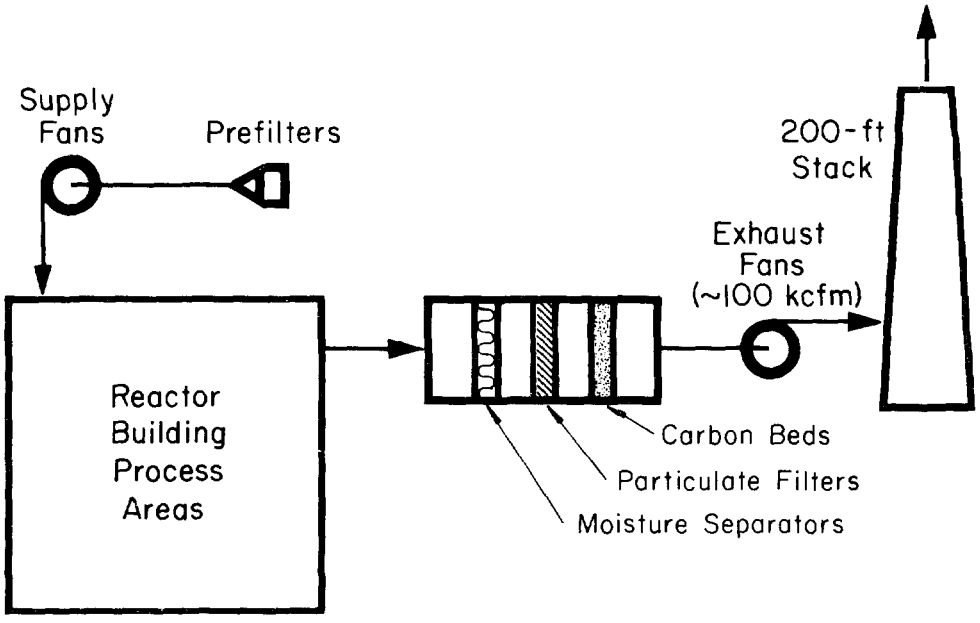

FIG. 1 Schematic of Ventilation System

Potential Accident Conditions

The most severe combination of steam-air exposure conditions that were considered credible for a Savannah River reactor accident were selected for simulated accident test development for the confinement filter systems. Temporary pressurization of the process areas by rapid release of steam from an inadequately cooled reactor was calculated to produce a flow surge through the filters that would peak at a maximum of ∿8.5 times normal flow and would last about 25 seconds. Following this flow surge, the flow would decrease to a value limited by the total developed head of the exhaust fans [∿6-in. H_2O] and the total flow resistance of the confinement system. Steam in the process areas would be diluted with building supply air flow causing the temperature of the steam and air mixture flowing through the confinement filters to decrease from ∿90°C to ∿30°C in about 5 hours.

Accident Simulation Test

Test conditions simulating the reactor accident conditions discussed are shown in Table I. Following the flow surge, the ΔP across the test filter must be limited to 5 inches of H_2O (by reducing the steam-air flow through the filter) to simulate the maximum filter ΔP which could be produced by the exhaust fans in the confinement system. Test filter ΔP and flow were monitored throughout every test to determine moisture pluggage as a function of test exposure time.

Filter Rupture Test

Although calculations indicate the most severe steam-air flow surge through the confinement filters would not last longer than ~25 seconds, a more severe test, intended to rupture the test filter, was developed to characterize more completely the different filters being tested. This rupture test exposes the filter to a steam-air mixture at 80°C and three times the normal flow rate until gross rupture occurs. A steam-air mixture temperature of 80°C was chosen because the greatest liquid water entrainment occurs when steam is mixed with air at 25°C to give a mixture temperature of 80°C. Maximizing this liquid entrainment produces the most severe condition for the test filter.

III. Test Facilities

Test Filters

Irradiation and testing of full-size (1000 ft^3/min rated flow) HEPA filters would require very large and expensive facilities. Smaller filters with internal construction identical to full-size filters (filter media, separator arrangement, and spacing) were fabricated by manufacturers of full-size HEPA filters using filter media designated Type F and Type E in Reference 5. These test filters (10 to 15 ft^3/min rated flow) are shown in Figure 2.

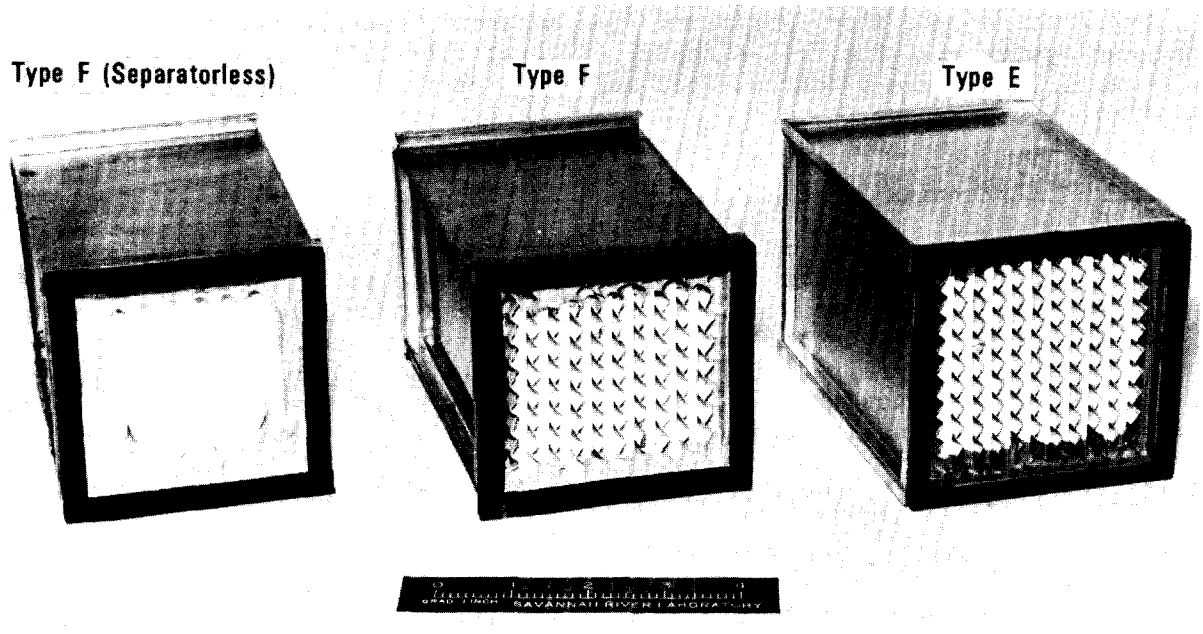

FIG. 2 Test HEPA Filters

Because the internal spacing of media and separators is identical to that in a full-size filter, moisture pluggage and media rupture in these filters is considered representative of the performance of a full-size filter. However, performance of small separator-less filters or adhesives in small test filters cannot be considered completely representative of a full-size filter, especially following radiation exposure, because of the geometric differences between full-size and small test filters and the resulting stresses applied to the filter pack. Gross failure of a filter by blowing the filtration media completely out of the casing would probably occur at a lower ΔP for the full-size filter than for the smaller filter, because the filter pack face area is much larger for the full-size filter, and the center of the full-size filter pack is not as strongly supported as the center of the smaller filter pack. In 1962, SRL tests of full-size filters with separators indicated the filter media would rupture, thereby reducing the filter ΔP before the filter pack could be blown out of the casing.[6]

Type F Filters

Six groups of test filters were fabricated by combining either all-glass fiber or glass-asbestos fiber filter media (Media F in Reference 5) and a foam or a rubber-base adhesive (Adhesives A and B, respectively, in Reference 5) into filters with and without aluminum separators. For purposes of identification the following abbreviations have been combined to designate each filter group:

G - all-glass media
GA - glass-asbestos media
S - aluminum separators
NS - no separators
RB - rubber-base adhesive
FA - foam adhesive

For example, G-NS-RB identifies a filter with all-glass media, no separators, and a rubber-base adhesive. All Type F filters have chromized steel casings.

Type E Filters

Test filters were also fabricated from materials used in SRP confinement filters by the manufacturer of the full-size SRP filters. The filter media (Type E in Reference 5) is a glass-asbestos fiber media enclosed in cadmium-plated steel frames with aluminum separators.

Type E Filters with Service Exposure

Type F and Type E test filters are currently being exposed to confinement system air flows prior to performance testing. However, these filters have not yet accumulated sufficient service exposure. To indicate the expected performance of these service-exposed filters, test filters were fabricated in the laboratory from media removed from full-size filters following service in the confinement system. Type E filter casings were used for the laboratory fabricated filters following rupture testing with the original filter pack.

^{60}Co Irradiation Facility

The SRL ^{60}Co Irradiation Facility[5] was used for irradiating test HEPA filters and other materials at a dose rate of $\sim 3.5 \times 10^7$ rad/hr. Dry air flowed through each test filter during irradiation to maintain an air temperature of $\sim$60°C and to remove gases from radiolysis of air and decomposition of materials.

Service Exposure Facility

A facility to measure the effects of service exposure *in situ* is located adjacent to the confinement filter compartments in one SRP reactor area. Air flow upstream of the confinement filters is drawn through a full-size moisture separator, through 36 HEPA test filters, and finally through 40 test carbon beds. HEPA filters exposed in this facility will be used to confirm results of tests with laboratory-fabricated, service-exposed filters.

Steam-Air Flow Test Facility

A schematic of the accident-simulation filter test facility is shown in Figure 3. This facility is designed with the following key features:

- Two modules provide steam-air flow to the HEPA filter being tested. The upper (high-flow) module shown in Figure 3 supplies steam-air mixtures at flow rates of about 85 ft^3/min for the first 25 seconds of the test. The lower (normal flow) module supplies steam-air mixtures at normal or below normal flow rates to prevent exceeding a ΔP across the test filter of 5-in. H_2O for the remaining 5 hours of the test. The facility is constructed of *Lexan** to permit observation inside the modules (Figure 4). The high flow module was used for filter rupture tests.

- Both modules are preheated before a filter is tested by flowing steam and air at the desired test conditions through the modules which vent into a laboratory hood through bypass ducts. The test filter is isolated from the steam-air flow during preheating by slide plate dampers. At the start of the test, the slide plate damper is opened and the bypass damper is closed to force full flow through the test filter. Operation in this manner allows reproducible short-duration exposure of the unpreheated filter and minimizes unwanted steam-air condensation on duct walls.

- Both modules contain 2-in.-thick moisture separator units. Because of the relatively small distance between the moisture separator and the test HEPA filter (needed to minimize wall condensation), a vertical offset downstream of the moisture separator prevents water droplets (which may fly off the downstream side of the moisture separator media) from reaching the face of the test HEPA filter. The relatively larger spacing in the full-size confinement compartments would prevent this occurrence during an actual reactor accident.

- A fraction of the steam-air flow through the normal flow module can be vented upstream of the moisture separator and test filter during a test to maintain a constant ΔP across the test filter. This venting is done after the limiting filter ΔP of 5 in. H_2O is reached. An additional orifice measures the net steam-air flow rate through the moisture separator and the test filter. This orifice is calibrated over the needed flow range for each steam-air temperature because the density of the steam-air mixture changes as the mixture temperature varies.

- Both modules contain shielded safety rupture diaphragms (set at 4.0 psig) to prevent accidental overpressurization of the facility if dampers are misoperated.

---

* Registered tradename of General Electric Company.

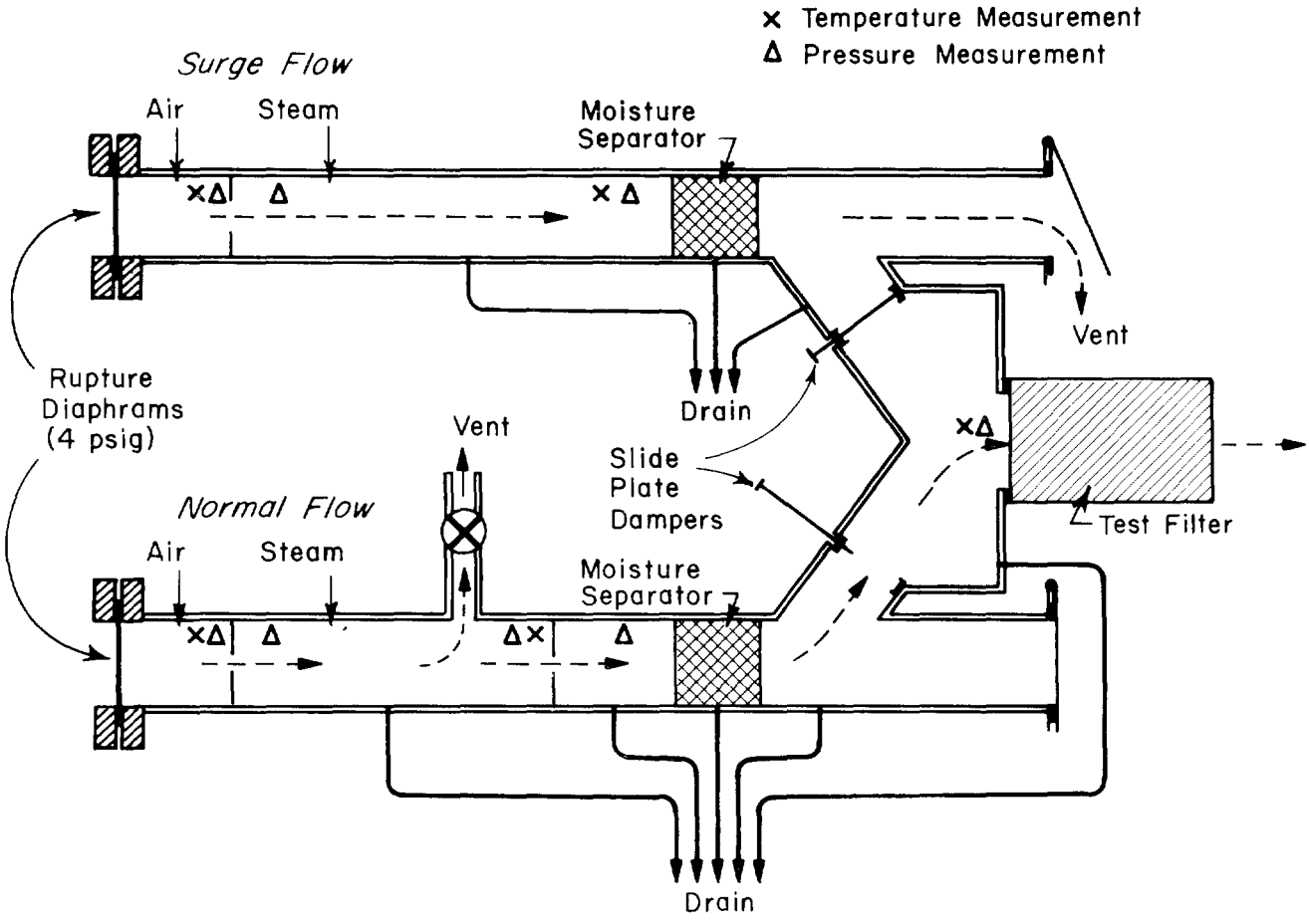

FIG. 3 Schematic of HEPA Filter Test Facility

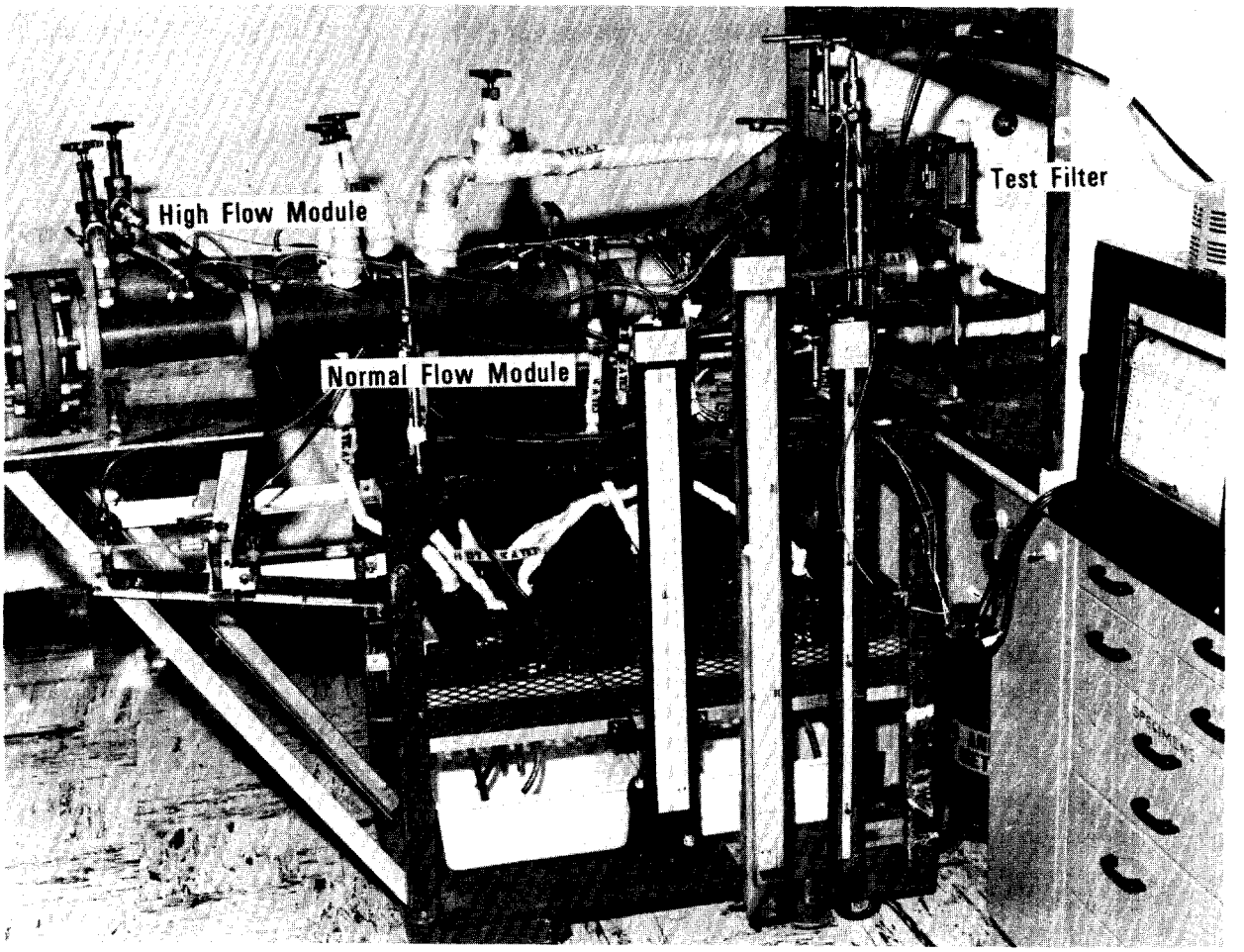

FIG. 4 HEPA Filter Test Facility

IV. Test Results

HEPA Filter Rupture

Type F Filters

Exposure of Type F filters to ∿3 times the normal flow of steam and air at 80°C caused moisture pluggage, which is shown as increasing filter ΔP with increased exposure time in Figure 5. Filters exposed to 2 x 10^8 rads in the ^{60}Co facility prior to testing became plugged and ruptured in from 100 to 250 minutes. Unirradiated filters plugged so slowly that the tests were terminated after 120 minutes as rupture in a reasonable period of time appeared unlikely.

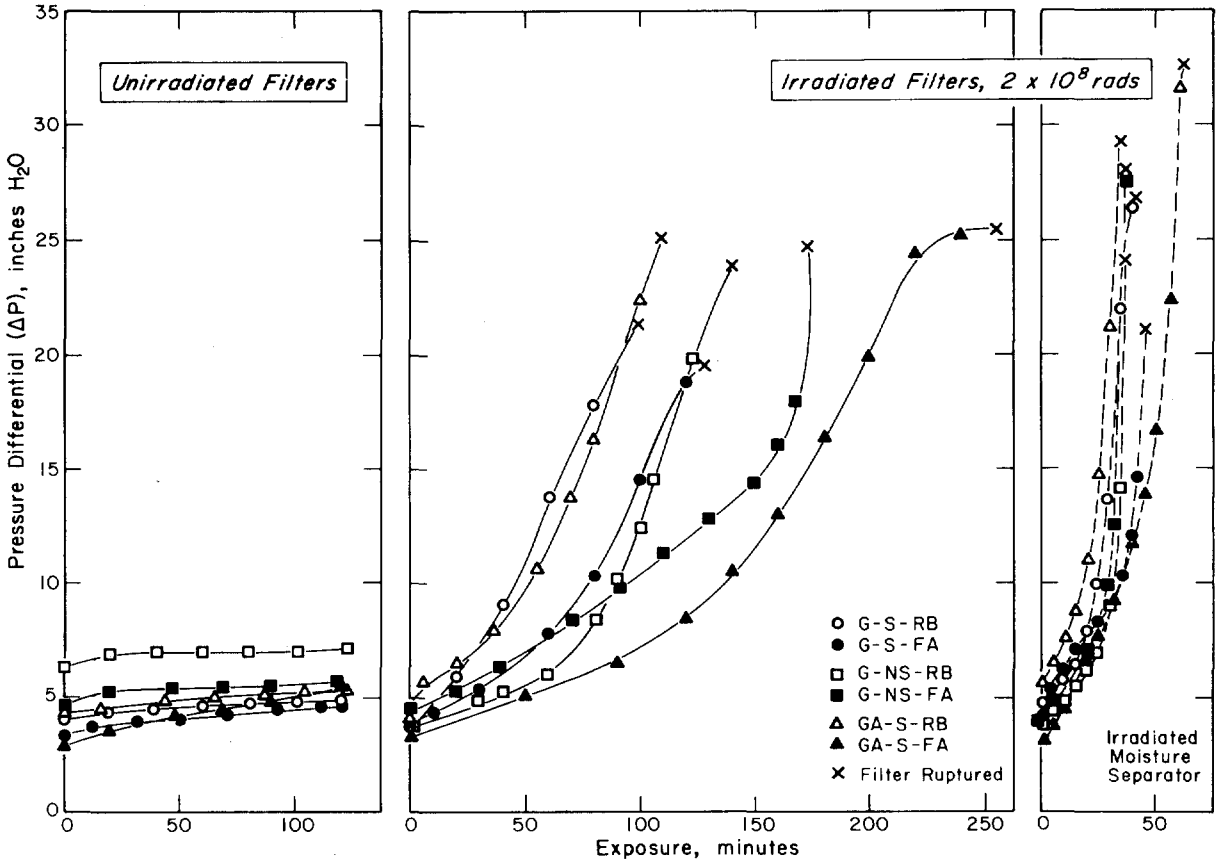

FIG. 5 Rupture of Type F HEPA Filters

Exposure to flowing steam-air mixtures continued until a rupture in the filter was visible, even though in one test the filter ΔP stabilized indicating a possible rupture prior to visible rupture. Rupture ΔP varied widely. It depended partially on whether the filter media ruptured initially at a fold around the end of a separator, or between pleats in a separator. Partial collapse of folds occurred in some irradiated filters without separators. Several ruptured filters, shown in Figures 6 and 7, are typical.

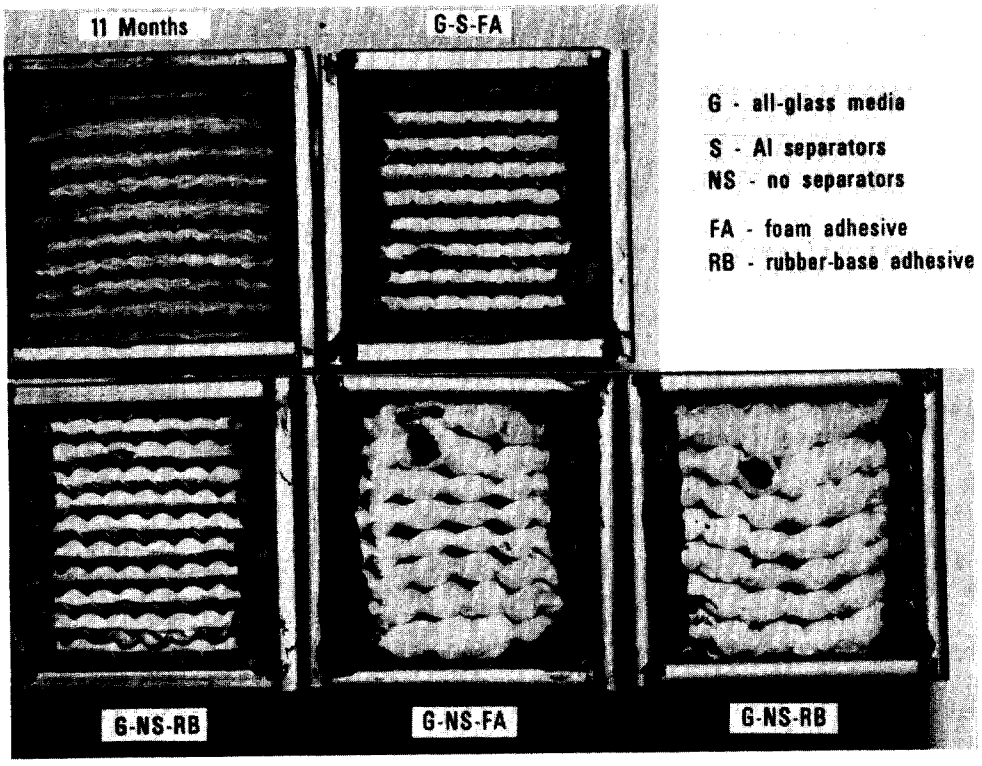

FIG. 7 Ruptured Type F HEPA Filters (Upstream Face)

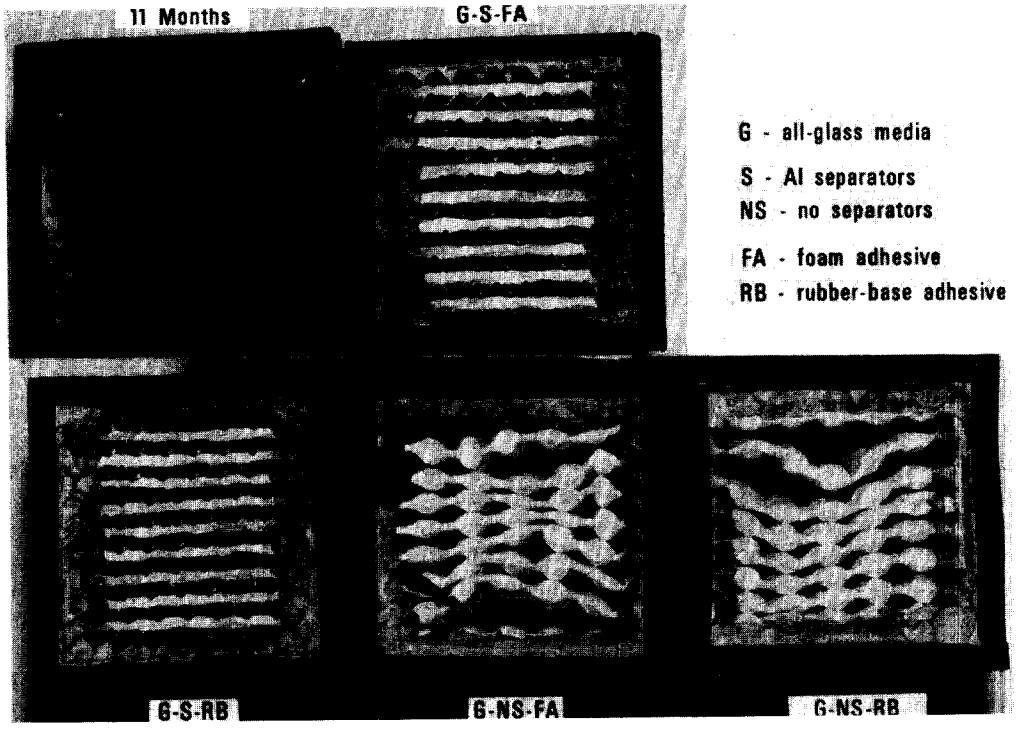

FIG. 6 Ruptured Type F HEPA Filters (Downstream Face)

Replacement of test facility moisture separator units with units that had been exposed to ~8 x 10^8 rads in the ^{60}Co facility caused more rapid filter pluggage and rupture. The *Teflon* fibers in the irradiated moisture separators were washed completely from the stainless steel wire mesh in the first two minutes of steam-air exposure, allowing entrained moisture to pass through the separator and collect on the test filter.

Filters constructed with the foam adhesive appeared to plug more slowly than filters with the rubber-base adhesive. Such behavior would not be expected unless flow bypassed the filter media by leaking through the foam adhesive. During tests, however, no leakage through either adhesive was observed. Post-test examination revealed the rubber-base adhesive tended to curl away from the metal filter casing after irradiation and exposure to steam-air flow; and, infrequently, loss of bonding between the foam adhesive and the metal casing was observed.

Type E Filters

Several type E (SRP) filters were exposed to rupture test conditions following irradiation to 1 x 10^8, 2 x 10^8, and 6 x 10^8 rads.

Comparison with a new, unirradiated Type E filter is shown in Figure 8. After 120 minutes of exposure, rupture of the unirradiated filter appeared unlikely, while pluggage and rupture of irradiated filters occurred more rapidly with increased radiation exposure. Substitution of an irradiated (8 x 10^8 rads) moisture separator in the test facility resulted in more rapid moisture pluggage and rupture, as was observed with the Type F filters.

Although filters with the greater radiation exposure ruptured more rapidly, they ruptured at higher pressure differentials, apparently contradicting previous data which showed decreased wet strength of filter media with increased radiation exposure.[5] This behavior could result from less penetration of moisture into the media during the shorter exposure time before rupture, or from random differences in individual filter construction.

A typical ruptured Type E filter is shown in Figures 6 and 7. The filter adhesive showed some curling away from the casing following irradiation and steam-air exposure, which was similar to the behavior of the rubber-base adhesive on Type F filters.

Type E Filters with Service

Test filters fabricated with media from full-size filters with 4-, 7-, 11-, and 13-months service in the confinement system were exposed to rupture test conditions. Filters with 4- and 7-months service plugged with moisture but did not rupture in 400 minutes of exposure, but filters with greater service ruptured rapidly. Substitution of an irradiated (8 x 10^8 rads) moisture separator resulted in even more rapid pluggage and rupture of downstream filters (Figure 9). Filters with 7- and 11-months service were exposed to 2 x 10^8 rads and then were exposed to rupture test conditions with a new, unirradiated moisture separator in the test facility. Both filters plugged more slowly initially than unirradiated 7- and 11-months service filters, but did rupture.

The more rapid moisture pluggage of filter media having confinement system service was caused by the hygroscopicity of the soot layer collected on the media during continuous air flow. This soot layer absorbed moisture from flowing steam-air mixtures much more readily than did clean, nonhygroscopic, glass-fiber filter media, even when the moisture repellency of the clean filter media was completely

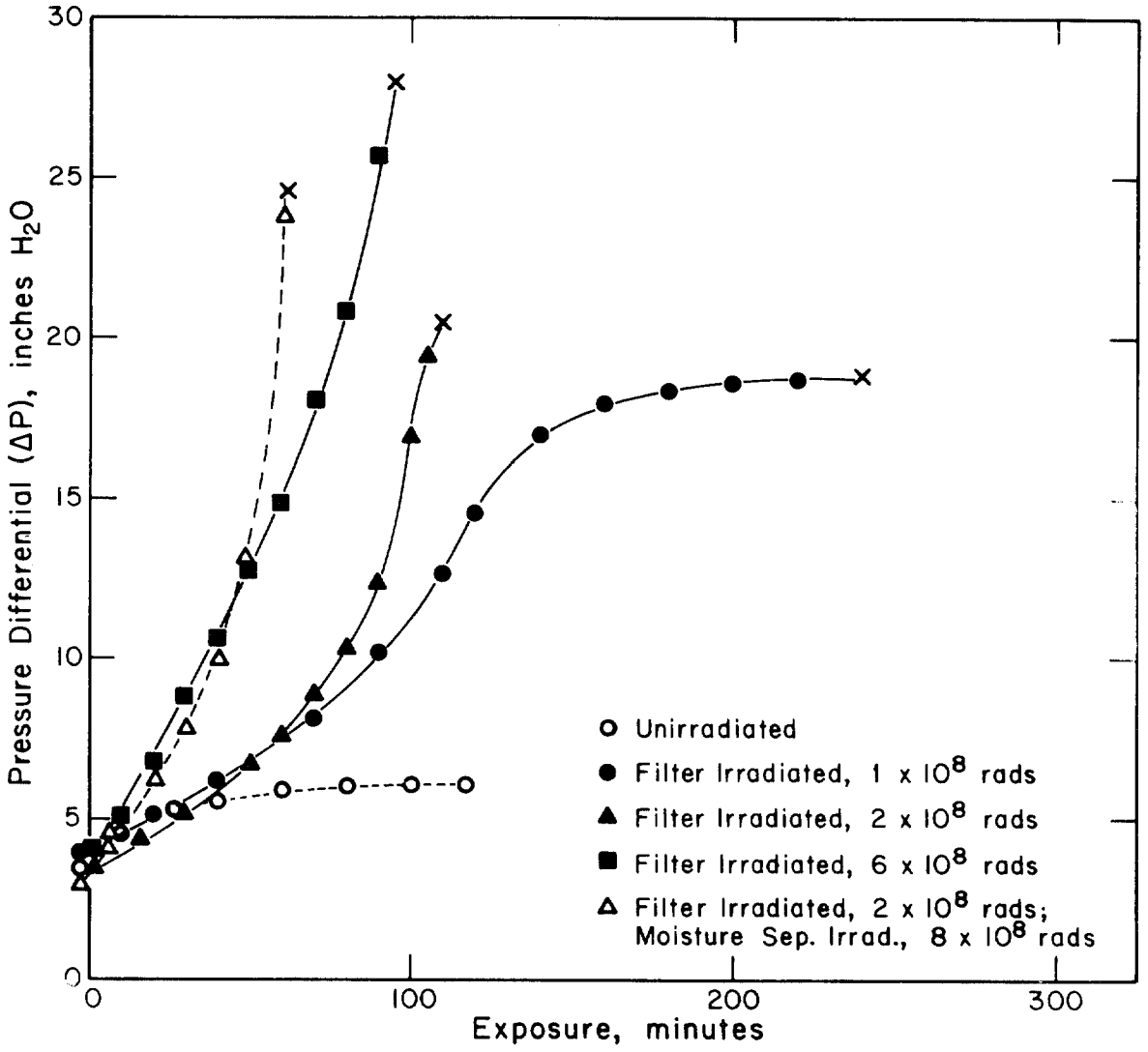

FIG. 8 Rupture of Type E HEPA Filters

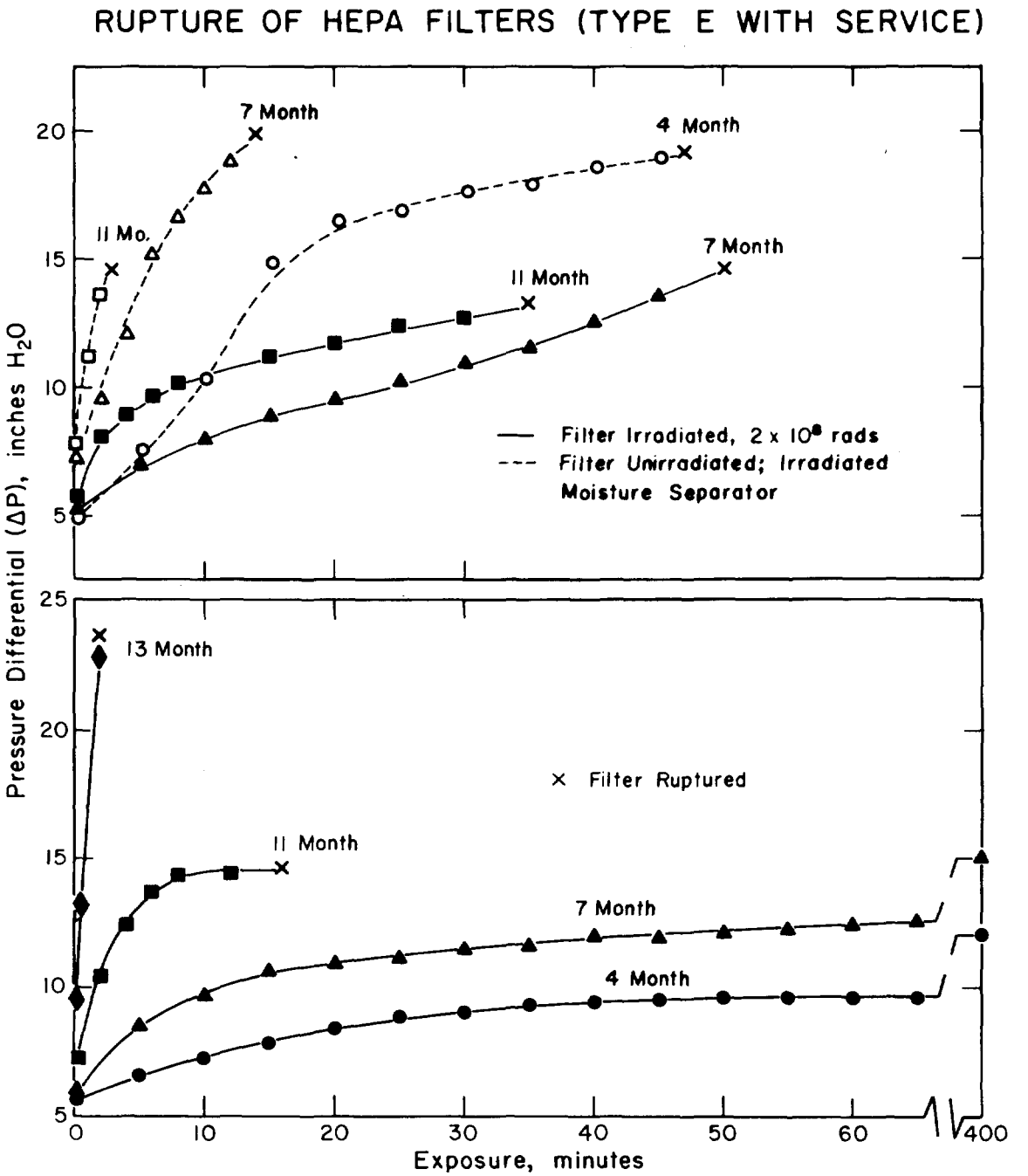

FIG. 9 Rupture of HEPA Filters (Type E with Service)

destroyed by radiation exposure. The presence of irradiated moisture separators aggravated the problem. The reduced removal of entrained moisture by the irradiated moisture separator exposed the hygroscopic soot on the filters to even higher moisture levels. However, the data (Figure 9) indicate irradiation reduces the hygroscopicity of the service-accumulated soot layer and also reduces the residual moisture repellency of the filter media.

HEPA Filter Simulated Accident Performance

Type F Filters

Type F filters (both unirradiated and following exposure to 2×10^8 rads) were exposed to simulated accident test conditions (Table I). Filter flow and ΔP were monitored during each test to determine moisture pluggage.

Moisture pluggage can be expressed as the measured ΔP across the filter at a selected flow rate of steam-air mixture divided by the measured (or calculated) ΔP at that same flow rate of clean, dry air adjusted for fluid density differences. This ΔP ratio was determined for each test filter at various times throughout each five-hour test.

TABLE I. HEPA FILTER ACCIDENT SIMULATION TEST CONDITIONS

Time	Multiple of Normal Flow Rate	Temperature of Steam-Air Mixture, °C	HEPA Filter ΔP, in. H_2O
0 to 25 sec	8.5	92	No Limit
25 sec to 4 min	1.0	92	<5
4 min to 14 min	<1.0	80	<5
14 min to 20 min	<1.0	70	<5
20 min to 30 min	<1.0	60	<5
30 min to 40 min	<1.0	50	<5
40 min to 2 hr	<1.0	40	<5
2 hr to 3 hr	<1.0	35	<5
3 hr to 5 hr	<1.0	30	<5

Calculated confinement system flow is expressed in percent of calculated normal flow with clean, dry HEPA filters (Figure 10) for each group of Type F filters (except group G-S-FA which is shown in Figure 11 for comparison with Type E filters). With the exception of group G-NS-RB filters, the initial calculated flow reduction from pluggage of Type F filters was less than 10%. As will be discussed in a later section, this initial flow reduction is of more importance than similar flow reductions at later times. The characteristic dip found during the first 25 minutes exposure is caused by maximum liquid entrainment occurring in the flowing steam-air mixture at a temperature of 80°C (period from 14 to 20 minutes in test sequence, Table I). Liquid entrainment decreased at lower temperatures.

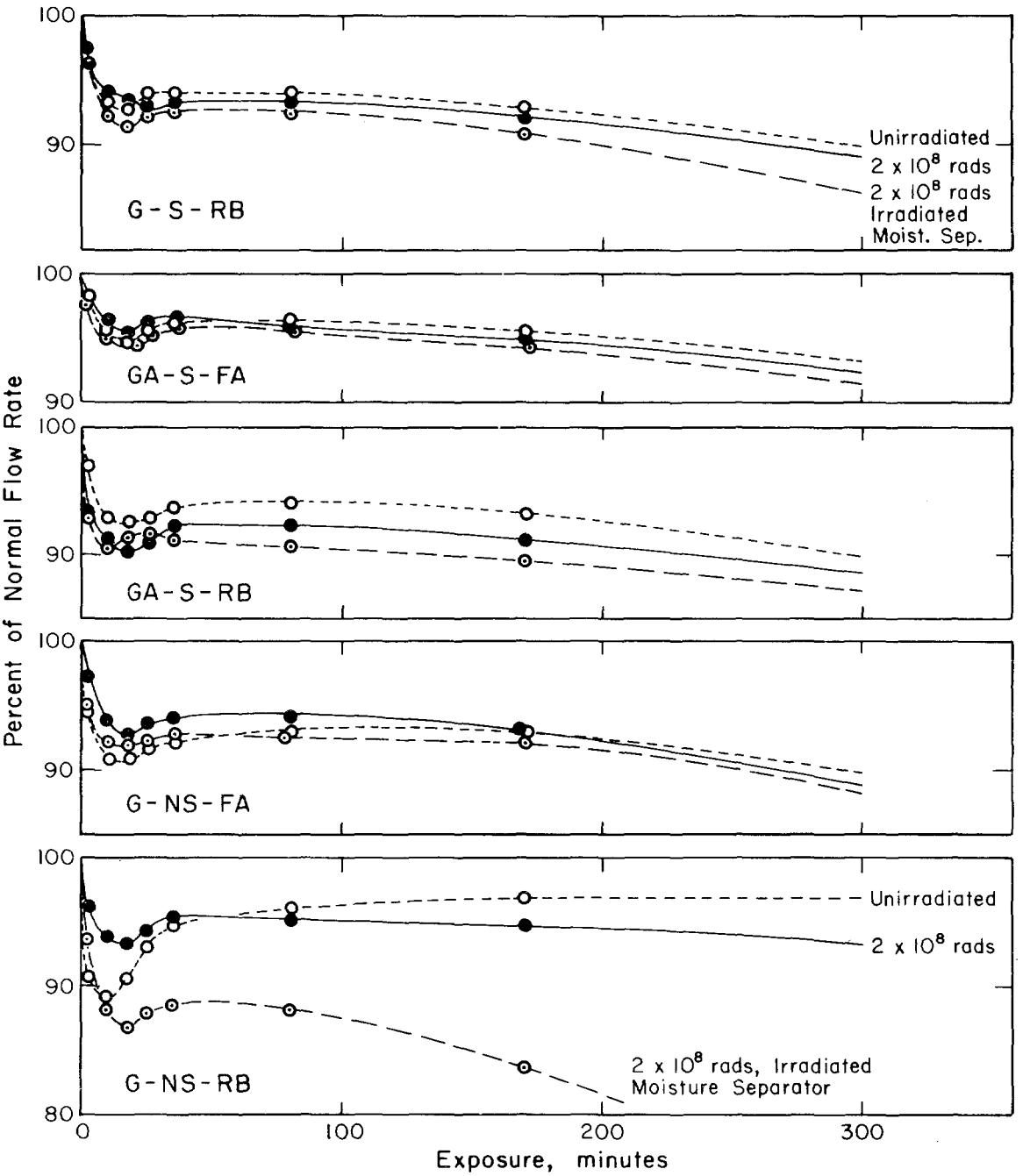

FIG. 10 Reduced Flow through HEPA Type F Filters with Time Under Simulated Reactor Exposure Conditions

Again with the exception of group G-NS-RB filters, performance of Type F filters was only slightly affected when filters were exposed to 2 x 10^8 rads and when an irradiated moisture separator was substituted in the test facility. The unique behavior of the group G-NS-RB filters, especially with an irradiated moisture separator, may be the result of irregular moisture repellency treatment of the media, although this supposition was not confirmed.

Type E Filters

Simulated accident performance of Type E filters was determined following exposure to 1 x 10^8, 2 x 10^8, and 6 x 10^8 rads. Calculated confinement system flows for each of these filters (Figure 11) were compared to that for a new, unirradiated Type E filter. Although initial flow reduction was similar to that for the Type F filters, the unirradiated Type E filter showed better flow recovery, while the irradiated filters showed slightly greater decreases in flow with continued steam-air exposures. Substitution of an irradiated moisture separator resulted in only a small effect, similar to that for Type F filters.

Type E Filters with Service

Test filters fabricated with media removed from full-size filters with 4-, 7-, 11-, and 13-months service in the confinement system were tested under simulated accident conditions. Calculated confinement system flow is shown in Figure 11 as a function of filter history. More severe flow reductions occurred for filter media with greater service exposures. Further flow reductions with substitution of an irradiated moisture separator were also more severe for media having longer service. Irradiation significantly improved performance of filters with 11- and 13-months service.

V. Application of Results

Because the most severe flow surge postulated through the SRP confinement system is calculated to last no longer than 25 seconds, rupture of confinement HEPA filters, even if radiation damage to moisture separators occurs, appears unlikely for filters with less than 13 months service and/or radiation exposure of less than 6 x 10^8 rads.

Tests in operating SRP reactor buildings have shown that sufficient subatmospheric pressure following a reactor accident could be maintained in process areas at lesser air flows than have been calculated for any of the filters tested.

The reduction in confinement system flow when HEPA filters plug with moisture depends on: fixed pressure-flow characteristics of the system (pressure losses in ducts, fan head, etc.); variable operating conditions (number of exhaust fans, filter compartments on line, etc.) at the time of the postulated accident; and the increased pressure loss across the HEPA filters. Carbon adsorbers would be heated by decay of radioiodine adsorbed from the flowing air stream. Carbon temperatures following the accident would depend on the quantity of radioiodine reaching the adsorbers and several transient parameters.

The temperature of the steam-air mixture reaching the carbon adsorbers has been discussed previously (Table I) and would be expected to decrease exponentially with time causing carbon adsorber temperatures to decrease following the accident. Radioiodine decay (especially for the short-lived isotopes) would reduce the rate of heat generation, and thus carbon adsorber temperatures, following the accident. Reduced confinement system flow would result in slower removal of decay heat and higher carbon adsorber temperatures. Such reduced flow would also retard the trans-

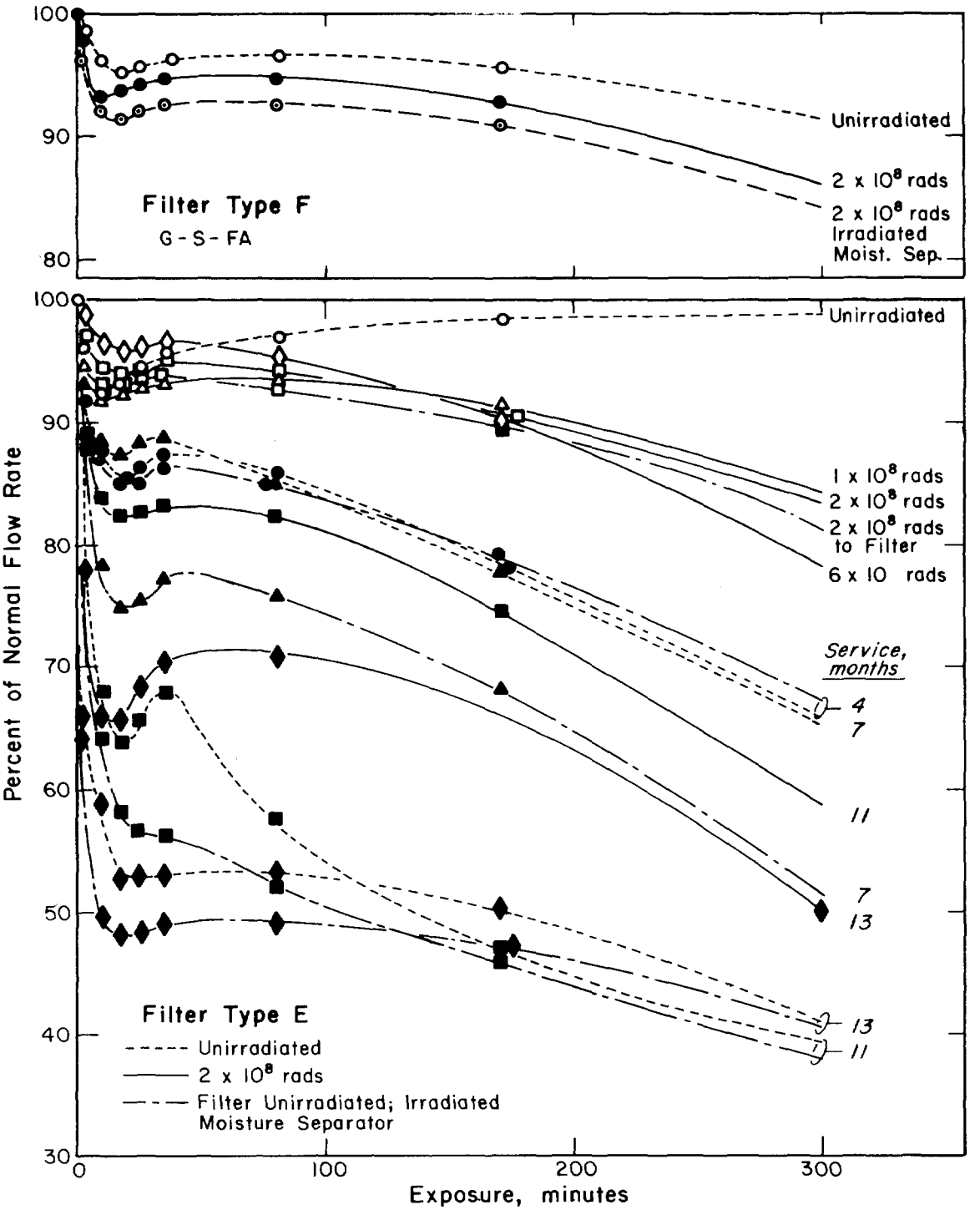

FIG. 11 Reduced Flow through HEPA Type E Filters with Time Under Simulated Reactor Exposure Conditions

port of the radioiodine from the process areas to the carbon adsorbers, thereby allowing greater decay before adsorption.

The combined effect of these transient parameters is that calculated carbon temperatures are increased by reducing system flow; however, the actual temperatures are strongly affected by the time interval between the accident and the occurrence of significant flow reduction. Temperatures calculated from performance data on a number of test filters and the worst combination of assumed confinement system operating conditions are at a maximum 20 to 30 minutes after the accident occurs. The maximum calculated temperature at the carbon beds is 220°C. Although this temperature is well below the ignition temperatures of most carbons, significant thermal desorption of iodine from carbon has been measured at temperatures of 180 to 200°C.[3]

VI. Conclusions

Six different groups of Type F filters performed as well in laboratory tests as Type E filters (presently used for SRP reactor confinement) when the filters were new or after gamma radiation exposure. Gamma irradiated filters, with no confinement system service, ruptured after 1 to 4 hours exposure to three times rated steam-air flow. Filters with greater radiation exposure ruptured more rapidly. Irradiated filters ruptured after less than 1 hour exposure to steam-air flow when the moisture separator upstream of the filter was replaced with an irradiated moisture separator. Moisture pluggage under more credible test conditions was also dependent on radiation exposure and moisture separator condition, although the effects were less significant than in filter rupture tests.

Filters made from media with greater than 8-months service in the confinement system ruptured after less than 15 minutes exposure to three times rated steam-air flow. Filters having only four months service also ruptured when the moisture separator upstream of the filter was replaced with an irradiated moisture separator. Moisture pluggage under more credible test conditions was similarly dependent on filter media service age and on the condition of the moisture separator. Gamma irradiation of service-aged filters slowed moisture pluggage and filter rupture.

In general, gamma radiation exposure impaired the performance of new filters only slightly under credible test conditions, and temporarily improved performance of service-aged filters. Normal confinement system service significantly impaired filter performance although not enough to prevent adequate performance of the SRP confinement system following an unlikely reactor accident.

VII. References

1. W. S. Durant, R. C. Milham, D. R. Muhlbaier, and A. H. Peters. *Activity Confinement System of the Savannah River Plant Reactors.* USAEC Report DP-1071, E. I. du Pont de Nemours & Co., Savannah River Laboratory, Aiken, S. C. (1966).

2. W. S. Durant. *Performance of Activated Carbon Beds in SRP Reactor Confinement Facilities - Progress Report: September 1961-September 1965.* USAEC Report DP-1028, E. I. du Pont de Nemours & Co., Savannah River Laboratory, Aiken, S. C. (1966).

3. R. C. Milham and L. R. Jones. *Iodine Retention Studies - Progress Report: January 1969-June 1969.* USAEC Report DP-1213, E. I. du Pont de Nemours & Co., Savannah River Laboratory, Aiken, S. C. (1969).

4. A. G. Evans and L. R. Jones. *Confinement of Airborne Radioactivity - Progress Report: July 1973-December 1973.* USAEC Report DP-1355, E. I. du Pont de Nemours & Co., Savannah River Laboratory, Aiken, S. C. (1974).

5. L. R. Jones. "Effects of Radiation on Reactor Confinement System Materials." *Proceedings of the Twelfth AEC Air Cleaning Conference, Oak Ridge, Tenn., August 28-31, 1972.* USAEC Report CONF-720823, Vol. 2, 655-76 (1972).

6. A. H. Peters. *Application of Moisture Separators and Particulate Filters in Reactor Containment.* USAEC Report DP-812, E. I. du Pont de Nemours & Co., Savannah River Laboratory, Aiken, S. C. (1962).

DISCUSSION

MURROW: The pictures show test filters with separators and media lying horizontally. Was the test made with the filters in those positions or were the separators vertical?

L.R. JONES: In the tests, the separators were always vertical. The reason they were shown that way was for better camera angle.

KNUTH: You used small filters but kept the depth the same as 24" by 24" filters. If 24" by 24" filters were used, wouldn't you expect them to rupture in less time because of the larger face area and the greater distance between end supports?

L.R. JONES: These filters did not have the same depth as full sized filters. In tests we did at Savannah River about 10 or 12 years ago with full sized filters, rupture occurred between separators or at the media fold around the end of the separator. We consider these small filters to be representative in that respect. The only case where they would not be representative would be if we blew the entire pack out of the filter. What we were looking for mostly was moisture pluggage and, for moisture pluggage, we would expect these filters to behave the same as full-sized filters. Since the fold and separator spacing are identical to those in full-sized filters, it shouldn't make any difference how big the filter is.

KNUTH: I would think that, as you are further away from the filter frame, you would have more weakness in the standard 24" x 24" x 12" filter than in a smaller one.

L.R. JONES: You wouldn't as long as the filter retains its geometry and separator spacing. You noticed the separators did retain their geometry and spacing. Rupture at the end of a fold should not depend on how deep the filter is. That one part of the media ruptures and that is the end of the test. Blowing the filter pack completely out would be entirely different.

BENDIXSEN: Would you care to comment on two questions: Why did you pick a radiation level of 2×10^8? If the radiation level was two or three orders of magnitude below 10^8, what might be the radiation damage you would expect?

L.R. JONES: We picked 2×10^8 rads out of convenience for irradiating as many filters as we could. We looked at the E type at 6×10^8 rads. Once you get above 7 or 8×10^8 rads, the media is pretty well shot and only retains what strength you have left in the glass fiber material.

BENDIXSEN: I also asked if radiation were two or three orders of magnitude less, than what you have found?

L.R. JONES: If it were significantly less; very little damage. I believe you could get information on this by looking at the 12th Air Cleaning Conference data.

BURCHSTED: Another environmental aspect of HEPA filters is possible exposure to heat and smoke under fire conditions or a fire in the operating area. We have a ventilation fire and smoke program established now. Jim Anderson is going to give you a discussion of their findings at Lawrence Livermore Laboratory.

THE HEPA-FILTER SMOKE PLUGGING PROBLEM*

J. R. Gaskill and M. W. Magee
University of California, Lawrence Livermore Laboratory
Livermore, California 94550

Abstract

Actual experiences indicate that during the early stages of a fire, pyrolysis and incomplete combustion of organic materials used in the furnishings or interior finishes of laboratories yield copious quantities of smoke particulates, both liquid and solid. Furthermore, the use of fire retardants in materials used for the above purpose interferes with the combustion process, so that burning of such materials in later stages of a fire will yield dense smoke. These particulates can plug up a HEPA filter or even a more porous prefilter, and thus effectively shut off the exhaust ventilation. In this case, the fire room will pressurize and contamination may spread in an uncontrolled manner.

Both small- and large-scale tests have been conducted to evaluate the nature and degree of the problem as a function of materials involved, rate of exposure to the fire, and kinds and temperatures of smokes so generated. Some test work has also been done on scrubbing of smoke. Proposed future work is described.

I. Introduction

At the previous Air Cleaning Conference in Oak Ridge,[1] my colleague and I reported on experimental work and tests we were doing to try to ameliorate the effects of unwanted fires on exhaust ventilation systems in buildings and laboratories where radioactive materials are handled. Figure 1 shows one kind of air flow system used in such a building. Figure 2 shows a schematic diagram of the apparatus we used and reported on at that time.

At this same conference we reported success in abating heat effects on HEPA filters by use of water sprays on graded, metal mesh scrubbers. We also indicated that we were starting a study of smoke plugging effects and would attempt some techniques to minimize this problem. The report today will cover the various aspects of the program, some of the results, and our proposed future work.

II. Program History — 1972 to date

Inasmuch as our work has undergone several changes in viewpoint and secondary goals, it is simpler to break down today's discussion into five parts as follows:

1. Systematic smoke plugging studies — 1972-1973.
2. The April 1973 conference at AEC Headquarters and the consequences.
3. The September 1973 large-scale tests.
4. The work in 1974 done and planned.
5. The proposed work for 1975.

*Work performed under the auspices of the U.S. Atomic Energy Commission.

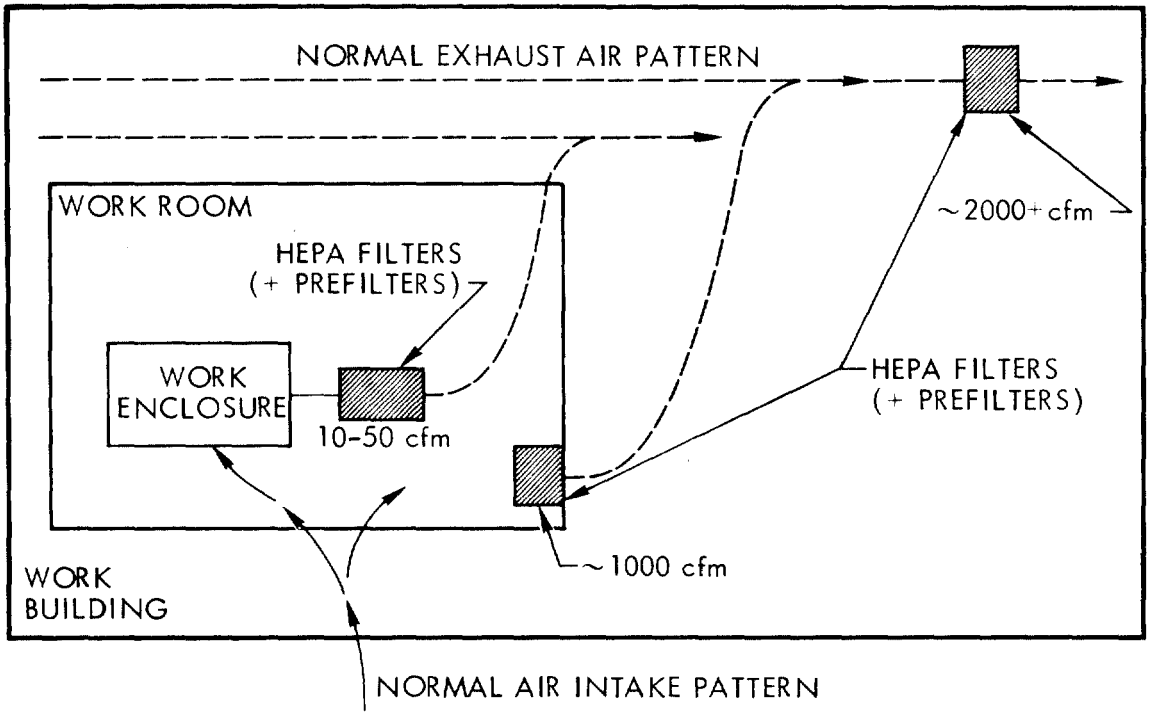

Fig. 1. Schematic diagram of one type of airflow system in a building where radioisotopes are used.

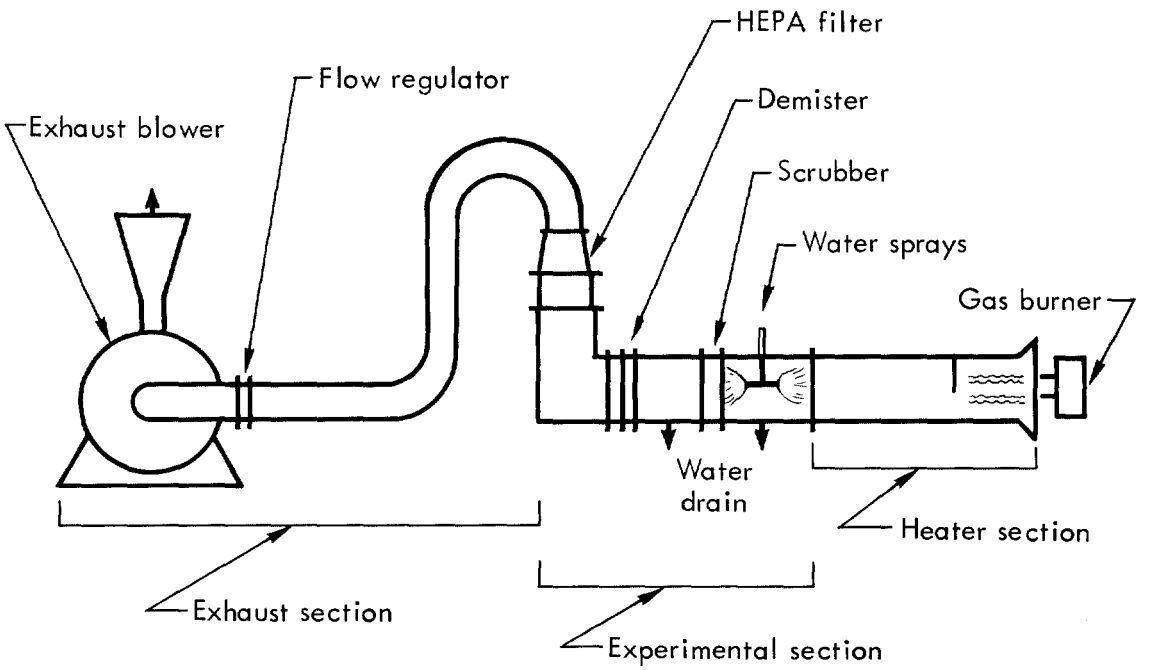

Fig. 2. Schematic diagram of LLL experimental spray damper setup.

III. Systematic Smoke Plugging Studies — 1972-1973

In our initial experiments we tried to answer the question, "How much smoke does it take to plug a filter?" For this purpose we used the setup illustrated schematically in Fig. 3 and shown photographically in Figs. 4 and 5.

In essence, we modified the existing outdoor duct test system by introducing a source of smoke drawn into the air stream by a venturi-like action. The source of smoke was obtained by modifying a wood-burning stove as follows: An ignited, forced-air — gas mixture introduced into the bottom of the stove impinged on a stainless steel pan onto which were either uniformly pumped small quantities of oil or onto which were fed small squares of likely solid fuels at a fairly uniform rate. The smoke so generated was mixed with the air stream and impinged upon the filter, or in some cases a prefilter.

The temperature of the smoke-air mixture was adjusted to the "cold" condition by preheating the air so that the mixture was at about 40°C; to a "warm" condition by preheating the mixture to approximately 150°C; or to the "hot" condition by preheating the mixture to approximately 400°C. Fuel rates were chosen at 50-, 100-, and 200-g/min, which represented our best judgments as to likely feed or burning rates of these items in a real fire.

The results of these tests are shown in Table I[2-4] from which it may be noted that filter plugging times using our original criterion of a pressure drop of

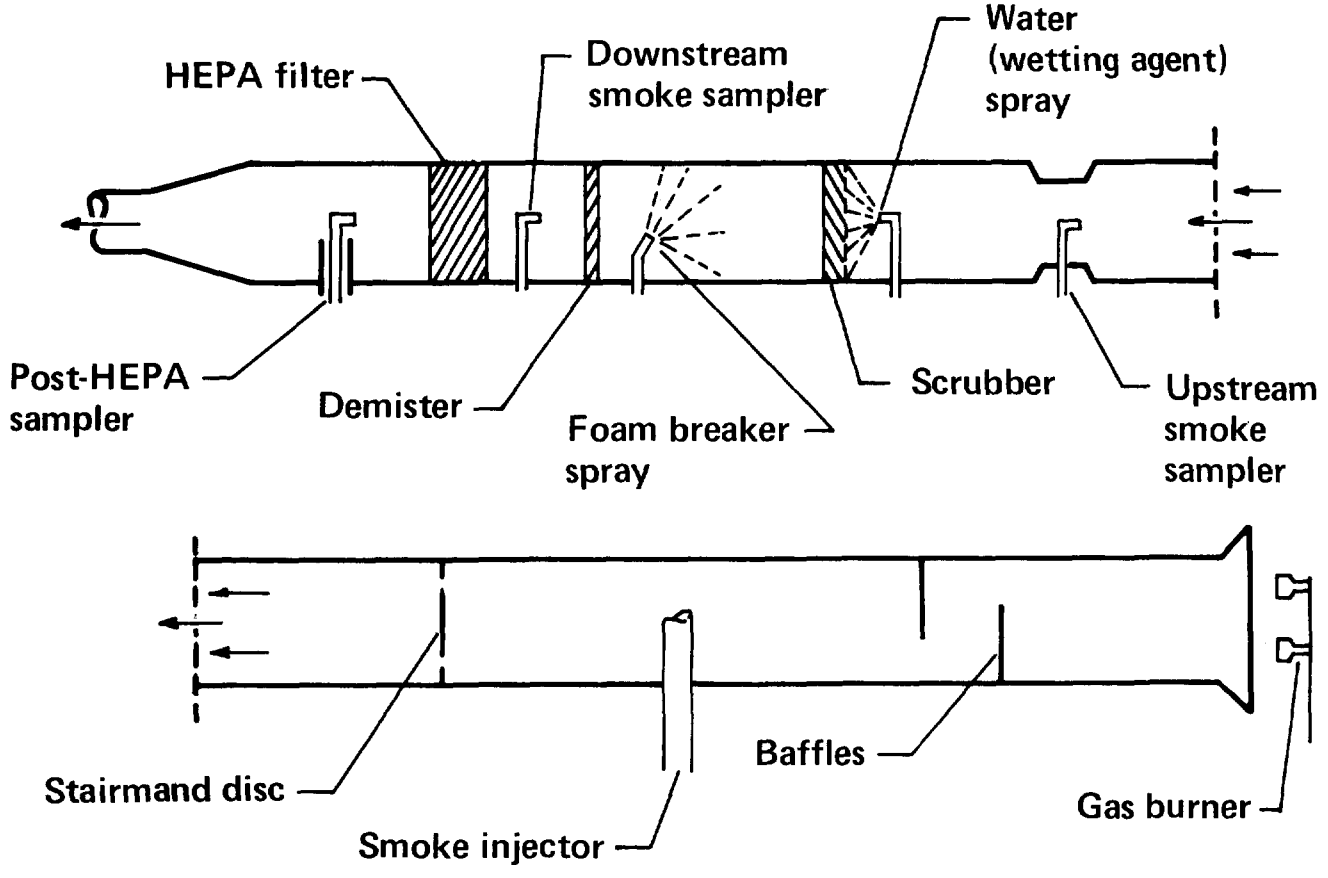

Fig. 3. Schematic diagram of typical duct arrangement for smoke experiments.

Table I. Summary of HEPA filter smoke plugging data.

Fuel	Smoke temp.	Run	Date	Feed rate (g/min)	Test duration (min)	HEPA filter ΔW(g)	HEPA filter ΔP(Pa)	Final air flow (ℓ/s)	$\frac{d}{dt}(\Delta P)$ (Pa/hr)	Chloride analyses[c]
Pump oil	Cold	PCS-1	7-13-72	--	10	--	747	432	--	
		-2	7-18-72	63.1	27	--	1244	378	2314	
		-6	7-26-72	62.6	96	407	1543	340	747	
		-7	7-27-72	98.2	30	470	1418	345	2314	
		-8	8-8-72	65.5	55	191	1244	363	1170	
		-9	8-10-72	60.6	55	340	1344	363	1194	
	Warm	PWS-1	8-2-72	60.3	60	355	1468	340	1145	
		-4	8-11-72	63.9	55	155	1394	340	1145	
Neoprene slabs	Cold	PCS-4	7-24-72	52	108	358	1568	340	722	
		-13	2-12-73	50	130	249	1717	293	672	
		-14[a]	2-13-73	53	70	48	398	205[a]	249	
		-15[a]	2-20-73	54	65	63	597	120[a]	398	
	Warm	PWS-3	8-3-72	52	60	65	1294	354	1020	
		-5	8-15-72	52	55	131	1269	359	995	
PMMA-FR	Cold	PCS-3	7-19-72	42	300	1890	1369	340	224	
		-10	12-19-72	52	55	--	1244	378	1070	
		-11	12-20-72	80	75	--	1518	354	1866	
		-12	1-17-73	104	40	302	1394	363	1070	
		-27	7-9-73	100	100	986	2041	236	1294	
	Warm	PWS-6	8-16-72	79	65	448	1269	354	896	
		-9	12-21-72	80	65	--	1369	340	1045	
		-10	7-10-73	100	85	630	1866	236	1170	
PMMA-NFR	Cold	PCS-17	4-23-73	193	50	234	1294	356	1269	
		-18[b]	4-24-73	193	100	356	1891	279	995	
		-19	5-3-73	200	100	416	1891	290	995	
PVC 0.5 mm film	Cold	PCS-5	7-25-72	100	40	855	1642	333	2115	
	Warm	PCS-7	8-17-72	50	40	219	1244	354	1394	
	Warm	PCS-8	8-22-72	100	25	367	1269	354	2339	
0.88-mm gloves-modified polyethylene	Cold	PCS-20	5-29-73	100	90	732	2090	236	1866(0-40)[d] 722(55-90)	--
0.4-mm gloves-modified polyethylene	Cold	PCS-21	5-30-73	113	70	760	2215	236	1742(20-45) 896(45-70)	25
0.4-mm gloves-neoprene	Cold	PCS-22	5-31-73	100	100	1646	1991	274	10.95	51
0.8-mm gloves-neop./mod. polyethylene	Cold	PCS-23	6-5-73	117	60	916	1518	340	1344	34
Gloves-leaded neoprene	Cold	PCS-24	6-6-73	200	75	2416	1518	330	1020	39[e]
6-mm window-chlor. polyester	Cold	PCS-25	6-8-73	105	60	503	1618	316	1369	--
6-mm window-allyl polycarbonate	Cold	PCS-26	6-11-73	115	90	120	1120	370	672	--
6-mm oil-impreg. pressed board	Cold	PCS-28	7-11-73	188	120	100	1468	319	597	--
25-mm impregnated pressed board	Cold	PCS-29	7-12-73	200	80[f]	0	547	406	274	--

[a]Original flow 236 ℓ/sec.
[b]Unsuccessful attempt to increase burning rate by forced air on stove.
[c]Chloride analysis: Cl^- mg/g of filter media.
[d]During minutes of test.
[e]Lead analyses for this test was Pb^{++} = 29 mg/g of filter media.
[f]Run stopped because filter showed no increase in plugging.

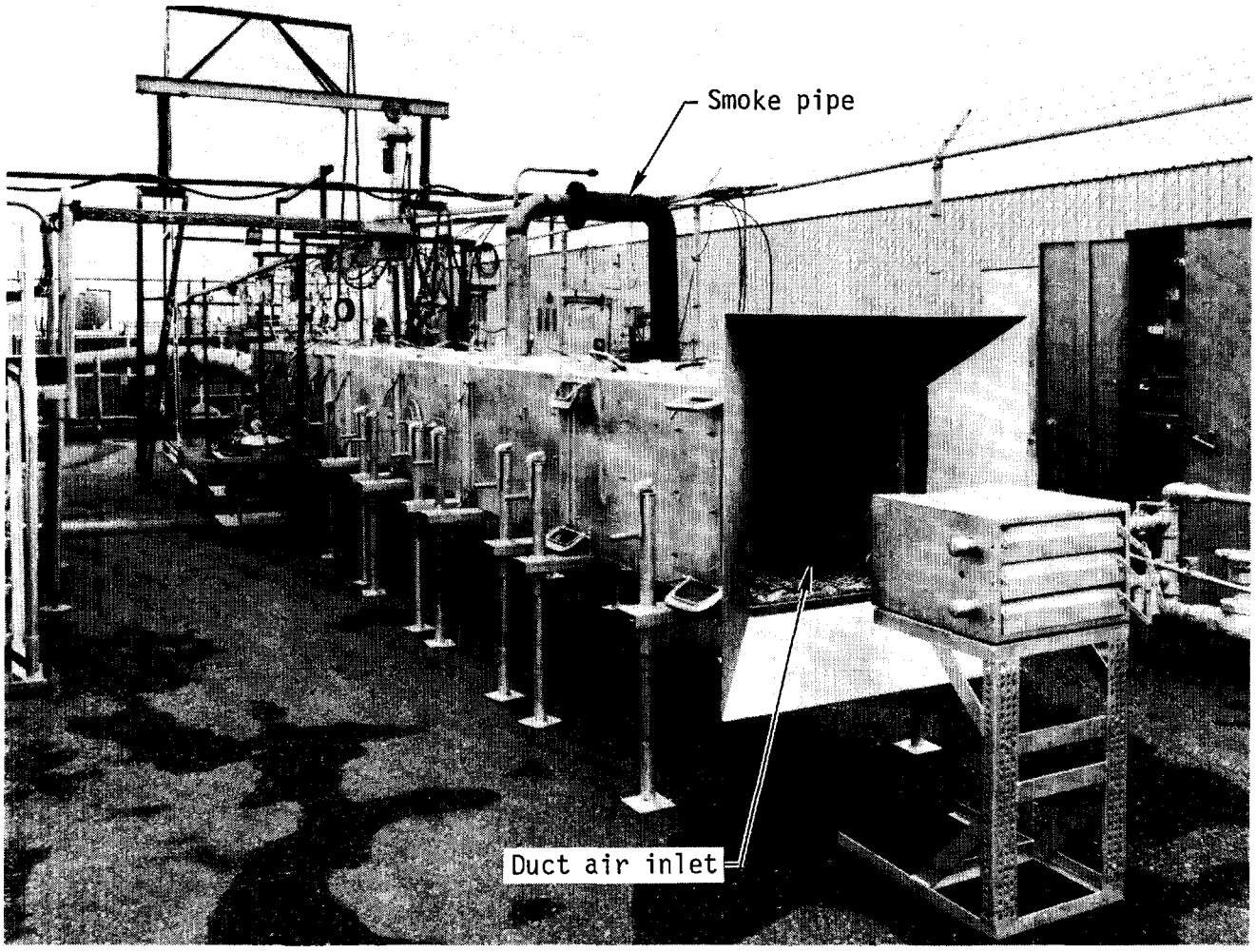

Fig. 4a. Duct arrangement for smoke experiments, general view.

about 800 pascals (5- to 6-in. water gauge) occurred in times varying from 30 to 120 min, depending upon the kind of material used and the rate at which it was fed.

Our initial attempts to scrub out smoke using water sprays proved fruitless since there was no decrease in filter-plugging time, even though we could observe smoke particles in the waste water overflow. Likewise, we had no success in using anionic surfactants injected into the water feed. However, we had done previous bench tests using these surfactants in varying concentrations and on samples of soot from various smoke scraped out of the stack, and these tests had indicated that two of the surfactants would indeed wet the smoke and cause it to disperse in water. As we shall show later, analysis of the particles of the smoke being generated revealed they were so small they probably could not be targeted by the large water droplets. We believe this is the reason for our failure to scrub smoke successfully using the above techniques.

Prefilter/HEPA-Filter Plugging Tests

Since in normal operation a prefilter is usually employed ahead of a HEPA filter, we decided to test the effect of smoke on a combined system. For this purpose we used a furnace filter, a prefilter with an indicated efficiency of 80% and

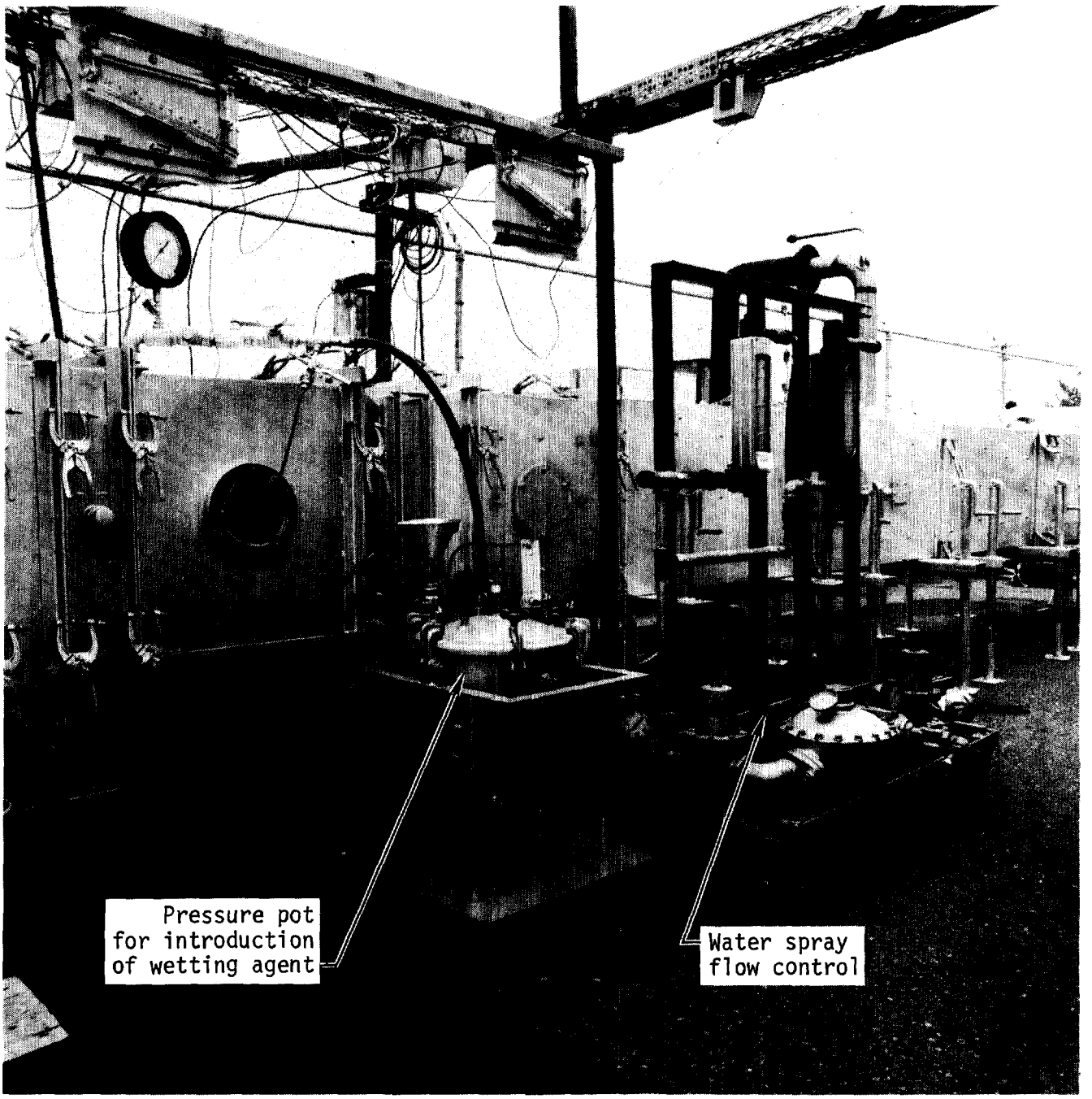

Fig. 4b. Duct arrangement for smoke experiments. Side view showing water spray flow regulator and pressure pot for introduction of wetting agent.

another prefilter with an indicated efficiency of 90%. We used neoprene slabs, fire-retardant polymethylmethacrylate, and 0.5-mm-thick polyvinyl chloride film as sources of smoke.

The data are summarized in Table II and the time histories of the tests are shown in Figs. 6, 7 and 8. The graphs dramatically illustrate that whereas even an inefficient furnace filter will "protect" the HEPA filter from smoke plugging, it

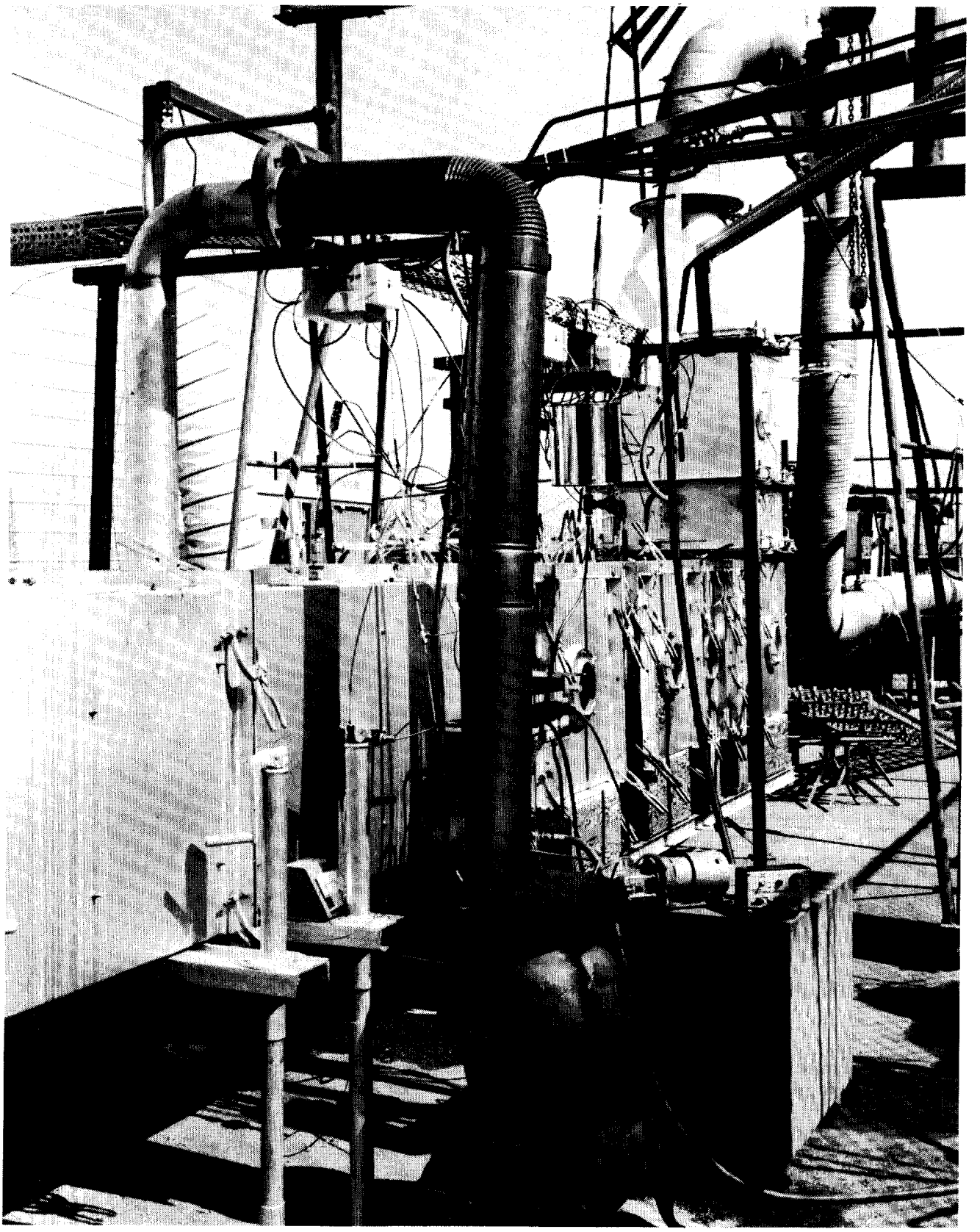

Fig. 4c. Duct arrangement for smoke experiments, side view showing stove for pyrolyzing/combusting materials to generate smokes.

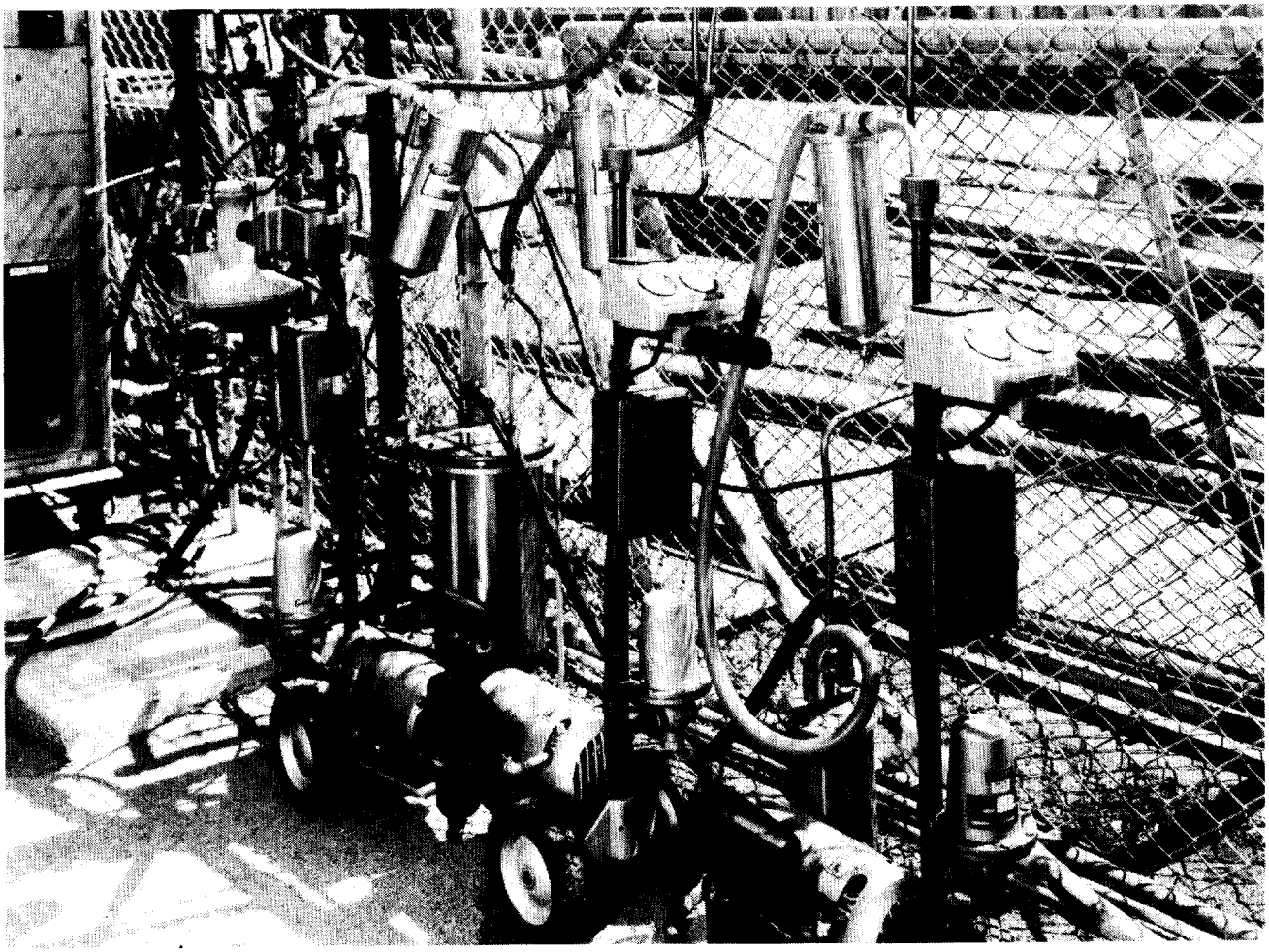

Fig. 5. Pump system for sampling smoke particulates.

Table II. Summary of prefilter/HEPA smoke plugging data.

Fuel	Smoke temp.	Prefilter eff. (%)	Run	Date	Feed (g/min)	Run time (min)	Δ Weight Prefilter (g)	Δ Weight HEPA (g)	ΔP(Pa) Prefilter	ΔP(Pa) HEPA	Final airflow (ℓ/sec)	
Neoprene slabs	Cold	90	PPCS-1	3-1-73	54	125	29	269	747	373	255	
		~30	-2	3-2-73	54	100	51	213	747	1319	326	
		80	-3	3-5-73	50	85	--	--	747	224	356	
		~30	-4	3-22-73	50	130	54	281	1344	1219	302	
		90	-5	3-23-73	50	120	22	18	1244	224	212	
		90	-6	3-27-73	50	120	411	161	2314	224	182	
		80	-7	3-28-73	50	120	395	23	1568	224	274	
		90	-8	3-28-73	50	120	395	135	2065	398	203	
Neoprene slabs	Warm	90	PPWS-1	8-3-72	52	30	48	(1)	1120	(1)	(1)	No HEPA
		90	PPWS-2	1-15-73	53	40	39	20	1020	224	354	
PMMA fire retardant	Cold	90	-9	3-29-73	110	75	669	348	174	1841	238	
		90	-10	4-3-73	103	80	527	181	299	1618	260	
		~30	-13	4-6-73	105	60	90	531	1244	1095	366	
PVC 0.5-mm film	Cold	90	-11	4-4-73	98	30	259	107	1916	149	215	
		~30	-12	4-4-73	98	30	33	157	498	1269	366	

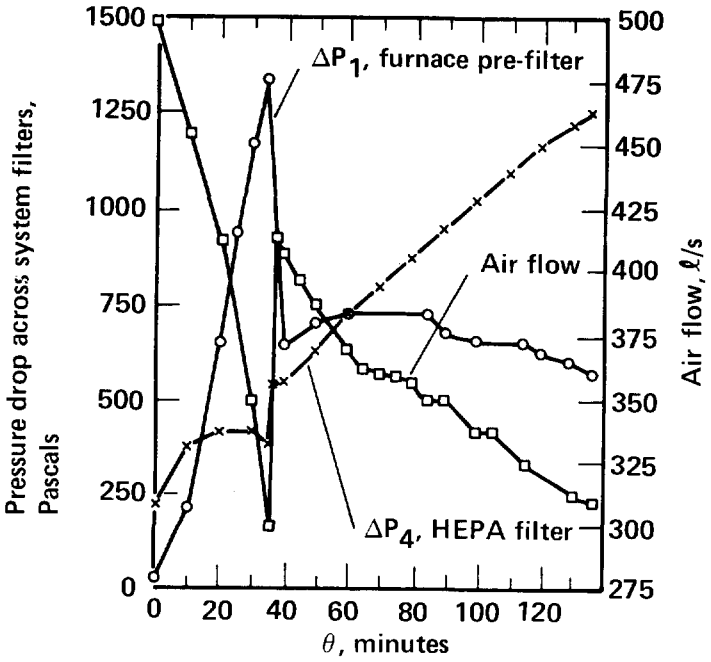

Fig. 6. Pressure drop and airflow of ventilation system with prefilter and HEPA filter subjected to neoprene smoke — furnace-type prefilter.

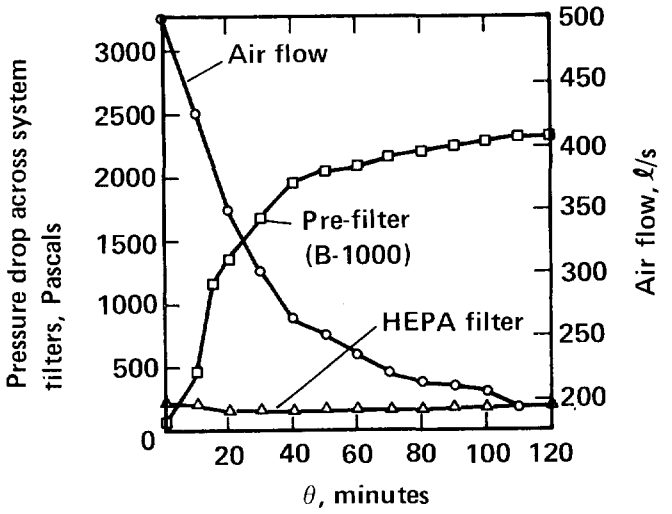

Fig. 7. Pressure drop and airflow of ventilation system with prefilter and HEPA filter subjected to neoprene smoke — 90% prefilter.

does so at the expense of airflow, and hence results in inadequate ventilation. Figures 9, 10, and 11 are photographs of filters in the new and smoke-plugged conditions.

During these filter- and prefilter-plugging tests, we took smoke samples at various times in the freshly generated condition and at a location just before the filter or prefilter. Then using a cascade impactor we determined the particle size distribution by weight. Whereas these data are not shown in this report, a typical analysis is shown in Fig. 12. In this particular example, we attempted to age the smoke 3 min using the smoke chamber in our laboratory setup. As will be noted, in fresh smoke and that aged approximately 1-3 min, most of the weight of the particles is very much less than 1 μ in size. We have calculated that the smoke generated in our outdoor experiments is less than 1 min old when it sees the filter or prefilter.

We have summarized all the data we have obtained on these outdoor tests in Tables III and IV; we have normalized the data where possible to 50% of the rated flow of the filter (Table V); and in Table VI we show the comparison of the HEPA loading for various materials and various pressure drops across the filter. These data may be regarded as handbook values to be used by researchers and designers once we determine the real burning rates of materials under actual fire conditions.

IV. AEC Conference — April 1973

During the course of the work just reported the question frequently arose, "What are the actual burning or decomposition rates of the kinds of materials used in AEC laboratories and processing facilities?" These materials are for the most part synthetic polymers. Our investigations and inquiries of a number of research and

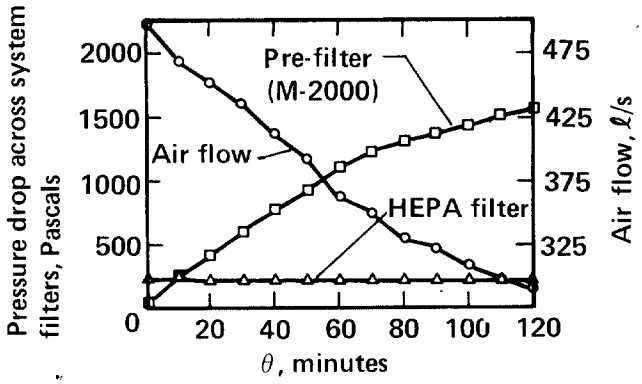

Fig. 8. Pressure drop and airflow of ventilation system with prefilter and HEPA filter subjected to neoprene smoke — 80% prefilter.

testing organizations throughout the country yielded essentially no information in this respect. In fact, as one prominent fire researcher put it over the telephone, "We have lots of burning rate data on materials we used to build things out of."

As a result of this lack of knowledge and other considerations, a meeting was called in April of 1973 at AEC Headquarters and attended by some 20 contractor and consulting personnel both interested in and deemed to have some knowledge on the subject. The following points summarize what appears to be the consensus of this meeting:

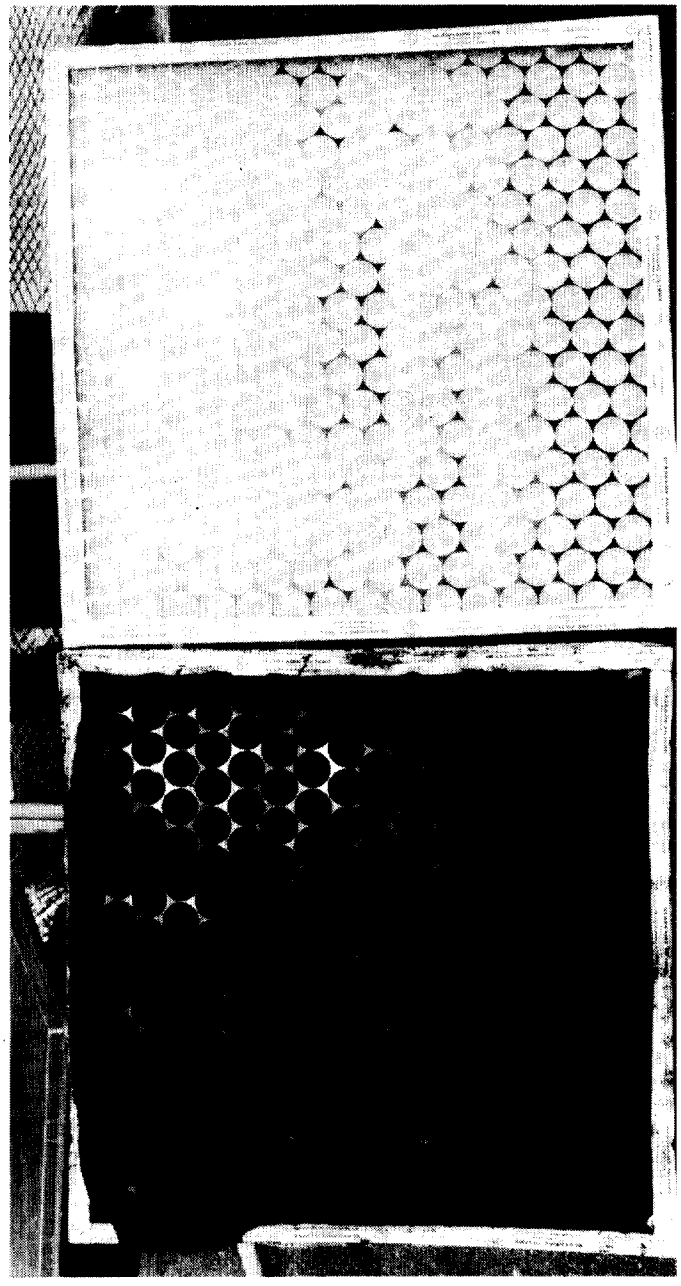

Fig. 9. Photograph of furnace prefilter before and after plugging (and rupture) by neoprene smoke.

- For experimental and design purposes, a filter is considered to be plugged when the flow through it drops to 50% of its rated value. (From our Table V reported here, a 50% flow is reached at a pressure drop approximating 2300 pascals or about 9.2 in. water gauge.)
- Little reliable information exists to permit a quantification of the smoke problem.
- Much information is needed on burning rates, characteristics of the smokes which reach the filter, smoke scrubbing, and actual burning times. Furthermore, "cold" smokes (including condensables) which occur in the early stages of a fire are important considerations.

Table III. Filter fire protection. (Fuel feed, air flow, and ΔP[a] versus time for various materials.)

Run No.	Material[b]	Date	Flow rate (ℓ/sec) versus ΔP			Total fuel feed versus ΔP			Time to reach		
			ΔP-1	ΔP-2 (Pa)	ΔP-3	ΔP_1	ΔP_2 (kg)	ΔP_3	ΔP_1	ΔP_2 (min)	ΔP_3
PCS-4	Neoprene	7-24-72	363	328	--	3.85	6.29	8.68	74	121	167
-5	PVC (0.5-mm film)	7-25-72	366	311	--	2.60	4.80	7.70	26	48	77
-6	DTE oil	7-26-72	349	307	--	4.95	6.76	9.70	79	108	155
-7	DTE oil	7-27-72	354	307	--	2.55	4.03	5.40	26	41	55
-8	DTE oil	8-8-72	354	307		3.28	5.11	6.55	50	78	100
9	DTE oil	8-10-72	354	316	--	3.09	4.61	6.24	51	76	103
-10	Neoprene	12-17-72	345	290	--	2.86	4.16	--	55	80	--
-11	PMMA-FR	12-21-72	359	335	--	4.48	6.80	--	56	85	--
-12	PMMA-FR	1-17-73	366	335	--	3.65	5.51	7.49	35	48	72
-13	Neoprene	2-12-73	354	283	--	3.90	6.75	8.60	78	135	172
Average			356	312							
± Standard deviation			±7	±17							
PCS-17	PMMA II	4-23-73	361	321	276	9.26	12.7	16.4	48	66	85
-18	PMMA II	4-24-73	363	293	271	8.9	16.4	23.2	46	85	120
-19	PMMA I	5-3-73	368	304	248	9.6	17.6	25.0	48	88	125
-20	Modif. polyethylene gloves 0.4 mm	5-29-73	354	293	219	3.1	5.5	9.5	31	55	95
-21	Modif. polyethylene gloves 0.4 mm	5-30-73	356	304	236	2.6	4.5	7.9	23	40	70
-22	Neoprene gloves 0.4 mm	5-31-73	366	304	236	5.7	8.5	11.5	57	85	115
-23	Neoprene mod. polyethylene gloves 0.76 mm	6-5-73	359	314	262	5.6	8.2	10.8	48	70	93
-24	Neoprene/lead gloves	6-6-73	363	307	257	11.8	17.4	23.0	59	87	115
-25	Chlor. polyester	6-8-73	356	304	254	4.6	6.8	9.9	44	65	86
-26	Allyl polycarbonate	6-11-73	340	304	236	11.2	16.7	23.0	97	145	200
Average			359	305	249						
± Standard deviation			±9	±8	±18						

[a] ΔP_1 = 1250 Pa (5-in. w.g.)
ΔP_2 = 1750 Pa (7-in. w.g.)
ΔP_3 = 2250 Pa (9-in. w.g.)
[b] Except as indicated, material was in form of squares 6.4 mm thick.

- Until more knowledge is gained, a reasonable approach to the problem is to reduce the smoke-producing material in building materials and equipment wherever possible.

- The question still persists as to whether a filter-plugging problem exists in the event of a real fire.

V. September 1973 — Large Scale Tests

In an effort to resolve the question as to whether filters will likely plug in the event of a real fire, we decided to conduct some experiments on as large a

Table IV. Filter fire protection, HEPA loading versus ΔP (pascals).

Run No.	Fuel	Rate fuel feed (g)	Duration of run (min)	Actual HEPA loading (g)	Calculated HEPA loading (g) 1.25 kPa	1.75 kPa	2.25 kPa	Actual ΔP at run end (Pa)
PCS-4	Neoprene	52	111	358	239	390	539	1593
-5	PVC	100	40	855	556	1027	1648	1642
-6	DTE oil	62.6	96	407	335	558	657	1543
-7	DTE oil	98.2	30	470	407	642	861	1418
-8	DTE oil	65.5	50	191	191	298	382	1244
-9	DTE oil	60.6	55	340	315	470	637	1344
-10	Neoprene	52	45	Unknown	--	--	--	1045
-11	PMMA-FR	80	75	Unknown	--	--	--	1543
-12	PMMA-FR	104	40	302	264	400	544	1394
-13	Neoprene	50	125	249	155	269	342	1717
-17	PMMA II	193	50	237	228	313	403	1294
-18	PMMA II	193	100	356	164	303	427	1891
-19	PMMA I	200	100	416	200	366	520	1891
-20	Modif. poly-ethylene	100	90	732	252	447	772	2090
-21	Modif. poly-ethylene	113	70	760	250	434	760	2215
-22	Neoprene 0.4 mm	100	100	1646	938	1400	1893	1991
-23	Neoprene/mod. P.E. 0.8 mm	117	60	916	733	1069	1420	1518
-24	Neoprene/lead	200	75	2416	1900	2800	3700	1518
-25	Cl-polyester	105	60	503	369	545	721	1618
-26	Allyl poly-carbonate	115	90	120	129	193	267	1120
-27	PMMA-FR	100	100	986	503	730	1183	2041
-28	Pressed bd. 6.4 mm	188	120	100	91	112	--	1468
-29	Pressed bd. 25 mm	200	80	--	--	--	--	547

scale as possible within our capabilities. First, we surveyed the fuel loadings in the laboratories in our plutonium research building. The values in three rooms representing reasonable variations in both the quantity of fuel and kinds of fuel are shown in Table VII. Next we chose a vacant Quonset hut and attached the outdoor spray damper duct system to one end of it and sealed the other end except for a small opening. We scaled down the fuel loadings to the same concentration per unit floor area (as shown in Table VII), loaded the fuels onto a pallet mounted on top of a load cell system, and set fire to the fuel in each of three experiments. Figure 13 shows a schematic diagram of the setup.

The results of these three tests are shown in Table VIII and Figs. 14, 15, and 16, and may be summarized as follows:

- In test 1 with a fuel loading of 8.2 kg/m^2 and containing 94% cellulosics (wood and paper), the temperature at the ceiling rapidly rose to and was maintained at about 350°C. However, the filter showed little or no sign of plugging until a hose stream (6.3 ℓ/sec — 100 gpm for 30 sec) was applied

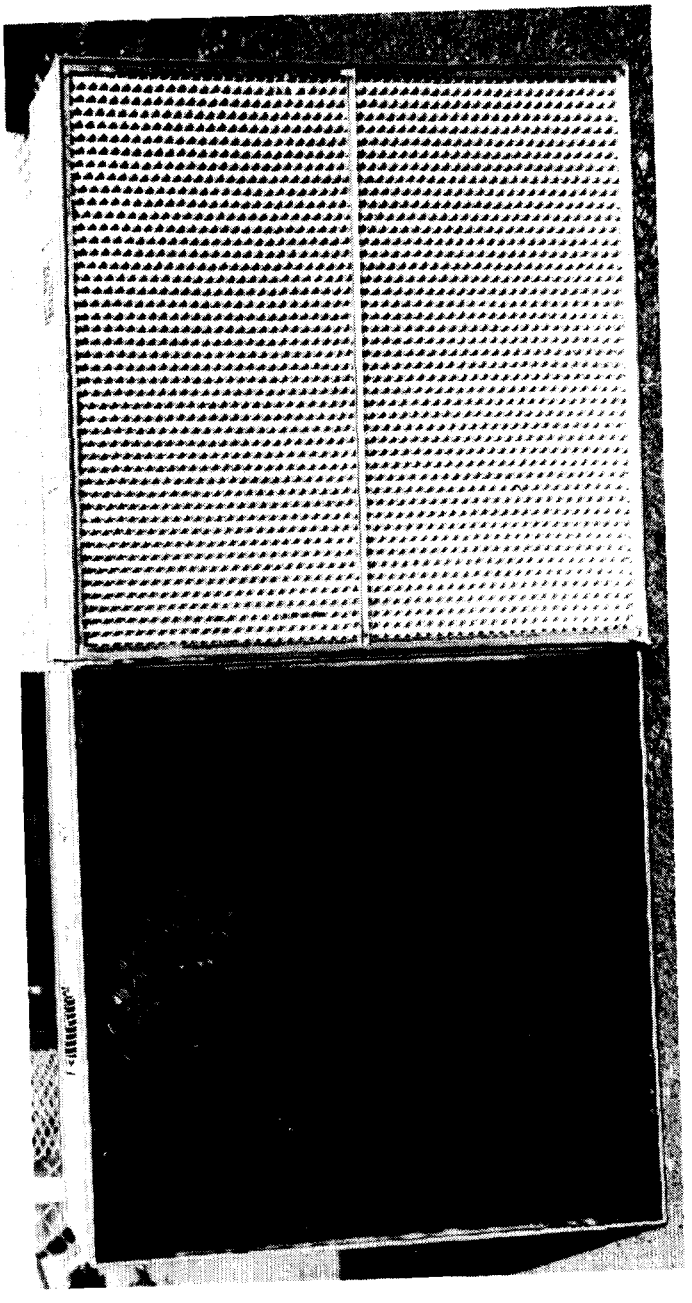

Fig. 10. Photograph of 90% prefilter before and after plugging by neoprene smoke.

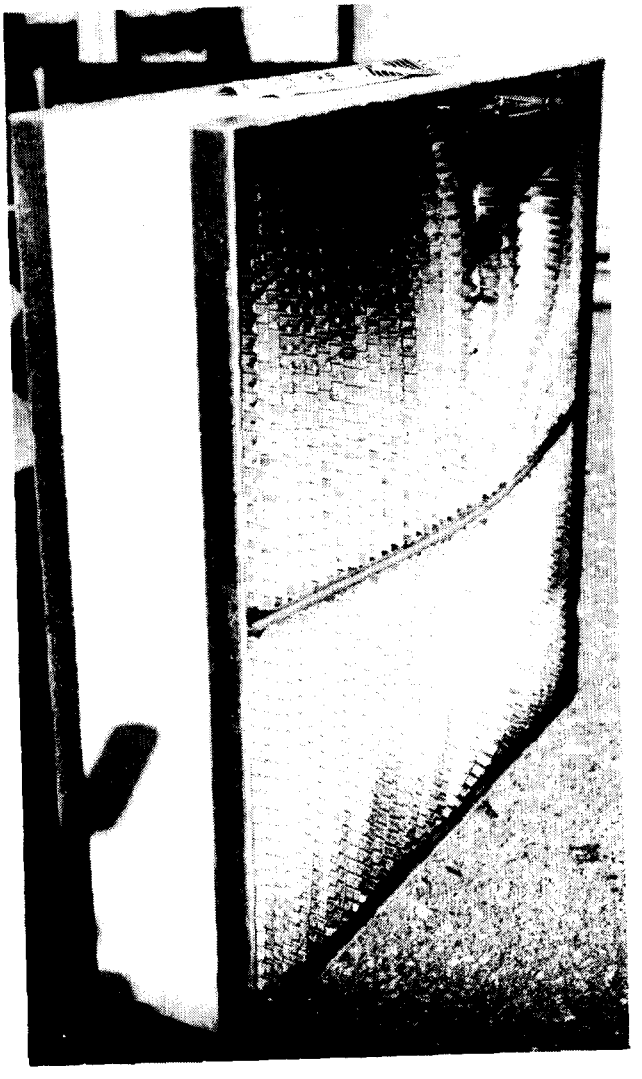

Fig. 11. Photograph of 80% prefilter after plugging by neoprene smoke.

45 min into the test, at which time a sudden release of soot plugged the filter and simultaeously decreased the flow to approximately half the initial value.

- In test 2 with a fuel loading of approximately 12 kg/m^2 and containing 78% plastics, the exhaust system was plugged in approximately 5 min due in large part to accumulation of tars on the scrubber. We believe that these tars consisted of partly depolymerized or repolymerized compounds.
- In test 3 containing 4 kg/m^2 of fuel and including 58% plastics, the system plugged up in about 12 min. In this particular case the ceiling

Table V. HEBA filter smoke plugging; data normalized to 50% of rated air flow (~250 ℓ/sec).

Run	Date (1973)	Material	Feed rate (g/min)	Run time (min)	ΔP-HEPA (Pa)	Time to reach 5-Pa duct suction (min)	Smoke particle size[a]
17	4-23	6-mm PMMA II	193	105	--	90	64 ± 3
18	4-24	6-mm PMMA II	193	120	2165	105	75 ± 2
19	5-3	6-mm PMMA I	200	160	--	--	60 ± 1
20	5-29	0.8-mm modif. P.E. gloves	100	102	2314	--	49 ± 0.5
21	5-30	0.4-mm modif. P.E. gloves	113	70	2215	70	56 ± 3
22	5-31	0.4-mm neoprene gloves	100	120	2314	143	68 ± 2
23	6-5	0.8-mm neoprene gloves	117	103	2488	107	52 ± 5
24	6-6	Leaded neoprene gloves	200	125	2240	94	16 ± 1
25	6-8	6.4-mm chlor. polyester	105	91	2339	90	62 ± 0.5
26	6-11	6.4-mm allyl polycarbonate	115	205	2289	--	58 ± 2
AVERAGE					2289 ± 44 (9.2 ± 0.58 in. w.g.)		

[a]Weight percent of smoke particles less than 1 μ.

temperature reached only 230°C and the plugging was mostly on the filter, although the scrubber did show some increase in pressure drop.

We should note that there are two differences in these experiments from what would exist in a real fire situation. First, the geometry of the Quonset hut is quite different from that of a real laboratory in that the length-to-width ratios are quite different, and the ceiling is much lower. Second, all the fuel was piled together and ignited at once, and this is unlikely in a real situation. However, we believe that there is sufficient evidence both from these experiments and the actual experience in the fire at Rocky Flats several years ago to warrant the conclusion that a serious problem exists relative to the plugging of the HEPA filters as a result of a fire in a facility where large quantities of polymeric materials exist and where the continued operation of the exhaust filtration system is mandatory.

VI. Work in 1974

We reported the results of these tests and our conclusions at AEC Headquarters last October 1973,(5) and, at a subsequent meeting of the Project Review Board, we outlined a program for future work. As a result of these discussions, LLL has decided to build a full-scale fire test facility. Our design criteria call for a fire test cell with inside working dimensions of 6.0 m long by 3.7 m wide with a ceiling height of 4.5 m. The working volume will thus be 100 m^3. (Dimensions are 12.1 × 19.7 × 14.8 ft high; volume = 3525 ft^3). There will be a small enclosed viewing gallery at one end.

The cell will be equipped with both a high and a low exhaust ventilation takeoff leading to an external duct system similar to the one we have been using and capable of being varied, depending upon the experiment. The cell will also be equipped with a sprinkler system which can be used at will.

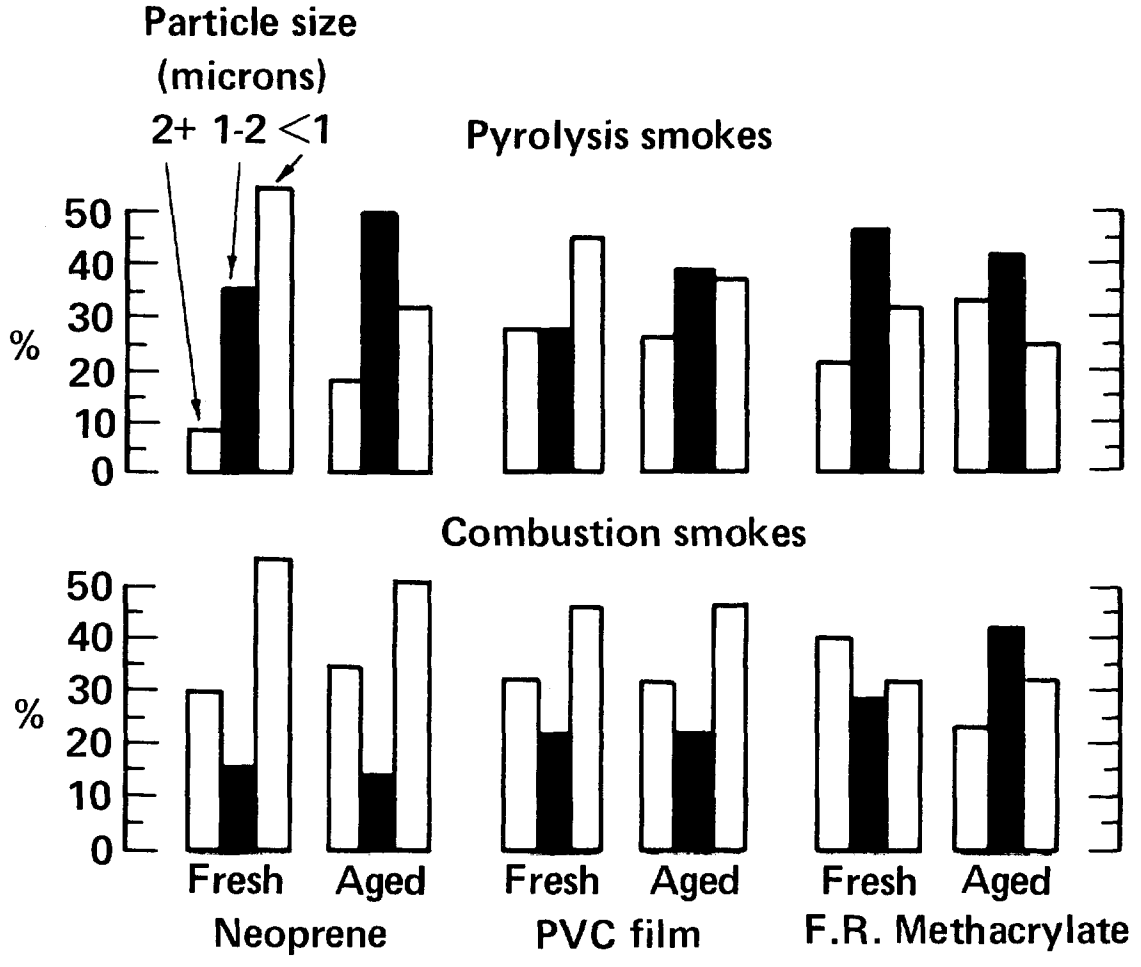

Fig. 12. Particle size distribution by weight of fresh smoke and smoke aged 1-3 minutes for materials of interest.

With funds provided by the Division of Operational Safety, AEC, we are buying a data acquisition system which will enable us to measure rapidly (and subsequently evaluate) temperature conditions, smoke optical density, smoke particle size, air- and water-flow rates, and pressure differences both between the building and atmosphere and also across the various prefilters and filters in the exhaust system.

While we are waiting for the building to be designed and built, and this will take us to the end of calendar year 1974, we are continuing our experimental work using the outdoor duct system.

Sometime ago Mr. Warren Ng of our Plant Engineering Department suggested we try a new two-fluid nozzle (air-water) which the manufacturer claimed would produce very small water droplets. We obtained two of these, rated respectively at 0.063- and 0.24-ℓ/sec (1.0 and 3.8 gal/min) of water, and have used them quite successfully to reduce the temperature of "hot fire gases." A picture of this nozzle is shown statically in Fig. 17(a) and in actual operation in Fig. 17(b). A summary of the results of several tests using hot air to simulate fire gases is shown in Fig. 18. Note that at a feed temperature of approximately 800°C, the temperature ahead of the prefilter (below the demister) is maintained at or below 150°C (300°F). This temperature is deemed to be the critical point above which the adhesive binding the filter media to it's frame will deteriorate. Note also that this effect was achieved

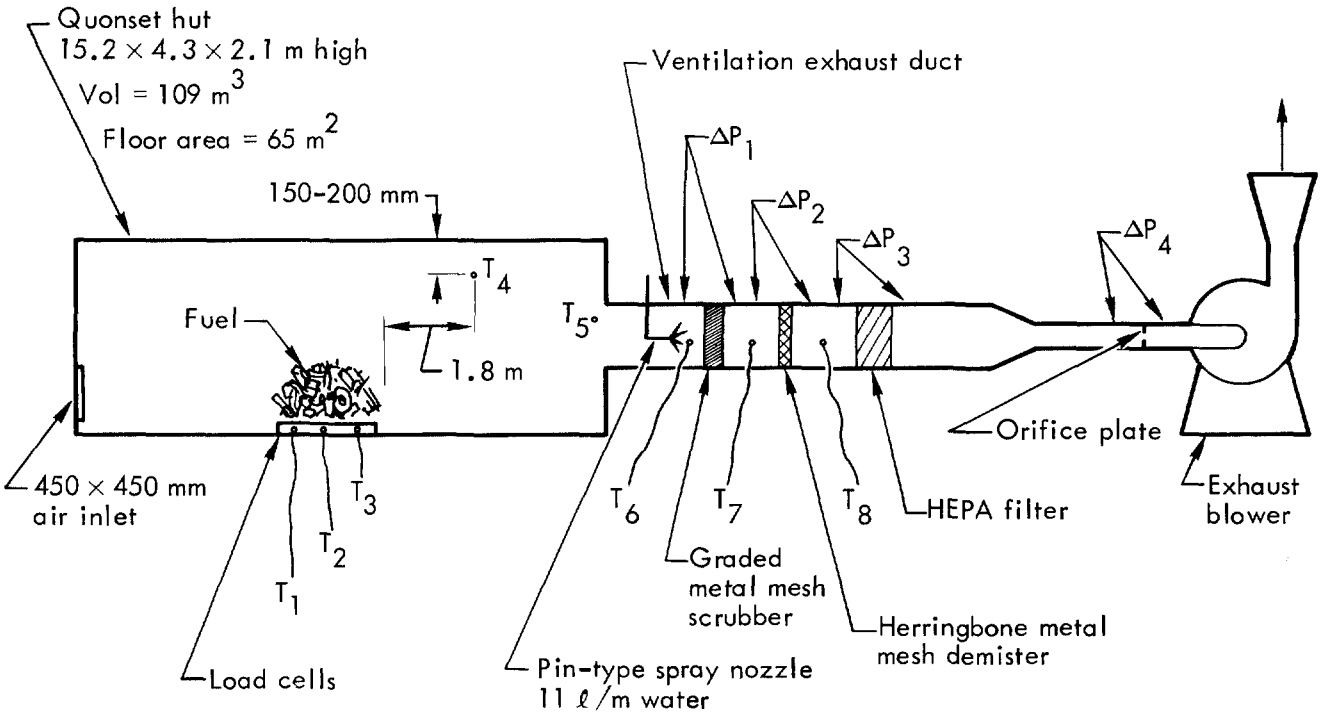

Fig. 13. Schematic diagram of LLL large scale fire-smoke filter test setup.

first with the use of less than 0.09 liters of water per sec (1.5 gpm of water) and with complete evaporation. This means that the use of this nozzle will effectively cool the hot fire gases without any "contaminated water overflow." The disadvantage to the use of this system, of course, is that there must be a guaranteed supply of air for the nozzles.

During the balance of this summer and early fall we shall use this nozzle with and without the addition of surfactants to the feed water to determine whether it is effective in scrubbing smoke and thus reducing the filter plugging problem.

VII. Proposed Work 1975

When our new fire test cell is constructed, equipped and checked out, we propose to conduct a series of full-scale fire tests using real furniture and equipment mounted on load cells and employing realistic ignitions to determine the following kinds of things: (1) how do fires grow in temperature, time, and in smoke development; (2) how effective are sprinklers in mitigating the effects of the fire; (3) how much smoke generated by a fire actually reaches the exhaust system; (4) is a high exhaust better than a low exhaust; and (5) the effects of various techniques employed in the exhaust system in mitigating the filter plugging effect. In this latter regard, we propose to try to answer such questions as: (1) will the use of water sprays with or without added surfactants and without the use of a scrubber cause condensible tars to precipitate sufficiently on the walls of the duct system so that the filter life will be extended? (2) will a rolling type prefilter adjusted to move as the pressure drop across it increases collect enough smoke so that the filter will be protected until the fire either dies out or is put out? (3) can smoke particles be forced to agglomerate before they reach the filter to such an extent that they can be scrubbed away?

Table VI. Filter fire protection — comparison of HEPA loading for various materials.

D.T.E. oil	Calculated HEPA loading		
	ΔP = 1.25 kPa	ΔP = 1.75 kPa (g)	ΔP = 2.24 kPa
	335	558	657
	407	642	861
	191	298	382
	315	470	637
Average ± Std. Dev.	312 ±77	492 ±128	
PMMA-(non-fire-retardant)	228	313	403
	164	303	427
Average	196 ± 30	300 ± 5	
Modif. poly-ethylene	252	447	772
(glove) (0.4 and 0.8 mm)	250	434	760
Average	250 ± 1	440 ± 5	
Neoprene (glove) (0.4 mm)	938	1400	1893

Table VII. Fire loading data — actual in three laboratory rooms at LLL versus those used in large-scale tests.

Fire test No.	1			2			3		
Room No.	1313			1329			1361		
Floor area (m^2)	113			86			90		
Fire loading	Room (tot. kg)	(conc. kg/m^2)	Test (kg)	Room (tot. kg)	(conc. kg/m^2)	Test (kg)	Room (tot. kg)	(conc. kg/m^2)	Test (kg)
Glove box window matl.	45.4	0.40[a]	25.4	227	2.64	68.0[b]	136	1.51	98.0
Vinyl-0.5-mm film	1.4	0.01	0.8	336	3.90	227	12.7	0.14	6.5
Vinyl-6-mm rigid sheet	0	0	0	390	4.54	259	0	0	0
Neoprene gloves	10.9	0.10	6.1	13.6	0.16	10.0	68.0	0.75	49.0
Wood	581	5.14	323	145	1.68	106	145	1.61	105
Paper	318	2.81	177	81.6	0.95	59.4	13.6	0.15	9.8
Polyethylene film	0	0	0	50.0	0.59	36.7	0	0	0
	956	8.46	532	1243	14.46	766	375	4.16	268
Test load conc. (kg/m^2)			8.18 (1.68 lb/ft^2)			11.78 (2.41 lb/ft^2)			4.12 (0.84 lb/ft^2)
Percentage of full-scale load (total wt. basis)			56			62			71
Percent plastics		6			82			58	

[a]70% fire-retarded variety; 30% non-fire-retarded.
[b]Equivalent to 1.0 kg/m^2 because of lack of material.
[c]100% fire-retarded variety.

Table VIII. Summary of large-scale fire-smoke filter plugging tests at LLL, September 1973.

Test No. / Date (1973)	1 / 6 Sept.	2 / 13 Sept.	3 / 27 Sept.
Fire loading			
Total wt. (kg)	532	766	268
Conc. kg/m^2	8.18	11.78	4.12
% plastics	6	78	58
Test duration			
Time to plug (min)	45	~5	12
Equiv. air flow (ℓ/sec)	~212	264	142-189
Time to 50% flow	43	4.5	11.5
Maximum temperatures			
At ceiling	345 C (650 F)	330 C (625 F)	230 C (445 F)
Time (min)	20	4	11
In exhaust duct	95 C (203 F)	35 C (95 F)	37 C (99 F)
Time (min)	25	Throughout	Throughout
Maximum ΔP			
Scrubber (Pa)	Not Measured	Not Measured	770
Time (min)	--	--	12
Filter (Pa)	1915	2240	1640
Time (min)	45	~5	12
Post-fire analyses			
Weight gain of filter (g)	1050	808	585
Soot content of filter media	24%	--	21%
HCl content of soot	1%	--	0.9%
HCl content of water from scrubber	--	0.6	0.4-0.03
Cause of ventilation failure	Sudden release of soot by steam generated by fire hose stream at 45-min test time.	Heavy accumulation of soot plugged scrubber.	Plugging of filter and to some extent the scrubber with soot.

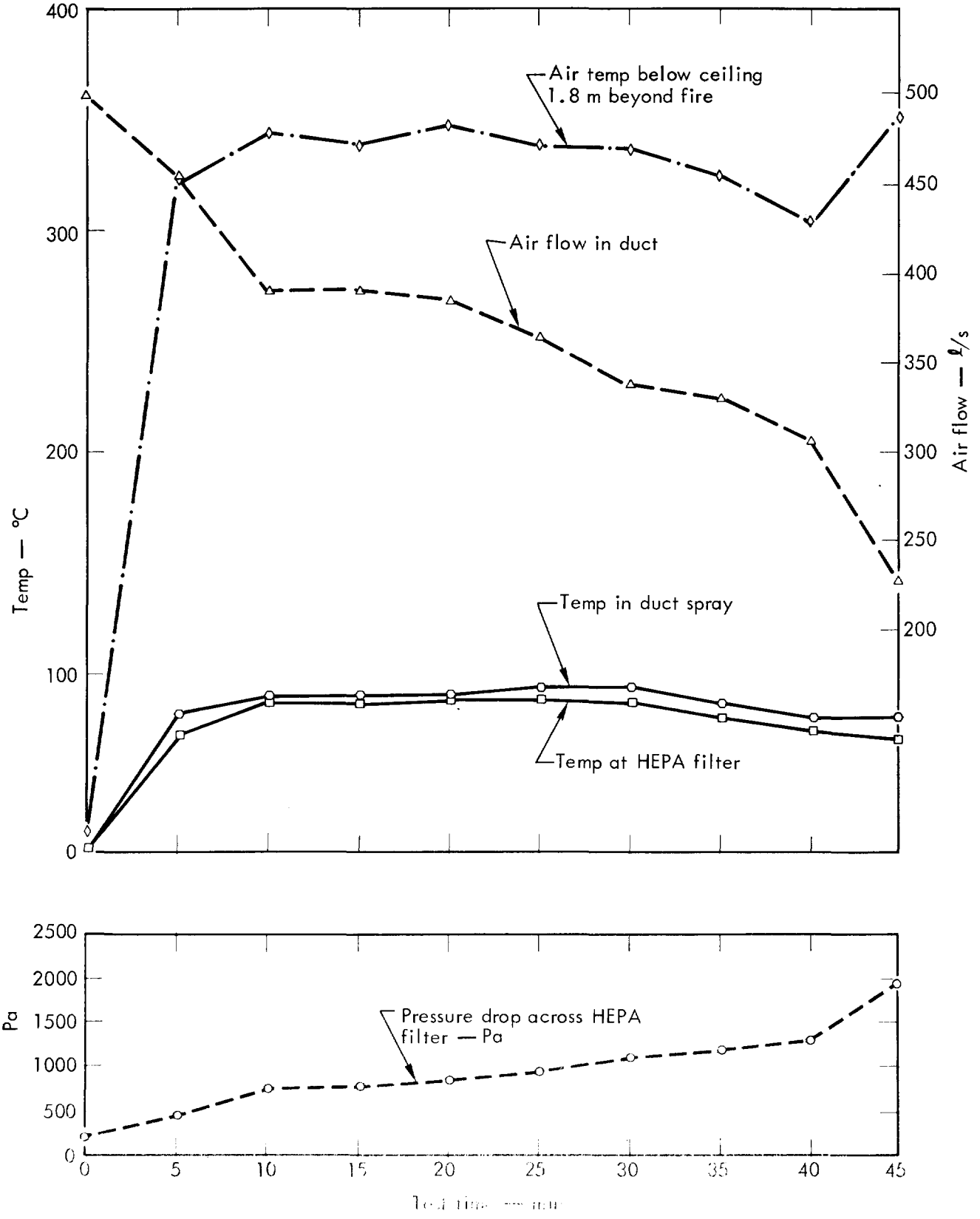

Fig. 14. Fire Test No. 1 — temperature, airflow and pressure drop versus time.

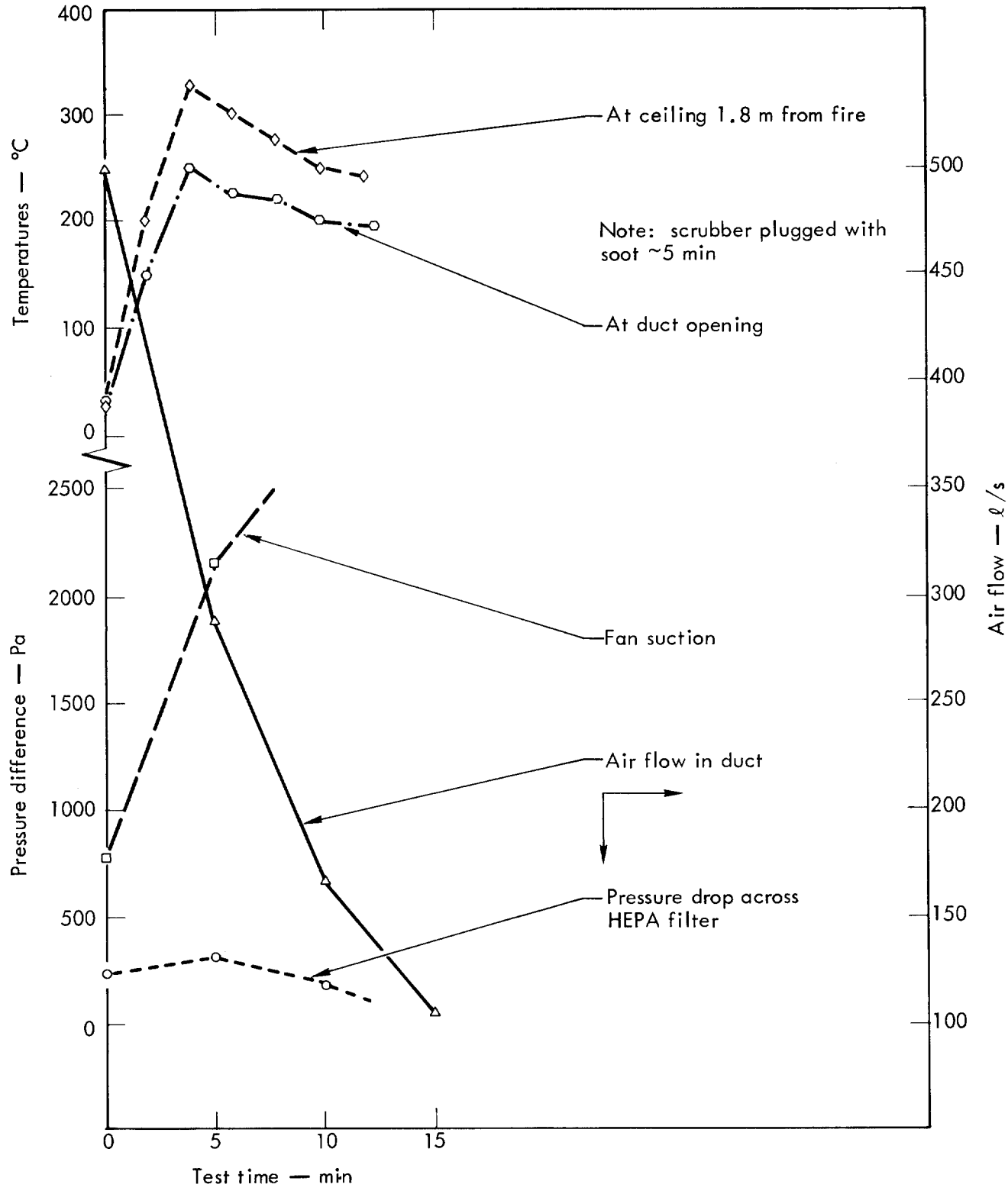

Fig. 15. Fire Test No. 2 — temperature, airflow and pressure drop versus time.

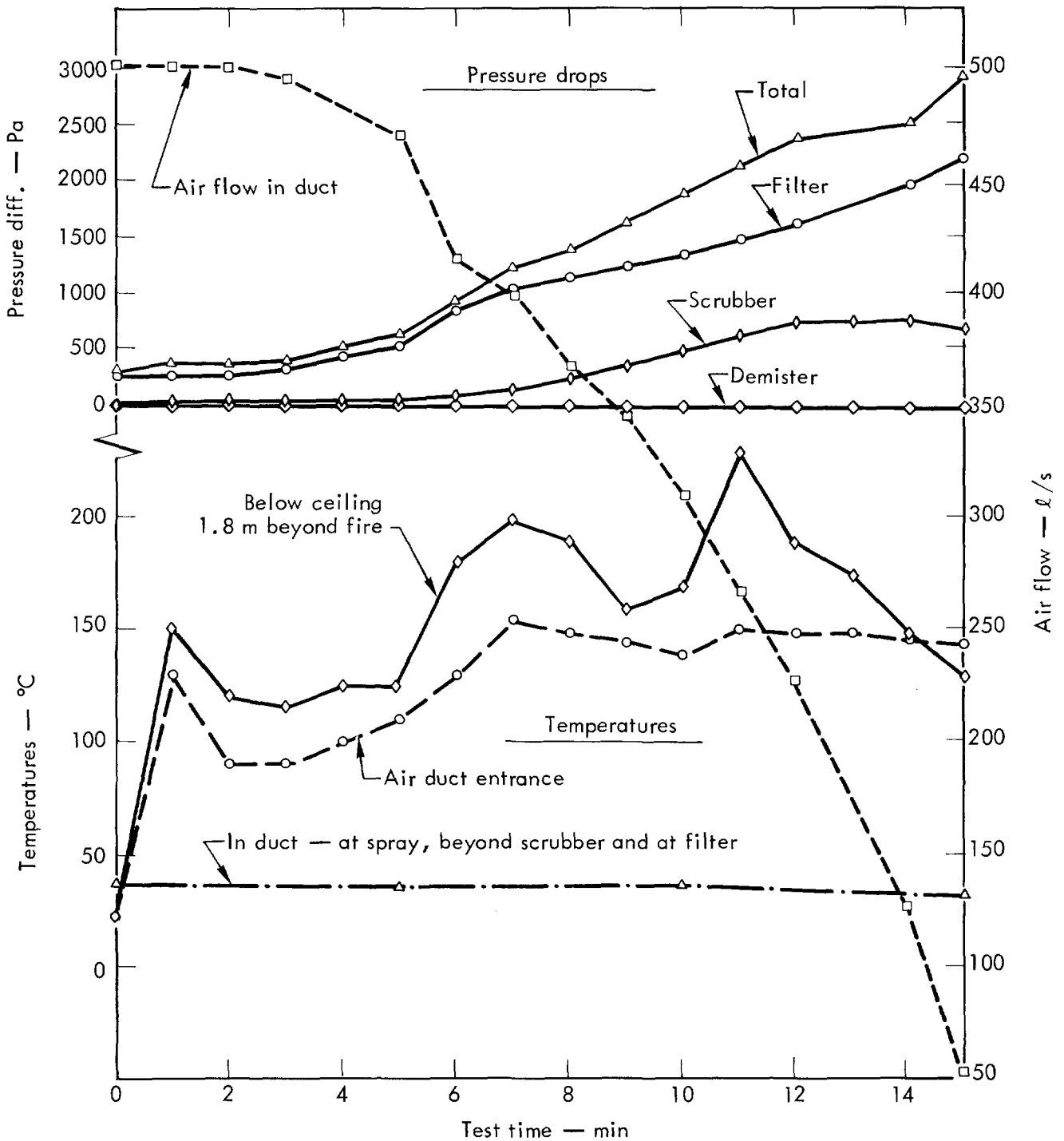

Fig. 16. Fire Test No. 3 — temperature, airflow and pressure drop versus time.

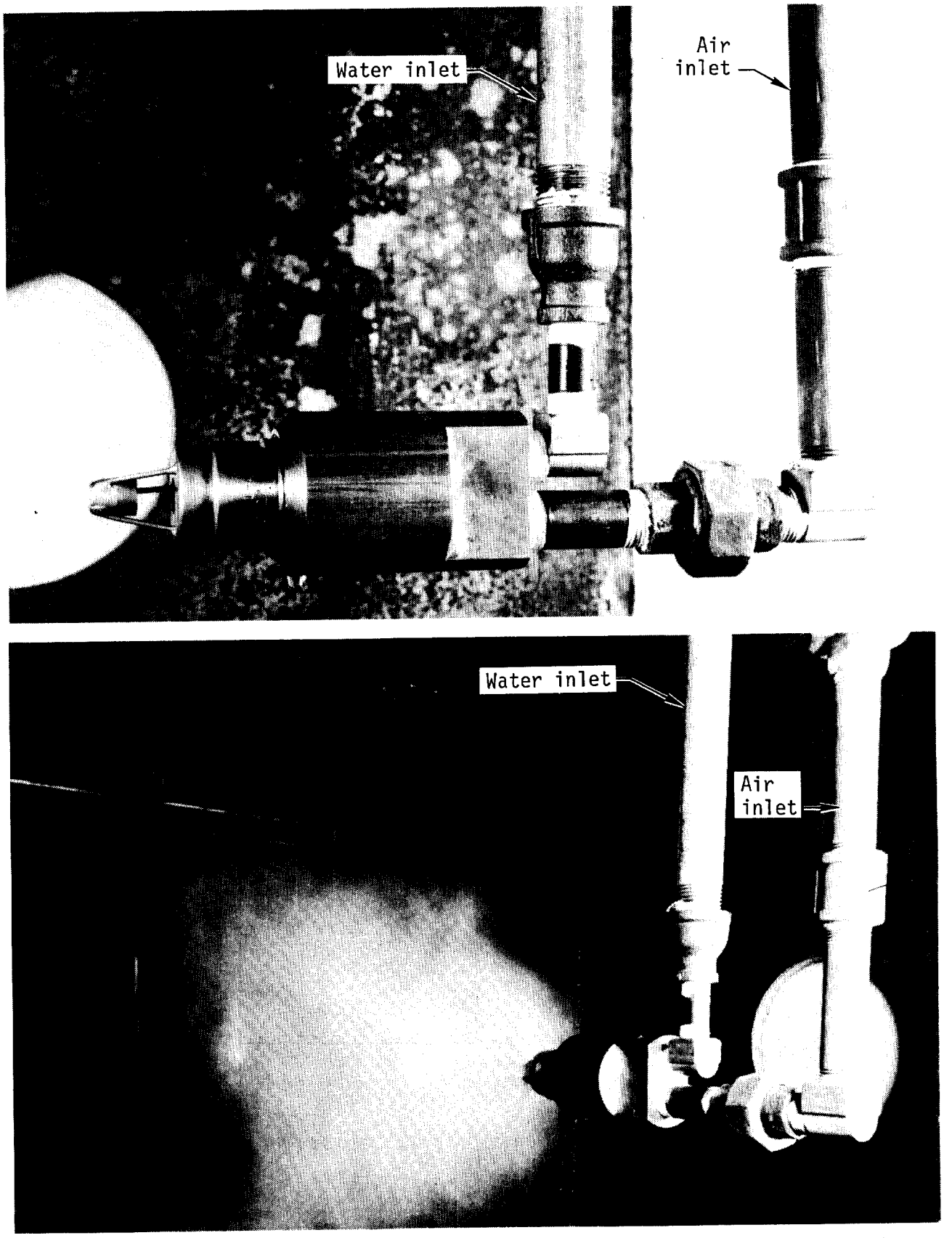

Fig. 17. New air-water ultrasonic spray nozzles. (a) Side view, (b) nozzle in operation.

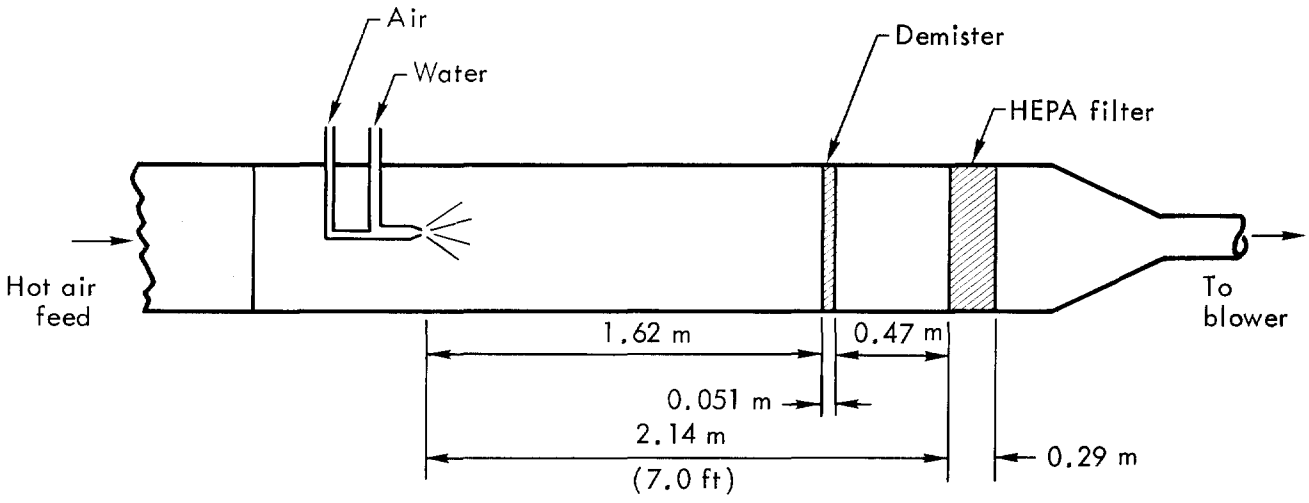

Temperatures (°C)	Results with small nozzle				Results with large nozzle			
Air feed	20	257	501	810	16	251	501	799
In spray	--	88	110	112	--	104	112	93
Becon demister	21	139	133	149	19	150	148	142
Becon filter	21	138	132	148	19	140	138	136
In aft duct	23	137	129	147	20	133	134	134
ΔP's (Paschals)								
Duct feed section to atm.	65	50	50	45	39	51	51	56
Across demister	15	13	10	7	24	20	20	19
Across filter	577 (572)*	416	393	368	317 (360)*	361	357	369
Water flow (ℓ/sec)								
In	0	.01	.052	.075	0	.01	.049	.089
Out	0	0	0	0	0	0	.002	.008
Water temp in (°C)	--	24	26	22	--	22	23	28
Out (°C)	--	--	--	--	--	--	41	59
Heat absorbed (kW)	--	24.3	126.2	183.0	00	24.4	119.6	197.9
(Btu/min)	--	1380	6900	10400	--	1390	6800	11250
Air flow (ℓ/sec)	577 (567)*	416	393	368	577 (548)*	436	406	379

*At ambient temp. after test.

Fig. 18. Summary of heat absorption test data and calculated values using sonic nozzles.

We hope that at the next Air Cleaning Conference we can report some measure of success in our efforts.

Acknowledgments

This work could not have been done without the support of the Division of Operational Safety and the Management of LLL and of the Hazards Control Department. In particular we cite Dr. R. E. Yoder, Mr. D. E. Patterson, Mr. James L. Olsen, and Dr. Joseph F. Tinney for their sponsorship and encouragement. Likewise, the successful setup and prosecution of the experimental work is due in large part to the efforts of such people as Donald Beason, Bruce Bigler, Herbert Ford, Richard Howell, William Kadi, Robert Kaifer, Homer Richardson, and Robert Taylor. We thank them all.

References

1. J. R. Gaskill and J. L. Murrow, "Fire Protection of HEPA Filters By Using Water Sprays" in *Proceedings of the Twelfth Air Cleaning Conference*, Vol. 1 (1972) pp. 103-122.

2. J. R. Gaskill, P. N. Bolton, B. Bigler, and T. M. Hofer, "Fire Protection of HEPA Filters: Preliminary Smoke Loading Studies," Hazards Control Prog. Report No. 43, UCRL-50007-72-2 (May-August 1972) pp. 9-10.

3. J. R. Gaskill, P. N. Bolton, B. Bigler, and H. Ford, Jr., "HEPA Filter Fire Protection," Hazards Control Prog. Report No. 44, UCRL-50007-72-3 (Sept.-Dec. 1972) pp. 8-11.

4. J. R. Gaskill, R. G. Purington, J. K. Hollingsworth, B. E. Bigler, and H. W. Ford, Jr., "HEPA Filter Fire Protection Smoke Plugging Problems," Hazards Control Prog. Report No. 45, UCRL-50007-73-1 (January-April 1973) pp. 10-17.

5. J. R. Gaskill, R. H. Howell, M. W. Magee, D. G. Beason, R. D. Taylor, H. W. Ford, Jr., and B. E. Bigler, "HEPA Filter Fire Protection Smoke Plugging Problem," Hazards Control Prog. Report No. 47, UCRL-50007-73-3 (Sept.-Dec. 1973) pp. 8-14.

Appendix — SI Conversion Chart for Filter Fire Protection Work.

Temperatures	Old values	Equiv. SI values	New SI benchmarks
	70°F	21°C	20°C
	100	37.8	38
	300	149	150
	500	260	250
	1000	538	550
	1500	815	820
Flow — air (20°C/50% RH)	1000 cfm	472 ℓ/sec	500 ℓ/sec
	750	354	375
	500	236	250
	250	118	125
Flow — water	5 gpm	0.315 ℓ/sec	0.32 ℓ/sec
	2.5	0.158	0.16
	2.0	0.126	0.13
	1.5	0.095	0.10
	1.0	0.063	0.06
	0.5	0.032	0.03
Pressure difference	0.1 in. w.g.	24.9 Pa	25 Pa
	0.25	62.3	60
	0.50	124.5	125
	0.75	187	190
	1.0	249	250
	2.0	498	500
	3.0	747	750
	4.0	996	1000
	5.0	1245	1250
	7.5	1868	1900
	10.0	2490	2500

EVALUATION OF MULTISTAGE FILTRATION TO REDUCE SAND FILTER EXHAUST ACTIVITY*

D. B. Zippler

E. I. du Pont de Nemours and Company
Savannah River Plant
Aiken, South Carolina 29801

Abstract

Air from the Savannah River Plant Fuel Reprocessing facilities is filtered through deep bed sand filters consisting of 8½ feet of gravel and sand. These filters have performed satisfactorily for the past 18 years in maintaining radioactive release levels to a minimum. The apparent filter efficiency has been determined for many years by measurements of the quantity of radioactivity in the air stream before and after the filter. Such tests have indicated efficiencies of 99.9% or better.

Even with sand filter efficiency approaching a single stage HEPA filter, new emphasis on further reduction in release of plutonium activity to the environment prompted a study to determine what value backup HEPA filtration could provide. To evaluate the specific effect additional HEPA filtration would have on the removal of Pu from the existing sand filter exhaust stream, a test was conducted by passing a sidestream of sand-filtered air through a standard 24 × 24 × 11½ in. HEPA filter. Isokinetic air samples were withdrawn upstream and downstream of the HEPA filter and counted for alpha activity. Efficiency calculations indicated that backup HEPA filtration could be expected to provide an additional 99% removal of the Pu activity from the present sand-filter exhaust.

Introduction

The efficiency of a filter system is a measure of its ability to collect particles from an air stream. A high efficiency filter is designed to provide an efficiency of 99.97% for 0.3 μm particles. At the Savannah River Plant (SRP) the radioactively contaminated exhaust air from the canyon separations facilities is passed through a sand filter. This filter was described in the August 1968 IAEA Symposium on Treatment of Airborne Radioactive Wastes[1]. A cross section of the sand filter is shown in figure 1. The sand filter efficiency is determined empirically on a routine basis by measurements of the quantity of radioactivity in the air stream before and after the filter. The measurements have indicated efficiencies of 99.9% except during short periods of malfunction caused by structural failure and loss of sand filtering media. Following the development of a large DOP smoke generator by the Hanford Environmental Health Foundation, a standard in place DOP penetration test was made; and the efficiency of the sand filter was confirmed to be 99.97% for an average aerosol particle size of 0.7 μm.

*Information in this document was developed during the course of work under Contract AT(07-2)-1 with the U. S. Atomic Energy Commission.

Plutonium releases from the Savannah River Plant have always been well within established guide values. However, new emphasis on further reduction of Pu activity release to the environment prompted a study to determine what value backup HEPA filtration could provide. Studies of HEPA filters in series on Pu facilities have not always indicated high efficiencies for each filtration stage. Some preliminary SRP testing of 2nd and 3rd stage HEPA filtration indicated efficiencies less than 99.97%. Work done by Los Alamos[2] on backup filters for Pu aerosol showed 99.8% or better. Before proposing spending large amounts of money to back up the sand filter exhaust stream with HEPA filters, tests were needed to prove the effectiveness of HEPA filters in removing residual minute quantities of Pu from the sand filtered air stream.

Summary

Tests at SRP show that backup HEPA filtration on the sand filter exhaust should provide a further reduction of 99% in ^{238}Pu* stack releases. In the event of future sand filter failure, adequate backup filtration would prevent increased releases to the environment. The sand filter would continue to provide a highly efficient pre-filter as well as an excellent protection against fire and explosion to the HEPA bank.

Discussion

The sand filter handles 115,000 ft^3/min of contaminated exhaust air. This study was conducted by passing a 1000 ft^3/min sidestream of sand filter exhaust air through a 24 X 24 X 11½-inch HEPA filter. Measurements of radioactivity before and after the HEPA filter were made to determine filter efficiency.

Test Equipment and Techniques

The equipment (figures 2, 3, and 4) consisted of an exhaust blower, HEPA filter, ducting to supply air from the top of the sand filter to the HEPA filter and to exhaust discharge air back into the sand filter plenum. The discharge was returned at a suitable location to eliminate the possibility that HEPA filtered air could be recirculated thus diluting the test sample. Returning the HEPA exhaust air to the filter also eliminated the need to overcome a ΔP of 12 inches of water which exists between the sand filter and the atmosphere. A manometer was provided to measure the ΔP across the HEPA filter as the test progressed. Sample taps were provided in the duct for DOP testing of the filter system prior to start of the test. All joints were sealed with duct seal and taped to prevent inleakage of air. A Stairmand disk was provided to assure adequate mixing of DOP aerosol during initial testing of the system.

Sample pumps (Bell & Gossett), flowrators, elapsed time meters and filter paper holders were provided for upstream and downstream sample collection. Sampling probes installed in the duct were sized for isokinetic sampling. Prior to commencing the test, the system was DOP tested and confirmed to have an efficiency of 99.97%. Air flow through the system was adjusted to 1000 cfm. Pressure drop across the filter was measured at 0.9 inch of water.

* The same efficiency would be expected for other Pu isotopes.

Sampling

Two vacuum pumps, equipped with rotameters and elapsed time meters, were used to collect 3-cfm air samples upstream and downstream. Samples were collected simultaneously on 3-inch-diameter Hollingsworth & Vose No. 70 filter paper. The first samples were collected for 24 hours. It was determined that this period of time was insufficient to determine an efficiency value for the HEPA filter. Longer sample collection periods were then evaluated. It was generally found that a minimum sampling period of 72 hours was required. One sampling period extended for 240 hours.

Efficiency Determination

Alpha and beta-gamma activity was measured on upstream and downstream samples by using standard radioactive counting techniques. Considerable initial activity was found on both the upstream and downstream samples. Samples were recounted daily until all short-lived material had decayed. A typical decay graph is shown in figure 5. The short-lived material had an effective half-life of about 10.6 hours which corresponds to thorium B, a thoron daughter decay product. After one week decay (168 hours) the short-lived material was no longer significant, and the activity remaining was attributed to long-lived plutonium isotopes. Since Pu removal by the HEPA filter was of primary concern, each air sample was subjected to a Pu chemical separation. The activity remaining on the upstream and downstream samples was determined. Results for 12 samples are shown in table I.

A PHA analysis confirmed that in all cases the remaining alpha activity was due to ^{238}Pu. Figures 6 and 7 show a typical PHA analysis of the Pu detected on the upstream and downstream samples. Figure 8 is a PHA of a Pu standard run for comparison.

The first four samples listed in table I were obtained by exhausting the sand filter discharge air from the top of the sand filter plenum. This is approximately seven feet above the surface of the sand bed. To eliminate the possibility that certain particle sizes were being swept away by the sand filter exhaust fans and thus were not being properly sampled, an extension was attached to the test equipment intake duct. This extension reached to within 18 inches of the sand bed. There was no detectable difference in the results obtained with or without the extension.

Material Balance Check

During the first two weeks of continuous operation, the ΔP across the HEPA filter remained constant at 0.9 inch of water. To determine the amount of radioactivity collected by the HEPA filter, it was removed and the filter medium was analyzed. The filter medium was gamma counted using a Ge(Li) detector to ascertain the major gamma-emitting isotopes on the filter. The largest portion of the observed gamma activity was from the daughters in the thoron decay chain which decayed away with the characteristic 10.6-hour half-life of thorium B. Following further decay, three samples of paper from different portions of the HEPA filter were analyzed for alpha emitters. Only ^{238}Pu was detected, amounting to $0.36 \pm 0.04\ \mu$Ci collected on the HEPA filter.

A material balance calculation was made comparing the difference in radioactivity between the upstream and downstream samples vs. the amount of radioactivity collected on the HEPA filter. The amount collected was within 11% of the calculated value expected to be present.

Particle Size Study

An attempt was made to characterize the particle sizes in the sand filter exhaust as well as those penetrating the HEPA filter. This was accomplished by taking air samples simultaneously upstream and downstream through "Millipore" HA 0.45 μ filter paper.

The samples were counted for radioactivity and then analyzed on a Millipore - Bausch & Lomb π MC particle measurement computer. The radioactivity measured on these samples showed the same correlation as did the HV 70 filter samples. Particle size analysis indicated no measurable difference in particle size or the quantity of particles as detected before or after the HEPA filter. These findings were attributed to the very low particle concentration in the sand filter exhaust stream as compared with normal clean air. The particles detected downstream may have come from the duct work itself.

Table II compares the relative particle concentration between ambient air and sand filter exhaust air.

Further Testing

Following the HEPA study, additional testing was performed to determine the bed thickness of an additional sand filter in series to provide a similar (99%) decrease in release levels for ^{238}Pu. It was determined that an additional three feet of a special grade of sand would be needed.

References

1. G. H. Sykes, J. A. Harper, Design and Operation of a Large Sand Bed for Air Filtration. IAEA Symposium on Treatment of Airborne Radioactive Wastes, August 26 - 30, 1968.
2. H. T. Ettinger, J. C. Elder, M. Gonzales, Performance of Multiple HEPA Filters Against Plutonium Aerosols LA-5349-PR, January - June 1973).

TABLE I SAND FILTER HEPA TEST.

Sample Collection Period, hours	Sample Decay Time, hours	Pu Activity, d/m		DF	Efficiency, %
		Upstream	Downstream		
72	192	102	2.3	44.3	98
144	168	913	10.5	87	99
96	168	775	<1	775	99.9
240	168	1539	3.0	500	99.8
67	168	97	0.98	98	99
192	168	943	4.6	205	99.5
145	168	553	2.66	207	99.5
96	168	500	2.8	178	99.4
72	168	47	1.4	34	97
98	168	664	1.05	632	99.8
69	168	839	7.23	116	99.1
96	168	234	<0.9	315	99.7

The last 8 samples were taken with the intake approximately 18 inches above the "G layer" sand.

TABLE II TOTAL PARTICLE COUNT COMPARISONS.

Sampling Location	Particles/ft^3
Ambient Air	
Jackson, S. C.	287,000
Talatha, S. C.	480,000
Plant site	136,000
Sand Filter Exhaust Air	
Plant site	12,200

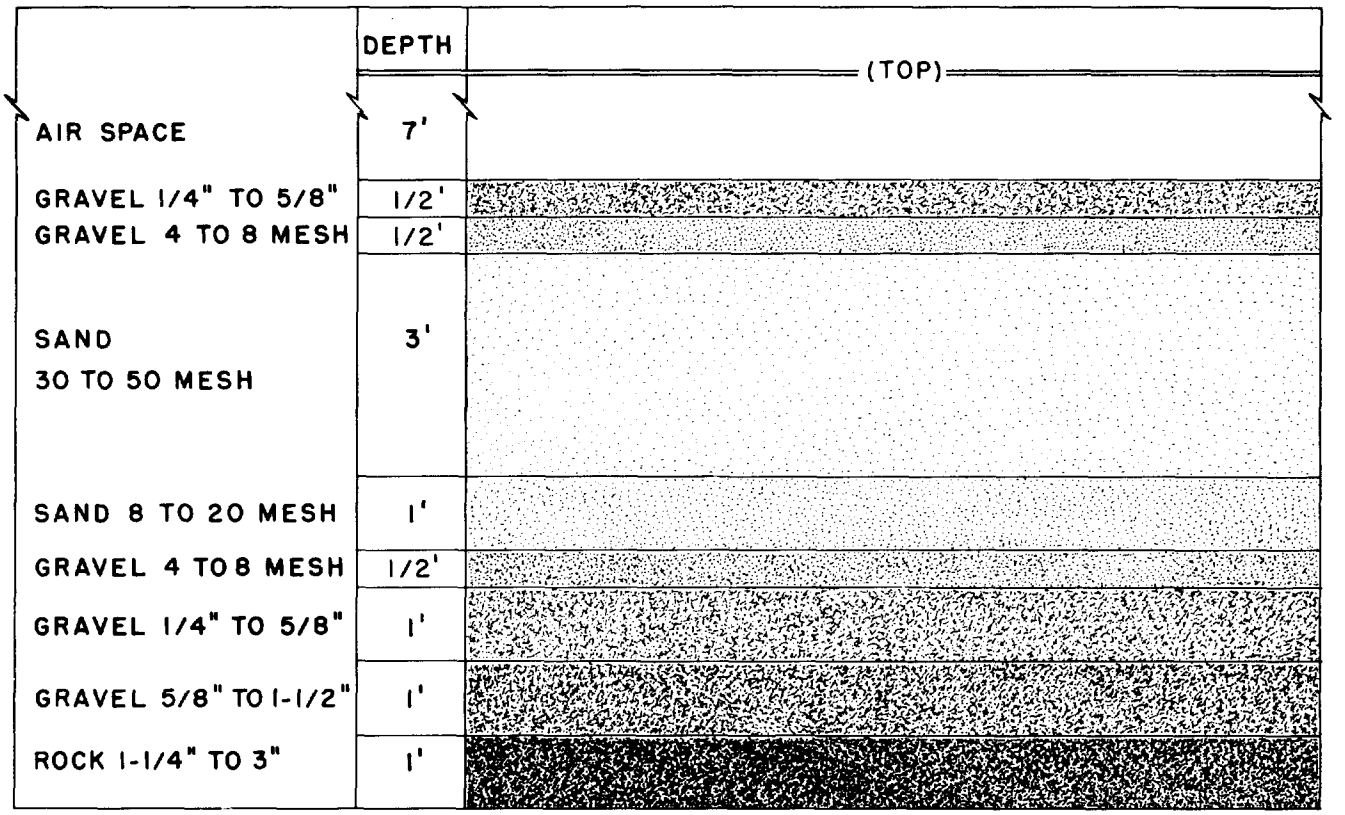

Figure 1. Sand filter cross section.

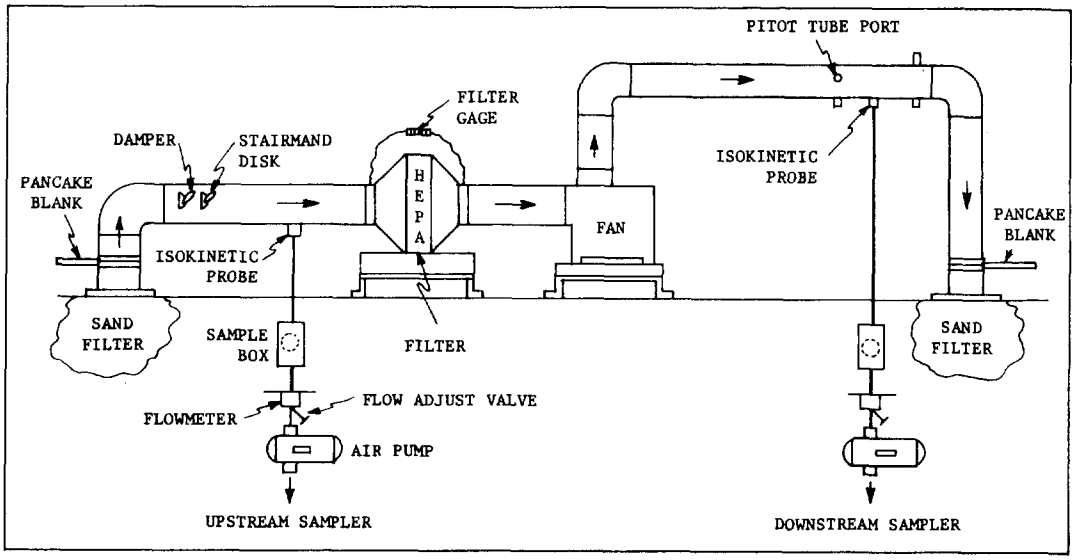

Figure 2. High efficiency particulate air filter test equipment.

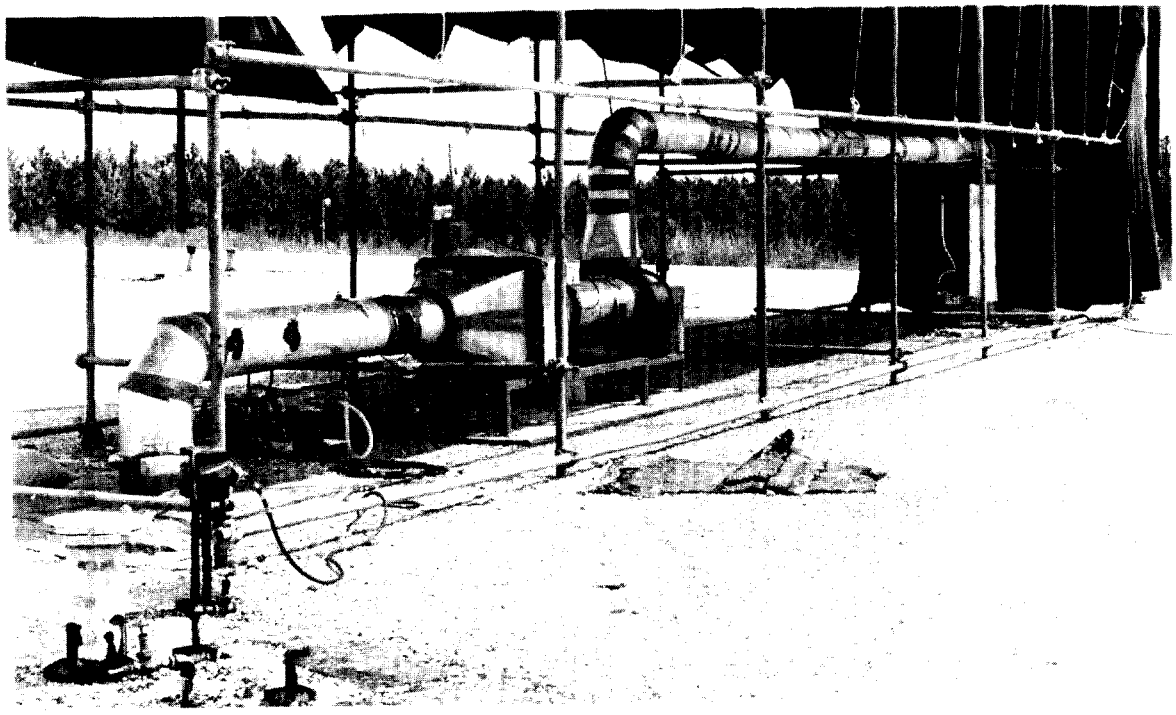

Figure 3. HEPA test equipment.

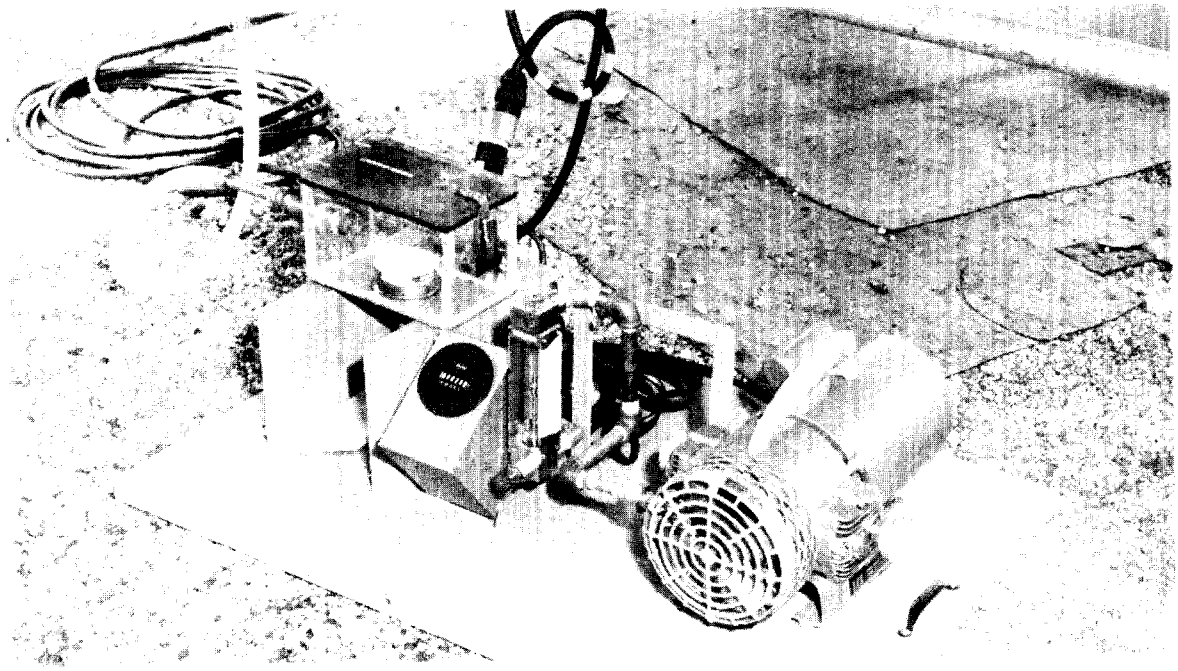

Figure 4. Sample collection box, pump, rotameter, and elapsed time meter.

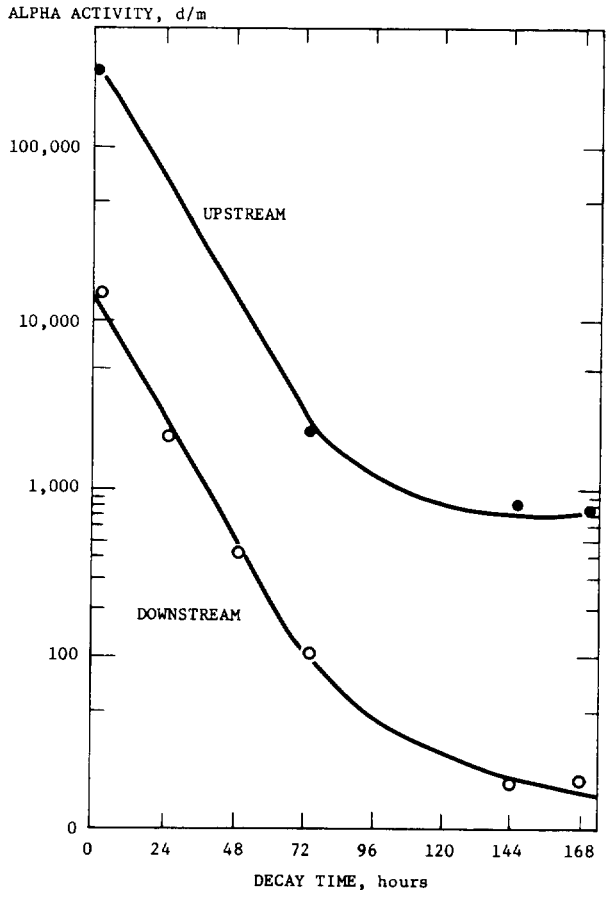

Figure 5. Sand filter HEPA filter test, 144-hour sample (alpha).

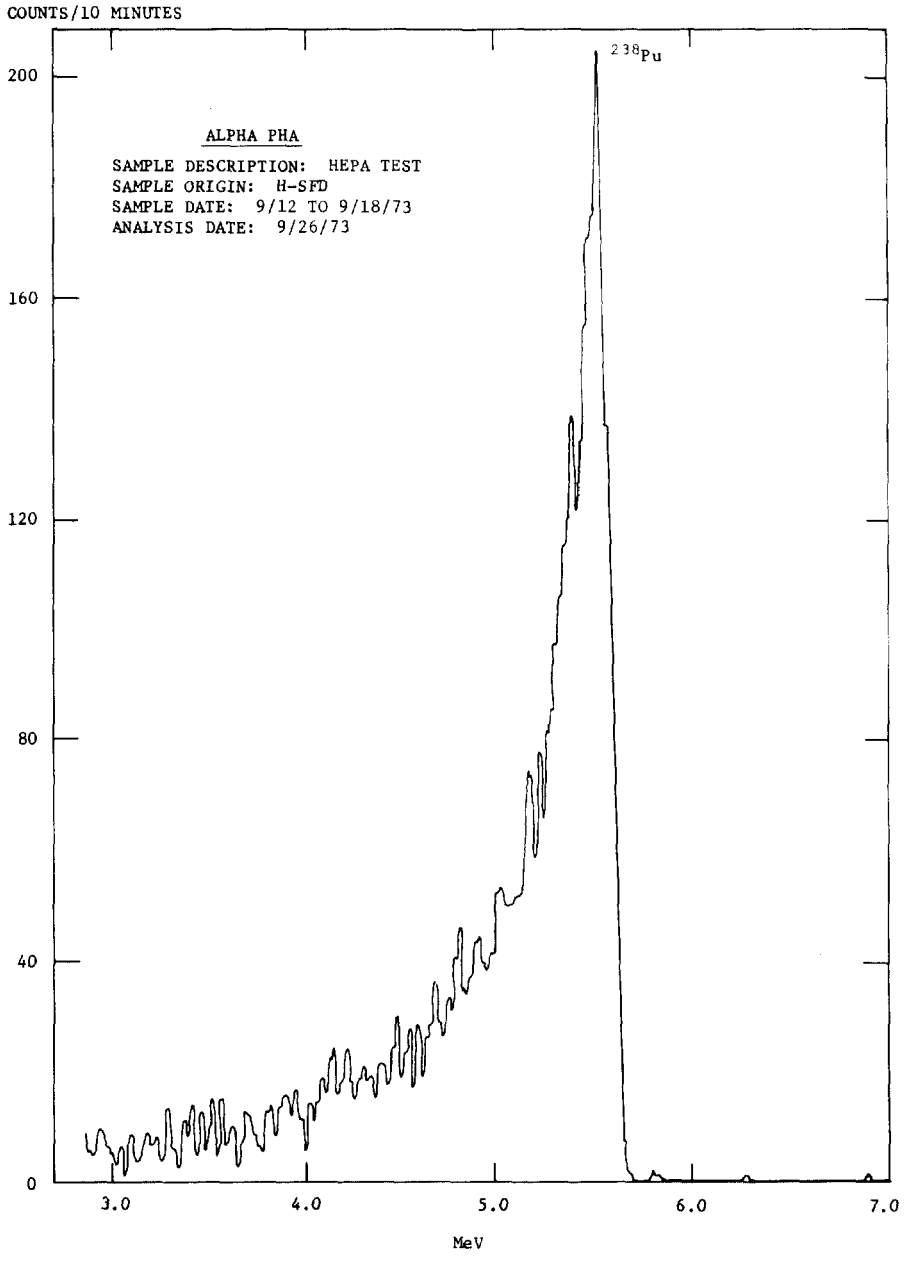

Figure 6. Upstream sample.

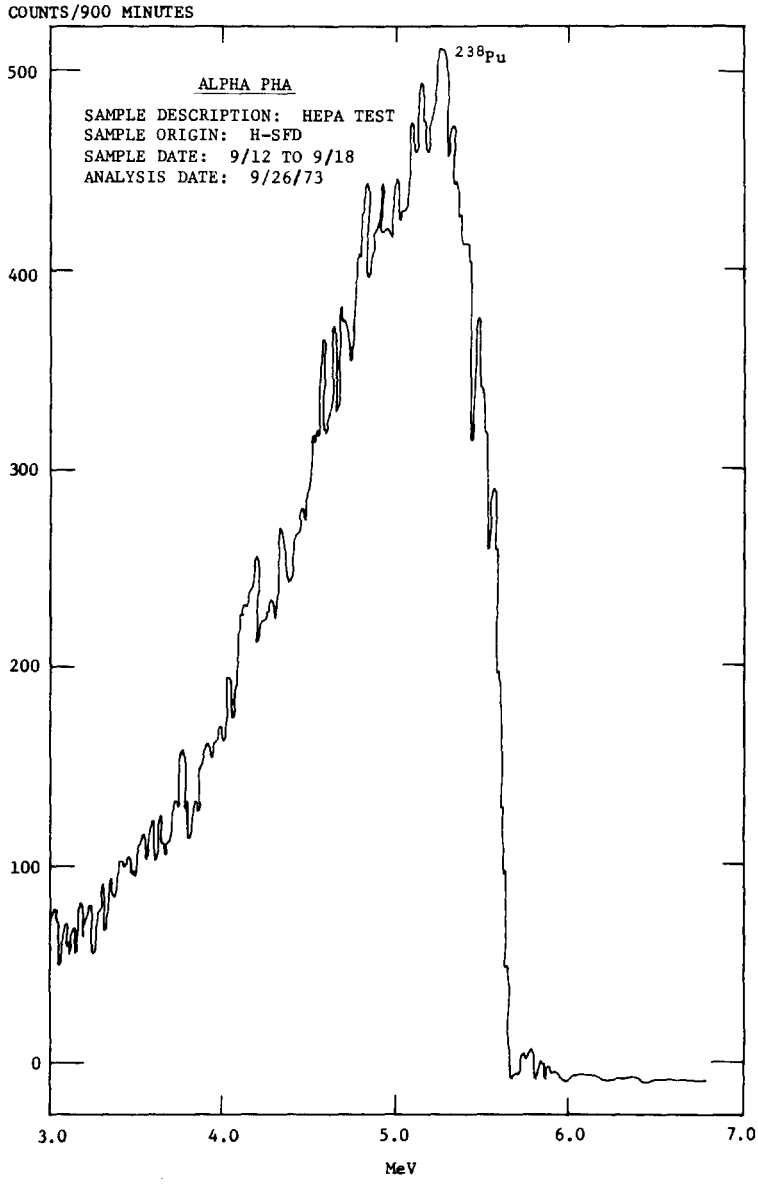

Figure 7. Downstream sample.

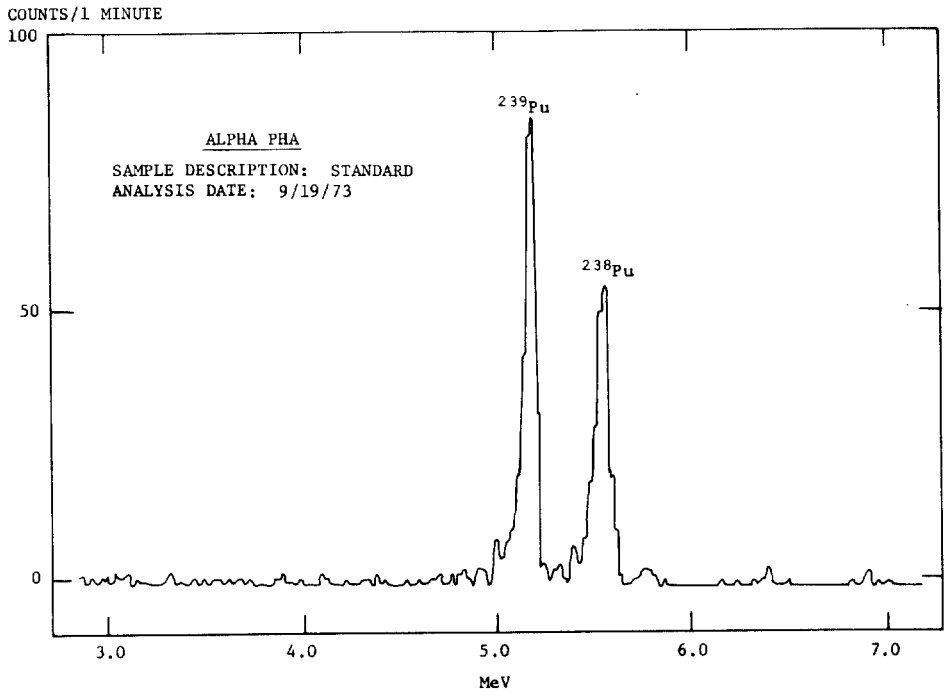

Figure 8. Plutonium-238-239 standard.

THE OFF-GAS FILTER SYSTEM OF THE SNR-300

L. Böhm, S. Jordan, W. Schikarski

Nuclear Research Center
Karlsruhe, Germany

Introduction

In Liquid Metal Fast Breeder Reactors sodium is used as cooling medium. This sodium has temperatures of about 500°C. Accidents at these nuclear installations may happen by leaking pipes or in case of accidents with major spills of sodium.

To minimize the release of radioactivity to the environment of the reactor in case of a major accident a special venting and filtration system is necessary.

A schematic diagram of the Reventing-Exventing-System of the German Liquid Metal Fast Breeder Prototype SNR-300 is shown in Figure 1. After an accident with major damage to the core the ventilation valves are closed fast. At the same time the blower of the reventing system evacuates the reventing gap up to a pressure difference of 2 mbar between the containment and the outer atmosphere. This pressure difference prevents a leakage from the containment to the outside. The revented gas is recirculated into the outer-containment. Leaks from the atmosphere and possibly from the inner containment into the reventing gap increase the pressure in the outer-containment.

Therefore depending on the pressure build-up which is determined by the course of the accident, it is necessary to exvent the containment after several days. As shown in Figure 1 the exvented gas is filtered by a filter combination consisting of pre-filters, charcoal-filters and HEPA-filters. Because accidental sodium fires produce high concentrations of sodium oxide-aerosols this filtersystem must resist chemical aggressive aerosols. Hot sodium reacts very fast with the atmospheric oxygen producing high concentrations of sodium-oxide aerosols. Even at low oxygen-concentrations of less than 1 % high aerosol production rates are observed[1]. In a number of experiments aerosol concentrations up to 50 gr/m^3 have been measured[2].

Up to now nuclear installations with the chance of sodium fires have been equipped with conventional fiber glass filters. These filters have high retention efficiencies for chemical inert aerosols of all sizes (HEPA-filters) but have not yet approved to resist aggressive sodium-oxide-aerosols.

Therefore in the Nuclear Research Center Karlsruhe a program is under way which has the following goals:

1. Testing and determination of performance of commercial glass fiber filters for removal of sodium and sodium oxide aerosols.
2. Development and testing of sandbed-filters to be used in the exventing system of Liquid Metal Fast Breeder Reactors.
3. Optimisation of design and performance of sandbed-filters according to retention, load and pressure drop.

Test facility

Fiberglass- and sandbed-filters were tested in the NABRAUS facility which is essentially a closed gas loop (Figure 2) and a vessel in which the sodium-oxide aerosols are produced. Sodium-oxide-aerosols were generated by melting and burning about 5 - 10 Kilogramm of sodium in a electrically heated pan of 1 m^2 area. The sodiumoxide aerosol production rate was nearly 20 kg Na per m^2 and hour. The aerosol-concentration reached values of nearly 50 g/m^3. The gas was drawn through the test filter and a security filter by a pump.

Temperature, oxygen- concentration and flow-rate was measured in the loop. Before and in the test filter temperature, pressure and relative humidity was measured. For all tests the oxygen-concentration was held constant at 21 %. The mean aerosol mass diameter was measured by a spectral particle scintillation counter. The particle size was found to be in the range of 0,1 - 0,6 µm diameter.

The mass-concentration of sodium-oxide aerosols before the test-filters was determined by washing out the aerosols in water with subsequent titration.

Behind the filter the concentration was measured by an aerosol mass monitor over the time of the run. Filter efficiencies varied slightly with time during the experimental runs. Therefore the average values are reported which are integrated over the total time of experiment.

Experiments with HEPA-Filters

Glass-fiber filters of the size 305 x 305 x 150 Millimeter with a metal-frame and an effective filter area of 2.6 m^2 were loaded with sodium-oxide aerosols. The flow rate was 4000 liter per minute according to the instruction of the manufacturer. This flow rate corresponds to a gas velocity of 2.6 cm/sec. The pressure drop at the filter increased very rapidly with load. At a specific load of 100 Gram per squaremeter the pressure difference of the filter increased from 20 mm WG to 300 mm WG, which is the maximum permissible pressure drop for this filter-type. Higher loads and corresponding pressure drops lead to destruction of the filter material.

After several days of storage loaded HEPA-filters showed exothermal chemical reactions in the filter. The filter-fibers were destroyed by overheating. This reaction was presumably due to delayed sodium-water reactions at high relative humidity of the atmosphere. Furthermore the seperators, gaskets and filter-frames were severly corroded by sodium oxide aerosols.

Experiments with Sand-bed-Filters

For the sand-bed-filter-experiments a special housing consisting of a 5 mm steel sheet was constructed and built. A cross-section of the filter box shows figure 3. The housing was gas-tight and took up about 2 m^3 of sand. The gas flow was directed from above to below. We used only fractions of basalt sand. Four basalt fractions have been available: 0.0/0.6, 0.6/2, 2/5, 5/11 mm. Figure 3 shows the housing filled with three typical different layers of graded sand. At the bottom of the housing special formed steel-sheets were installed to provide a good gas flow. Just above these steel-sheets a supporting layer of about 10 - 20 cm thickness was arranged followed by a layer of fine graded sand. The first layer from above was coarse grained sand.

In a first series of experiments we determined for a simple arrangement of sand layers the filter efficiency at different air flow rates (Table 1). High collection efficiencies and good specific loading capacities were achieved for low flow rates at 400 1/min corresponding to air velocities of 0.9 cm/sec, whereas at large air flow rates of 2000 1/min (4.5 cm/sec) good collection efficiency but moderate load capacity were measured. In the medium range of the flow rates the optimum filtering conditions were not achieved. Figure 4 represents the increase of pressure drop with increasing specific load. For low air-velocities the pressure does not increase substantially up to a load of 300 g/m^2.

Table 2 shows a selection of some test runs with different sand-layers at gas flow rates of 400 1/min, where the different sand layers have been optimized in respect to filter efficiency and load-capacity. These filters have been obtained as result of several test-runs, which were carried out to increase the filter-efficiency. Filter number 1 represents the simple sand arrangement already mentioned in Table 1. By adding a thin layer of very fine sand (layer 2 c in table 2) the filter-efficiency increased substantially. Simultaneously the initial pressure drop increased as well (filter 2 and 3). In these filters an additional coarse first sand-layer was added.

In Figure 5 the pressure drop depending on the specific load for these filters is shown. The lower sand bed filter curve represents filter number 1 of table 2: By adding a fine graded sand-layer to the arrangement the initial pressure difference increases substantially (upper curve in figure 5). From the slope of this curve it can be concluded that due to the additional coarse graded layer on the top of the filter the load capacity was increased. For comparison the pressure drop of a commercial available fiber-glass-filter during load with sodium-oxide-aerosols is shown in Figure 5. The pressure difference of HEPA-filters increase more rapidly with load compared to sand-bed-filters.

Two physical filtration processes determine mainly the quality of the sand-bed-filter: Impaction and diffusion. An aerosol penetration model was developed for multilayer sand-bed-filters. This model is based on the theory of capillarity. One result of this theory is shown in Figure 6. The aerosol penetration through the different sand-bed-layers is shown as function of the flow velocity. The calculated results of total penetration of aerosols through the filter are identical with our experimental results, namely good filter efficiency at low and at high gas flow velocities.

Summarizing the advantages and disadvantages of glass-fiber-filters and sand-bed-filters especially for the filtration of aggressive sodium-oxide-aerosols we can conclude:

- Fiber-glass-filters can be loaded with sodium, sodium-oxide-aerosols up to 100 gramms per squaremeter. At higher loading break through has been observed. Delayed exotherm reactions may destroy the filter-material.

- Sand-bed-filters are inert against aggressive sodium aerosols.

- Sand-bed-filters with different layers of graded sand have efficiencies in the same order of magnitude as HEPA-filters.

- High collection efficiencies and high loading capacities of about 500 gr/m^2 have been achieved at low gas velocities of about 1 cm/sec.

- Sand-bed-filters are good sinks for heat of hot off-gas and for decay heat of fission products.

- Sand-bed-filters for LMFBR plants exceed fiber-glass-filters in all important characteristics of performance even in collection efficiency.

- Sand-bed-filters are somewhat more expensive than fiber-filters in respect to initial costs. Considering long therm use sand-bed-filters can be much cheeper depending on the frequences of replacement of filter material (sand) or filter-cells (HEPA-filter).

- Due to the good performance of the sand-bed-filters of our design the installation in the off-gas filter system of the SNR-300 together with charcoal and fiber-glass-filters has been desided.

References

(1) L. Böhm, S. Jordan, W. Schikarski
Aerosolverhalten bei Natriumbränden im SNR-Containment
Reaktortagung Karlsruhe, 1973

(2) L. Böhm, S. Jordan, W. Schikarski
Versuche zum Verhalten von Faser- und Sandbettfiltern gegenüber Natrium- bzw. Natriumoxid-Aerosolen
Reaktortagung Berlin, 1974

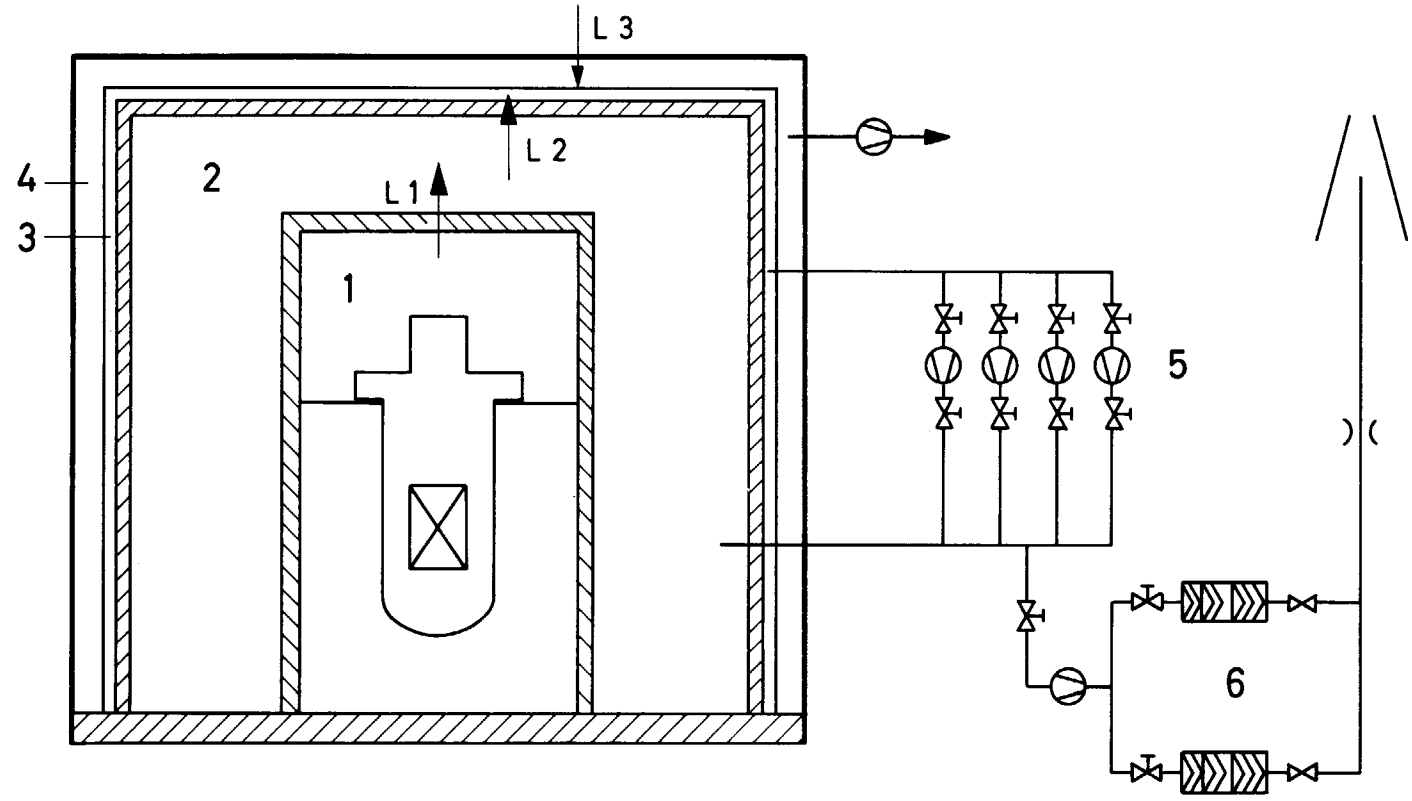

1. Jnner Containment
2. Outer Containment
3. Reventing Gap
4. Ring Gap
5. Reventingsystem
6. Exventingsystem

Figure 1	Reventing - and Exventingsystem of SNR 300	

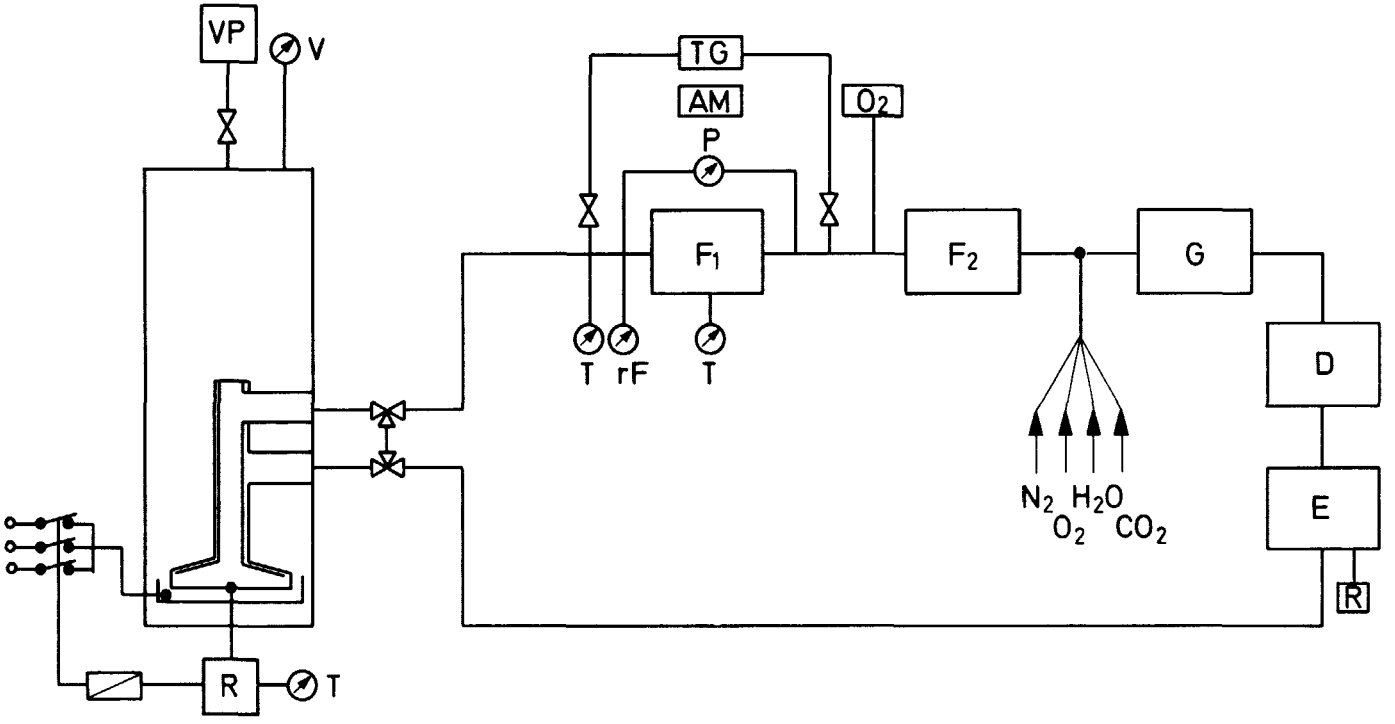

VP - Vacuumpump
F1 - Test Filter
F2 - Safety Filter
G - Blower
D - Flowmeter

E - Gasheater
R - Heatcontrol
V - Vacuummeter
T - Temperaturemeter
rF - Humiditymeter

P - Pressuremeter
O2 - Oxygenmeter
AM - Aerosol - Massconc.-meter
TG - Particle - Size - Analyzer

Figure 2 Diagram of the Filterloop

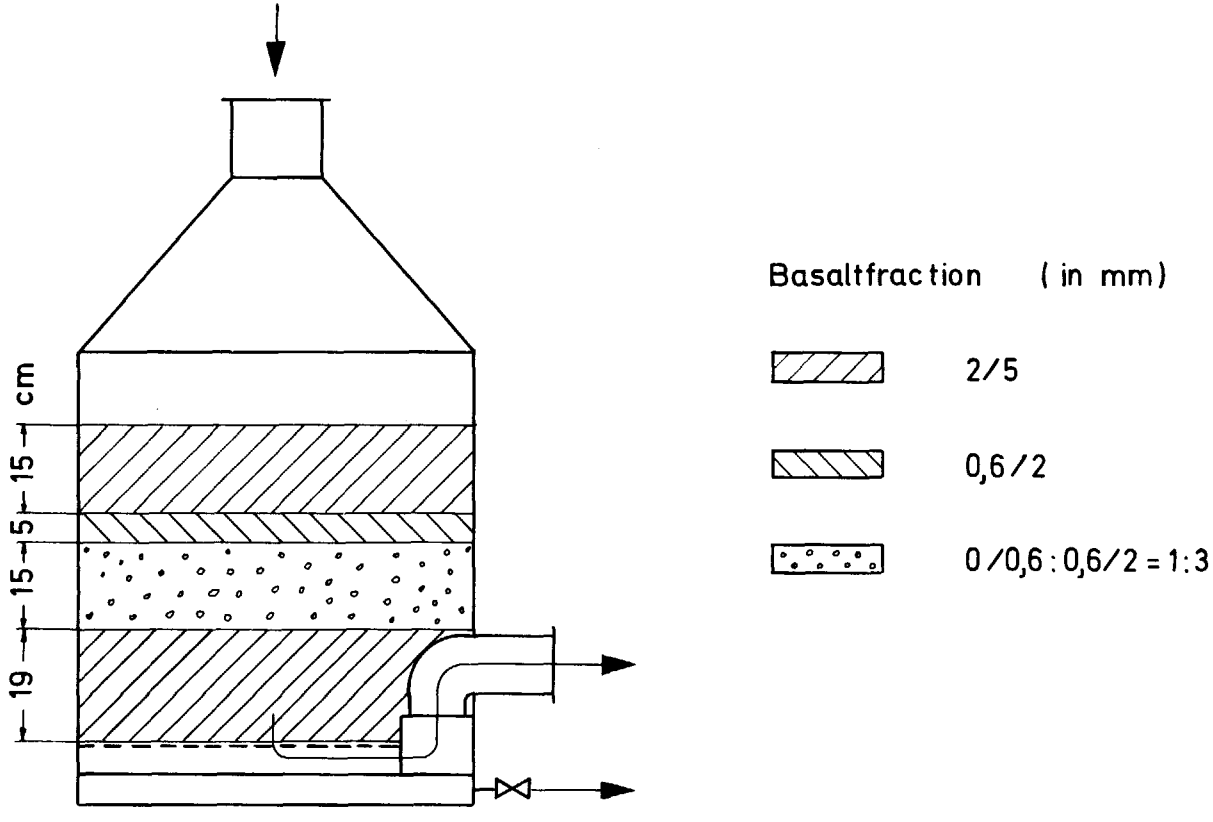

Figure 3 — Cross-Section of a Sandbedfilter

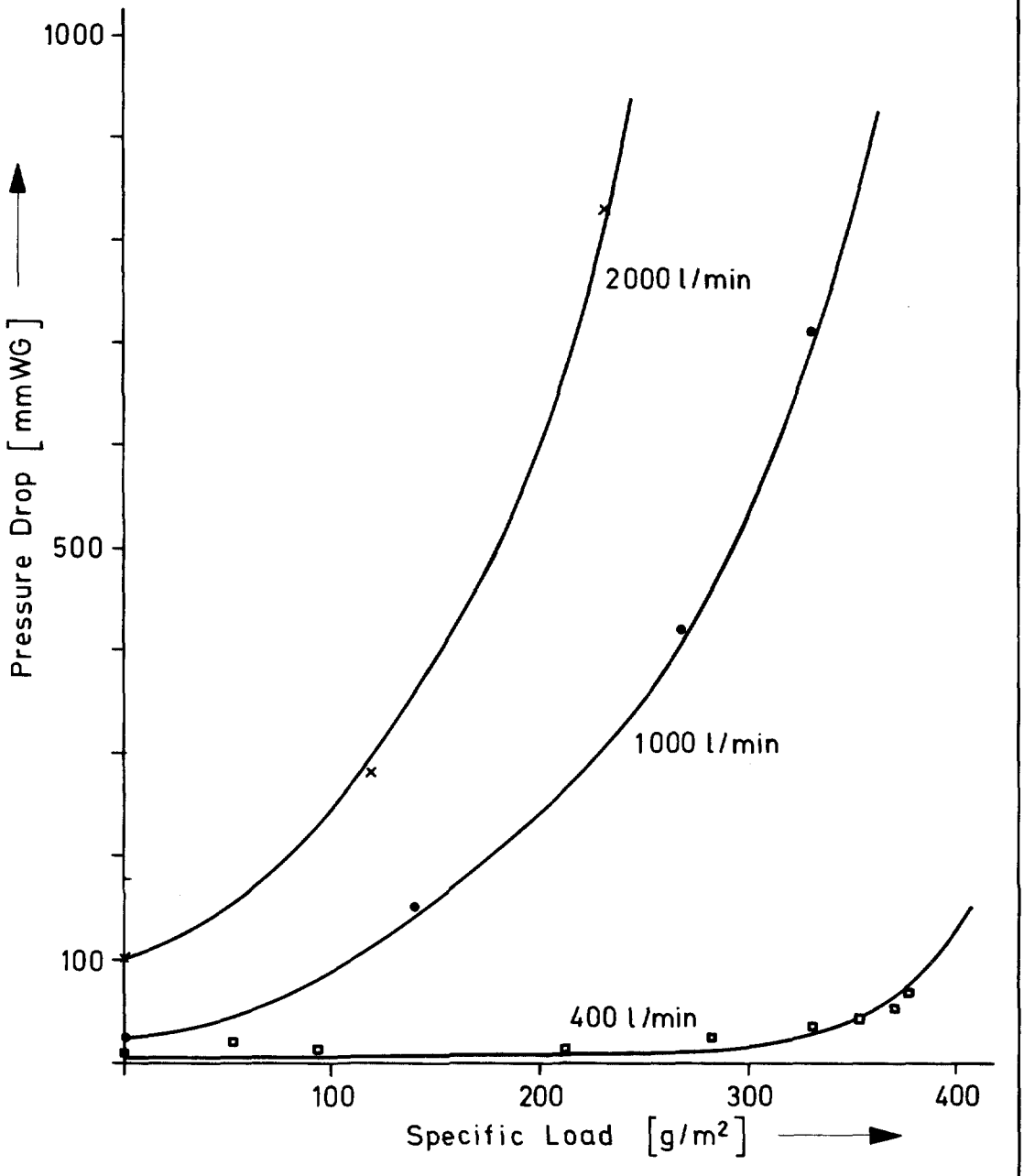

Figure 4 Pressure Drop of a Sandbed-Filter during Load with Sodiumoxid - Aerosols at different Flowrates

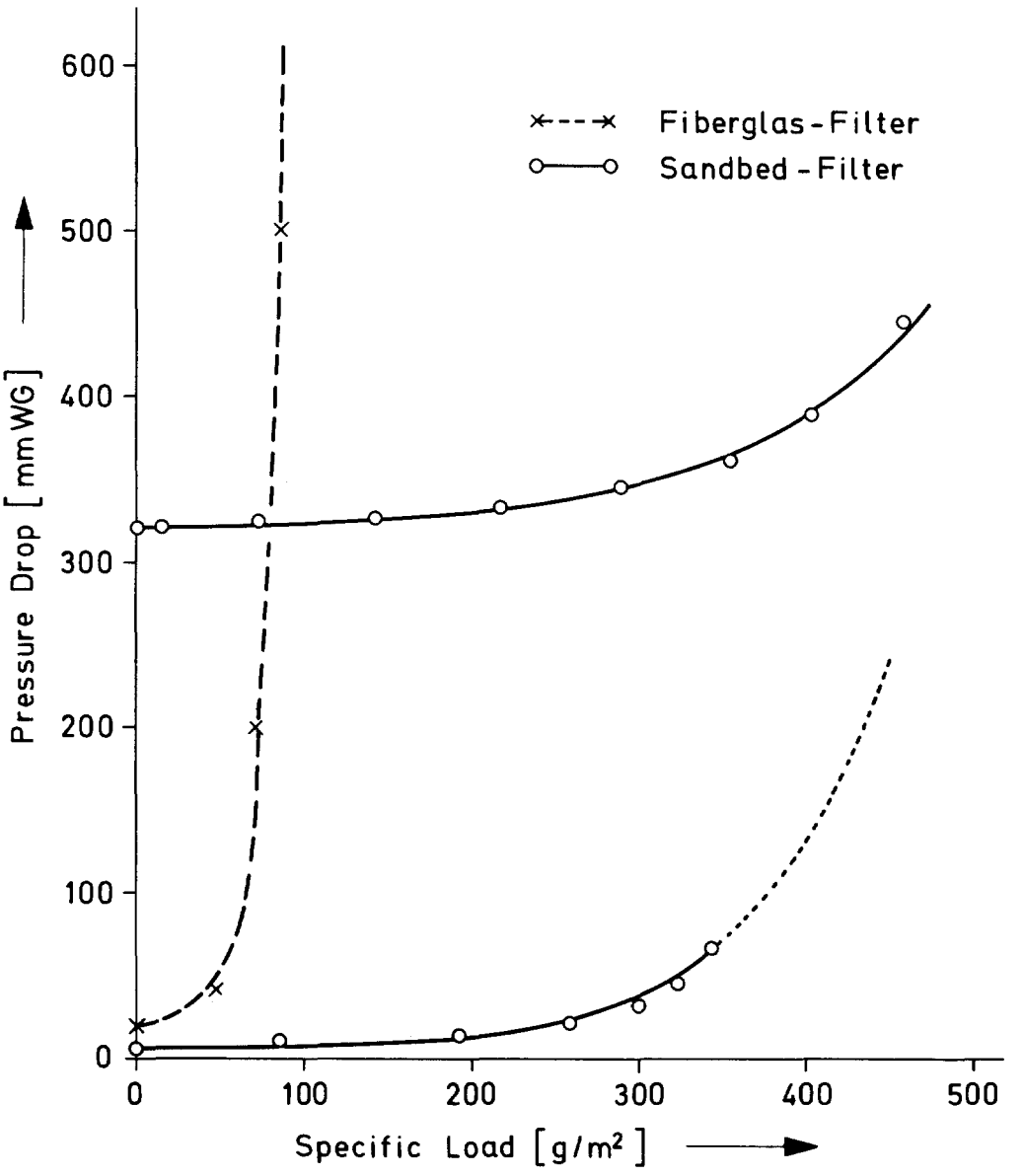

Figure 5 Pressure Drop of different Filters during Load with Sodium - oxide - Aerosols

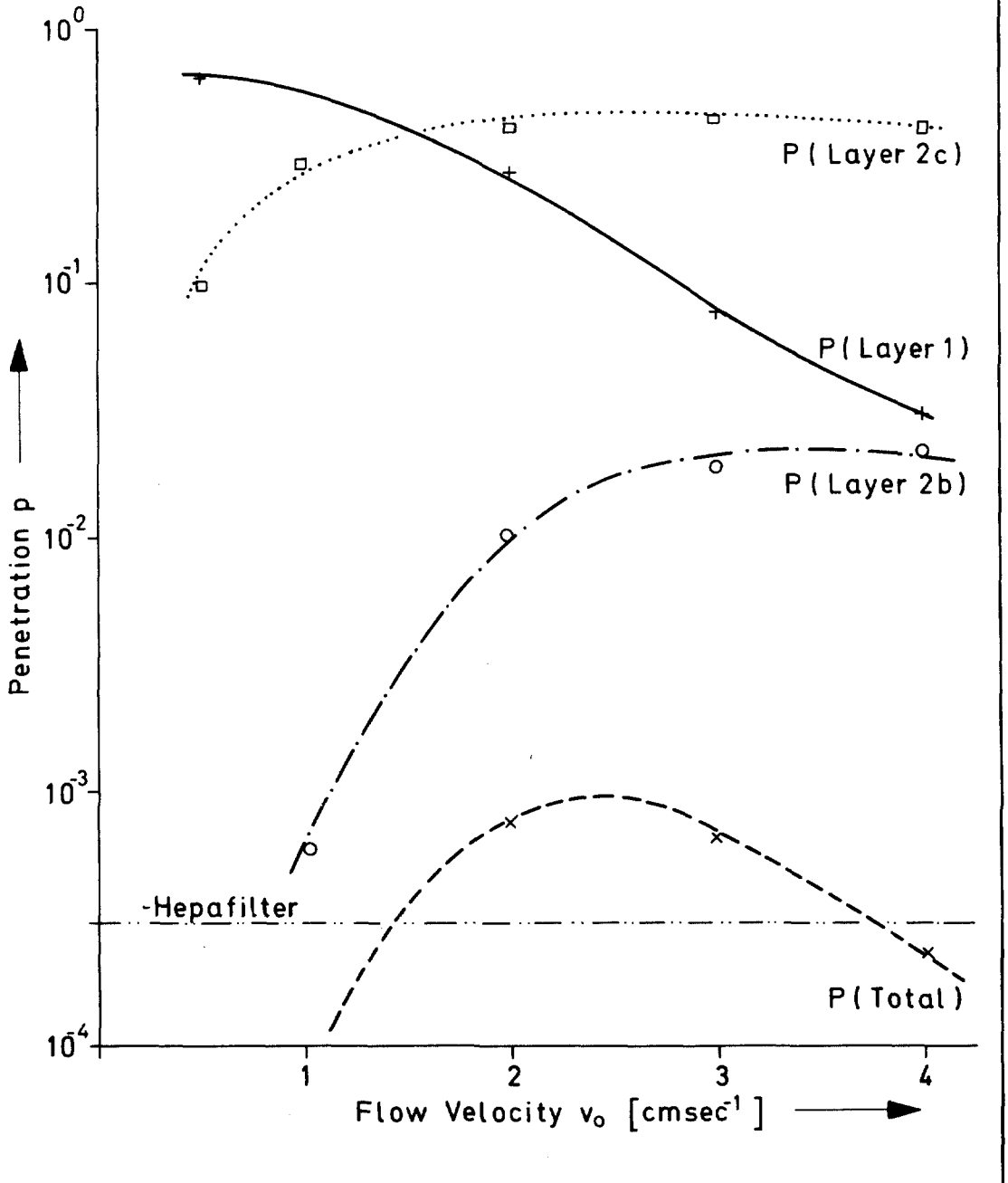

Figure 6 Aerosol Penetration Model of a Multi-layer Sandbed-filter

Gas-Flow l/min	Load g/m²	Filter-Efficiency %
2000	352	99,99
1500	-	99,93
1000	465	99,60
400	446	99,96

Basaltfraction (mm)
Layer 1: 2/5
Layer 2: 0/0,6 u. 0,6/2
Layer 3: 2/5

Table 1 Jntegrated Efficiency of a Sandbedfilter at different Air-Flows

Filter Number	Sand - Layers		Filter - Efficiency %	Specific Load g/m²	Jnitial Press. Drop mmWG
1	1 2a 2b 3	15 cm 2/5 5 cm 0,6/2 20 cm 0/0,6 : 0,6/2 = 1 : 3 20 cm 2/5	99,96	446	20
2	1a 1b 2a 2b 2c 3	10 cm 5/11 15 cm 2/5 5 cm 0,6/2 20 cm 0/0,6 : 0,6/2 = 1 : 3 5 cm 0/0,6 20 cm 2/5	>99,99	450	320
3	1a 1b 2a 2b 2c 3	10 cm 2/5 : 5/11 = 1 : 3 15 cm 2/5 5 cm 0,6/2 20 cm 0/0,6 : 0,6/2 = 1 : 3 5 cm 0/0,6 20 cm 2/5	99,999		315

Table 2 — Efficiency of Sandfilters with different Sand-Layers loaded with Sodiumoxide-Aerosols, Gasflow 400 l/min

DEEP-BED SAND FILTER AT SAVANNAH RIVER LABORATORY*

R. A. Moyer
J. H. Crawford
R. E. Tatum

Savannah River Laboratory
E. I. du Pont de Nemours & Co.
Aiken, South Carolina 29801

Abstract

A deep-bed sand filter was placed in service during June 1974 at the Savannah River Laboratory. This filter provides a back-up for HEPA filters in the primary exhaust system. HEPA filters can fail due to deterioration, faulty seating mechanisms, fire, and/or pressure excursions. The deep bed filter area is 103 feet by 140 feet and consists of layers of rock, gravel, and sand to a depth of seven feet 6 inches. Design flow is 74,000 cfm at 5.15 linear feet per minute. Most of the pressure drop occurs in the 36-inch layer of the "G" sand (sieve size #50 to #30) where the submicron particulates are captured. The filter is described, and operating characteristics are summarized, including pressure drops and filter efficiencies as determined with DOP.

I. Introduction

The Savannah River Laboratory (SRL) is conducting research and development programs involving kilocurie quantities of radioactive nuclides, such as fission products, ^{60}Co, $^{238,239}Pu$, ^{244}Cm, and ^{252}Cf. The main laboratory building, Building 773-A, consists of a group of laboratory modules equipped with hoods and glove boxes (for work with small quantities of radionuclides) and a number of hot cells equipped with remote handling equipment for work with larger quantities. Prior to release to the building stacks, exhaust gases from these facilities are filtered and monitored. Each stack is equipped with continuous monitors and alarm systems to detect any abnormal releases.

The laboratory building was originally designed for work with irradiated and unirradiated fuels, fission products, and ^{239}Pu. As research emphasis shifted to ^{238}Pu, ^{244}Cf, and ^{252}Cf, ventilation was improved to contain these alpha emitters with higher specific activity. Multiple stages of high-efficiency particulate air (HEPA) filters were installed, an on-line filter testing program was established, and a deep bed sand filter was put in service in early June 1974.

The sand filter was installed to provide additional protection against the release of radionuclides to the environment in the event of an accident, such as a fire or explosion, that could breech the containment provided by the existing HEPA filter systems. The sand filter is also expected to provide a secondary benefit in the form of additional reduction in the very low level emissions associated with minor leaks in the HEPA systems during normal operations.

---

* Work performed under Contract AT(07-2)-1 with the U. S. Atomic Energy Commission.

II. Sand Filter System Description

The sand filter system consists of the sand filter itself and its auxiliaries including the inlet duct work, two exhaust fans, effluent duct work, a discharge stack, emergency power generator, a control house, and radiological monitoring equipment.

Sand Filter

The sand filter is a massive reinforced concrete structure about 140 ft x 103 ft x 16 ft. About 15 ft of the filter is underground. The walls and floor are 16 in. thick and the roof is 10 in. thick. The roof is supported by 30-in.-diameter concrete columns (Figure 1).

Air enters the bottom of the filter bed from the inlet tunnel and flows into distribution trenches provided across the bottom of the filter at 20 ft intervals. From the distribution trenches, air passes through stainless steel support gratings and into a single layer of hollow tiles with slotted openings on one side. This layer of hollow tiles is inverted over the distribution trenches (Figure 2) and serves to distribute the air to the first layer of stone in the filter bed.

The size, configuration, and content of the filter bed were based on field tests with a model filter and on experience with other Savannah River Plant (SRP) sand filters. The resulting filter bed was a compromise between flow rates, distribution, pressure, and efficiency. Specifications for the composition of the 7.5 ft filter bed are shown on Figure 1. There is about 7.5 ft of air space above the top (G) layer of the sand.

Auxiliary Equipment

Air is supplied to the sand filter inlet through a 7-ft-inside-diameter underground reinforced concrete pipe, which in turn is fed by a large system of steel ducts, individual system fans, and HEPA filter banks within the laboratory building (Figure 3). High potential systems such as off-gas, glove box, and "hot-cell" exhausts are supplied to the sand filter on a continuous basis. Normally, lower potential systems, such as room and hood exhausts, exhaust directly through building stacks after one or two stages of HEPA filtration. If a release occurs through the HEPA filters on one of these low potential systems, the contamination is automatically diverted to the sand filter by a continuously operational contamination monitor.

An instrument is installed in the inlet duct to measure flow. Fittings and sample lines are provided for introducing dioctylphthalate (DOP) aerosol to measure filter efficiency. Four 6-in.-diameter monitoring tubes extend from the roof to the bottom of the bed for radiation surveys as needed. Also, static lines and probes are installed at strategic locations for measuring pressure drop and for pulling air samples.

Air exits the sand filter from the air space above the bed through ports to a plenum, then through one of two 150 hp fans, and finally discharges to the atmosphere from a 6-ft-diameter, 100-ft-tall stack. The fans were designed for 75,000 cfm at 9 in. H_2O static pressure. At the design flow of 74,400 cfm, the apparent face velocity across the bed is 5.15 ft/min. Fans were fabricated of mild steel and were coated to prevent corrosion. The exhaust ducts and stack are fabricated

Layer	Depth, in.	Specifications
A	12	1-1/4-in. to 3-in. gravel
B	12	5/8-in. to 1-1/2-in. gravel
C	12	1/4-in. to 5/8-in. gravel
E	6	#8 to 1/4-in. sand
F	12	#20 to #8 sand
G	36	#50 to #30 sand

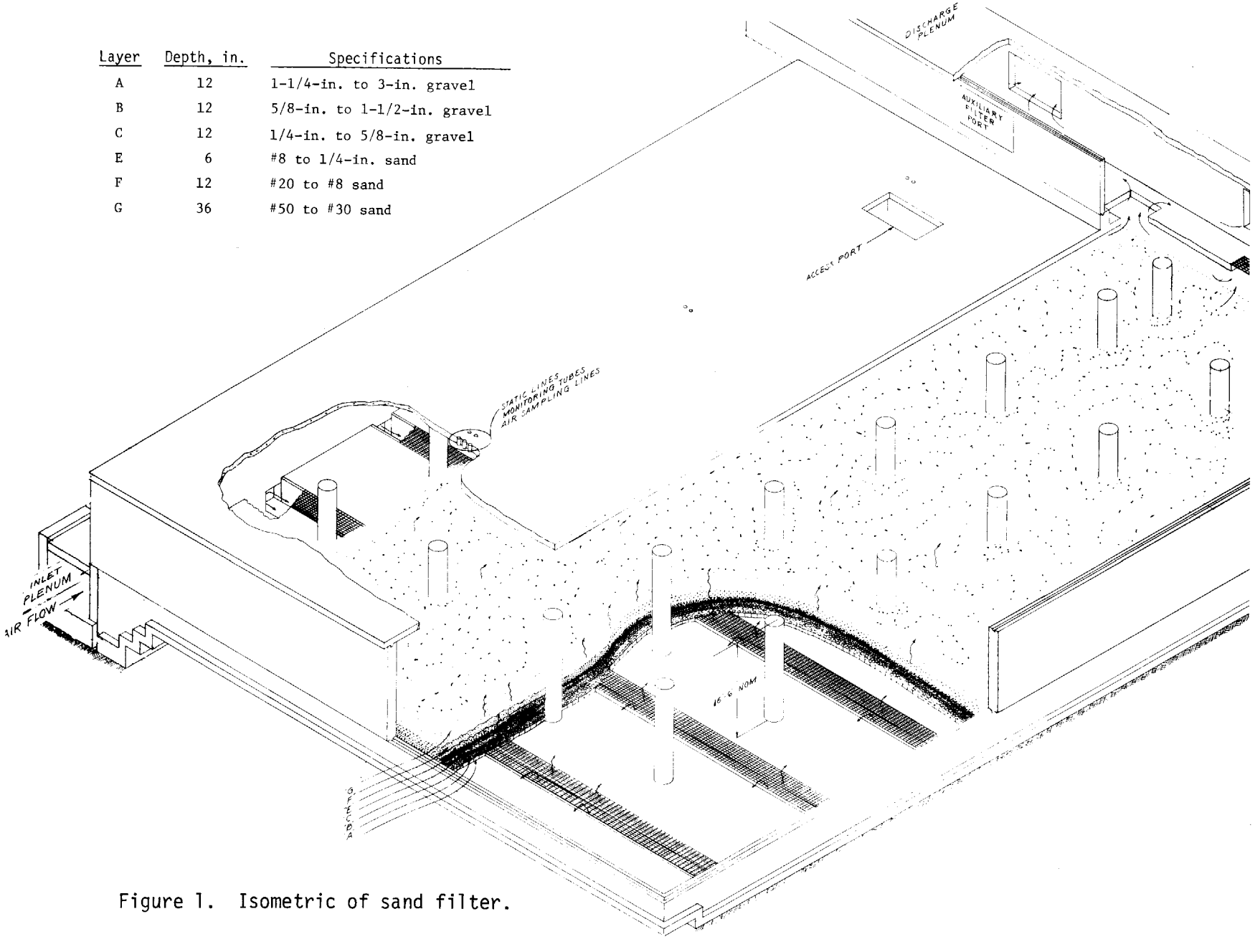

Figure 1. Isometric of sand filter.

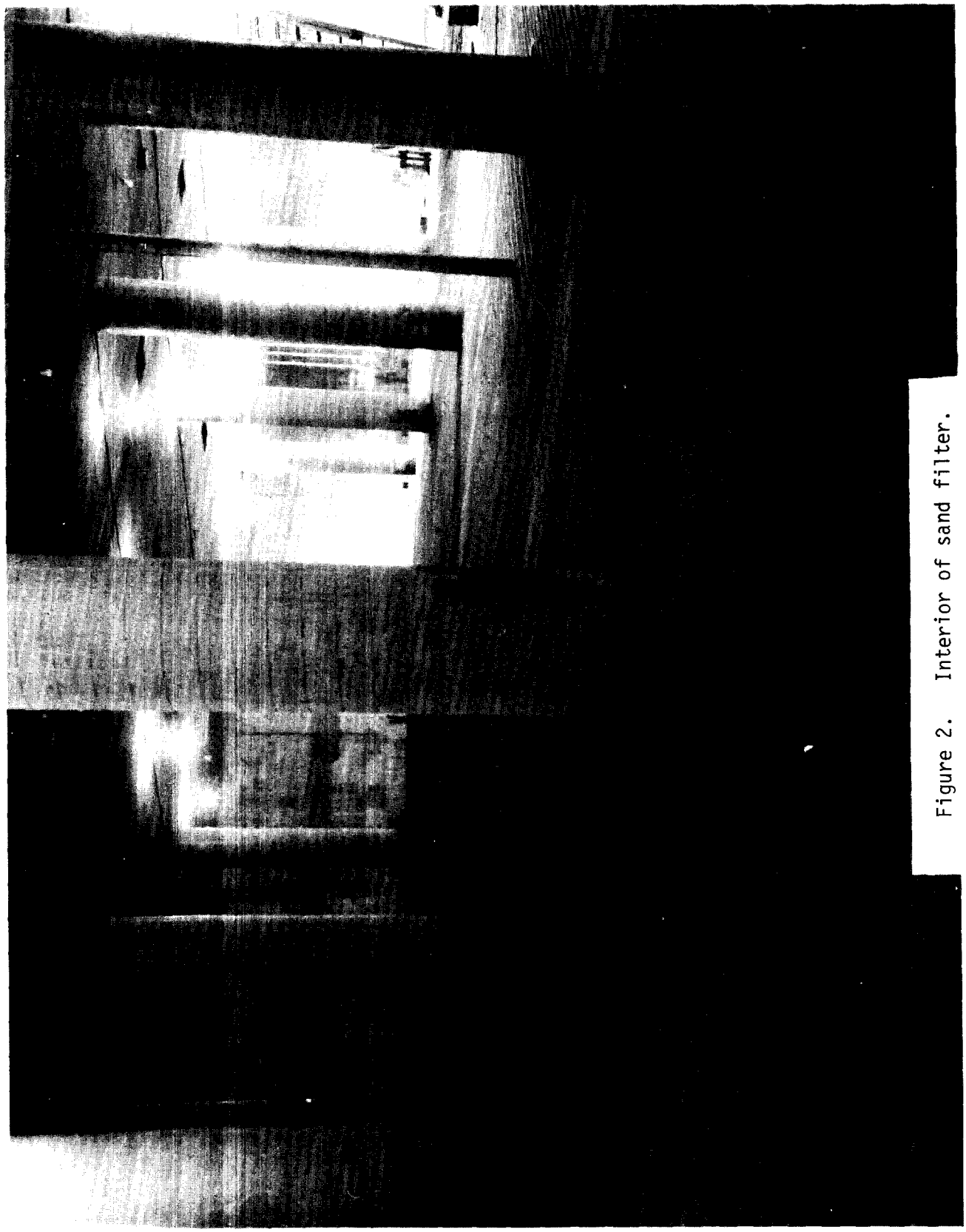

Figure 2. Interior of sand filter.

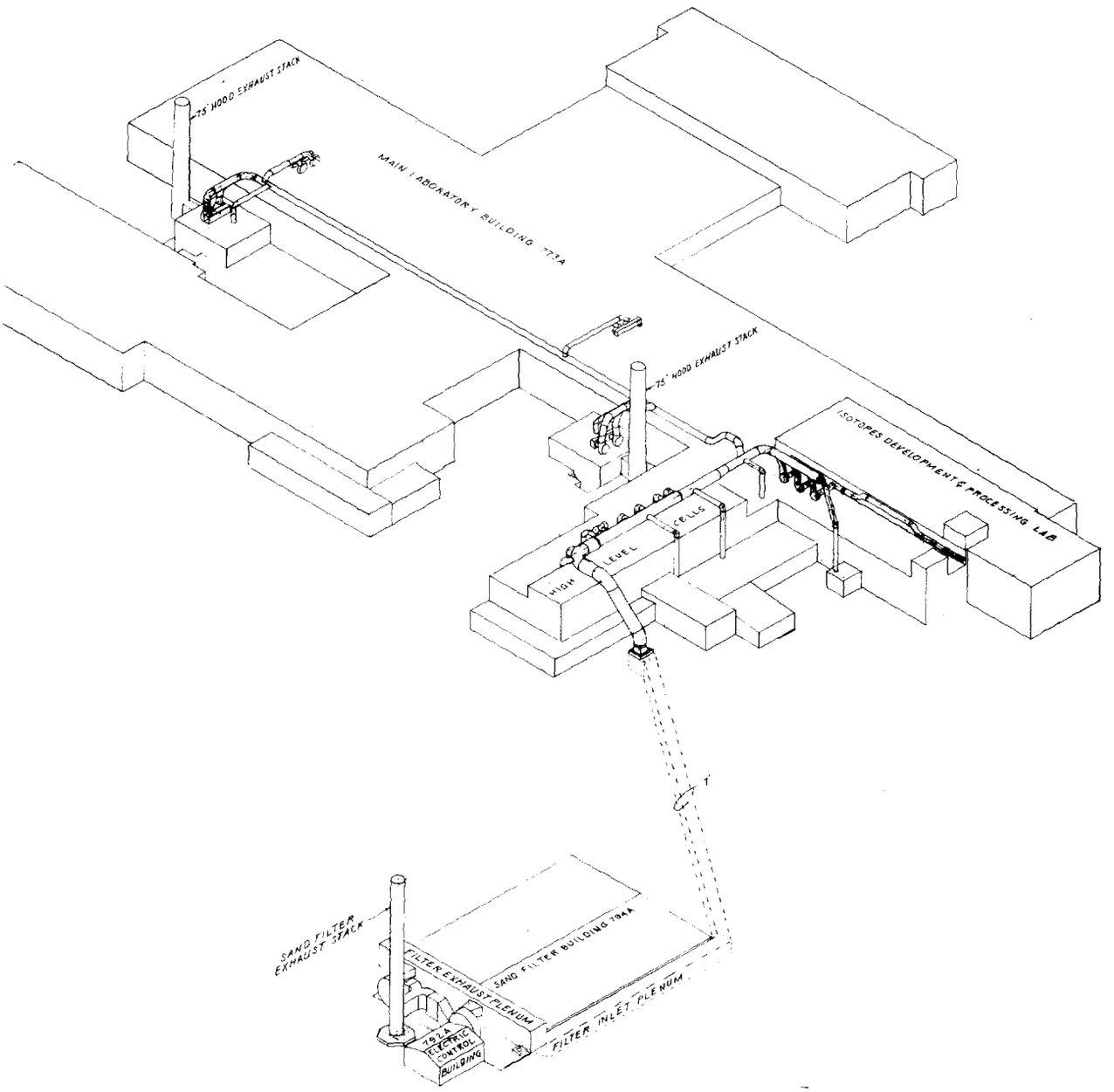

Figure 3. Isometric of system including above-grade ducts.

of *Cor-ten** steel.

Radiological Monitors

The sand filter stack and the two auxiliary stacks are sampled continuously for radioactive particulates and radioiodine. The monitor used is a wide range unit that was reported in detail at the 12th Air Cleaning Conference.[1] The monitor is designed to give an alarm for a release of as little as a few microcuries and to remain on scale for any credible accident. The alarm is based on the gross measurement of alpha and beta-gamma activity collected on a glass fiber filter sample, and on gamma activity collected on a charcoal-filled canister.

An alarm on these monitors causes a protective action plan to be initiated to protect personnel from a potential stack release. Pre-alarm stages trigger a concentrated effort to define the source of the release and correct the problem. Also, if the alarm is from one of the systems monitoring an auxiliary stack, this stack effluent is automatically diverted to the sand filter.

III. Sand Filter Test Program

The engineering data for design of the new sand filter was obtained from performance tests of a model filter[2] and from experience gained from about 17 years of operation of two sand filters in the SRP chemical processing areas. The original model filter tests, completed to determine efficiency of the SRL design for submicron particles, compared efficiencies of various sand deposits, determined effects of compaction and bed moisture on efficiency, and evaluated the duct loading characteristics. The results of these tests were reported in detail at the 12th AEC Air Cleaning Conference.[2]

To provide a direct correlation between the original test data and the new sand filter as actually constructed, an all-welded version of the model sand filter housing used in the original engineering tests was loaded with the same sand bed material as used in the installed filter. The sand and gravel used in the new filter was obtained locally (Dawes Silica Mining Co., Thomasville, Ga.), after initial comparative tests in a small 6-in. column indicated comparable performance with the sand in the two operating SRP sand filters. It should be noted that the sand from Dawes Silica which was used in the original model tests was not from the same batch as finally purchased and used in the sand filter.

Model Tests

Efficiency tests were made by standard procedures using DOP submicron particles and measurement of the relative concentrations both before and after the model bed. A DOP aerosol generator manufactured by Air Techniques Inc. (ATI), Baltimore, Maryland, which is used routinely for inplace HEPA filter tests, produced the aerosol. A forward light-scattering photometer, TDA-2DN, also manufactured by ATI, was used to measure the DOP concentrations.

Figure 4 compares the efficiency of the original model unit loaded with sand and gravel from the Northern Sand and Gravel Co., Muscatine, Iowa, with the model unit loaded with local materials from Dawes Silica. The efficiencies of both filter beds are comparable at a velocity of 5 ft/min (design velocity of the installed

* Tradename of U. S. Steel Corp., Pittsburgh, PA.

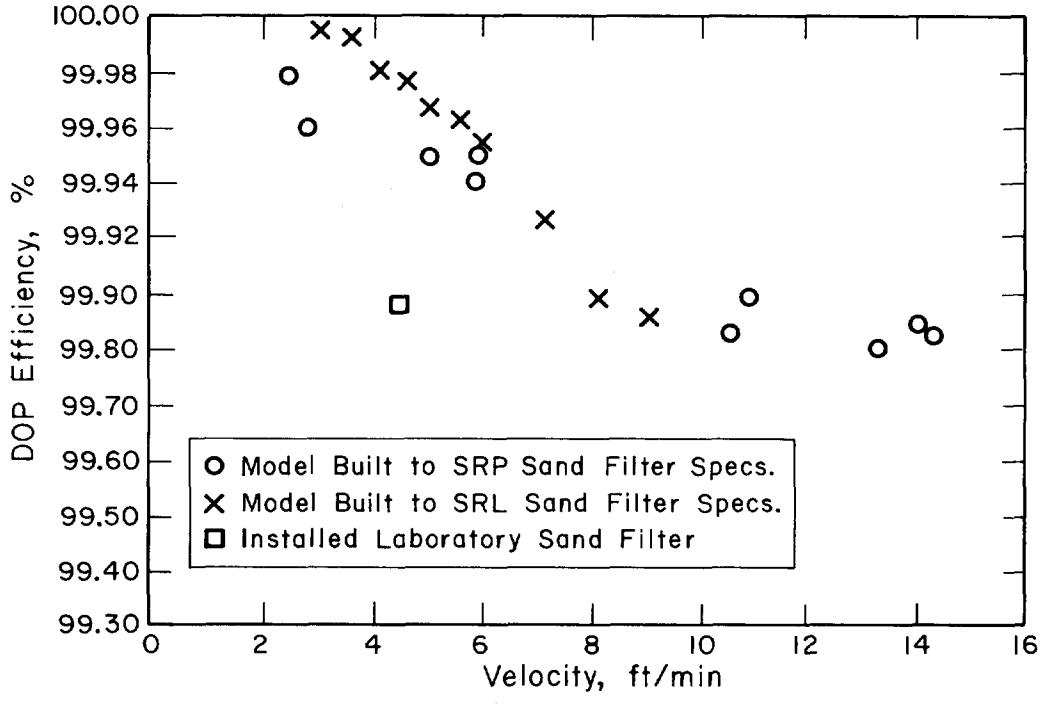

Figure 4. Sand filter efficiency vs velocity.

sand filter) with some slight advantage for the Dawes Silica material at the lower velocities. Figure 5 shows that the pressure drop in the two model unit loadings is comparable at the lower flow rates.

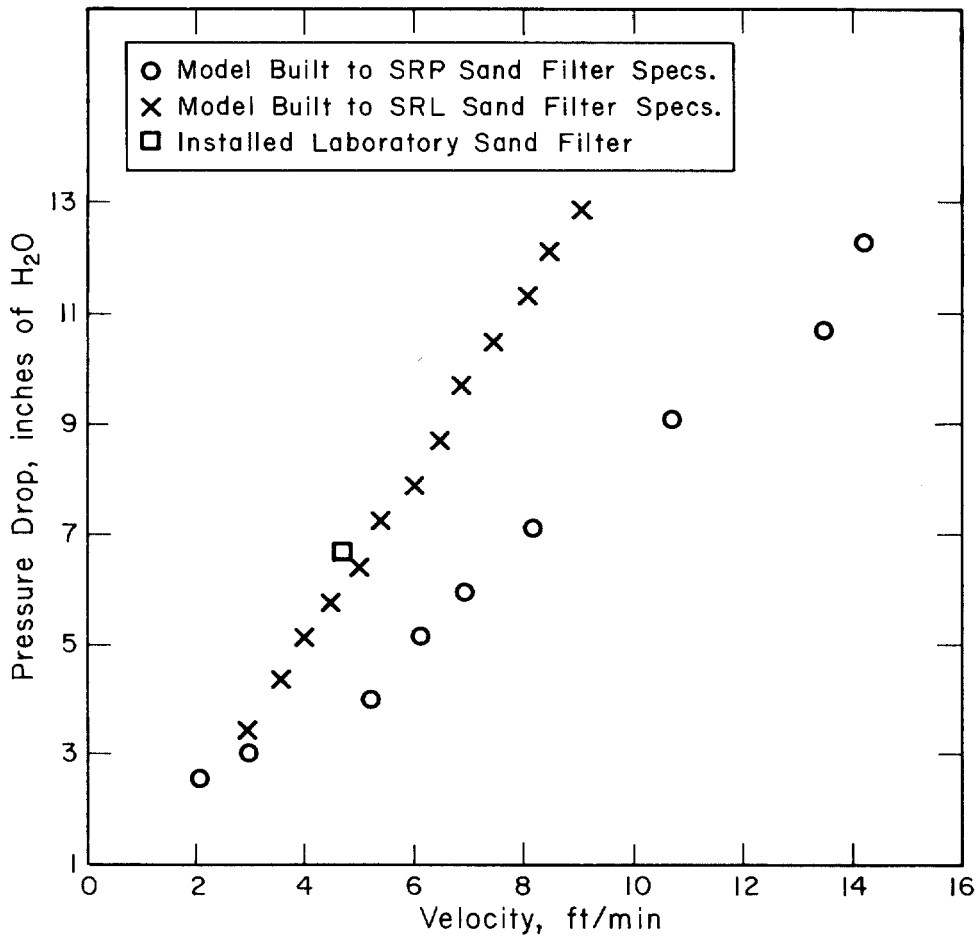

Figure 5. Sand filter pressure drop vs velocity.

Sand Filter Tests

The large volume of air flowing through the installed sand filter (65,000 cfm) required additional DOP generating capacity to complete similar inplace efficiency tests. Large volume (rated at flow rates to 40,000 cfm) ATI DOP generators were obtained for this purpose. On June 6, when the filter had been on line about 6 days, two of the large volume DOP generators were discharged into the 66-in.-diameter duct just before it enters the underground plenum. The flow rate at this time was 65,000 cfm and the pressure drop across the sand filter was 6.8 in. H_2O. Penetrometer (ATI TDA-2DN) measurements indicated an efficiency of 99.9%. Because the penetrometer could not be adjusted for a 100% baseline, the test was repeated on June 17, with three of the large volume DOP generators discharging into the sand filter intake plenum. A 100% baseline was obtained and the indicated efficiency with the same penetrometer was 99.88%. The DOP concentration in the exhaust remained constant for a period of 5 minutes during the test.

IV. Conclusions

The deep bed sand filter as installed at SRL provides a final stage of filtration for laboratory off-gases with an efficiency for radioactive particulates close to that of an HEPA filter. It is virtually impervious to fire, moisture, and other common failures which beset HEPA filters and greatly reduces the potential for a radioactive release during a potential accident.

V. References

1. R. A. Moyer and G. Hayes, "Monitors for Alpha and Beta Activity in Air Exhaust Ducts and Stacks," *Twelfth AEC Air Cleaning Conference*, USAEC Report CONF-720823, Vol. 2, pp 311-319 (January 1973).

2. G. A. Schurr, D. B. Zippler, and D. C. Guyton, "Deep Bed Filter Performance Tests," *Twelfth AEC Air Cleaning Conference*, USAEC Report CONF-720823, Vol. 1, pp 596-616 (January 1973).

DISCUSSION

SHAVER: Was any check made in your sand specification relative to moisture? Would moisture have any effect to speak of on pressure drop after being wetted? What were pressure drop differentials before and after wetting?

MOYER: Yes, there was some work done relative to moisture effects and, generally, moisture increased efficiency somewhat.

SHAVER: How is the sand loaded into the filter: bulk loaded or in bags?

MOYER: The sand was bulk loaded into the filter through the port in the top of the filter. Trucks were backed up and dumped into the slide. But, rather than dumped, the sand was dropped into position.

SHAVER: It wasn't bagged and placed in the filter in individual bags?

MOYER: No, it was not.

BLANCO: Your paper reported data on the use of a sand filter after two banks of HEPA filters in series. In designing a new facility, what efficiency would you assign to the sand filter for use after two HEPA filters in series?

MOYER: The efficiency we have achieved is something like 99.9 percent. We feel this is good: very good in fact.

GOVERNMENT-INDUSTRY MEETING ON FILTERS, MEDIA, AND MEDIA TESTING

W. L. ANDERSON
Naval Weapons Laboratory
Dahlgren, Virginia

Many of the accomplishments of the AEC air filtration program achieved thus far have been due to the efforts of an informed working group concerned with high efficiency filters. The existence of this group has now spanned six air cleaning conferences and has shown successive growth and participation at each one. At the 7th Conference a small group of interested individuals assembled in a smoke-filled hotel room and discussed the current problems in the popular bull-session format. This session proved to be so interesting and productive that the ad-hoc group was convened at all subsequent conferences. At the 10th Conference in New York, 32 people comprised the working group, thus necessitating a formal organizational structure with Mr. Gilbert as its chairman. At the 11th Conference in Hanford, 42 persons were in attendance and a prepared agenda was instituted. At the 12th Conference in Oak Ridge, sufficient interest was expressed so that attendance was limited to invitation only. A total of eleven agenda items were addressed with 48 participants contributing to the discussions. At this the 13th Conference in San Francisco over 70 persons comprised the assembled body; although the majority were from industry, representatives from government, contractors, academic institutions and four foreign governments were present. Many other individuals and/or companies had expressed a desire to participate but the restriction of the attendees was considered to be mandatory in order to keep the active discussions under rational control.

The most recent session of this working group was held this past Monday morning and was devoted to a series of discussions on subjects of current interest. This session, following the precedent of earlier meetings, related the operating requirements placed on the high efficiency filter and the capacity of industry to meet them. To this end, the collected talents of the assembled body were unified toward the solution of the problems of the particulate filter, its components, and methods of test. Representatives of all of the facets of the industrial complex were present, from the basic fiber suppliers, through the media producers, and finally to the filter unit fabrication. Research organizations from R&D government laboratories and academic institution contributed status reports on work currently underway. Users at various levels expressed their problems and actively participated in the discussion.

At the present session, six separate subjects were discussed. The following review of the discussions may seem to be an agglomeration of information and show little continuity of thought. It is my intent to review for you, in abstract form, the items of committee

deliberations. The items will be addressed in the order of their relative importance. Because of the lengthy agenda, prepared papers were reviewed and the intimate discussions and deliberations of previous conferences were conspicuous by their absence.

1. Specifications for Media and Filtration Units - The proposed revision of the combined military-AEC specifications for media (MIL-F-51079) and units (MIL-F-51068) were reviewed and critiqued by the assembly. A position paper on several problem areas was presented by Dexter and specific items of concern identified. A number of technical deficiencies were emphasized; comments on radiation source, acceptance criteria, paper - acidity, caliper, tensile strength, etc. were deliberated. In general it was emphasized that physical requirements should not be restricted without economic and/or practical tradeoff considerations. No specific conference action was established; however, all input from interested parties will be coordinated by AEC and where supported by experimental data and/or need, a specific revision will be negotiated with Edgewood.

2. Qualified Products Listing - Edgewood is currently establishing a qualified products listing for HEPA filtration units under specification MIL-F-51068. All units will be subjected to the proscribed tests and only those passing in all respects will be listed. A deadline of August 30 has been set for companies to file a declaration of intent to participate in the product qualification. Only 3 out of a potential of 8 contractors have indicated their intent thus far. Several filter units have already been received and first tests have begun. Specific performance data has not been received on the units submitted for test. Since the listing stated that this submission was a requirement of qualification, no approval can be given until the documentation has been received. The initial tests will take 9 weeks to complete at a one time charge of $500 per group; government subsidy will provide the remaining funds. If correctable faults are revealed and retest is required for certification then a charge of $2800 per group will be instituted. Much of the test time is required for environmental testing; a test schedule will be published and the contractor is invited to observe any or all of his QPL tests during their conduct. A final report on all lots will be prepared and the acceptable listings published.

3. HF-resistant HEPA Filters - At the last conference a hydrogen-fluoride resistant glass fiber (L-134) was described by Johns Manville. After overcoming fiber production problems, sufficient fiber was prepared to prepare filter media for test. Filter media developed from the acid resistant L-134 fiber and asbestos formulations (50-50) established by Hertz Foundation has been fabricated into filtration units for operational evaluation. Rocky Flats reported that four of these units have been installed in the corrosive processing air systems of their plant for evaluation. HF concentrations of up to 40 ppm and nitric acid up to 100 ppm are

being experienced in this exposure. In this environment an all glass filter will be effective about 2 weeks and the presently utilized glass-asbestos from 10 to 12 weeks before destruction. The recently developed L-134 units were examined at 10 weeks and were shown to be intact with adequate performance. Two of the four units were removed for analysis; the remaining two were left in the system and are still presently acceptable after a total of 14 weeks exposure. Analyses of the removed units have shown adequate residual fibers and tensile strength. Lab exposures of various media to 40% HF shows that ordinary glass fibers dissolves but the L-134 remains intact. It is anticipated that a total operational life factor will be determined and that a final report on all aspects (fiber, media, to final performance) will be issued by the AEC in the near future. In summary, the L-134 media shows great promise for use in the acid environments of the off gas production systems.

4. Dioctyl Phthalate (DOP) Shortages - Due to material shortages, the availability of high quality DOP from Carbide has been seriously curtailed. Several groups associated with the AEC in-place testing programs have stockpiled DOP against future needs; Nuclear Consulting, Columbus Ohio, and Air Techniques, Baltimore will make the DOP available as required. A current price of $1.55 per pound in 55 gallon containers was quoted. Alternate means of procurement (including foreign) and/or purification of inferior grade materials will be explored to provide continuity of the test programs.

5. JM Fiber Composition Changes - Raw material shortages are also reflected in glass microfiber availability. The present fibers (475 formulation) have been supplied by Johns Manville. Extreme shortages of high purity barium oxide has resulted in a proposed change to a new composition glass (753 formulation). The total forces of the working group were committed to this problem on a crash basis to determine impact and effect on the operational needs of the industry.

JM has reported that since the initial shortage was identified, they have obtained additional raw materials sufficient to supply the 475 formulation through July 1975; this in effect will buy time to accumulate additional operational evaluation data. Based on present estimates, March 75 will be a decision point for transition probability. JM now plans to phase out 475 and supply only the 753 formulation about one year hence.

Considerable information was supplied by the fiber producer showing that the fiber characteristics of the two formulations are the same. Identical fiber diameters and size distributions will be available in all the listed size codes. Physical characteristics such as softening point, % water, pH, and densities are nearly identical and costs per pound of fiber will be the same. Other researchers have determined that the fiber solubility of the new fiber is similar; slightly more soluble in NaOH and slightly less

soluble in acids. Fiber dispersion techniques at pH of 3 have not been a problem. Filter media producers have evaluated the fiber with respect to media specifications. Three separate media producers have successfully produced acceptable filter media. Some difficulty was experienced in adjusting the media formulations for mismarked fiber diameters; however, once this was evaluated, specification media has been commercially produced. Tensile strengths, filtration performance, waterproofing, radiation resistance were found to be comparable in both formulations.

Weber from ORNL presented data on accelerated exposures in the acid environments. His tests on the fibers confirmed the solubility differences but concluded that both fibers would exhibit the same performance in the operational environment. Based upon information developed to date no problem areas are foreseen for the fiber formulation change.

6. Chairman Change - From the beginning, Mr. Gilbert has served as the chairman of the working group. He has ably directed the deliberations of the sessions and has been responsible for the groups growth into the impressive role that it now occupies. In line with his recent retirement from the AEC, he has requested that he likewise relinquish the group leadership. It should be pointed out that the action was entirely voluntary and no articles of impeachment are either planned or anticipated. The working group reluctantly accepted Mr. Gilberts' request and heartedly endorsed his recommendation that Dr. First of Harvard School of Public Health be acknowledged as his successor. Mr. Gilbert expressed his desire to remain active in the field and will serve as a member of the working group for future sessions. Cliff Burchsted of ORNL will continue as secretary of the group. Dr. First in his new role as chairman expressed the groups appreciation for Mr. Gilberts contributions and pledged that the role of the working group would continue along the lines of its charter and/or mission.

In conclusion, it should be reemphasized that this informal working group, with its diversified representation, provides a means for a comprehensive and expedient solution to the problems of the filtration industry. The total effort has proven invaluable because it permits the surfacing and exposure of problems that might otherwise be lost in the quagmire of bureaucracy and management. The meetings are intended to be an actually are a working level distribution of data and expertise as well as a progress report of ongoing projects in the particle filtration areas. To this end, we feel that we have been successful and future sessions under our new leadership are comtemplated.

CHAIRMAN'S SUMMATION (BURCHSTED):

I would like to say that in view of the questions that have been raised here this morning, there does seem to be one question remaining which you may wish to discuss among yourselves this afternoon: What kind of filtration efficiency can we expect on a two-stage or three-stage, relatively large capacity, real life, high efficiency filter system?

This is an area of importance to many people in the audience today and I suggest some further discussion might be advisable among those of you who presented papers this morning, Mr. Gonzales, in particular.